A University of Sussex PhD thesis

Available online via Sussex Research Online:

http://sro.sussex.ac.uk/

This thesis is protected by copyright which belongs to the author.

This thesis cannot be reproduced or quoted extensively from without first obtaining permission in writing from the Author

The content must not be changed in any way or sold commercially in any format or medium without the formal permission of the Author

When referring to this work, full bibliographic details including the author, title, awarding institution and date of the thesis must be given

Please visit Sussex Research Online for more information and further details

Drug target development and analysis of genome stability in cancer cells lacking the BAF180 subunit of the PBAF remodelling complex

Suzanna Hopkins

University of Sussex

2017

Thesis submitted for the degree of Doctor of Philosophy

Candidates Statement

I hereby declare that this thesis has not been and will not be submitted in whole or in part to another University for the award of any other degree.

Signed:

Date: 23/03/2017

Acknowledgements

I would first like to thank my incredible supervisor Prof. Jessica Downs for being my guiding light and always having faith in me, even when I had no faith in myself. You are such an inspiration and I am so grateful to have had the opportunity to work with you for the past four years. Secondly, a big thanks to all my friends in the Downs lab, past and present. Being part of such a fantastic lab has made my PhD experience really great. I don't know what I would have done without you guys at times. With a special thanks to Conny Meisenberg who provided brilliant advice in times of utter desperation. Thank you to other members of the GDSC, especially the 'lunch club' who have provided great friendship and guidance. I'd like to say a huge thank you to my Gnomey girls, sharing the PhD experience with you has been amazing. Again, with a special thank you to Catrina Miles, who has been my writing buddy/support system/general rock. Finally, a massive thank you to my family and friends outside of the GDSC. My brothers Paul and Steve who have always believed in me. My 'core four' girls Meg, Sarah and Grace who have done so much to shape the person I am today. To Tom, for all your support, love and for always bringing wine. And to my parents, who are just the best people I can think of, without your love and unwavering support I would have never made it here, so thank you from the bottom of my heart for everything.

This work was funded by the MRC and Cancer Research UK.

Publications

Hopkins, S. R., G. A. McGregor, J. M. Murray, J. A. Downs and V. Savic (2016). "Novel synthetic lethality screening method identifies TIP60-dependent radiation sensitivity in the absence of BAF180." DNA Repair (Amst).

Niimi, A., **S. R. Hopkins**, J. A. Downs and C. Masutani (2015). "The BAH domain of BAF180 is required for PCNA ubiquitination." Mutat Res 779: 16-23.

University of Sussex
Suzanna Hopkins
Doctor of Philosophy (Genome Damage and Stability)

Drug target development and analysis of genome stability in cancer cells lacking the BAF180 subunit of the PBAF remodelling complex

SUMMARY

In eukaryotes, DNA is packaged into a highly condensed structure, known as chromatin. Several complexes facilitate the remodelling of chromatin, for example, INO80, NURD and SWI/SNF, which attach to tightly bound chromatin, allowing its relaxation by nucleosome sliding, unwrapping, histone eviction and exchange of histone variants. The activities carried out by these chromatin remodelling complexes are thought to be integral in the prevention of cancer cell formation. Recently, whole exome sequencing has identified frequent mutations in subunits of the SWI/SNF chromatin remodelling complex, at a frequency that rivals p53. Strikingly, the BAF180 (PBRM1) subunit of the PBAF variant of SWI/SNF remodelers is mutated in over 40% of clear cell renal cell carcinoma (ccRCC), a cancer with typically poor prognosis and limited treatment options to date.

This work embodies four main results chapters that aim to identify novel synthetic lethal gene candidates with BAF180, with a view to targeting these gene candidates with chemotherapeutic drugs. In the first chapter we work through a short list of hypothesis driven potential synthetic lethal candidates and identify the genes KAT2A, RNF4, EZH2 and BAP1 as potential synthetic lethal partners for BAF180. Chapter two describes the development of both stable shRNA and CRISPR/Cas9-derived BAF180-deficient cell lines that were used both in this study as well as for other ongoing projects. The third chapter outlines the set-up of a high-throughput synthetic lethal siRNA (HTS) screen and determines potential synthetic lethal interactions identified here. The final chapter examines various PARP genes, identified as hits in HTS screening, to further explore the interaction between PARP and BAF180. We find that PARP1 and PARP3 are synthetic lethal with BAF180 and treatment with various siRNA's and PARP inhibitors in BAF180 deficient mammalian cells results in specific cell death. A phenotype that could be clinically exploited for treatment of ccRCC.

Table of Contents

List of tables and figures

Tables

Figures

Chapter 1

Chapter 2

Chapter 3

Chapter 4

Chapter 5

Chapter 6

Appendix

1 Introduction

1.1. Genome Damage and Stability

The maintenance of genome stability by the correct replication of DNA and repair of damage is vital for optimal fitness in all living organisms. Genomes hold all the biological information needed for life and are made of DNA (Deoxyribonucleic Acid). When unwanted alterations are made to the DNA sequence it is possible to develop cancer, broadly described as a group of diseases that are capable of abnormal cell growth. Hanahan and Weinberg described, in 2000 and again in 2011, the hallmarks of cancer, encompassing the capabilities acquired by tumours for sustained growth (Hanahan and Weinberg 2000, Hanahan and Weinberg 2011). These included, but aren't limited to evading growth suppressors, inducing angiogenesis, avoiding immune destruction and most importantly for the discussion in this thesis, genome instability and mutation (Hanahan and Weinberg 2011). Genome maintenance systems within cells have a vital role in resolving defects or damage acquired on DNA to ensure spontaneous rates of mutation are low during each cell generation (Hanahan and Weinberg 2011). This DNA-maintenance machinery is diverse and components of this machinery are often referred to as "caretakers" of the genome, which have tumour suppressing activity (Kinzler and Vogelstein 1997). The tumour suppressor TP53, has a key role in the surveillance of genetic integrity and is known as the "guardian of the genome" (Lane 1992). It is when genome maintenance by components of the machinery like this fail, for any number of reasons, that leads to the onset and progression of cancer. Currently the leading treatments for cancer include resection by surgery, which is an invasive process, as well as radiation and chemotherapy, which work by severely damaging DNA to trigger cancer cell death, none of which are entirely successful and can be damaging by themselves alone, thus leaving scope for development of new treatments. The research field of genome stability and DNA repair is important for the advancement of cancer treatment. Study in this field generates vital knowledge about the biology of cancer and how these diseases develop over time,

as well as studying how they respond to current treatments and ultimately aims to improve and identify new therapies for the treatment of cancer. This first section of this introduction chapter will aim to introduce DNA damage and the pathways that are involved in the repair of this damage.

1.1.1. Deoxyribonucleic Acid

DNA was first discovered in the late 1860's by a Swiss biochemist, Johann Friedrich Miescher, defining what he found as being acidic, rich in phosphorous and having the potential to have large individual molecules. It wasn't until much later, in 1953 when James Watson and Francis Crick as well as other research teams headed by Maurice Wilkins and Rosalind Franklin, made their seminal discovery about the structure of DNA (Franklin and Gosling 1953, Watson and Crick 1953, Wilkins, Stokes et al. 1953). Rosalind Franklin's data, based on X-ray diffraction studies, supported the theory of a DNA double helix, but it was in fact Watson and Crick who first solved the double helix structure of DNA, a discovery which has come to be known as the single most important biological breakthrough of the twentieth century.

The DNA double helix exists as two hydrogen-bonded DNA polymers that run alongside each other in opposite directions, therefore making anti-parallel strands (Watson and Crick 1953). A pentose sugar-phosphate backbone is the supporting scaffolding of these polymers, joining together four chemically distinct nitrogenous bases cytosine (2'-deoxycytidine 5'-triphosphate, dCTP), thymine (2'-deoxythymidine 5'-triphosphate, dTTP), which are single ring pyrimidines and adenine (2'-deoxyadenosine 5'-triphosphate, dATP) or guanine (2'-deoxyguanosine 5'-triphosphate, dGTP), which are double-ring purines (Figure 1.1a). 2'-Deoxyribose is a pentose sugar that consists of five carbons named 1',2' (one prime, two prime) etc. Phosphate groups are composed of one, two or three linked phosphate units, designated α, β and γ. Nucleotides, the single unit of the DNA polymer, are formed when a nitrogenous base is attached to the first carbon of the 2'-deoxyribose pentose sugar and when the α-phosphate unit

joins to the 5’-carbon of the sugar (Figure 1.1b). Polynucleotides are formed when individual nucleotides are joined by phosphodiester bonds (Figure 1.2) between their 5’ and 3’ carbons. This type of bonding gives the polymer a chemical direction, denoted as 5’→3’, in which all natural DNA polymerase enzymes follow during DNA replication. In eukaryotic cells, DNA is tightly packaged with proteins in a structure called chromatin, which will be fully introduced in section 1.2.

(A)

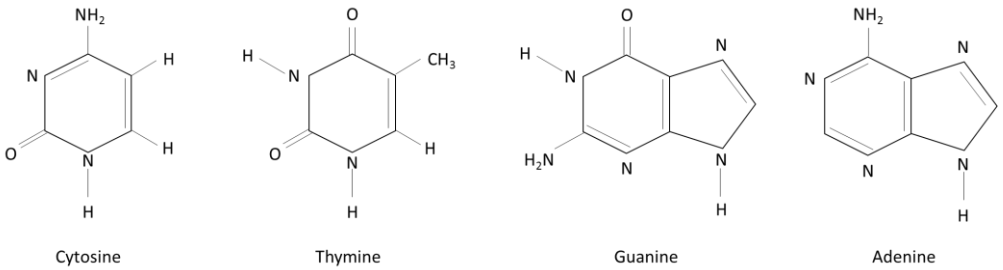

(B)

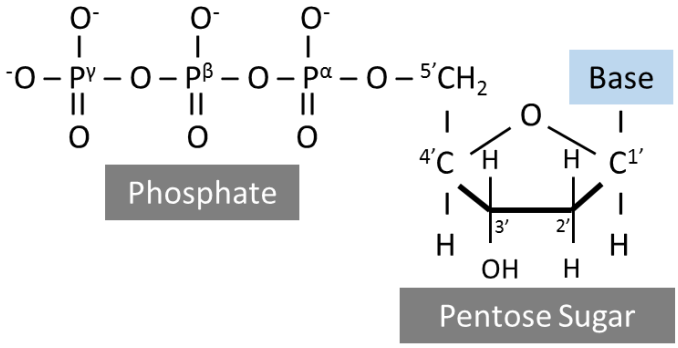

Figure 1.1. Nucleotide Structure (A) The four nitrogenous bases, the pyrimidines cytosine and thymine and the purines guanine and adenine. (B) Composition of a typical deoxyribonucleotide found in DNA.

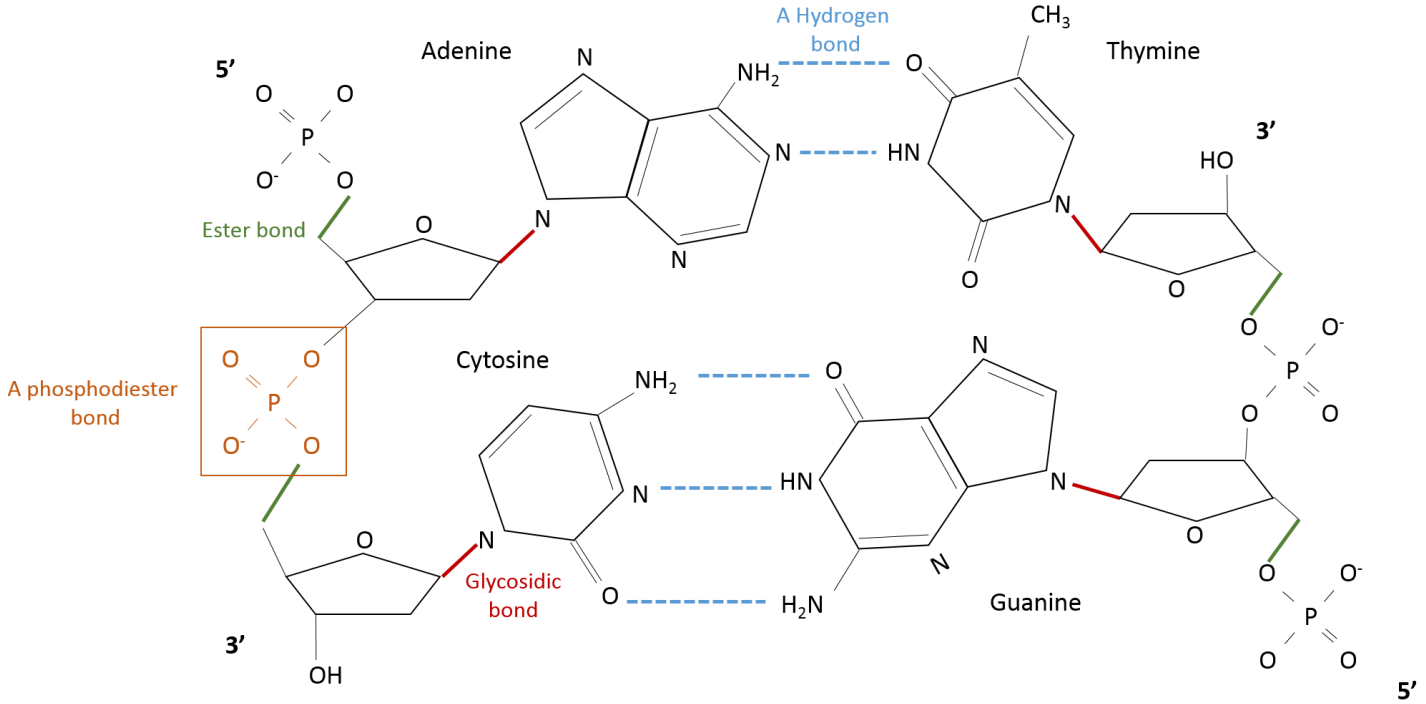

Figure 1.2. The double helix structure of DNA. Two polymers of DNA, represented here by two units each, are joined by the formation of hydrogen bonds between the bases. Glycosidic bonds join the nitrogenous bases to the 2'-deoxyribose sugar and the formation of phophodiester bonds between the sugars results in the joining of two single units of a DNA polymer.

1.1.2. DNA Damage and Repair Pathways

Damaging agents that lead to the generation of cytotoxic or mutagenic DNA adducts via both endogenous and exogenous sources threaten the genomic integrity of all living organisms. If DNA is damaged in this way, it is imperative that it be effectively and swiftly repaired for proper DNA replication and proper chromosome segregation to preserve chromosomal integrity. Replication of damaged DNA can lead to mutations that could become tumorigenic or cause lesions that result in cellular senescence or cell death via the block of replication or transcription. Per cell cycle it has been estimated that a eukaryotic cell can come under assault from up to 10,000 single-stranded DNA lesions caused by endogenous sources of damage that they are forced to repair, a number that is increased by lesions caused by exposure to environmental toxins, ultraviolet (UV) damage and other radiations.

To add to the complication of trying to overcome thousands of DNA lesions at any one time, these lesions occur within and must be detected and repaired in the context of chromatin, which is a dynamic and highly complex structure. To deal with the day to day onslaught of DNA lesions a complex DNA damage response has evolved within cells that encompasses several different DNA repair pathways, which include nucleotide excision repair (NER), base excision repair (BER), mismatch repair (MMR), non-homologous end-joining (NHEJ) and homologous recombination (HR), which will be further described in the text below.

1.1.2.1. Reversal Repair

In addition to the repair pathways named above, there are also mechanisms that have evolved to initiate repair by directly reversing the damage through direct removal, usually carried out by a single repair protein without needing to alter the physical structure of DNA. Only a small set of DNA lesions benefit from this direct DNA repair, including some UV induced damage and some forms of alkylated bases. The process is thought to be quite simple and essentially error-

free and can be divided in to three major mechanisms. The first mechanism by which UV light-induced photolesions are reversed by photolyases, the second where *O*-alkylated DNA damage is reversed by O^6-alkylguanine-DNA alkyltransferases (AGTs) and the third where the AlkB family dioxygenases reverse N-alkylated base adducts (Yi and He 2013). These mechanisms all work to catalyse the reversal of damage done to the DNA with a view to restoring the DNA to its original state.

1.1.2.2. Nucleotide Excision Repair

Bulky DNA lesions in mammalian cells, for example, those that are caused by UV induced cyclobutane pyrimidine dimers (CPDs) and 6-4 photoproducts, environmental mutagens and some cancer chemotherapeutic agents such as cisplatin, are mainly subjected to repair by the nucleotide excision repair (NER) pathway (Scharer 2013). NER can be divided in to two sub-pathways; global genome NER (GG-NER) or transcription-coupled NER (TC-NER) (Gillet and Scharer 2006, Hanawalt and Spivak 2008). GG-NER can occur at both transcriptionally active and inactive regions of DNA, opposed to TC-NER, which is responsible for repair at transcriptionally active regions of DNA only. The study of rare autosomal recessive disorders, such as Xeroderma pigmentosa (XP), which is associated with patients being extremely prone to developing skin-cancer, and Cockayne syndrome (CS), which is associated with microcephaly, helped to identify and characterise the GG-NER and TC-NER pathways (Diderich, Alanazi et al. 2011). Both pathways require the core NER factors (Figure 1.3) for the process of excision and thus repair. Specifically, GG-NER is initiated by XPC-RAD23B, whereas TC-NER is initiated by RNA polymerase stalled at a lesion, which uses the TC-NER specific factors CSA, CSB and XAB2 (Scharer 2013). A detailed overview of the model for the core NER reaction is described in Figure 1.3.

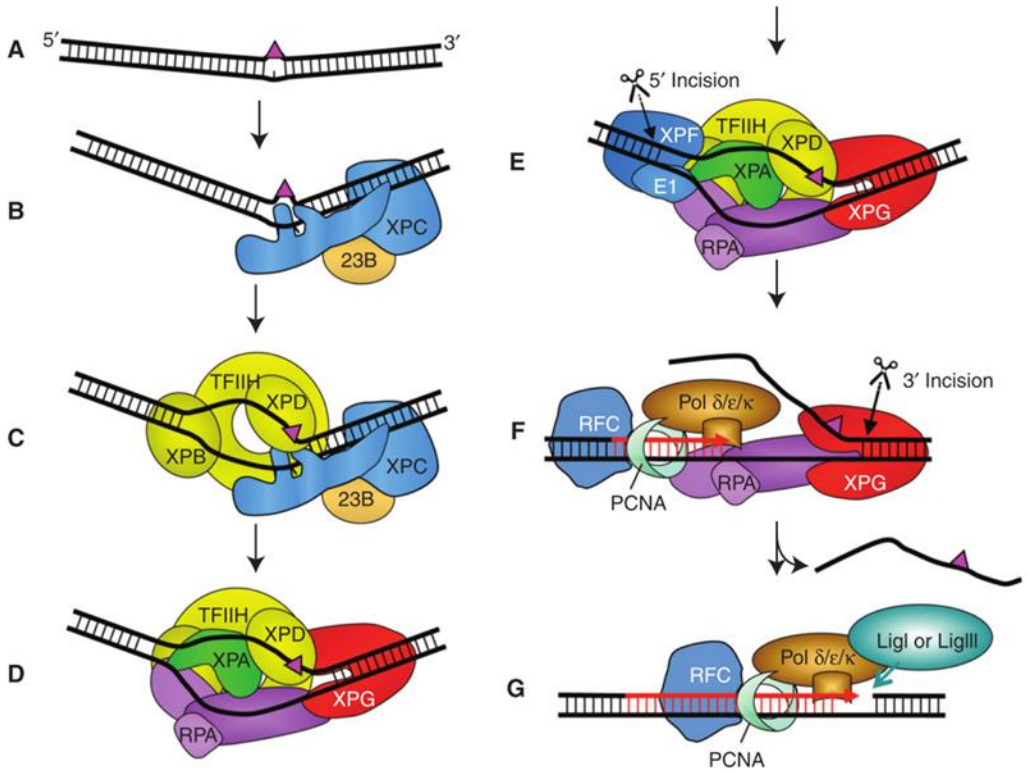

Figure 1.3. Model for the core NER reaction, taken from (Scharer 2013). (A) Bulky DNA lesions are introduced into DNA by a damaging agent. (B) In GG-NER lesions are detected by XPC-RAD23B and binds the undamaged strand of DNA opposite the lesion. (C) TFIIH interacts with XPC-RAD23B. The XPB subunit of TFIIH opens DNA allowing XPD to move along DNA until it identifies/verifies the lesion. (D) XPA, RPA and XPG are recruited to the complex when XPD has stopped at the specific lesion. (E) ERCC1-XPF is recruited by XPA and initiates an incision 5' to the lesion. (F) Pol δ, Pol κ, Pol ε and their associated factors initiate repair, subsequently allowing the 3' incision by XPG. (G) DNAligaseIIIα/XRCC1 or DNA ligase I then complete the repair process and seals the nicked DNA.

As with all DNA repair mechanisms, NER is carried out in the context of chromatin, which requires the coordination between NER factors and chromatin modifying enzymes to allow the chromatin to be accessible for repair. Multiple chromatin remodelers have been implicated with NER, with varied roles and level of contribution. The complex UV-DDB, which is composed of a damage binding protein DDB2 and an adaptor protein DDB1, and also forms a ubiquitin ligase complex with CUL4A and ROC1 (Groisman, Polanowska et al. 2003), is thought to have an influential role in NER. At the sites of UV induced lesions, DDB2 targets the XPC-RAD23 complex to facilitate early NER steps (Wakasugi, Kawashima et al. 2002, Fitch, Nakajima et al. 2003). After UV damage the UV-DDB/CUL4A/ROC1 complex localises at chromatin and destabilises the nucleosome structure through the ubiquitination of histones H2A, H3 and H4 (Bergink, Salomons et al. 2006, Kapetanaki, Guerrero-Santoro et al. 2006). XPC and DDB2 are also ubiquitinated by this complex, resulting in the degradation of DDB2 and the stabilisation of XPC to DNA (Sugasawa, Okuda et al. 2005, Nishi, Alekseev et al. 2009). The localisation of XPC to damaged sites in chromatin where NER takes place is thought to be facilitated by this ubiquitination (Fei, Kaczmarek et al. 2011).

DDB2 can also mediate chromatin modification by aiding PARP-mediated polyribosylation and recruitment of ALC1, an enzyme part of the SNF2/SWI2 family of chromatin remodelers (Pines, Vrouwe et al. 2012). Poly(ADP)ribosylation (which will be introduced fully in section 1.7) of DDB2 prevents it from exposure to ubiquitination and degradation and this is thought to provide enough time to aid chromatin decondensation (Pines, Vrouwe et al. 2012). Post-translational modifications, such as this, stabilise DDB2 and therefore control its activity as well as the time spent on chromatin damaged by UV irradiation.

Other chromatin remodelers have been implicated in NER, for example the SWI/SNF subunits BRG1 and SNF5 (which will be introduced in section 1.4), which are recruited to NER complexes in an XPC-dependent manner (Ray, Mir et al. 2009, Zhao, Wang et al. 2009). These subunits are presumed to work downstream of the initial recognition of DNA damage and are thought to complete the NER process by aiding the decompaction of chromatin (Scharer

2013). Following NER, the repaired DNA must be reassembled in to chromatin. The histone chaperone CAF-1 (chromatin assembly factor) allows this chromatin reassembly to occur (Scharer 2013).

1.1.2.3. Base Excision Repair

The base excision repair (BER) pathway repairs spontaneous DNA damage caused by oxidation, deamination and alkylation that must be repaired, but is not significant enough to impede the helical structure of DNA (Krokan and Bjoras 2013). A choice of several mammalian DNA glycosylases initiates BER, which then allows for the removal and replacement of a damaged base. Once removed an abasic site is processed by short-patch repair, which is the main type of BER, or by long-patch repair (Figure 1.4). Both of which use multiple different proteins to facilitate the resultant repair. The process of these types of repair and the choice between them have been extensively reviewed by Kim and Wilson, Krokan and Bjoras and others (Kim and Wilson 2012, Krokan and Bjoras 2013).

An understanding of the involvement of chromatin remodelling complexes in different DNA repair pathways is emerging. It has been suggested that chromatin remodelling is important for several DNA repair mechanisms, including BER. The SWI/SNF remodelling complex was found to facilitate the processing of induced 8-oxoG lesions by OGG1 and APE1 (Menoni, Gasparutto et al. 2007).

BER can occur in the nuclei as well as the mitochondria of a cell and is known to protect against cancer, aging and neurodegeneration (Krokan and Bjoras 2013). BER has been linked to the cellular response to chemotherapeutic agents and radiotherapy and it is thought that activation of BER enzymes can lead to resistance to DNA-damaging agents (Kim and Wilson 2012). Introduction of BER inhibitors to the clinic could work to overcome resistance to chemotherapeutic drugs, by re-sensitising the cancer cells to the effects of these drugs (Kim and Wilson 2012).

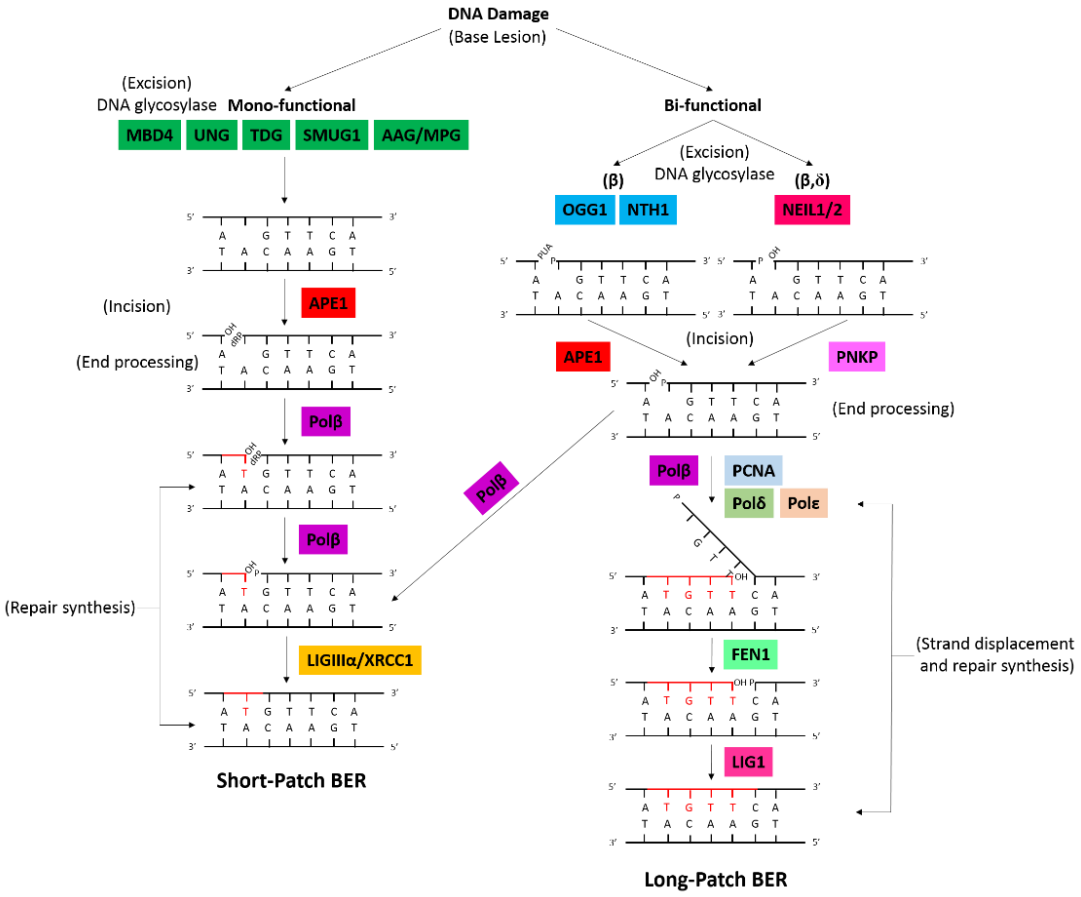

Figure 1.4. The base excision repair pathway. BER can occur via Short-Patch BER or Long-Patch BER.

1.1.2.4. Mismatch Repair

During DNA replication, errors can occur that lead to incorrectly incorporated bases, strand misalignments and small loops of extrahelical nucleotides that form as a result of slippage. These errors are dealt with by the mismatch repair (MMR) system, which removes them by excising the piece of nascent DNA with the mis-pair and facilitating its error-free re-synthesis (Jiricny 2013). Mismatches can only be recognised while two strands of DNA are annealed together, so repair must happen quickly. If two strands of DNA with a mismatch separate, the 'damaged' DNA will no longer be recognisable by MMR and the strands will continue through to replication, resulting in 50% of the progeny DNA containing a mutation (Jiricny 2013). The MMR system is thought to be integral for genomic integrity, errors here can lead to genomic instability and the development of cancer. Cancers that arise because of a malfunction in MMR include hereditary nonpolyposis colon cancer (HNPCC), also known as Lynch syndrome (reviewed in (Lynch, Lynch et al. 2009)). The defect in MMR is characterised by microsatellite instability (MSI), brought about by unrepaired insertion/deletion loops (IDL's) within repeated sequences of DNA (microsatellites) (Jiricny 2013). This phenotype of microsatellite instability has been useful as a diagnostic tool for characterising the status of MMR tumours (Hampel, Frankel et al. 2005).

In mammals, MMR is regulated by the MutS heterodimers, MutSα and MutSβ, as well as the MutL heterodimers, MutLα, MutLβ and MutLγ. Distortions or mismatches that occur during replication are recognised and bound to by the MutS heterodimer, subsequently initiating the recruitment of MutL heterodimers to the site of the mismatch (Drotschmann, Yang et al. 2001). MutL has intrinsic endonuclease activity, which is activated when bound to replication factors such as proliferating cell nuclear antigen (PCNA) and replication factor C (RFC) (Kadyrov, Dzantiev et al. 2006). This activation facilitates MutL to generate a nick in the DNA backbone, which is used by the exonuclease Exo1 to remove the damaged base. Repair is completed by the replicative polymerase, DNA polδ and the ligase, DNA ligase I (Iyama and Wilson 2013).

1.1.3. Double Strand Break Repair

DNA double-strand breaks (DSBs) can occur after exposure to multiple endogenous and exogenous agents. In eukaryotes the repair of these breaks is either undertaken by the homologous recombination (HR) or non-homologous end-joining (NHEJ) pathways (Liu and Huang 2016). It is important to repair DSBs as they are the most dangerous example of DNA damage. Cells that are unable to repair DNA DSBs can undergo apoptosis or fall in to senescence, alternatively, if a DSB is mis-repaired it can result in genomic instability, for example in the form of chromosome translocations and can ultimately lead to carcinogenesis (Davis and Chen 2013). Choosing between the HR and NHEJ pathways in response to DNA DSBs is well studied, but still not fully understood, here I will give a brief overview of these two complex and vital pathways.

1.1.3.1. Non-Homologous End Joining

Non-homologous end-joining (NHEJ) is a major DNA DSB repair pathway and is known to function in all cell cycle phases (Jeggo and Downs 2014). The term NHEJ can refer to canonical NHEJ (c-NHEJ), which is well studied and has clear roles in the response to DNA DSBs, or to alternative NHEJ (alt-NHEJ), which is thought to be a less efficient mechanism of repair. Regardless, both pathways work to re-join two DNA DSB ends without using extended homology as a guide, by detection, processing and ligation (Chiruvella, Liang et al. 2013). As well as repairing DNA DSBs, NHEJ is also essential for V(D)J (V (variable) D (diversity) J (joining)) recombination, a site specific recombination process that occurs during T- and B-cell lymphocyte development (Malu, Malshetty et al. 2012, Davis and Chen 2013). On recognition of a DNA DSB, the abundant Ku heterodimer initiates NHEJ by binding at the break site (Cary, Peterson et al. 1997, Walker, Corpina et al. 2001). DNA-PKcs, the catalytic subunit of the DNA-dependent protein kinase complex, is recruited to the break by Ku and facilitates end-processing steps as well as allowing for a complex cellular response, for example cell cycle checkpoint

activation that helps to prevent replication errors (Gottlieb and Jackson 1993, Yaneva, Kowalewski et al. 1997). The Mre11-Rad50-Nbs1 (MRN) complex, which is known for its role in HR-mediated DSB repair and damage signalling (Tauchi, Kobayashi et al. 2002) is additionally recruited to work with Ku and DNA-PKcs to stimulate end resection and enhances DNA-PKcs autophosphorylation (Zhou and Paull 2013). When ends require processing (~10-15% of DSBs in G2), the end processing factor Artemis is bound to DNA-PKcs and generates reconcilable DNA ends, via its exonuclease and endonuclease activity, that can be ligated by the XRCC4-DNALigaseIV-XLF ligation complex (Figure 1.5) (Grawunder, Wilm et al. 1997, Ma, Pannicke et al. 2002, Goodarzi, Yu et al. 2006). Although there are three components to the ligation complex, only XRCC4 directly interacts with DNA ligase IV (Critchlow, Bowater et al. 1997). DNA ligase IV is the enzyme required for ligation of the repaired ends and its activity is dependent on XRCC4 for stabilisation (Jeggo and Downs 2014). XRCC4 interacts with XLF for the alignment of DNA ends (Ahnesorg, Smith et al. 2006, Tsai, Kim et al. 2007, Andres, Vergnes et al. 2012) and more recently it has been suggested that the two could form heterofilament bundles that surround DNA in a sheath (Ropars, Drevet et al. 2011, Wu, Ochi et al. 2011, Andres, Vergnes et al. 2012, Mahaney, Hammel et al. 2013, Brouwer, Sitters et al. 2016). It has been postulated that the potential flexibility of these XRCC4/XLF heterofilaments could either wrap around chromatin-bound DNA or that it provides stabilisation to the DNA strands after nucleosome disassembly (Jeggo and Downs 2014). Cells deficient in NHEJ proteins, such as those described above, are found to present with various phenotypes, including radio-sensitivity (Goodarzi and Jeggo 2013).

If a DNA DSB is not repaired by NHEJ in G2, then DNA resection promotes repair by homologous recombination (HR) (Goodarzi and Jeggo 2013).

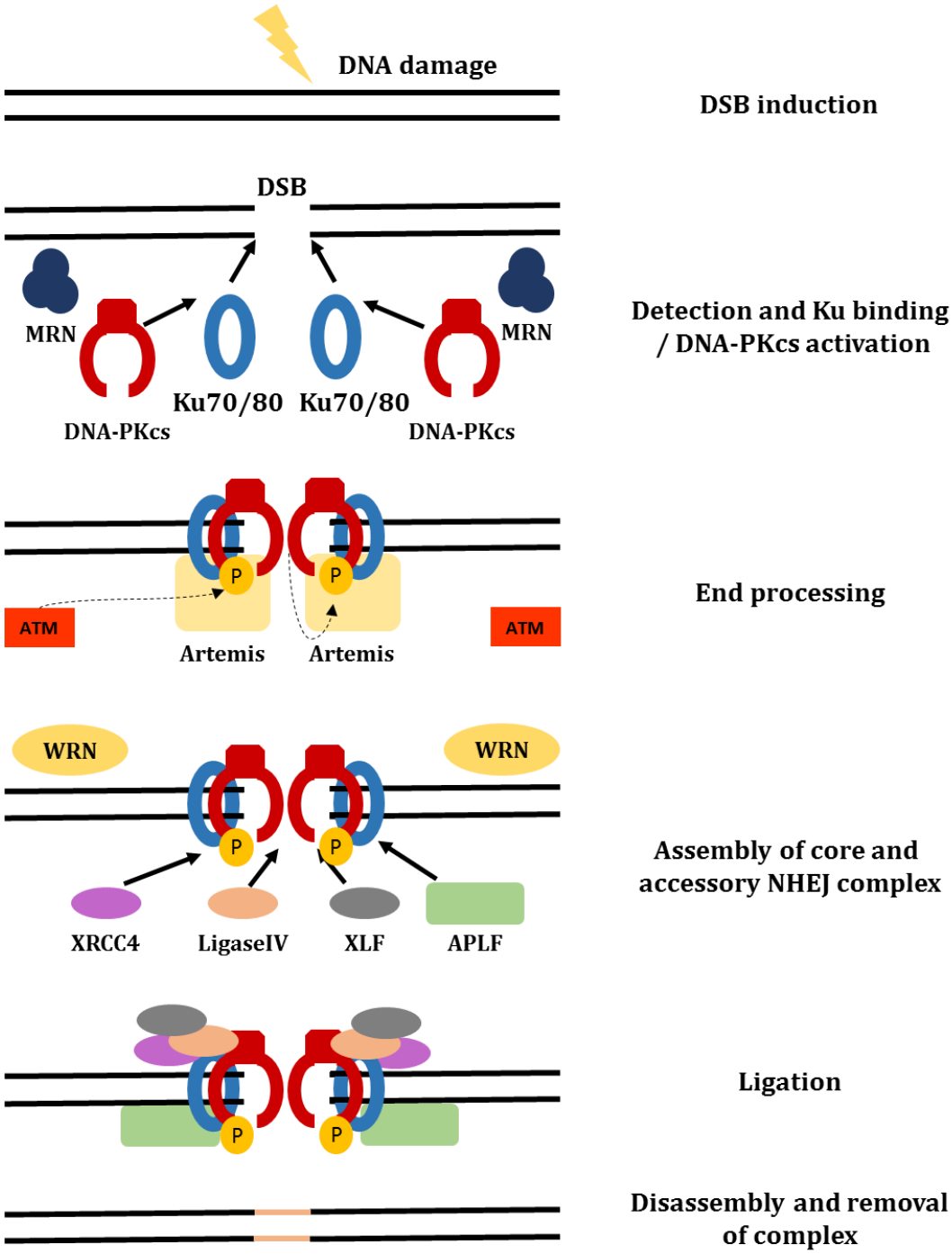

Figure 1.5. The non-homologous end-joining pathway. The Ku70/Ku80 heterodimer binds DNA double strand breaks. DNA-PKcs initiate the recruitment of end processing factors, such as Artemis that allow the XRCC4-LigaseIV-XLF ligation complex to complete the DNA repair Adapted from (Davis and Chen 2013).

1.1.3.2. Homologous Recombination

The repair of DNA double strand breaks can also be carried out by homologous recombination (HR). This process uses the intact sister chromatid as a template for repair and is thought to be relatively error-free because it is able to use this DNA as a template. HR takes place during the S and G2 stages of the cell cycle, this is due to the requirement of the sister chromatid. HR is initiated by the resection of DNA, which is followed by invasion of the homologous sequence and subsequent resolution of these intermediate structures. Crossover between the homologous DNA sequences is determined by how these intermediate structures are resolved, resulting in crossover or non-crossover products (Figure 1.6).

The MRN complex plays a key role in the early response to DSBs by recognising the break and recruiting ataxia telangiectasia mutated (ATM), a protein kinase, to the site of damage and activating its catalytic activity via its direct interaction with ATM and Nbs1 (Lee and Paull 2004, Lee and Paull 2005, Hartlerode and Scully 2009). In the DNA damage response there are many substrates that are phosphorylated by ATM, for example the H2A histone variant, H2AX. Therefore, phosphorylation of H2AX is frequently used as an early indication of DSB formation on chromatin (Matsuoka, Ballif et al. 2007, Hartlerode and Scully 2009, Savic, Yin et al. 2009). CtIP, BRCA1 and BARD1 work together with the MRN complex to facilitate resection and subsequent processing of the 5'-ends of the DSB, thus leaving a 3'-overhang for invasion of the sister chromatid template (Sartori, Lukas et al. 2007, Yun and Hiom 2009). The exposed overhang of ssDNA is bound by the large subunit of RPA and is subsequently displaced by Rad51, which is recruited by factors including BRCA2. The formation and stabilisation of Rad51 filaments stimulates the invasion and displacement of the homologous strand. This displacement results in Rad54 promoting D-loop formation, which can be extended by DNA pol δ or ε via the 3' strand (Holmes and Haber 1999, Krejci, Altmannova et al. 2012).

Double Holliday junction formation occurs when the 3'-overhang is 'captured' on the other side of the break, these junctions must be resolved by endonucleases. It

is the resolution of these Holliday junctions that results in either crossover or non-crossover products.

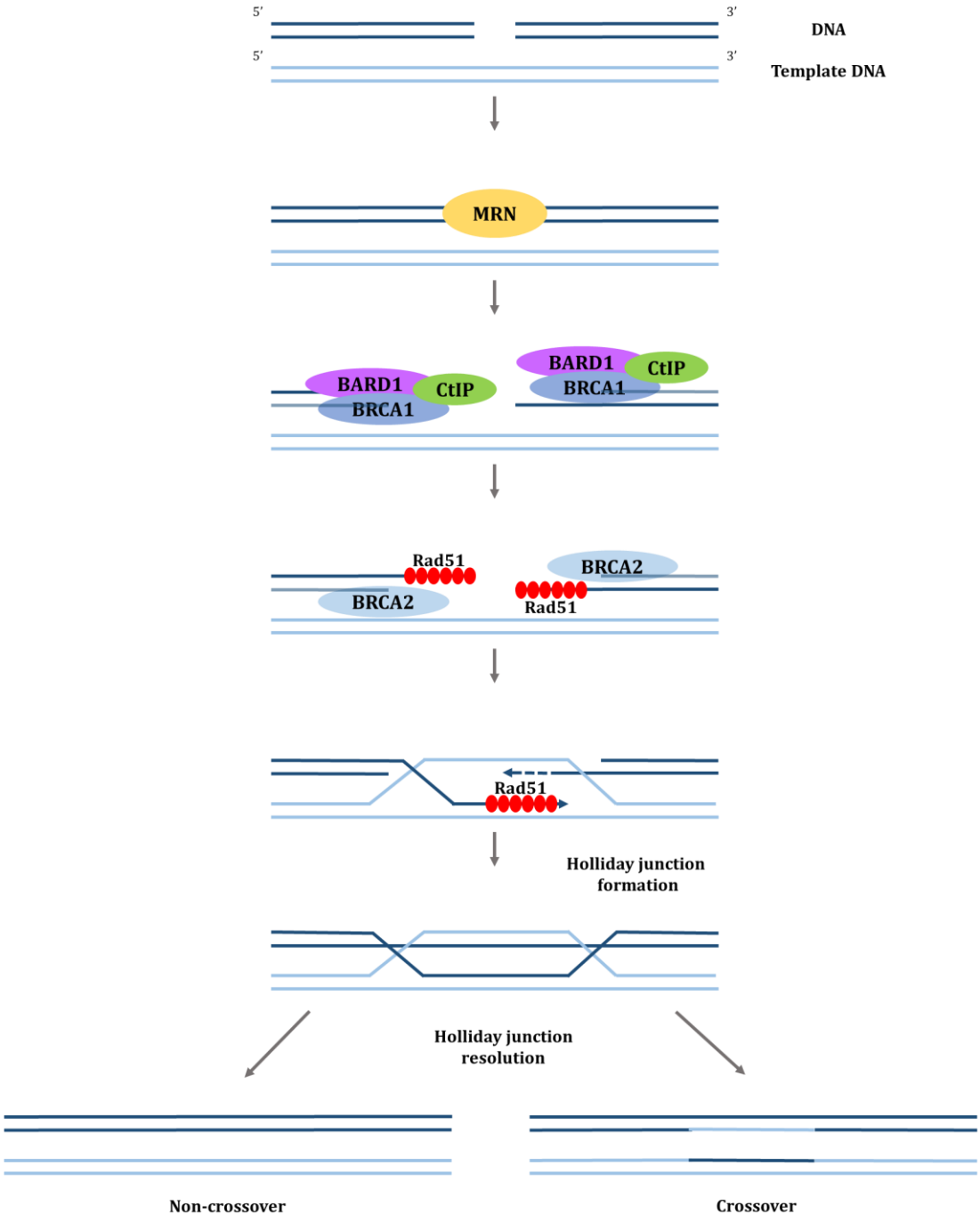

Figure 1.6. The homologous recombination pathway. DNA double strand breaks are repaired by HR proteins and result in either Non-crossover or Crossover products.

1.2. Chromatin Structure and Remodelling

In eukaryotes, genomic DNA is tightly packed together in a protein-DNA complex structure known as chromatin. The nucleosome is the basic unit of chromatin, where 147bp of DNA is tightly wrapped in left-handed ~1.7 superhelical turns around an octomer of histone proteins, comprised of a heterodimer (two copies) of histone proteins H2A and H2B, and a tetramer of histones H3 and H4 (Luger, Mader et al. 1997, Richmond and Davey 2003). One molecule of the linker histone H1 associates with the external interface of the nucleosome, sealing the ~1.7 turns of DNA, where the DNA enters and exits the nucleosome (Kamakaka and Biggins 2005).

The condensation and organisation of the genome is regulated by the packaging of DNA by nucleosomes. Chromatin actively participates in numerous DNA transactions including transcription, chromosome segregation, replication, recombination, DNA repair and the maintenance of genome integrity. This section will introduce chromatin structure, histone variants and the post-translational modification of histones as well as chromatin remodelling families and how mutations found in these families is strikingly linked to cancer formation.

1.2.1. Chromatin Structure

As mentioned, the nucleosome is formed from the four core histones H2A, H2B, H3 and H4, created in a 'hand-shake motif' due to the interaction of electrostatic, hydrophobic and hydrogen bonds between the histone pairs (Kamakaka and Biggins 2005). The core histones share a conserved C-terminal histone fold domain and N-terminal tails that are directly involved in the interaction with other proteins and nucleosomes (Kamakaka and Biggins 2005). The extremely recognisable 'beads on a string' structure represents chromatin in its most basic form, a linear arrangement of nucleosomes that can be bound to a number of structural and/or functional proteins, for example, linker histones, transcription factors etc. (Figure 1.7) (Woodcock and Dimitrov 2001).

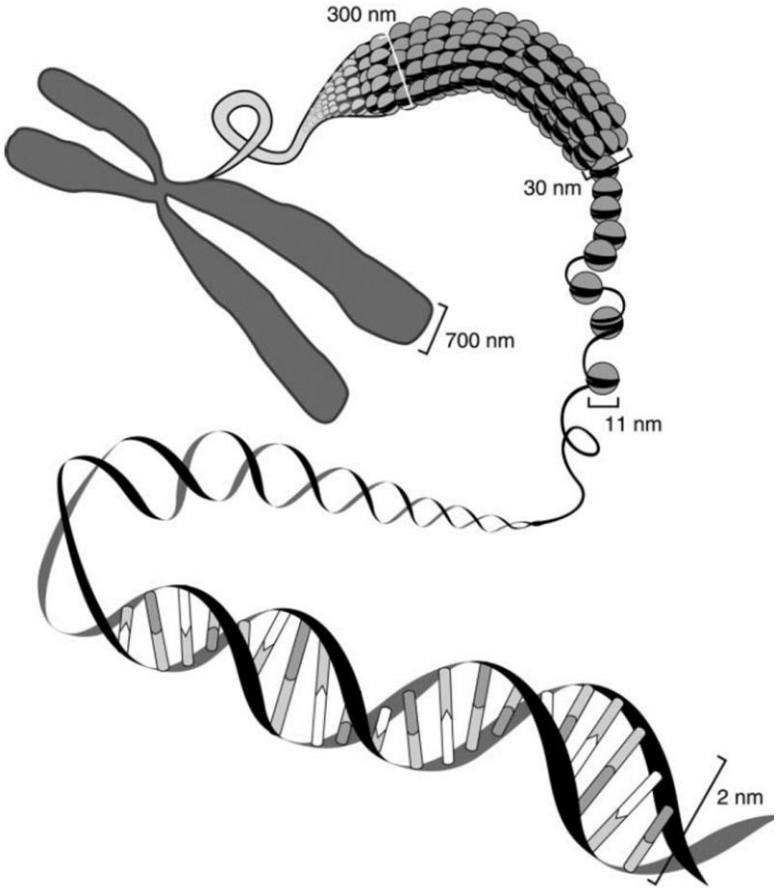

Figure 1.7. The packaging of DNA in to chromatin. Image taken from (Weier 2001). DNA molecules are tightly wound around histone proteins that compact themselves in to 30 nm chromatin fibres. Additional packaging forms chromosomes that have a diameter of 300 nm and a thickness of 700 nm.

The folding of nucleosomes into its secondary three-dimensional structure, known as a 30 nm fibre, is driven by interactions between nucleosomes. The 30 nm fibre associates with linker histones, for example H1 or H5 to stabilise this secondary structure. Self-association of these 30 nm fibers into 100 to 400 nm filaments forms the tertiary structure organisation (Belmont and Bruce 1994, Gordon, Luger et al. 2005). Additional levels of packaging allow for the eventual formation of chromatids by chromosomes.

A three-helix bundle of histones is denoted a histone fold motif (or domain) and it is these that mediate a histone's interaction with other histones (histone-histone interaction) as well as with DNA (histone-DNA interaction) (Peterson and Almouzni 2013). The modulation of chromatin for the facilitation of multiple cellular processes is carried out in various ways. For example, histones are subject to various post-translational modifications, for example phosphorylation, methylation, acetylation and ubiquitylation, modifications which can alter histone properties (Iizuka and Smith 2003, Kamakaka and Biggins 2005). The use of chromatin remodelling complexes and their catalytic ATP core subunit, which will be further introduced in section 1.2.4, also facilitates the movement of chromatin by nucleosome sliding, ejection and the repositioning of histones etc. The incorporation of histone variants is also important in the modulation of chromatin.

1.2.2. Histone Variants

Canonical replicative histones H2A, H2B, H3 and H4 are mostly restricted to being produced during S phase of the cell cycle (Peterson and Almouzni 2013). These canonical histones make up the dominant proportion of cellular histones, however nonallelic variants of these core histones also exist, exhibiting very different biophysical characteristics (Kamakaka and Biggins 2005). These non-canonical histone variants are not restricted to expression during S phase, and are therefore expressed throughout the cell cycle (Peterson and Almouzni 2013). Histone variants are thought to have specialised functions in the regulation of

chromatin dynamics, this could be due to a multitude of factors, for example, in contrast to canonical histones, variants contain introns and are often polyadenylated, suggesting an importance for the post-translational regulation of these proteins (Old and Woodland 1984, Kamakaka and Biggins 2005). The exchange of histones for histone variants, which then become preferentially expressed, also suggests a specialised function with regards to the dynamics of chromatin (Wunsch, Reinhardt et al. 1991). Below I will briefly introduce a subset of the different histone variants.

1.2.2.1. Histone H1

Eleven sequence variants such as $H1^0$, H5 and the spermand testis-specific variant all belong to the histone H1 variants, with the N and C-terminal tail domains being the sites of sequence variation from canonical H1 (Kamakaka and Biggins 2005, Millan-Arino, Islam et al. 2014). The histone H1 family is the most diverse in comparison to the core histones H2A, H2B, H3 and H4, having the most variants or subtypes (Happel and Doenecke 2009, Millan-Arino, Islam et al. 2014).

1.2.2.2. The histone variants of H2A and H2B

Of the core histones H2A, H2B, H3 and H4, it is known that H2A has the most diverse range of histone variants, including the very important H2A.Z and H2A.X (Redon, Pilch et al. 2002). The H2A variants are distinguishable from canonical H2A by their C-terminal tails that vary in length and sequence and have a divergent genome distribution. Broadly, H2A.Z has been linked to both transcriptional repression and activation and is ~60% identical to canonical H2A (Jackson and Gorovsky 2000). H2AX has important roles in DNA double strand break induction. At DNA DSBs H2AX becomes rapidly phosphorylated at serine 139, gaining the nomenclature γ-H2AX and serving as a sensitive indicator of DSBs (for reviews of both H2A.Z and H2AX see (Redon, Pilch et al. 2002, Zlatanova and Thakar 2008, Bonisch and Hake 2012, Tsabar and Haber 2013)). H2B has

very few variants, however the ones that have been documented have specialised functions in chromatin compaction and transcription repression, particularly during gametogenesis (For review see (Poccia and Green 1992, Green, Collas et al. 1995)).

1.2.2.3. The centromeric histone H3 variant, CENP-A

There are two major histone H3 variants, H3.3 and centromeric H3, known as CENP-A in mammalian cells. CENP-A is a conserved essential protein that binds to centromeres, is expressed throughout the cell cycle and often localizes to transcriptionally active regions of the chromosome (Ahmad and Henikoff 2002, Kamakaka and Biggins 2005). CENP-A shares similarity in histone-fold domain with canonical H3, but has highly divergent N-terminal tails (Kamakaka and Biggins 2005).

1.2.2.4. Histone H4

Histone H4, to date, has no known variants, with some suggesting that it is a slowly evolving protein (Malik and Henikoff 2003, Kamakaka and Biggins 2005). It is not clear why this core histone isn't represented by multiple variants or subtypes.

1.2.3. Post-translational Modification of Histones

For the regulation of chromatin structure and function, histones are subject to a diverse set of post-translational modifications (PMTs). These PMTs include lysine acetylation, methylation, SUMOylation and ubiquitination, serine/threonine phosphorylation, proline isomerization, argenine methylation and ribosylation (Peterson and Almouzni 2013). PMTs can occur in the nucleosomal core, but the

majority of events affect the N- and C-terminal tail regions(Peterson and Almouzni 2013). Two broad mechanisms can explain how chromatin dynamics are regulated by post-translational modification. Firstly the creation or elimination of binding sites for non-histone proteins by PMTs can affect the structure and function of chromatin. Secondly, the stability of nucleosomes individually as well as the ability of chromatin fibres to fold into higher order structures is directly influenced by histone PMTs (Peterson and Almouzni 2013). The formation of a DNA double strand break can rapidly induce post-translational modifications and the modification of histones in this way is thought to have a key role in the DNA damage response (DDR) (Figure 1.8) (Peterson and Almouzni 2013). An example of this role in the DDR can be seen in the phosphorylation of the histone variant H2A.X at S139 by ATM, ATR and DNA-PK. This phosphorylation of H2A.X (termed γH2AX) is an early event in the response to DNA DSBs and affects around a megabase of chromatin either side of the break, promoting the binding of DNA damage checkpoint mediators like MDC1, thus pausing the cell cycle and therefore mediating the repair of the damaged DNA (Rogakou, Boon et al. 1999, Stucki, Clapperton et al. 2005, Peterson and Almouzni 2013). Below I will briefly introduce the most well-known PMTs: acetylation, methylation and phosphorylation.

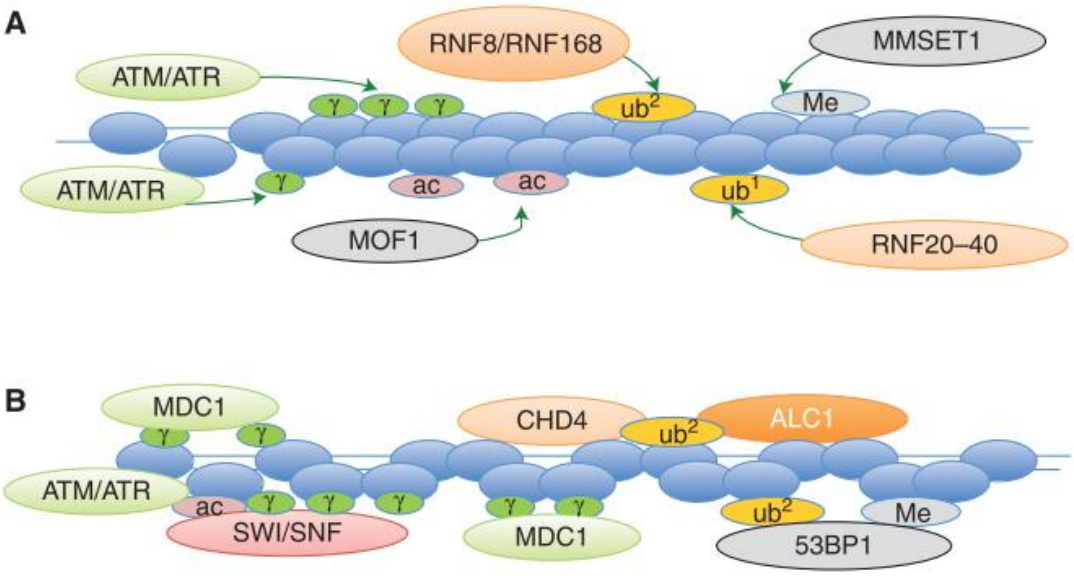

Figure 1.8. The effect of histone modifications in chromatin on the DDR response. (A) Histone modifications that occur on chromatin with a DSB and the proteins that are associated. (B) The binding partners or regulators of histone modifications. Taken from (Peterson and Almouzni 2013).

1.2.3.1. Acetylation

Lysine residues are able to undergo many post-translational modifications. The acetylation of lysine residues, meaning the transfer of an acetyl functional group from one molecule to another, at the ε-amino group neutralises the charge of the lysine and results in a change of the histone's electrostatic properties. This change results in a weakened interaction with the negatively charged DNA, forming a more relaxed chromatin structure that is typically associated with a transcriptionally active state (Musselman, Lalonde et al. 2012). Lysine residue acetylation can occur on H3 (K4, K9, K14, K18, K23, K27, K36 and K56), H4 (K5, K8, K12, K16, K20 and K91), H2A (K5 and K9) and H2B (K5, K12, K15, K16, K20 and K120) (Musselman, Lalonde et al. 2012). Histone acetylation or deacetylation can be carried out by enzymes known as Histone/Lysine Acetyltransferases (HATs/KATs) or Histone/Lysine Deacetylases (HDACs/KDACs), for example the transcriptional activator lysine acetyltransferase 2A (KAT2A aka. GCN5), which I will introduce further in Chapter 3. The relaxed chromatin structure created by lysine acetylation can be reversed by a de-acetylation event. Relaxed DNA that is transcriptionally active can be referred to as euchromatin and the corresponding condensed version of chromatin is referred to as heterochromatin (Grunstein 1997).

Acetylated lysines are recognised by three types of histone effectors; the bromodomain, PHD fingers and PH domains. Bromodomains are well characterised as acetyl-lysine readers(Dhalluin, Carlson et al. 1999, Sanchez and Zhou 2009). A well conserved four-helix bundle structure, comprised of αA, αB, αC, and αZ helices, folds together to form the typical bromodomain's structure. A deep hydrophobic cavity is created by inter-helical ZA and BC loops and it is within this cavity where the acetyllysine residue is inserted and have contact with several hydrophobic residues, for example two conserved tyrosines or the hydrogen bonding of a conserved asparagine which leads to stabilization (Musselman, Lalonde et al. 2012). Typically single bromodomains bind to acetylated lysines very weakly, however, binding can be substantially enhanced by a single bromodomains interaction with multiple acetylated sequences or the

recognition of the acetylated lysine by covalently linked tandem bromodomains (Musselman, Lalonde et al. 2012).

PHD domains, such as the double PHD finger (DPF) of DPF3b, a key epigenetic factor for the development of heart and muscle that is associated with the SWI/SNF chromatin remodelling complex BAF, have also been found to recognise acetylated lysines at histones H3 and H4 (Lange, Kaynak et al. 2008, Zeng, Zhang et al. 2010). PH (pleckstrin homology) domains, such as the double PH domain of Rtt106, a histone chaperone has specifically be linked to the binding of H3K56-acetylated histone H3-H4, implicating it in the regulation of nucleosome assembly during DNA replication and repair and disassembly during gene transcription (Su, Hu et al. 2012).

Histone deacetylase 1 and 4 (HDAC1 and HDAC4) are responsible for the deacetylation of N-terminal lysine residues of the core histones (H2A, H2B, H3 and H4). Epigenetic repression is marked by the deacetylation of histones, which play a key role in the progression of the cell cycle and developmental events as well as transcriptional regulation. HDACs can interact with a diverse range of non-histone proteins, thus making the terminology lysine de-acetyltransferases or KDACs more encompassing of the roles they actually carry out *in vivo*, although typically they are mostly referred to by their original nomenclature (Kadiyala and Smith 2014). There are currently eighteen mammalian HDACs that can be subdivided in to different families, decided by their homology with yeast HDACs (Bhaskara 2015). HDAC1 belongs to Class I HDACs, which is homologous to Rpd3 in yeast, this class also contains HDACs 2, 3, and 8. HDAC4 belongs to Class IIa HDACs, which also contains HDAC 7 and 9 and is homologous to Hda1 in yeast (Ropero and Esteller 2007).

HDAC1 is specifically recruited to sites of DNA damage during DNA repair as well as to chromatin around replication forks (Bhaskara 2015). HDAC1 is also involved with transcriptional repression that is regulated by the retinoblastoma protein Rb (Robertson, Ait-Si-Ali et al. 2000), as well as interacting with the nuclear receptor Estrogen receptor-α (ER-α), via its DNA-binding domain and activation function-2 (AF-2) domain (Kawai, Li et al. 2003).
As well as having the broad HDAC activity, HDAC4 is also involved in muscle

maturation though its physical and functional interaction with the transcription factor MEF2C. MEF2C can recruit HDAC4 via its N-terminal domain to aid transcriptional repression (Wang, Bertos et al. 1999). HDAC4 is also known to associate and co-localize with a protein that causes Huntington's disease, the aggregation-prone mutant huntingtin protein (mHTT) through its interaction with MAP1S (Yue, Li et al. 2015).

HDACs make an attractive group of synthetic lethal candidates as there are currently several small molecule histone deacetylase inhibitors (HDIs) that inhibit various HDACs already in clinical studies. These HDIs are potent anti-proliferative agents that are thought to selectively kill cancer cells (Bhaskara 2015).

1.2.3.2. Methylation

Methylation can occur on two residues, lysine and arginine, and each has three possible methylation states (Musselman, Lalonde et al. 2012). Unlike other modifications, methylation does not affect overall charge, however it does alter the hydrophobic character and size of the modified residue (Musselman, Lalonde et al. 2012). Lysine can be mono-, di- and trimethylated on its ε-amino group. For histone H3 methylation sites typically occur at K4, K9, K26, K27, K36 and K79, for histone H4 at K20 and for histone H1 at K26. Excluding H3K79, these are all located in the N-terminal tails of the histone proteins. Readers of lysine methylation include ADD (ATRX-DNMT3-DNMT3L), ankyrin, bromo-adjacent homology (BAH), chromo-barrel, chromodomain, double chromodomain (DCD), MBT (malignant brain tumour), PHD (plant homeodomain), PWWP (Pro-Trp-Trp-Pro), Tandem Tudor domain (TTD), Tudor, WD40 and the zinc finger CW (zf-CW) (Musselman, Lalonde et al. 2012).

In the context of cellular functions, methylation of lysine residues is the best characterised, with a defining role in transcriptional regulation. Methylation of H3K4 (H3K4me) is thought to be a gene-activation mark on global chromatin, with H3K4me1 distinguishing active enhancer elements, H3K4me2 being

associated with active or potentially active 'permissive' chromatin states and H3K4me3 occurring within active transcription (Bernstein, Humphrey et al. 2002, Schneider, Bannister et al. 2004, Jeong, Kim et al. 2011, Musselman, Lalonde et al. 2012).

H3K36me is also thought to have a role in transcription. A progressive shift from monomethylation to trimethylation of K36 between the 5' and 3' ends of genes was found by genome wide profiling (Bannister and Kouzarides 2005). H3K36me also has an additional roles in DNA damage response, DNA replication and mRNA alternative splicing (Musselman, Lalonde et al. 2012). H3K20me2 is a methylation mark that also has a role in the DNA damage response, being targeted by the TTD (Tandem Tudor Domain) of 53BP1 (Botuyan, Lee et al. 2006).

H3K9 and H3K27 are typically associated with the formation of constitutive and facultative heterochromatin and gene silencing. At pericentromeric heterochromatin regions the methylation marks H3K27me1 and H3K9me3 are found, conversely H3K27me3 and H3K9me2 are found in repressed euchromatin regions (Peters, Kubicek et al. 2003, Rice, Briggs et al. 2003).

Arginine can be monomethylated or dimethylated symmetrically or asymmetrically. It has been reported that arginine methylation can occur at H3R2, H3R8, H3R17, H3R26, H4R3, H2AR11 and H2AR29 (Musselman, Lalonde et al. 2012). Functionally, very little is known about the significance of methylarginine readout in histone proteins, but it is thought that the recognition of these methylated residues can influence transcription processes (Musselman, Lalonde et al. 2012).

1.2.3.3. Phosphorylation

Phosphorylation occurs at serine or threonine residues. Bulky, negatively charged groups are added to the modified residues, altering the electrostatic and topographic properties of histones. Histones are phosphorylated on histone H3 at T3, T6, S10, T11, S28 and T45, on histone H4 at S1, on histone H2A at S1 and T120, on H2AX at S139 and on histone H2B at S14. Phosphorylation at these

residues is important in the DNA damage response pathways, mitosis and transcriptional regulation (Musselman, Lalonde et al. 2012).

1.2.4. Chromatin Remodelling Families

As described, DNA is packaged in to chromatin and access to this tightly bound structure is integral to allow the participation of chromatin in roles such as the regulation of transcription and DNA repair to name a few. Specialised chromatin remodelling complexes have evolved to facilitate this access by dynamically mediating nucleosome composition in chromosomal regions (Clapier and Cairns 2009). The energy from ATP hydrolysis is utilised by chromatin remodelling complexes to aid the sliding, ejection and repositioning of nucleosomes as well as mediating the exchange of histone variants. Other chromatin related factors work with these ATPase remodelers to guide the packaging and un-packaging of DNA, with a view to controlling not only the tightly bound structure of chromatin, but the regulation of essential processes, including DNA repair (Clapier and Cairns 2009).

Four different chromatin remodelling families are currently known, including the ISWI family, the CHD family, the INO80 family and the SWI/SNF family of remodelers. All families give rise to multi-subunit complexes that share a similar core catalytic ATPase domain, surrounded by uniquely associated subunits (Clapier and Cairns 2009). Strong affinity for nucleosomes, the recognition of histone modifications, similar ATPase domains, proteins that regulate these ATPase domains and subunits that interact with other chromatin or transcription factors are the five essential properties shared by all four families of remodelers (Clapier and Cairns 2009). Though the families of remodelers share properties, they also serve different purposes and act in very different biological contexts. The subject of this thesis is the SWI/SNF family of remodelers, specifically the PBAF complex, and so a thorough introduction of this family is described in section 1.4.

1.2.5. Chromatin Remodelling Complexes and Cancer

Dysregulation of processes mediated by chromatin remodelling complexes including transcriptional regulation and DNA-damage repair have been implicated in cancer development. Genome-wide sequencing of human cancers in recent years have identified multiple genes involved in cancer progression. In those identified, somatic mutations affected multiple epigenetic processes such as DNA methylation or hydroxylation, as well as mutations being found in histone-modifying enzymes like EZH2 or SUZ12 (Masliah-Planchon, Bieche et al. 2015). ATP chromatin remodelling complexes, like epigenetic changes, are implicated in cancer formation. Most notably, mutations in subunits of the SWI/SNF family of remodelers have been found in a striking 19% of all human tumours, rivalling the frequency of TP53 mutations, which is found in 26% of all human cancers (Shain and Pollack 2013). I will discuss specific SWI/SNF subunits and their involvement in cancer in section 1.4.

Other chromatin remodelling families have been implicated as having roles in cancer, for example the NuRD complex , which belongs to the CHD family of remodelers. The NuRD complex components, MTA1-3, have been associated with metastasis when overexpressed in cells and is thought to be linked with the invasive behaviour in several cancers (Denslow and Wade 2007). To give one example, in breast cancer, estrogen receptors (ERs) are regulators of proliferation and differentiation, and expression of these receptors can be used as a prognostic tool as well as a therapeutic target. MTA3 expression has been found to correlate with ER expression, and it has been suggested that this MTA3 subunit is responsible for the regulation of invasive growth pathways and that mutations within this gene can lead to breast cancer development via direct inhibition of the transcriptional repressor Snail (Fujita, Jaye et al. 2003).

1.3. The Genetics of Renal Cell Carcinoma

Renal cell carcinomas (RCC) are a complex set of diseases that have a major socioeconomic impact and are seen to be rising in incidence throughout the world (Jonasch, Futreal et al. 2012). 338,000 new cases were diagnosed worldwide in 2012 and there is thought to be a five-year survival rate of just ~12% when advanced in stage. Affecting both men and women alike, it is biologically distinct from kidney cancer, in that it doesn't involve the renal pelvis or renal medulla and isn't a single entity, but instead is a class of tumours of renal epithelial origin, for example the renal tubules. RCC mostly tends to arise sporadically, but can also be heritable, accounting for 1-4% of cases, with genetic mutations being the cause of some RCC cancer-prone families (Pavlovich and Schmidt 2004). Four major autosomal dominantly inherited RCC syndromes have been identified as; von Hippel-Lindau syndrome (VHL), which is also mutated in sporadic RCC, Hereditary leiomyomatosis and renal cell cancer (HLRCC), Hereditary papillary renal cancer (HPRC) and Birt-Hogg-Dube syndrome (BHD). We know that *VHL* is the gene mutated in von Hippel-Lindau disease (Latif, Tory et al. 1993), *MET* mutations are drivers in familial papillary renal cancer (Schmidt, Duh et al. 1997), fumarate hydratase (*FH*) mutations are found in hereditary leiomyomatosis and renal cell cancer (Tomlinson, Alam et al. 2002), as well as folliculin (FLCN) mutations in Birt-Hogg-Dubé syndrome (Nickerson, Warren et al. 2002). Clear cell renal cell carcinoma (ccRCC) accounts for about 80% of sporadic RCC (Shenoy and Pagliaro 2016). This major subtype of kidney cancer is characterised by 80-90% of these tumours having a frequent inactivation of the von Hippel-Lindau (VHL) gene (Liao 2015) and the aberrant signalling of the hypoxia inducible factor (HIF) that subsequently ensues (Jonasch, Futreal et al. 2012). It is interesting to note that VHL can be considered as both a germline cancer susceptibility gene as well as one that can be somatically mutated. Most of these VHL mutations cause loss of the wild type (WT) allele via large-scale loss of heterozygosity of chromosome 3p, resulting in a loss of protein (Jonasch, Futreal et al. 2012). It is known that ccRCC tumours exhibit extremely diverse mutational heterogeneity and as well as VHL, there are known to be three other genes that are frequently mutated in ccRCC; PBRM1 (mutated in ~50%), BAP1 (~15%) and

SETD2 (~15%). These genes all cluster with VHL in a 43Mb region on chromosome 3p, a region that is deleted in over 90% of tumours due to the loss of one or more of these tumour suppressor genes (Pena-Llopis, Christie et al. 2013). Loss of these genes are oncogenic drivers, which are distinct from passenger mutations in that they occur at mutation frequencies that are higher than expected by chance alone (Pena-Llopis, Christie et al. 2013).

The genes frequently mutated in RCC are biologically very diverse and therefore multiple mechanisms and biological pathways can be implicated in the tumorigenesis of RCC (Pavlovich and Schmidt 2004). Currently it is not well understood how driver mutations in cancer genes can work together in the progression of tumorigenesis and RCC is a good example of the complex relationships that can arise between cancer genes (Pena-Llopis, Christie et al. 2013). The most commonly mutated genes in ccRCC have strong links to chromatin (Figure 1.9) and ccRCC tumours are known to lack the hallmark genetic features of solid tumours, such as KRAS and TP53 mutations and are unresponsive to angiogenesis inhibitors, traditional chemotherapies, as well as highly resistant to radiation (Jonasch, Futreal et al. 2012). Thus, the study of the identified key tumour suppressors is vital, not only for the understanding of the mechanism behind ccRCC tumorigenesis, but also to exploit these known mutations to develop novel therapeutic treatments for a cancer that has a clear unmet clinical need.

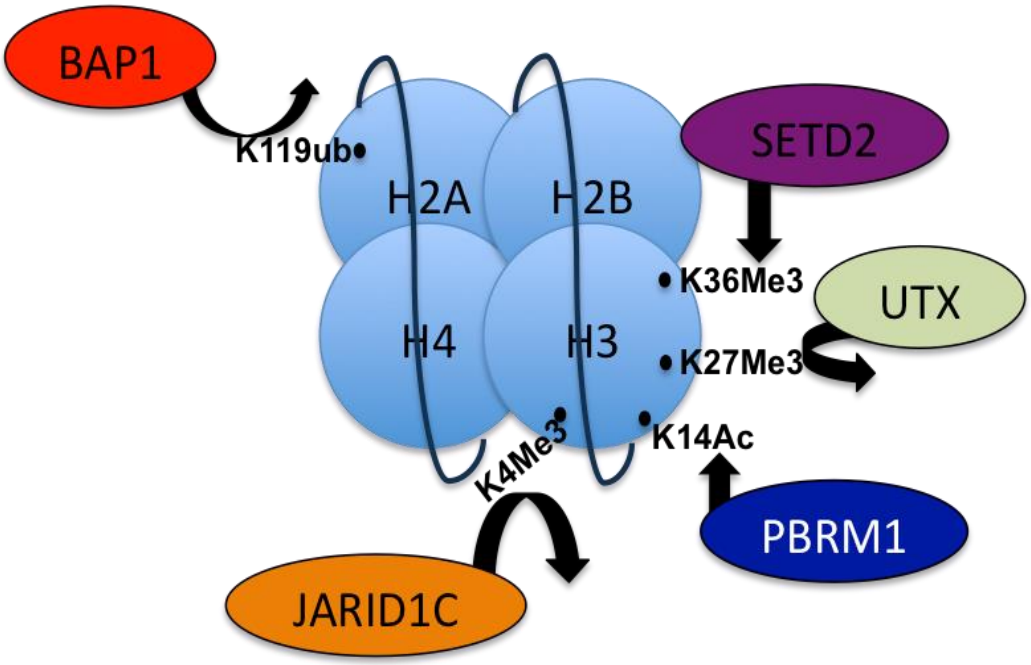

Figure 1.9. Genes involved in ccRCC interact with chromatin. Adapted from (Liao, Testa et al. 2015).

1.3.1. VHL is the most frequently mutated gene in ccRCC

Inactivation of the VHL tumour suppressor gene is the most significant driver of ccRCC, with 70-80% of all ccRCC tumours harbouring a biallelic inactivation of VHL through mutation, deletion, or hypermethylation of its promoter resulting in the loss of expression (Liao, Testa et al. 2015). Although loss of VHL is a key driver in the tumorigenesis of ccRCC, inactivation of this gene alone is not sufficient to cause ccRCC (Mandriota, Turner et al. 2002, Rankin, Tomaszewski et al. 2006). The VHL gene maps to chromosome 3p25 and is an established two-hit tumour suppressor gene, meaning that one allele is inactivated by mutation or promoter methylation and the other is inactivated through a large deletion resulting in loss of heterozygosity (LOH) (Gnarra, Tory et al. 1994, Gossage, Murtaza et al. 2014). Von Hippel-Lindau (VHL) gene mutations are associated with the development of both hereditary and sporadic clear cell renal carcinoma. The protein product of VHL (pVHL) forms an E3 ubiquitin ligase complex with Cul2 and Rbx1 that is able to regulate the hypoxia-inducible factor-1 (HIF-1), however the relationship between this function and ccRCC development is not clear (Mandriota, Turner et al. 2002, Liao, Testa et al. 2015). It has been demonstrated that in the kidneys of patients with VHL disease, HIF activation is an early event occurring in morphologically normal single cells within the renal tubules (Mandriota, Turner et al. 2002).

1.3.1.1. The role of Hypoxia Inducible Factor (HIF) in ccRCC

VHL is mutated in both hereditary kidney cancer as well as spontaneous clear cell renal cell carcinoma (Liao, Testa et al. 2015). The heterodimeric transcription factor hypoxia-inducible factor (HIF) contains α-subunits that are targeted by the VHL containing E3 ubiquitin ligase complex, resulting in poly-ubiquitination and proteosomal destruction (Liao, Testa et al. 2015). When HIFα is hydroxylated on either of the two prolyl residues by members of the Egl nine homolog family (otherwise known as either prolyl hydroxylase domain-containing proteins or

HIF prolyl hydroxylases), it can then be recognised by pVHL (Liao, Testa et al. 2015). A loss or inactivation of pVHL promotes the synthesis and accumulation of HIFα proteins, which then form a complex with HIF1β protein, resulting in the activation of a transcriptional response to hypoxia in the nucleus (Liao, Testa et al. 2015). Not all HIF-induced genes result in tumour development (Niu, Zhang et al. 2012), however constituently active HIF activity is known to promote tumourigenesis and stimulate growth in ccRCC tumours (Kaelin 2005). Activation of HIF is thought to be an important step in the development of VHL mutant ccRCC. Development of VHL mutant ccRCC has been described as a sequence of events, starting with the loss of VHL activity, followed by the consequential activation of the HIF pathway, followed by interaction of the HIF pathway with other oncogenic pathways, resulting in genome-wide epigenetic changes and further inhibition of multiple tumour suppressor genes, finally ending with immune evasion (Shenoy and Pagliaro 2016).

1.3.2. Intratumour heterogeneity and branched evolution

Vast heterogeneity within individual tumours has been identified by large-scale sequencing analysis of solid tumours (Parsons, Jones et al. 2008, Varela, Tarpey et al. 2011). Intratumour heterogeneity (ITH) is a phenotype expressed in ccRCC. Sequencing analysis of ccRCC recently identified multiple genetically distinct subclones within primary tumours and their metastases (Gerlinger, Rowan et al. 2012), revealing that the evolution of ccRCC was branched, rather than occurring in a linear fashion (Figure 1.10) (Gerlinger, Horswell et al. 2014). Genetic complexity of a tumour identified by single-biopsy may be therefore underestimated if ITH is not taken in to consideration. In ccRCC, mutations in VHL or PBRM1 are thought to be the main drivers or truncal mutations, however the clinical outcomes for patients with ccRCC can differ greatly from patient to patient. This is likely due to subclonal driver mutations acquired by tumours during progression (Gerlinger, Horswell et al. 2014). Subclonal driver events present in solid tumours may provide an explanation for the acquired resistance to targeted therapeutics in late stages of disease (Gerlinger, Horswell et al. 2014).

Greater knowledge of the evolution of truncal mutations and the consequential subclonal branches they form in ccRCC may be useful in future prediction of tumour evolution in patients and ultimately may be able to identify new targets for therapeutics.

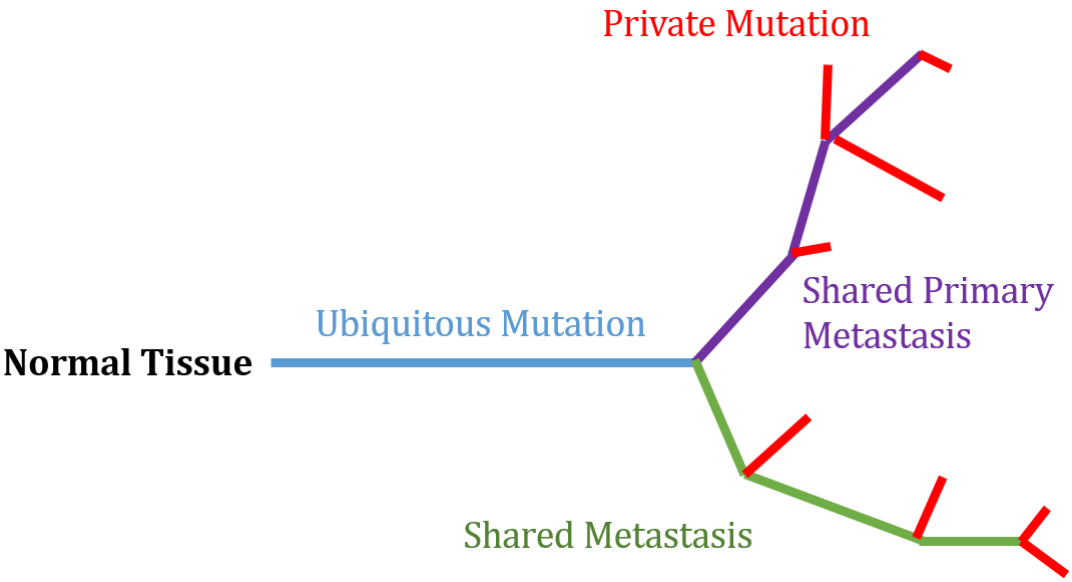

Figure 1.10. Phylogenetic tree for tumour analysis. Adapted from (Gerlinger, Rowan et al. 2012)**.** Normal tissue that acquires a ubiquitous driver mutation forming the 'trunk', the 'branches' that arise from this driver mutation represent the intratumour heterogeneity displayed in ccRCC.

1.3.3. PBRM1 is another key tumour suppressor in kidney cancer

Whole exome sequencing of ccRCC tumours has revealed that PBRM1, the gene that encodes BAF180, is mutated in over 40-50% of cases (Varela, Tarpey et al. 2011). Found on chromosome 3p21, PBRM1 mutations lead to loss of protein and are typically associated with gross chromosomal aberrations, such as loss of heterozygosity (LOH) (Varela, Tarpey et al. 2011). While we know that PBRM1 is frequently mutated in ccRCC and is known to be a driver of this cancer, we still require a greater understanding of the molecular mechanism of how this gene acts as a tumour suppressor, before we can fully exploit it for the development of cancer therapies.

PBRM1has multiple cellular functions that could contribute to tumorigenesis. This is the focus of our study and so will be discussed in much greater detail in Section 1.5,

1.3.4. BAP mutations in cancer and its tumour suppressor role in ccRCC

BRCA1- associated protein-1 (BAP1) is mutated in ccRCC at a frequency of around 15% (Liao, Testa et al. 2015). It was first identified as a protein that interacted with BRCA1's RING finger in a yeast two-hybrid screen (Jensen, Proctor et al. 1998). In the study from Jensen et al, BAP1 was found to enhance BRCA1-mediated inhibition of breast cancer cell growth and was suggested to be a new tumour suppressor gene that functions within the BRCA1 growth control pathway (Jensen, Proctor et al. 1998). BAP1 shares homology with the ubiquitin C-terminal hydrolases (UCH) family of deubiquitases and has deubiquitinase activity (Jensen, Proctor et al. 1998). As well as harbouring its deubiquitinase activity in its N-terminal domain, BAP1 also has a BARD1 interaction domain (BA), a UCH37 domain located in the C-terminus, a YY1-binding domain, two nuclear

localisation signals and its interaction with host cell factor-1 (HCF-1) requires its NHNY sequence (Liao, Testa et al. 2015).

BAP1's role in the BRCA1 growth control pathway is complex and not fully understood, however it is thought that BAP1, under circumstances such as in response to DNA damage, can then interact with BRCA1 (Yu, Pak et al. 2014). BAP1 has key roles not only in the DNA damage response (DDR), but in the control of cell cycle, cellular growth and regulation of chromatin architecture by de-ubiquitination of histone H2A (Piva, Santoni et al. 2015), and these subsequently allow for the promoters of several target genes to become accessible to transcription factors. It is interesting to note that BAP1 deubiquitinates the mono-ubiquitinated K119 residue on histone H2A, however this does not seem to associate with its ability to repress cell growth (Liao, Testa et al. 2015).

Mutations in BAP1 result in the development of metastases in uveal melanoma (UM) (Harbour, Onken et al. 2010) as well as other malignancies such as malignant pleural mesotheliomas (Bott, Brevet et al. 2011). BAP1 mutations have conflicting implications in cancer. They present as a paradox in which, both overexpression (Jensen, Proctor et al. 1998, Ventii, Devi et al. 2008), as well as knockdown (Pan, Jia et al. 2015), result in growth suppression and the down regulation of E2F-responsive growth-related genes. It has been postulated that this BAP1 paradox could be explained by BAP1 contributing to a delayed but more permissive G1/S checkpoint, where cells may in fact grow more slowly, but still in an uncontrollable manner (Bott, Brevet et al. 2011).

As previously mentioned, BAP1 is mutated in uveal melanoma metastases, the most important cytogenetic predictor of this being the loss of chromosome 3. BAP1, like VHL and SETD2, is located on chromosome 3, specifically on the short (p) arm of chromosome 3, at band location 3p21, which is extremely close to the PBRM1 gene. Like VHL, BAP1 is modelled as a two-hit tumour suppressor in ccRCC, where the wild type allele compensates for the mutated allele (Piva, Santoni et al. 2015).

Mutations of BAP1 in ccRCC are mostly inactivating mutations and that in a large portion of tumours studied, were subclonal rather than ubiquitous.

In almost all tumours where BAP1 is mutated, VHL is also inactivated. Mutation of VHL results in high allelic burden with mutations typically resulting in loss of heterozygosity (LOH), however tumours with subsequent mutations in BAP1 tended to show this burden as being significantly lower. BAP1 mutations may be more likely to be acquired in tumours with pre-existing VHL mutations and therefore subsequently contribute to tumour progression because of selection pressure (Sato, Yoshizato et al. 2013).

BAP1 mutations in ccRCC are associated with poor outcome, tumour aggressiveness and high Fuhrman grade, with more than 50% of tumours with mutant BAP1 exhibiting coagulative necrosis (Pena-Llopis, Vega-Rubin-de-Celis et al. 2012, Kapur, Pena-Llopis et al. 2013).

As mentioned, BAP1 is frequently mutated in tumours with a driver mutation in VHL. BAP1 and PBRM1 mutations, however, appear to be mutually exclusive (Pena-Llopis, Vega-Rubin-de-Celis et al. 2012, Kapur, Pena-Llopis et al. 2013).

When two genes function within the same pathway, they are often thought to have mutation exclusivity, however BAP1 and PBRM1 have been suggested to be involved in two separate processes as they are mutually exclusive in ccRCC (Brugarolas 2013). Evidence supporting this is first seen in the parallels in outcome prognosis after mutation in each gene. BAP1 mutations are associated with poor outcome and high Fuhrman grade as well as activation of mTORC1, however, PBRM1 mutant ccRCC's are thought to be low grade, have a lack of mTORC1 activation and have a markedly better outcome (Pena-Llopis, Vega-Rubin-de-Celis et al. 2012, Kapur, Pena-Llopis et al. 2013). Secondly, the gene expression signatures of BAP1-mutant and PBRM1-mutant tumours are highly specific and quite distinct from one another, which typically suggests tumours with different pathological features and different patient outcomes (Kapur, Pena-Llopis et al. 2013). Therefore, it would not infer that BAP1 and PBRM1 mutations are mutually exclusive because they act in the same pathway, in fact, it would suggests that the mutations define two different molecular subtypes of ccRCC,

which have different biology, act in different pathways and result in markedly different outcomes (Brugarolas 2013). The mutual exclusive relationship between BAP1 and BAF180 could be exploited therapeutically by harnessing synthetic lethality, which will be further discussed in section (3.8.4).

1.3.5. SETD2 in renal cancer

Set domain-containing 2 (SETD2), a gene known to produce at least three alternative splicing transcripts that produce histone methyltransferases, is known to trimethylate histone H3 at lysine 36 (H3K36me3) (Piva, Santoni et al. 2015). It is mutated in multiple cancers, including breast cancer and leukemias (Al Sarakbi, Sasi et al. 2009, Zhang, Ding et al. 2012), but first being identified as inactivating mutations in ccRCC in 2010 (Dalgliesh, Furge et al. 2010). It is now known to be mutated in 3-16% of all human ccRCC tumours (Wang, Liu et al. 2016) and is associated with loss of DNA methylation at non-promoter regions (Piva, Santoni et al. 2015). Most cases of ccRCC with a SETD2 mutation were found to have either a VHL or PBRM1 mutation also, and as previously mentioned, all three genes map to chromosome 3p. This suggests that the mutations are functionally non-redundant and that physical linkage of these three genes may be the driver for the loss of fitness and the large scale 3p loss of heterozygosity (LOH) seen in over 90% of ccRCC cases, perhaps due to haploinsufficiency (Varela, Tarpey et al. 2011).

It has been hypothesised that there may be high selection pressure for mutations of SETD2 after analysis of different SETD2 mutations in a panel of multiple ccRCC, show a tendency to be subclonal and showed that different regions of the same tumour could harbour different SETD2 mutations(Gerlinger, Rowan et al. 2012). In one example given by Gerlinger et al, the same tumour was biopsied in multiple sites and within these sites three different SETD2 mutations were found, including a missense mutation, a splice-site mutation, and a frameshift deletion (Gerlinger, Rowan et al. 2012). It is interesting to note that the ubiquitous loss of one gene allele could provide a foundation for the subsequent loss of protein function, driven by different mutations that are regionally separated. Tumours

that harbour missense or frameshift mutations of SETD2 have notably down-regulated trimethylation of H3K36 (Gerlinger, Rowan et al. 2012), which would suggest active transcription would not be carried out in these regions, however the H3K36me3 signature has also been linked with alternative splicing as well as transcriptional repression (Wagner and Carpenter 2012), making it unclear what role this down-regulation of H3K36me3 by SETD2 mutation plays in the biology of ccRCC.

In context of the DNA damage response, SETD2 is known to play an important role. It is thought to act in a similar way to RAD51, in that it promotes the repair of DNA DSB's through homologous recombination, by facilitating the recruitment of repair proteins (Pfister, Ahrabi et al. 2014). SETD2 mutated cancers are also thought to be unable to activate p53-mediated checkpoints, without the need for additional mutations in TP53, a known guardian of the genome that is very rarely mutated in ccRCC (Carvalho, Vitor et al. 2014).

SETD2 plays a significant role in ccRCC disease progression and like BAP1 mutations, is typically associated with poorer cancer-specific survival (CSS) (Hakimi, Ostrovnaya et al. 2013). However, unlike BAP1 mutations that are typically mutually exclusive with PBRM1 mutations, SETD2 mutations are often found to occur in tumours where PBRM1 was mutated more frequently that would be expected by chance alone, suggesting some level of cooperation between the loss of these two genes in the tumorigenesis of ccRCC (Pena-Llopis, Christie et al. 2013). While this study focuses on mutant PBRM1 ccRCCs, it is still important to note that study of SETD2 mutant cancers could too have translational potential in the clinic.

1.3.6. JARID1C/KDM5C mutation in ccRCC

Trimetylation of Histone H3 at Lysine 4 (H3K4me3) is an epigenetic modification, which identifies the transcription start sites (promoters) of active genes (Benayoun, Pollina et al. 2014). The methylation state of the lysine residues of histone H3 and the modification that takes place here is implicated in

transcriptional control by its regulation of chromatin structure (Varela, Tarpey et al. 2011). JARID1C, also known as KDM5A, is a histone demethylase that removes a methyl group from lysine 4 on histone H3 (H3K4Me3) and is mutated in 3-7% of ccRCC tumours, most of which are subclonal mutations (Dalgliesh, Furge et al. 2010, Liao, Testa et al. 2015). JARID1C mutation is linked with poor prognosis of ccRCC patients, having an association with advanced tumour stage and grade as well as overall tumour invasiveness (Sankin, Hakimi et al. 2014). Amplification or mutation of JARID1C can also be observed in other urological malignancies, such as prostate adenocarcinoma and papillary RCC to name a few (Liao, Testa et al. 2015). As mentioned previously, HIF's are known to increase the transcription of histone demethylases and so, unsurprisingly, JARID1C mRNA and protein expression are HIF-dependent (Niu, Zhang et al. 2012). VHL negative cells have low levels of H3K4me3 and this could be due to reduced methyltransferase activity or increased demethylase activity, or both. It has been suggested that there could be a HIF-induced JARID1C negative feedback loop that could be linked to tumour size. This model would see a loss of JARD1C leading to an increase in H3K4me3 in VHL-defective kidney cancer and would therefore form larger tumours (Niu, Zhang et al. 2012)

1.3.7. UTX/KDM6A mutation in ccRCC

The trimethylation of histone H3 at lysine 27 is the most prominent histone modification that is associated with transcriptional repression. Enzymes that modify this site, such as EZH2, are frequently mutated in cancer (Yamaguchi and Hung 2014). UTX, otherwise known as KDM6A, is a H3K27 demethylase that is mutated at low frequencies in ccRCC and at higher levels in bladder cancer and others (van Haaften, Dalgliesh et al. 2009, Dalgliesh, Furge et al. 2010, Liao, Testa et al. 2015). UTX mutations in a study of ccRCC samples, were found in a subset of cancer cells within a tumour, meaning these mutations are subclonal rather than driver mutations, although little is known about them and how they impact ccRCC tumorigenesis at present (Liao, Testa et al. 2015).

1.4. SWI/SNF Remodelling Family

Originally identified in *S. cerevisiae* by both genetic screens and biochemical purification, the SWI/SNF (switching defective/sucrose nonfermenting) family of chromatin remodelers are typically composed of 8 to 14 subunits (Clapier and Cairns 2009). The SWI/SNF subfamily of complexes work to remodel chromatin by moving or ejecting nucleosomes, allowing for the proper frequency and positioning of nucleosomes at genes and other loci (Kasten, Clapier et al. 2011). The complex, in most eukaryotes, centres around two variant catalytic subunits, which subsequently form two well-defined members of this sub-family of chromatin remodelers, BAF and PBAF (Brownlee, Meisenberg et al. 2015). The BRG1 catalytic subunit belongs to the PBAF complex, whereas the BAF complex can contain either BRG1 or BRM (Table 1) (Brownlee, Meisenberg et al. 2015). BRG1 and BRM are both catalytic ATPase subunits, comprised of an N-terminal HSA (helicase-SANT) domain, a post-HSA domain that is split in to two areas separated by a linker, called DExx and HELICc, as well as a C-terminal bromodomains (Clapier and Cairns 2009). Both BAF and PBAF share a number of core and accessory subunits and have additional subunits that are unique to each complex (Figure 1.11). As mentioned previously, the genes that encode these subunits are frequently mutated in human cancers, earning their title as tumour suppressor genes (Shain and Pollack 2013). SWI/SNF complexes have a well-described role in the regulation of gene expression (Wilson and Roberts 2011, Romero and Sanchez-Cespedes 2014, Masliah-Planchon, Bieche et al. 2015). More recently, SWI/SNF has been found to play a vital role in transcription-independent pathways, contributing to genome stability via DNA repair, sister chromatid cohesion and the DNA damage response (Brownlee, Meisenberg et al. 2015).

1.4.1. Discovery of the RSC chromatin remodelling complex

The SWI/SNF-family of chromatin remodelers exists as SWI/SNF and RSC (remodels the structure of chromatin) in budding yeast, with RSC being ten times

more abundant than SWI/SNF (Cairns, Lorch et al. 1996). The yeast SWI/SNF (ySWI/SNF) was first identified by genetic screening in 1984, where yeast mutants defective in either mating-type switching (*swi* mutants) or sucrose fermentation (*snf* mutants) were screened together (Neigeborn and Carlson 1984, Stern, Jensen et al. 1984, Breeden and Nasmyth 1987). The identification of RSC came slightly later, being isolated by mass spectrometry and limited sequence analysis based on the homology to the ySWI/SNF complex (Cairns, Lorch et al. 1996). The RSC subunits known to date are; Sth1, Rsc1, Rsc2, Rsc3, Rsc4, Rsc5, Rsc6, Rsc7, Rsc8/Swh3, Rsc9, Rsc10/Rsc56, Rsc14/Ldb7, Htl1, Sfh1, Arp7, Arp9 and Rtt102 (Kasten, Clapier et al. 2011), at least three of which are homologous to the ySWI/SNF components (Cairns, Lorch et al. 1996). The catalytic ATPase 'core' subunit of RSC, Sth1, closely resembles the ySWI/SNF catalytic subunit Swi2/Snf2, both being activated by single-strand, double-strand and nucleosomal DNA (Cairns, Lorch et al. 1996). As well as having similarities within the ATPase catalytic subunits, there is an extended conservation of four core subunits, Swi2/Snf2, Swp73, Swi3 and Snf5 in ySWI/SNF and their RSC homologs Sth1, Rsc6, Rsc8 and Sfh1 (Figure 1.11). This homology extends to higher eukaryotes, such as human SWI/SNF (hSWI/SNF), suggesting that conservation of the core proteins is functionally important (Cairns, Lorch et al. 1996), either to maintain the complex integrity or to preserve remodelling activity (Tang, Nogales et al. 2010). RSC and ySWI/SNF have many similarities, however, they are thought to regulate different regions of chromatin and the function of RSC is vital for cell survival (Tang, Nogales et al. 2010). It is plausible that the addition/subtraction of accessory subunits allows for this more specialised function of RSC, just as the addition of novel subunits to mammalian BAF and PBAF (Figure 1.11), for example, can allow for selective regulation of certain genes and functional specificity (Yan, Cui et al. 2005).

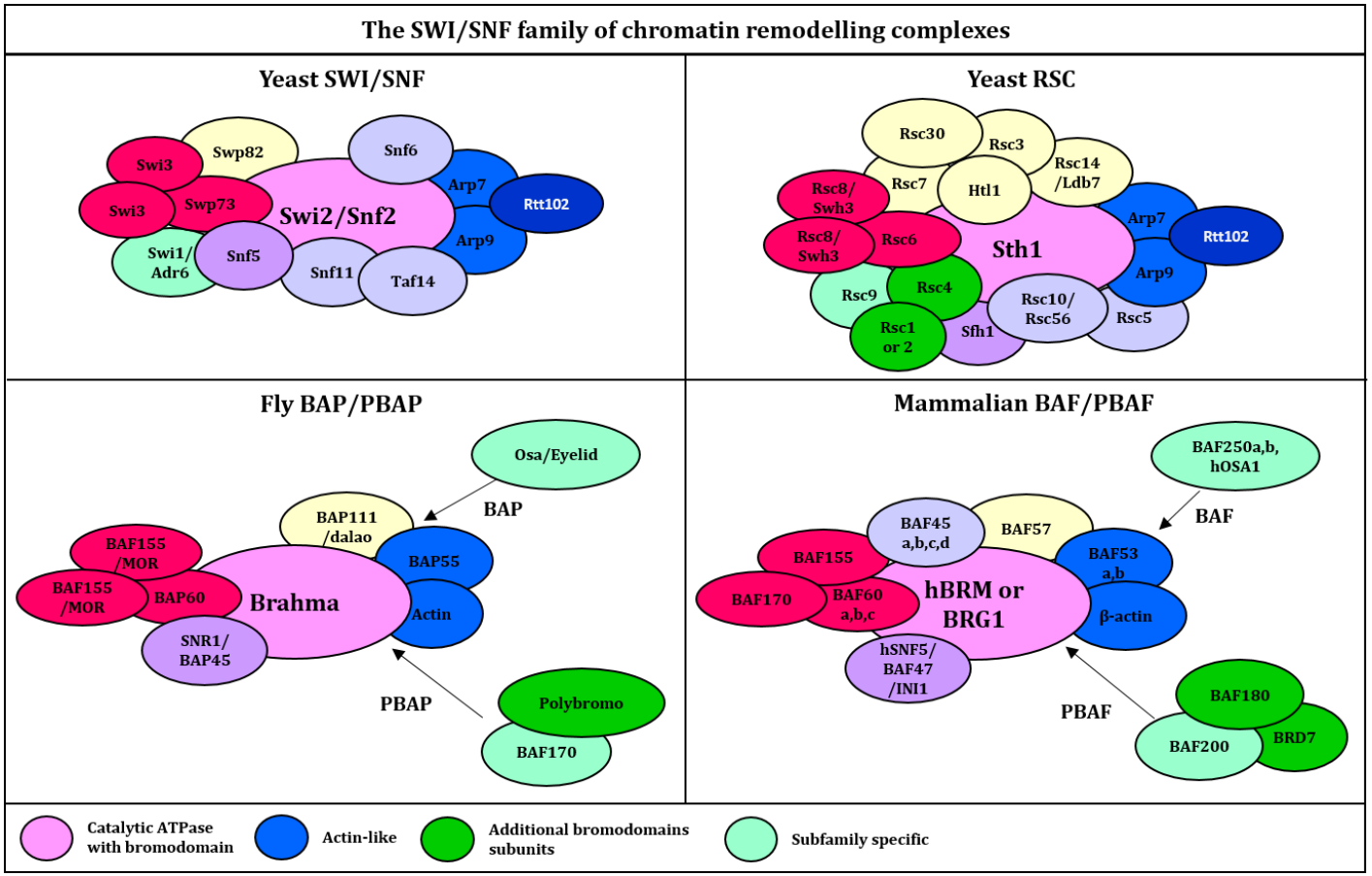

Figure 1.11. Composition of the SWI/SNF family of chromatin remodelers. Adapted from (Kasten, Clapier et al. 2011). Conserved catalytic subunits in each complex are shown in pink.

1.4.2. The RSC complex can exist as two distinct isoforms

It is known that in budding yeast, the RSC complex can exist as two related complexes containing either Rsc1 or Rsc2 (Cairns, Schlichter et al. 1999). The RSC complex, as previously described, was identified from yeast extracts in 1996 (Cairns, Lorch et al. 1996). Rsc1 and Rsc2 are similar in domain architecture, being composed of two bromodomains, an AT hook motif, a bromo-adjacent homology (BAH) domain and two regions in the carboxyl termini (C-terminal) of high and moderate identity respectively, CT1 and CT2 (Figure 1.12) (Cairns, Schlichter et al. 1999). The mammalian PBAF complex, interestingly carries a subunit, BAF180, which consists of six bromodomains, two BAH domains and a high-mobility group (HMG), therefore appearing to be a fusion of the yeast Rsc1, Rsc2 and Rsc4 (Figure 1.13) (Goodwin and Nicolas 2001, Mohrmann and Verrijzer 2005, Chambers, Pearl et al. 2013).

1.4.2.1. Bromodomains and AT hook functionality in RSC

Bromodomains, such as the ones found in the Rsc components as well as in many other proteins, are important for the regulation of transcription and the structural integrity of chromatin (Cairns, Schlichter et al. 1999). They exist as 110-amino acid acetyl-lysine binding motifs (Dhalluin, Carlson et al. 1999), binding to the amino-terminal tails of histones H3 and H4 (Ornaghi, Ballario et al. 1999). The second bromodomain (BD2) of Rsc1 and Rsc2 (Figure 1.12), with the BAH and C-terminal domain, are entirely required for function, where loss or mutation of these areas results in null phenotypes (Cairns, Schlichter et al. 1999). However, the first bromodomain (BD1) and the AT hook are only required in a subset of functions. Rsc1 can lose BD1 without impeding any function, however in Rsc2, BD1 was found to be required for its function in media supplemented with caffeine (effecting osmotic stability and cAMP signalling), a demonstration that Rsc1 and Rsc2 bromodomains are functionally distinct (Cairns, Schlichter et

al. 1999). The bromodomains found in the Rsc4 subunit of RSC, appear in tandem and both preferentially bind at different sites. It is thought that the BD1 domain binds directly to Rsc4 itself at the acetylated lysine K25, whereas the BD2 domain binds the acetylated lysine at K14 of histone H3 (H3K14ac) (VanDemark, Kasten et al. 2007). Gcn5 has activating and inhibitory roles with Rsc4, it is known that Gcn5 acetylates the ligands for BD1 and BD2, K25 and H3K14 respectively. These acetylated ligands are then thought to compete for binding to Rsc4, however it is known that Rsc4 K25 acetylation directly inhibits Rsc4 binding to acetylated H3K14. It has therefore been postulated that there is an auto-regulatory mechanism, with Gcn5 acting as a switch for RSC at sites of remodelling. In this model, Gcn5 would promote RSC-nucleosome binding by acetylation of H3K14, therefore enabling remodelling, with the subsequent acetylation of K25, releasing RSC from the interaction (VanDemark, Kasten et al. 2007).

AT hooks (Figure 1.12) associate preferentially with the minor groove of AT-rich DNA and were first identified as short DNA-binding motifs in the high-mobility group chromosomal protein HMG-I (Reeves and Nissen 1990, Aravind and Landsman 1998). The functional domains of chromatin proteins and DNA-binding proteins, such as histone folds and zinc fingers, are known to associate with AT hooks and they are commonly found preceding bromodomains by 20-40 amino acids (Cairns, Schlichter et al. 1999). It is thought that these AT hooks can facilitate changes in the structure of DNA either cooperating as part of a protein with multiple domains, like Swi2 in yeast, or as a single polypeptide, as in HMG-I (Aravind and Landsman 1998). In RSC, it is thought that the AT hook is only required for Rsc1, but not Rsc2 functions. The cooperation between AT hooks and bromodomains may facilitate specific interactions with defined nucleosomes. For example the AT hook in the catalytic subunit BRM of the BAF mammalian SWI/SNF complex has been found to bind DNA as well affecting the complexes association with chromatin (Bourachot, Yaniv et al. 1999). In contrast, the RSC catalytic subunit Sth1, does not contain an AT hook, therefore these specific functions may be carried out by Rsc1/Rsc2.

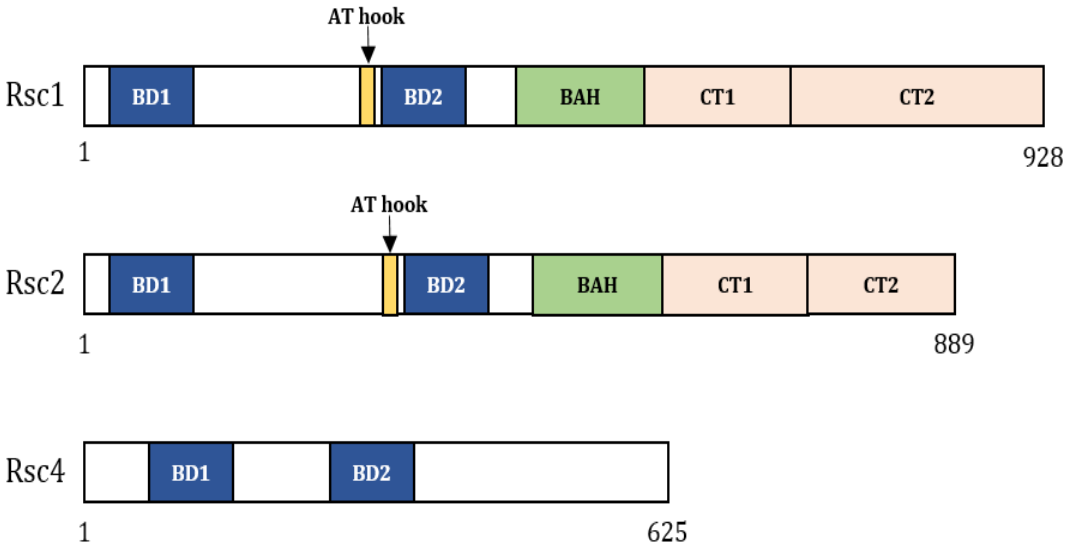

Figure 1.12. Rsc1, Rsc2 and Rsc4 are bromodomain containing members of RSC. Adapted from (Cairns, Schlichter et al. 1999).

1.4.2.2. BAH domain function in RSC

First identified in the chicken polybromo (BAF180) protein (gPB) (Nicolas and Goodwin 1996), Bromo-adjacent homology (BAH) domains are often associated with chromatin proteins, protein complexes and proteins that facilitate gene transcription and repression and are thought to be involved in protein-protein interactions (Goodwin and Nicolas 2001). BAH domains interact with nucleosomes and can be classified in two ways, the first being, 'Remodels the Structure of Chromatin (RSC)-like', which can be found in the yeast Rsc1 and Rsc2 and their mammalian homologue BAF180 (Chambers, Pearl et al. 2013). RSC-like BAH domains can also be found in transcription factors, such as Ash1, as well as the CpG-DNA methylase DNMT1 (Oliver, Jones et al. 2005). Secondly, BAH domains can be classified as 'Silent information regulator 3 (Sir3)-like' and this classification includes Orc1 homologues and the Sir3 protein found in budding yeast (Chambers, Pearl et al. 2013).

The BAH domains of Orc1 and Sir3 have a key role in the mediation of transcriptional silencing at telomeres (Norris and Boeke 2010) and can both bind nucleosomes (Noguchi, Vassilev et al. 2006, Onishi, Liou et al. 2007, Norris, Bianchet et al. 2008, Muller, Park et al. 2010). Interestingly Orc1 BAH domain nucleosome binding in mammals is determined by an interaction with the tail of histone H4 dimethylated at lysine 20, whereas the Sir3 BAH domain interacts with both H3 and H4, by binding nucleosomes at the Loss of Ribosomal Silencing (LRS) region of the nucleosome. As well as being able to bind nucleosomes, the Orc1 BAH domain can interact with the silent information regulator Sir1 and the heterochromatin-associated protein HP1 in yeast and higher eukaryotes respectively.

In the context of RSC, it is known that the BAH domains of both Rsc1 and Rsc2 are required for function and viability, but have no role in the assembly of the complex and relatively little is known about their binding partners (Cairns, Schlichter et al. 1999). However, recently in our lab, it was found that the Rsc2 BAH domain is able to bind specifically with histone H3 as well as being important for rDNA transcriptional silencing (Chambers, Pearl et al. 2013).

1.4.2.3. Structural conformation of RSC

The structure of the RSC complex has been determined using cryo-electron microscopy, revealing a ring of protein densities around a large central cavity with the size and shape that would be appropriate for nucleosome binding (Asturias, Chung et al. 2002). It has been suggested that this cavity acts as a nucleosome binding pocket, due to the observation that addition of nucleosomes to the complex experimentally leading to an increase in density in this region (Lorch, Cairns et al. 1998, Asturias, Chung et al. 2002, Skiniotis, Moazed et al. 2007). To accommodate a nucleosome in this binding pocket, RSC can exist in two conformations, 'open' and 'closed', which were determined when Rsc2-RSC (Leschziner, Saha et al. 2007) as well as the mixture of Rsc1-RSC and Rsc2-RSC were analysed (Skiniotis, Moazed et al. 2007, Chaban, Ezeokonkwo et al. 2008). The open conformation is thought to allow the entrance or release of a nucleosome, whereas in the closed conformation the movement/conformation of the distal portion of the bottom domain or 'arm', which becomes very close in proximity, is the most important for enveloping the docked nucleosome (Chaban, Ezeokonkwo et al. 2008). The dynamically mobile distal portion of RSC is thought to be stabilised by the presence of acetylated histone H3 N-terminal tail peptides (Skiniotis, Moazed et al. 2007). A portion of the complexes formed by the mixture of both Rsc1-RSC and Rsc2-RSC isoforms were found to appear in a third conformation, where ~16% of the complexes had either a reduced density or were completely lacking part of the distal arm, a conformation that could be attributed to Rsc1 isoform specificity (Skiniotis, Moazed et al. 2007, Chambers and Downs 2012).

1.4.2.4. Biochemical activity of RSC

In vitro assays have been carried out on mixed populations of Rsc1 and Rsc2-containing complexes as well as Rsc2 only containing complexes to establish the

biochemical activity of these chromatin remodelers. From these studies, the RSC complex is known to be involved in nucleosome remodelling, repositioning, disassembly and histone octamer transfer. DNA of at least 25bp in length is thought to be able to stimulate the ATPase activity of the RSC complex, at a rate of ~7.5 molecules ATP/second under optimal conditions, which is not further stimulated by the addition of nucleosomes (Cairns, Lorch et al. 1996, Boyer, Logie et al. 2000, Saha, Wittmeyer et al. 2002). The catalytic Sth1 subunit, when compared to the intact Rsc2-RSC complex, is thought to have approximately 2.5 times lower ATPase activity, suggesting that the cooperation of the other RSC subunits is necessary for maximal complex activity (Saha, Wittmeyer et al. 2002). Using atomic force microscopy, RSC was found to form relaxed supercoiled loops of around 400-700bp or 20-1200bp respectively on DNA that was tethered and stretched at low forces as well as on nucleosomal templates (Lia, Praly et al. 2006, Zhang, Smith et al. 2006). The loops formed in an ATP-dependent manner and slippage was observed in both templates. However, a greater translocation rate, >500bp/s compared to 12bp/s, was seen in the naked DNA, rather than the nucleosome-bound DNA template. The loops formed may provide a molecular basis for the functions of chromatin remodelling complexes (Zhang, Smith et al. 2006). It has been suggested that these loops may cause the formation of a bulge of DNA on the nucleosome surface that has the capability of forming a larger loop by translocation and on dissolution of this large loop can facilitate remodelling activities such as reverse translocation, nucleosome position jump or nucleosome sliding (Chambers and Downs 2012).

1.4.2.5. In vivo functions of RSC

It has been well established that the RSC complex is important for the activation and repression of transcription of multiple genes in *S. cerevisiae* and is found to be co-immunoprecipitated with all three RNA polymerases (Angus-Hill, Schlichter et al. 2001, Ng, Robert et al. 2002, Soutourina, Bordas-Le Floch et al. 2006). The RSC complexes role *in vivo* isn't restricted to transcriptional control however, it is also thought to be important for proper kinetochore function (Hsu,

Huang et al. 2003), adaption to the spindle assembly checkpoint (Rossio, Galati et al. 2010), correct localisation of the nuclear pore complex (Titus, Dawson et al. 2010), and sister chromatid cohesion (Baetz, Krogan et al. 2004) to name a few.

1.4.3. Mammalian SWI/SNF exists as BAF and PBAF

As previously described, mammalian SWI/SNF can exist as the BRG1- or hBRM-associated factor (BAF or SWI/SNF-A) or the polybromo BRG1-associated factor (PBAF or SWI/SNF-B) complexes (Wilson and Roberts 2011). Two mutually exclusive catalytic ATPase subunits define each complex, either brahma homologue (BRM) or BRM/SWI2-related gene 1 (BRG1), with the BAF complex containing BRG1 or BRM and the PBAF complex containing only BRG1 (Table 1.1) (Wilson and Roberts 2011). Both complexes contain a set of highly conserved 'core' subunits, SNF5, BAF155 and BAF170 (Table 1.1). Variant subunits associate with each complex and are thought to facilitate complex targeting, assembly and the regulation of lineage-specific functions of each complex (Wang, Cote et al. 1996, Phelan, Sif et al. 1999, Wilson and Roberts 2011). Subunits unique to the BAF complex include, AT-rich interactive domain-containing protein 1A (ARID1A) and ARID1B and subunits that are unique to the PBAF complex include, BAF180, BAF200 and bromodomain-containing 7 (BRD7) (Wang, Cote et al. 1996, Wang, Nagl et al. 2004, Mohrmann and Verrijzer 2005, Kaeser, Aslanian et al. 2008).

SWI/SNF complexes are able to remodel nucleosome structure by the mobilisation of nucleosomes by sliding and by catalysing the ejection and insertion of histone octamers (Saha, Wittmeyer et al. 2006, Wilson and Roberts 2011). The sequential steps of nucleosome sliding are thought to be initiated by SWI/SNF complex binding to a fixed position of nucleosome DNA, followed by the disruption of histone-DNA contacts, the ATPase subunit then can translocate DNA and DNA loop formation can then propagate around the nucleosome and subsequently generate sites that are accessible to DNA binding factors (Saha, Wittmeyer et al. 2006, Lorch, Maier-Davis et al. 2010, Wilson and Roberts 2011). Less is known about the mechanism employed for nucleosome ejection and

insertion, however it may be aided by histone chaperones. It has been suggested that histone ejection may not occur at nucleosomes directly bound by SWI/SNF complexes, but rather at adjacent nucleosomes as a consequence of repositioning the bound nucleosome (Dechassa, Sabri et al. 2010). SWI/SNF complexes may have effects on higher order chromatin structure other than nucleosome remodelling, which is the most studied, and this could be due to the complexes interaction with various other chromatin proteins (Wilson and Roberts 2011).

Protein	Gene Name	Complex(es)	Features	Notes
BRG1	SMARCA4	BAF and PBAF	Bromodomain, ATPase	Roles in NHEJ, HR, repression of transcription after DNA damage
BRM	SMARCA2	BAF	Bromodomain, ATPase	Role in NHEJ
BAF250a/b	ARID1A/B	BAF	ARID domain	Role in NHEJ, promotes BRM association with damaged chromatin, interaction with TopoIIa
BAF200	ARID2	PBAF	RFX-type winged helix, Zinc finger, ARID domain	
BAF180	PBRM1	PBAF	6 Bromodomains, 2 BAH domains, 1 HMGB domain	Promotes sister chromatid cohesion, repression of transcription after DNA damage
BRD7	BRD7	PBAF	Bromodomain	
BAF170	SMARCC2	BAF and PBAF	Chromo, SWIRM and SANT domains	Roles in HR and NHEJ, not needed for BRM accumulation at damaged chromatin, interaction with BRIT1
BAF155	SMARCC1	BAF and PBAF	Chromo, SWIRM and SANT domains	Roles in HR and NHEJ, not needed for BRM accumulation at damaged chromatin, interaction with BRIT1
BAF60a/b/c	SMARCD1/2/3	BAF and PBAF	SWIB	Role in NHEJ, promotes BRM association with damaged chromatin
BAF57	SMARCE1	BAF and PBAF	HMGB	No NHEJ defect when depleted
BAF53a/b	ACTL6A/B	BAF and PBAF	Actin related protein	No NHEJ defect when depleted
Actin	ACTB	BAF and PBAF	Actin	
BAF47 (SNF5)	SMARCB1	BAF and PBAF		Role in NHEJ, promotes BRM association with damaged chromatin
BAF45a/b/c/d	PHF10/DPF1/2/3	BAF and PBAF	2 PHD fingers	

Table 1.1. SWI/SNF subunits. Taken from (Brownlee, Meisenberg et al. 2015).

SWI/SNF complexes were originally identified in budding yeast because of their roles in transcriptional activation, but there is mounting evidence to suggest roles for mammalian SWI/SNF in transcriptional repression as well as activation. Some examples of the duality of the subunits in these complexes are highlighted below. For example, BRG1 and BAF57 are required for the reciprocal regulation of CD4/CD8 expression, acting to silence CD4 and to activate CD8 expression during mammalian T lymphocyte development (Chi, Wan et al. 2002). BRG1 is also thought to act as both a repressor that inhibits programs linked to differentiation and a facilitator of the expression of core pluripotency programmes in the BAF complex of embryonic stem cells (Ho, Jothi et al. 2009).

It was discovered that SNF5 deletion in murine fibroblasts (MEFS) leads to transcriptional activation (Isakoff, Sansam et al. 2005). In gene expression arrays comparing SNF5 deleted MEFS to appropriate controls, significantly more genes were defined as being upregulated compared to those that were down regulated (Isakoff, Sansam et al. 2005). Conversely to this, SNF5 has also been implicated in the repression of transcription. It is known that histone deacetylases (HDACs) can be recruited by SWI/SNF complexes, to aid the removal of transcriptionally activating acetyl marks from histone tails. SNF5 was found to exert tumour suppressor activity by mediating cell cycle arrest by the direct recruitment of HDAC activity to the cyclin D1 (CCND1) promoter and therefore causing repression (Zhang, Davies et al. 2002). The PBAF complex is also thought to have a role in DNA induced transcriptional repression, which will be discussed further in section 1.5.

These data suggest that mammalian SWI/SNF complexes have dynamic and essential roles in many gene expression programs by regulating both activation and repression.

1.4.3.1. Epigenetic antagonism between Polycomb and SWI/SNF complexes

The dynamic structure of chromatin is regulated by two classes of enzymes: those that mediate covalent modifications on either histone proteins or DNA, like the Polycomb (PcG) complex, and those that use energy created from ATP hydrolysis to remodel chromatin structure, like the SWI/SNF complexes.

There are two main PcG complexes; polycomb repressive complex 1 (PRC1) and 2 (PRC2). The catalytic subunit of the PRC2 complex is the protein methyltransferase, EZH2, and it is known to promote H3K27me3, a covalent chromatin modification associated with repressed heterochromatin. The H3K27me3 mark at PcG-regulated promoters facilitates PRC1 recruitment, subsequently repressing transcription by the BMI1-dependent promotion of H2A monoubiquitination at K119 (Cao, Tsukada et al. 2005). The catalytic activity of SWI/SNF complexes, mediated by either BRG1 or hBRM, results in a relaxed, open state of chromatin that is associated with active transcription. Epigenetic modifications, like those carried out by PcG and SWI/SNF complexes, can be defined as somatically heritable changes in gene expression that is derived from alterations in chromatin structure, rather than from DNA sequence changes. These modifications are important in cell fate decisions and have roles in oncogenic transformation (Jones and Baylin 2007, McKenna and Roberts 2009). However, unlike DNA mutations, epigenetic modifications are reversible and therefore are good targets for effective cancer therapy.

The antagonistic relationship between PcG and SWI/SNF complexes toward their roles in development was first identified by analysis of *Drosophila* mutants (Kennison and Tamkun 1988). The mechanism by which this antagonism occurred was discovered to be that the PcG proteins maintain repression of Hox genes during embryogenesis, while the SWI/SNF complex promotes Hox gene activation (Kennison and Tamkun 1988).

Mammalian complexes were also found to be antagonistic, due to PcG proteins counteracting the repositioning of nucleosomes and chromatin remodelling

carried out by the enzymatic activity of SWI/SNF (Shao, Raible et al. 1999, Francis, Saurin et al. 2001). A cancer based mechanistic relationship was identified between PcG and SWI/SNF when the SWI/SNF subunit, SNF5, was re-expressed in a SNF5-deficient rhabdoid tumour cell line, resulting in increased activation of the tumour suppressor protein $p16^{INK4a}$ and removal of PcG proteins at the *p16*^{INK4a} locus (Kia, Gorski et al. 2008). Additional evidence supporting a role for PcG and SWI/SNF complexes in cancer was seen when primary SNF5-deficient tumours as well as primary cells with experimentally inactivated SNF5 were found to have elevated EZH2 expression (Wilson, Wang et al. 2010). Elevation of EZH2 expression levels in both models infers that the effect is not a secondary consequence of oncogenic transformation. Wilson et al also showed that Polycomb targets are broadly H3K27-trimethylated and repressed in SNF5-deficient fibroblasts and cancers (Wilson, Wang et al. 2010). They also found that antagonism between the complexes is found in the regulation of stem-cell associated programs and that SNF5 loss activates those programs (Wilson, Wang et al. 2010). Furthermore in mouse models, inactivation of EZH2 blocks tumour formation that is driven by SNF5 loss (Wilson, Wang et al. 2010). An increase in EZH2 expression has also been reported in other types of cancer, some in which SWI/SNF mutations occur, for example ovarian and renal cell carcinomas (Wagener, Holland et al. 2008, Lu, Han et al. 2010). These data suggests there is an epigenetic antagonism between PcG and SWI/SNF complexes and this antagonism may be mechanistically important in the prevention of tumorigenesis.

1.4.3.2. SWI/SNF and DNA repair

As introduced in section 1.1.3, DNA double strand breaks can be repaired by HR or NHEJ. The choice between repair pathways after damaged DNA is recognised is thought to rely on the composition of chromatin that surrounds the break. Compaction of chromatin and the presence of active transcription prior to the induction of the break is thought to be important in the choice between repair pathways (Aymard, Bugler et al. 2014, Pfister, Ahrabi et al. 2014).

Both BAF and PBAF have been implicated in DNA double strand break repair via HR and NHEJ. Consistent with data from yeast, the SWI/SNF complex is recruited to sites of DNA DSBs and is thought to have a direct role at DNA lesions (Park, Park et al. 2006, Peng, Yim et al. 2009, Ogiwara, Ui et al. 2011). Several proteins and protein modifications have been implicated in the recruitment of SWI/SNF to damage. BRIT1 is known to interact with two subunits common to both BAF and PBAF, BAF170 and BAF155. It was found that globally and at DNA DSBs, BRG1 and hBRMs association with chromatin was impaired upon BRIT1 depletion. Depletion of BRIT1 results in defects in both NHEJ and HR activity. Therefore BRIT1 may be important for the mediation of SWI/SNF complex recruitment to DSBs (Peng, Yim et al. 2009). Subunits of BAF, but interestingly not PBAF, were recently found to promote NHEJ in a model where I-SceI-induced DSBs, which require some end processing, were used to monitor NHEJ (Watanabe, Ui et al. 2014).

In contrast, work in our lab identified that the PBAF, not BAF complex is required for the repair of a subset of DSBs in the area surrounding actively transcribed genes (Kakarougkas, Ismail et al. 2014). This is thought to reflect NHEJ activity as it was epistatic with LIGIV when repair was analysed following irradiation (Kakarougkas, Ismail et al. 2014). We have speculated that neither BAF or PBAF is essential for NHEJ, but perhaps that BAF might promote resection-mediated end joining, while PBAF may be required for NHEJ in the vicinity of actively transcribed genes (Jeggo and Downs 2014).

Histone acetylation has also been implicated in mediating the recruitment of SWI/SNF to chromatin at sites of DNA damage (Lee, Park et al. 2010, Ogiwara, Ui et al. 2011). At DSBs, histones H3 and H4 are acetylated by the histone acetyltransferase (HAT), CBP/p300. hBRM recruitment to DNA DSBs is impaired when CBP/p300 was ablated (Ogiwara, Ui et al. 2011). Recent work in our lab has also identified a role for BAF180 in the replication of damaged DNA, by repriming stalled replication forks (Niimi, Chambers et al. 2012, Niimi, Hopkins et al. 2015). This will be introduced in detail in section 1.5.

1.4.3.3. Mutation spectrum of SWI/SNF subunits

SWI/SNF mutations are widespread across a diverse range of human cancers (Reisman, Glaros et al. 2009, Weissman and Knudsen 2009, Wilson and Roberts 2011). SNF5 is a SWI/SNF subunit with a well characterised role as a tumour suppressor. It is known to be homozygously inactivated in nearly all rhabdoid tumours, a rare paediatric malignancy (Versteege, Sevenet et al. 1998). Consistent with this, SNF5 knockout mice are prone to forming similar tumours (Roberts, Galusha et al. 2000). SNF5 and other SWI/SNF subunit mutations, for example BRG1, have also been implicated in lung cancer (Medina, Carretero et al. 2004, Medina, Romero et al. 2008).

Whole exome sequencing surveys of human cancers have identified frequent mutations in SWI/SNF subunits in various single cancer types (Jones, Wang et al. 2010, Wiegand, Shah et al. 2010, Birnbaum, Birnbaum et al. 2011, Li, Zhao et al. 2011, Varela, Tarpey et al. 2011, Wang, Kan et al. 2011, Shain, Giacomini et al. 2012). To appreciate the spectrum of human cancers with SWI/SNF subunit mutations on a larger scale, Shain and Pollack exploited whole-exome sequencing studies, mining 24 studies, representing 669 patient samples across 18 different cancer diagnosis (Shain and Pollack 2013) . Strikingly, SWI/SNF mutations rates were highest in ovarian clear cell carcinoma, with 75% of the samples harbouring a mutation. SWI/SNF mutations were also found in clear cell renal cell carcinoma (57%), hepatocellular carcinoma (40%), gastric cancer (36%), melanoma (34%) and pancreatic cancer (36%) (Shain and Pollack 2013). The overall rate of mutation across all tumour types for SWI/SNF subunits was 19%, rivalling that of TP53, comparatively mutated at 26% across all tumour samples (Shain and Pollack 2013). The authors show that SWI/SNF genes with mutations had an increased tendency to be deleterious mutations, i.e. frameshift, nonsense, rearrangement, splice-site and missense-damaging) at a frequency greater than predicted, compared to missense-benign and missense-damaging. Thus, SWI/SNF mutations are most likely driver mutations (Shain and Pollack 2013). Of the SWI/SNF mutations identified in this study, the majority appeared to preferentially effect the enzymatic and targeting subunits, inferring they may be

critical for SWI/SNF function. ARID1A (9%), PBRM1 (4%), SMARCA4 (3%), ARID1B (2%) and ARID2 (2%) were the five most frequently mutated SWI/SNF genes, with other mutations being found in scaffolding subunits at much lower rates (Shain and Pollack 2013). The main impact of mutations may be to compromise in part or whole the functional activity of SWI/SNF, reinforced by the fact that mutations were found across a varied range of SWI/SNF subunits (Shain and Pollack 2013). Assessing the frequency at which SWI/SNF gene mutations occur together with other mutations in known oncogenic or tumour suppressor pathways revealed that SWI/SNF and TP53 mutations are frequently mutually exclusive (Kadoch, Hargreaves et al. 2013). ARID1A and TP53 mutations, for example, were found to be mutually exclusive, but coincided with PIK3CA and CTNNB1 mutations in clear-cell ovarian carcinoma (Kadoch, Hargreaves et al. 2013).

SWI/SNF is known to control the expression and activity of specific genes and pathways including, Rb, TP53, Polycomb, sonic hedgehog, Myc, stem cell programs and nuclear hormone receptor signalling (Guan, Wang et al. 2011, Wilson and Roberts 2011). The regulation of these genes/pathways may be how SWI/SNF exerts its tumour suppressor activity. We also know that SWI/SNF, specifically PBAF, have roles in the DNA damage response as well as in correct sister chromatid cohesion. It is well known that defects in the DNA damage response and sister chromatid cohesion can contribute to tumorigenesis, therefore SWI/SNF complexes, namely PBAF, may exhibit their tumour suppressing function by the regulation of these factors. I will develop this theory in the following section and in subsequent chapters.

1.5. The BAF180 subunit of PBAF

BAF180 is a protein encoded for by the Polybromo-1 (PBRM1) gene and is one of three subunits that are unique to the PBAF (SWI/SNF-B) chromatin remodelling complex, with the other two being BRD7 and ARID2. These unique subunits distinguish the PBAF complex from the BAF (SWI/SNF-A) complex (Wilson and Roberts 2011).

Little is known about the specific biological functions of BAF180, however its high mutation in cancer has suggested its role as a tumour suppressor gene. BAF180 is mutated in a diverse range of cancers, for example in bladder cancer (Huang, Peng et al. 2015) and in breast cancer (Xia, Nagase et al. 2008, Mo, Li et al. 2015), but its strikingly high mutation frequency in clear cell renal cell carcinoma (ccRCC) has drawn the most attention.

BAF180 is the second most frequently mutated gene in (ccRCC) and is thought to be mutated at a frequency of around 41% in all ccRCC (Varela, Tarpey et al. 2011), however this is reportedly higher in other studies, with some showing mutation frequency at ~50% (Brugarolas 2013). Mutation of BAF180 is believed to be an early event in carcinogenesis, but how it functions as a tumour suppressor is not well understood. As described previously, ccRCC is a disease that effects several thousands of people, with very limited treatment options and poor prognosis, therefore the continued study of BAF180 and its function as a tumour suppressor is important for the progression of new cancer therapeutics.

1.5.1. BAF180 structure and domains

BAF180 is conserved from yeast to humans, with BAF180 appearing to be a fusion of the budding yeast genes Rsc1, Rsc2 and Rsc4 (Figure 1.13) (Chambers, Pearl et al. 2013). BAF180 contains six tandem bromodomains responsible for binding acetylated histones, two bromo-adjacent homology (BAH) domains that can mediate protein-protein interactions and a high-mobility group (HMG) box that

can bind nucleosomal DNA (Figure 1.13) (Wilson and Roberts 2011, Brownlee, Chambers et al. 2012). The functional activity of these domains, in particular the bromodomains and their binding of acetylated histones, is thought to facilitate the recruitment, targeting, retention and orientation of the PBAF complex on chromatin (Brownlee, Chambers et al. 2012). The binding targets of BAF180's bromodomains are yet to be conclusively identified. Two studies to date have examined the ability of BAF180's bromodomains to bind acetylated histone peptides and they come to different conclusions. In one study they found that the first five bromodomains of BAF180 had binding affinity with different acetylated peptides, BD1-H3K4Ac, BD2-H3K9Ac, BD3-H3K9Ac, BD4-H3K23Ac and BD5-H3K14Ac, with BD6 having no preference for any of the tested H3 peptides (Chandrasekaran and Thompson 2007). Contrary to this study, another found entirely different binding of BAF180s bromodomains to acetylated peptides, observing binding between BD1 and H3K36Ac, BD2 and K3K14Ac and H2BK116Ac, BD3 and H3K115Ac, H4K12Ac, H2BK15Ac and H2BK120Ac, BD4 and H3K14Ac and H3K11Ac, BD5 and H3K36Ac and BD6 and H2BK24Ac and H2BK116Ac (Charlop-Powers, Zeng et al. 2010). It is unusual that these two studies come to such different conclusions as in each study all six bromodomains were individually expressed and purified before being used in *in vitro* binding assays, but perhaps the discrepancies could be accounted for in the different methodologies used by each lab (Brownlee, Chambers et al. 2012). This conflicting data does not help answer the question of what are the physiological targets of BAF180's bromodomains. However, recent work in out lab has found that the BAH domain of Rsc2 and the homologous second BAH domain of mammalian BAF180 has the ability to bind to unmodified H3 (Chambers, Pearl et al. 2013). We can infer from this that the bromodomains of BAF180, like the BAH domains, may also have preference for histone H3, recognising acetylated lysine residues on this histone or neighbouring histones.

It is unclear what role BAF180 plays in the prevention of tumorigenesis in cells, but what is known is that mutation within the bromodomains of BAF180 could lead to loss of function of the protein itself, potentially resulting in the onset of cancer (Brownlee, Chambers et al. 2012).

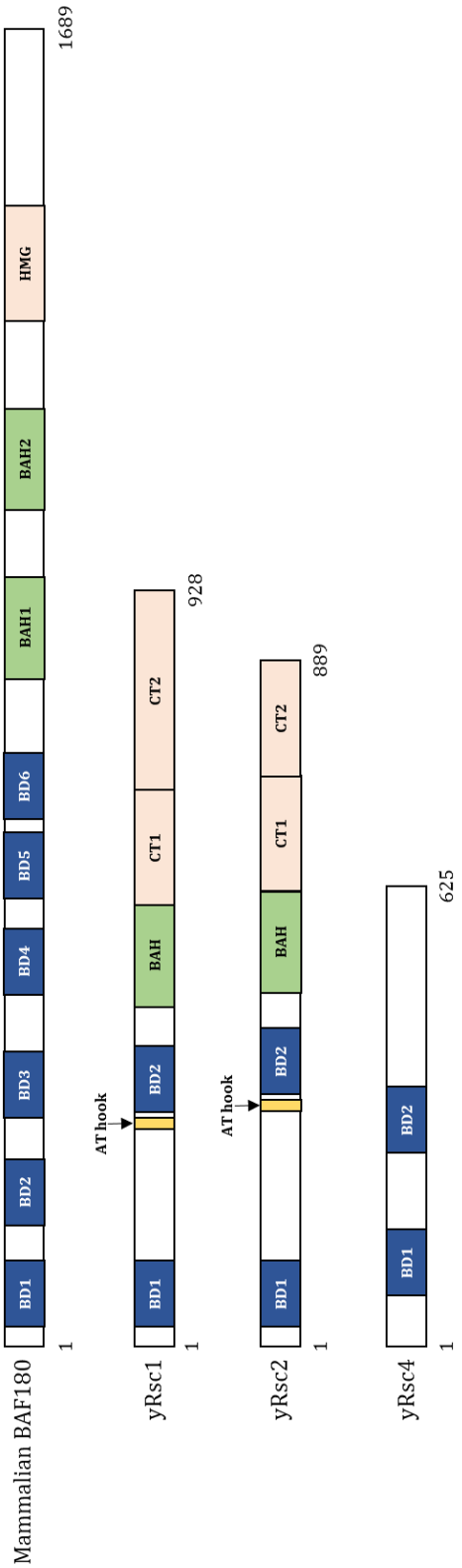

Figure 1.13. Mammalian BAF180 is homologous to Rsc1, 2 and 4 – Adapted from (Cairns, Schlichter et al. 1999, Brownlee, Chambers et al. 2012).

1.5.2. BAF180 and DNA damage

It was shown recently that the yeast homolog of BAF180, Rsc2, has a role in repriming stalled replication forks at sites of damage (Niimi, Chambers et al. 2012). DNA lesions, such as damaged bases, block DNA polymerases and in order to bypass the lesion, traditional DNA polymerases must be replaced for a group of specialised translesion synthesis (TLS) polymerases (Lehmann, Niimi et al. 2007). Mono-ubiquitination of PCNA is required for this switching from replicative to TLS polymerases at stalled replication forks (Lehmann, Niimi et al. 2007). RSC2 deletion, but not deletion of RSC1, results in a significant reduction in PCNA ubiquitination after DNA-damage caused by UV irradiation, or treatment with either HU or MMS (Niimi, Chambers et al. 2012). It was also found that siRNA depletion of BAF180 after DNA-damage with UV-irradiation, resulted in a reduction of PCNA ubiquitination as well as unmodified chromatin-associated PCNA and the STUbL E3 ligase that ubiquitinates PCNA, Rad18 (Niimi, Chambers et al. 2012). Interestingly, we recently found that specifically, the BAH domains of BAF180 are required for the ubiquitination of PCNA (Niimi, Hopkins et al. 2015).

Another role for BAF180 in the DNA damage response was shown by recent work in our lab. The PBAF complex, which uniquely harbours the BAF180 subunit, was identified as important for DSB-induced transcriptional silencing (Kakarougkas, Ismail et al. 2014). PBAF also promotes repair of a subset of DNA DSBs at early time points, which can be rescued by inhibiting transcription globally. Phosphorylation of BAF180 is required for both processes (Kakarougkas, Ismail et al. 2014). Transcription is repressed in response to a DSB in an ATM-dependent manner and leads to H2A monoubiquitination at Lysine 119 (H2-K119ub) (Shanbhag, Rafalska-Metcalf et al. 2010). H2A-K119ub levels are dependent on the PBAF complex and therefore could mediate the regulation of H2A-K119ub at both sites of damage as well as transcription repression (Kakarougkas, Ismail et al. 2014). Work from other members in our lab had previously identified two cancer-associated mutations of BAF180, which were found to not de-stabilise the protein (Brownlee, Chambers et al. 2014). In context

of transcriptional repression, these BAF180-mutants were unable to restore the ability of BAF180-depleted cells to repress transcription-flanking DSBs or promote efficient repair at early time points (Kakarougkas, Ismail et al. 2014). This data suggests that PBAFs role in repressing transcription near DSBs may contribute to its tumour suppressor activity.

The yeast homologues of BAF180, Rsc1 and Rsc2, have been shown to have defects in HR-dependent DNA repair (Chai, Huang et al. 2005, Oum, Seong et al. 2011). The RSC complex was found to physically interact with the recombination protein Rad59 and functions in HR (Oum, Seong et al. 2011). Studies have revealed that RSC is required for recombination between sister chromatids by its ability to promote sister chromatid cohesion by the recruitment of cohesin at DNA break sites (Oum, Seong et al. 2011). The defective sister chromatid HR at double strand break sites, in Rsc2 mutant cells specifically, is thought to be due to impaired accumulation of DSB-induced cohesin at the break (Oum, Seong et al. 2011). It is possible that mammalian BAF180, like its yeast homologues, cooperates with cohesion factors to facilitate cohesin-dependent HR.

Before this study, work in our laboratory had previously never directly looked at BAF180's role in HR. However, BAF180 was found to be hypersensitive to mitomycin C (MMC), resulting in increased levels of structural chromosome aberrations after treatment. This mimics phenotypes seen in cells with defects in HR or cohesin subunits after MMC treatment (Brownlee, Chambers et al. 2012). We can infer from this that BAF180 may have a role in HR-dependent DNA repair.

1.5.3. BAF180 and the PBAF complex have a role in sister chromatid cohesion

Work in our lab has recently identified a transcription-independent role for BAF180 in promoting sister chromatid cohesion (Brownlee, Chambers et al. 2014). Sister chromatid cohesion is dependent on the activity of several regulatory factors, including the cohesin loader components Scc2 and Scc4 and the cohesion establishment factors Eco1, Scc3, Pds5 and Wapl. In mammalian

cells, Scc3 homologs are SA1 (STAG1) and SA2 (STAG2), Eco1 homologs are ESCO1 and ESCO2 and Pds5, whose homologs are PDS5A and PDS5B. SA1, ESCO2 and PDS5B are thought to promote cohesion, specifically at pericentromeric regions (Canudas and Smith 2009, Whelan, Kreidl et al. 2012, Carretero, Ruiz-Torres et al. 2013). Chromosome biorientation and segregation is reliant on centromeric cohesion and defects here result in aneuploidy, defined as the presence of an abnormal number of chromosomes in a cell, a typical characteristic of cancer cells.

In yeast, interactions have been found to occur between genes involved in sister chromatid cohesion and the Rsc2 gene (Chambers and Downs 2012). Furthermore, studies have shown that when looking at Rsc1 and Rsc2 deletion strains in G2 phase of the cell cycle, increased separation of sister chromatids can be observed as well as a greater tendency to lose chromosomes in comparison to a wild type strain (Chambers and Downs 2012). There is evidence showing an interaction between the cohesin complex and RSC, however it a matter of debate as to whether RSC's role in sister chromatid cohesion is during loading of cohesin or the establishment of cohesion (Chambers and Downs 2012).

Loss of BAF180 in mouse and human cells results in defective sister chromatid cohesion at the centromeric locus, as opposed to chromosome arms, implying that BAF180 specifically regulates centromere cohesion (Brownlee, Chambers et al. 2014). This study also found increased levels of micronuclei formation, abnormal anaphase events and aneuploidy associated with BAF180-depletion. This suggests both chromosome instability (CIN) and consequently genome instability after the loss of BAF180-mediated centromere cohesion (Brownlee, Chambers et al. 2014).

BAF180 is known to localize to the kinetochores of mitotic chromosomes and it has been implied that BAF180 therefore plays a role there during mitosis (Xue, Canman et al. 2000). In yeast, there is evidence showing that chromosome kinetochores can promote cohesin loading by Scc2-Scc4 (Natsume, Muller et al. 2013). We can hypothesise that PBAF, via BAF180s localisation to kinetochores, may in turn aid cohesin loading.

1.5.4. Transcriptional roles for BAF180

BAF180 is thought to contribute to transcriptional regulation by altering chromatin structure and controlling the accessibility of DNA (Thompson 2009). p53 is a well characterised tumour suppressor protein whose normal activity prevents tumorigenesis. It is well known as a transcription factor that regulates the expression of many genes involved in apoptosis, genome stability and angiogenesis. Recently it was demonstrated that PBRM1 regulates p53 function by influencing p53 transcriptional activity and is required for p53-induced senescence and proper p21 expression (Xia, Nagase et al. 2008, Burrows, Smogorzewska et al. 2010, Macher-Goeppinger, Keith et al. 2015). It was suggested that BAF180 acts together with BRD7 to promote p53 transcriptional activity directed towards a plethora of target genes and that loss or disruption of the PBAF complex results in compromised p53 function (Burrows, Smogorzewska et al. 2010).

Another transcriptional role for BAF180 is seen in association with p21, BAF180 has been described as a physiological mediator of p21 expression (Xia, Nagase et al. 2008).

BAF180 has also been found to interact with the bromodomain containing 1 (BRD1) gene, which is implicated with transcriptional regulation, brain development and susceptibility to schizophrenia and bipolar disorder (Fryland, Christensen et al. 2016).

1.5.5. BAF180 is frequently mutated in human cancers

Truncating mutations in PBRM1 that abrogated protein expression, were first identified in breast cancer in a screen for novel breast cancer tumour suppressor genes (Xia, Nagase et al. 2008). They identified four truncating mutations in the bromodomains of BAF180 that were associated with loss of wild-type BAF180. Microsatellite markers that flank the locus of BAF180 on 3p21 were used to screen tumour samples and of the 52 samples tested, 48.1% (25 samples) had

BAF180 loss of heterozygosity, suggesting that BAF180 loss may contribute to tumour progression (Xia, Nagase et al. 2008). In addition to this study, further work has identified low PBRM1 expression in breast cancer tissues, correlating with more advanced tumour stage, lymph node metastasis and lower overall survival (OS) for patients compared to those with higher PBRM1 levels. This data strengthens the argument for BAF180 acting as a tumour suppressor in breast cancer and identifies the potential as a valuable prognostic marker (Mo, Li et al. 2015).

Although the first BAF180 cancer mutations were identified in breast cancer, arguably the most influential study in regards to BAF180 cancer mutations was carried out by Varela et al, identifying BAF180 truncating mutation in a striking 41% of clear cell renal cell carcinoma (ccRCC) (Varela, Tarpey et al. 2011). In this study exome sequencing was used to elucidate the mutation spectrum of seven ccRCCs, in which four cases presented with truncating mutations in PBRM1, three of which were frame-shift insertions and the fourth being a nonsense mutation. They next sequenced a further 257 cases of RCC, which included 36 cases of papillary chromophobe and other non-ccRCC cancers, finding PBRM1 truncating mutations in 88/257 (34%) cases, all of which were from the 221 ccRCC tumour samples. In 38 tumours sequenced, PBRM1 mutations were all found in the context of chromosome 3p loss of heterozygosity (LOH). ccRCC tumours with PBRM1 mutations were also frequently found to have mutations in VHL (Varela, Tarpey et al. 2011). Of the 38 PBRM1-mutant tumours studied, 36 exhibited a hypoxia signature, which is often linked to loss of VHL, however this signature was found in cases that did not have a detectable VHL mutation (Varela, Tarpey et al. 2011). Increased proliferation was observed in four out of five RCC cell lines after PBRM1 siRNA knockdown. The cell line with the outlying result was found to have a homozygous truncating mutation in PBRM1 and had no PBRM1 protein expression (Varela, Tarpey et al. 2011), this was the RCC cell line A704, which we have subsequently used in our study. Knockdown of PBRM1 was also associated with increased colony formation potential in soft-agar and increased cell migration, suggesting an increase in transformed phenotype (Varela, Tarpey et al. 2011).

In a panel of 727 cancer cell lines, with various histologies, exome sequencing was carried out to elucidate PBRM1's contribution in other cancers. Congruent to the study carried out by Xia et al, PBRM1 homozygous deletion was found in the HCC-1143 breast cancer cell line (Xia, Nagase et al. 2008). Five homozygous truncating mutations in PBRM1 were identified in this study, including a frame shift deletion in the RCC line, A704, the small-cell lung cancer cell line NCI-H2196 and the gall bladder cancer cell line TGBC24TKB. Nonsense mutations were found in two lines, the squamous-cell lung cancer cell line NCI-H226 and the pancreatic adenocarcinoma line PANC-10-05 (Varela, Tarpey et al. 2011).

In addition to the data put forward by Varela et al, multiple other studies have linked PBRM1 mutation with loss of tumour suppressor activities in multiple cancers.

PBRM1 maps to chromosome 3p21, interestingly, structural abnormalities were also frequently detected in this region in bladder cancers (Abat, Demirhan et al. 2014). In a study by Huang et al, PBRM1 was found to be downregulated in bladder cancer cell lines and was associated with shorter overall survival in bladder cancer patients (Huang, Peng et al. 2015). They also found that PBRM1 induced G2 cell cycle arrest by repressing cyclin B1 and suggest that it is this PBRM1-dependent block of the G2/M transition that allows PBRM1 to function as a tumour suppressor in bladder cancer (Huang, Peng et al. 2015).

Recently PBRM1 mutations were also identified in a study of 68 diffuse large B-cell lymphomas (Morin, Mendez-Lago et al. 2011, Pasqualucci, Trifonov et al. 2011, Lohr, Stojanov et al. 2012), as well as in a sample of head and neck cancers (Agrawal, Frederick et al. 2011, Stransky, Egloff et al. 2011). Truncating mutations in PBRM1 were also reported in a mutational screen of pancreatic cancers (Jones, Zhang et al. 2008).

To conclude, while it is not known the exact mechanism by which BAF180 functions in cell biology, we do know that loss of this protein impacts on repair, replication, cohesion, DNA-damage induced transcriptional silencing and regulation of gene expression. The impairment of these factors, together with the wide mutation spectrum of BAF180 in human cancers, solidifies the notion that BAF180 is an important tumour suppressor gene. In this work we will discuss

how we have tried to exploit BAF180's mutational status, specifically in ccRCC, to identify novel opportunities for therapeutic intervention.

1.6. Synthetic Lethality and Cancer Therapy

The identification of chemical compounds that will kill cancer cells has never been a barrier to the progression of medical oncology. The challenge we are faced with instead, is how to use these identified chemical compounds at concentrations that will specifically target cancer cells, without effecting healthy cells. Traditional chemotherapeutic drugs aim to damage rapidly dividing cells, which encompasses cancer cells rather than normal non-cancer cells. However, some normal cells such as skin, hair and the healthy lining of the digestive system, can also rapidly divide and be at risk of damage from these non-specific agents. Most clinically available chemotherapeutic agents have limited efficacy for late stage patients and are associated with toxic side effects, such as hair loss and severe sickness (Chan and Giaccia 2011). A challenge facing current chemotherapies is in finding the concentration of drug needed to produce a therapeutic effect, while also taking in to consideration that high drug concentrations cause unwanted toxicity. Finding this perfect balance is known as the therapeutic window, which is often very narrow in current chemotherapeutics. Thus, there is a clear unmet clinical need for the development of new anti-cancer agents and the concept of synthetic lethality could provide scaffolding for the development of new, more cancer-cell-specific, cytotoxic agents.

1.6.1. Synthetic Lethality

The concept of synthetic lethality was first described in the fruit fly *Drosophila melanogaster* by Dobzhansky in the 1940's, where he found that mutations in two different genes could promote a synthetic lethal interaction (Dobzhansky 1946). Two genes are typically referred to as 'synthetic lethal' if a mutation in both leads to cellular death, but mutation in either of the genes alone is consistent with viability (Hartwell, Szankasi et al. 1997, Hartman, Garvik et al. 2001, Kaelin 2005, Boone, Bussey et al. 2007). This type of interaction can also exist in an

intermediate state, where mutation in two genes result in a non-lethal impaired growth phenotype, referred to as 'synthetic sickness' (Kaelin 2005). Identification of a synthetic sick interaction between two genes can further be enhanced by acquiring additional mutations in one or more non-essential genes (Canaani 2014). The terms synthetic lethality and synthetic sickness are generally grouped together to encompass a broader definition of synthetic lethality as a whole. Under this more general description of synthetic lethality an identified pair of synthetic lethal genes may actually only cause a partial, rather than a total decrease in viability. There are three different mechanisms in which synthetic lethal genes interact to cause cellular lethality. Firstly, mutation of two genes in one essential pathway can result in synthetic lethality. Secondly, synthetic lethality can occur if two genes that exist in parallel pathways were mutated, consequently hindering the formation of an essential product that would normally arise from both functional pathways. Finally, a mutation in two genes that are located on two independent survival pathways can also result in synthetic lethality (Canaani 2014).

Synthetic lethality typically describes two genetic perturbations, however, a revolutionary hypothesis by Hartwell and Friend in the 1990's has allowed us to broaden the scope of this phenomenon to include cellular synthetic lethality caused by a combination of a genetic mutation, for example loss of a tumour suppressor gene and chemical inhibition (Hartwell, Szankasi et al. 1997). It was this revelation that revealed the potential exploitation of chemical and genetic synthetic lethal screening for the development of new therapeutics/drug targets for cancer therapy. To date, multiple synthetic lethal screens have been performed in various model organisms, such as *Saccharomyces cerevisiae* (Bender and Pringle 1991), *Drosophila* (Lucchesi 1968) and human cancer cell lines e.g. (Bryant, Schultz et al. 2005, Farmer, McCabe et al. 2005, Helleday 2011). The use of screens like these to identify new synthetic lethal interactions is on track to becoming advanced enough to identify interactions in specific cancer types and even individual tumours, a progression within the field that would be an invaluable addition to therapeutic decision making.

1.6.2. Exploration of synthetic lethal interactions in Saccharomyces cerevisiae

In the study of synthetic lethal gene interactions, a well characterised model organism is the budding yeast, *S. cerevisiae*, having been examined on a genome-wide scale. This high-throughput survey of synthetic lethal interactions in *S. cerevisiae* has led to the discovery of multiple genetic interaction networks and allowed for a more diverse functional annotation of multiple genes (Pan, Ye et al. 2006, Hillenmeyer, Fung et al. 2008, Lin, Qi et al. 2008, Costanzo, Baryshnikova et al. 2010, Nijman 2011). For example, *RSC1*, which is known to be an important factor in transcriptional regulation, was subsequently found to be required for chromosome stability (Measday, Baetz et al. 2005).

In yeast, the evolution of high-throughput screening for synthetic lethality has been facilitated by the development of synthetic genetic array (SGA) analysis (Tong, Evangelista et al. 2001). Tong and Boone carried out the first example of SGA analysis of high-throughput synthetic lethal screening in 2001; they used two individually viable mutants and showed that when mutated together the result was a substantial fitness defect. It was found that genes were more likely to exhibit synthetic lethal phenotypes if the mutated genes were located in either the same essential pathway or two parallel non-essential pathways (Tong, Evangelista et al. 2001). They extrapolated data between two gene sets, identifying the number of genetic interactions and used statistical analysis to organise genetic interaction networks (Tong, Evangelista et al. 2001, Lin, Qi et al. 2008). The evolvement of this type of screening and analysis has expanded our knowledge of DNA integrity and the understanding of functional relationships among different processes (Pan, Ye et al. 2006), as well as broadening our assessment of post-translational modifications of histones (Lin, Qi et al. 2008) to name a few contributions. Whether using yeast gene interactions, as a prediction of synthetic lethality in higher eukaryotes is actually accurate and useful, remains unclear. There is debate to whether the general lack of conservation of synthetic lethal interactions is due to technical limitations, or the fact that some interactions may only be conserved in certain biological processes (Nijman 2011).

However, there are examples where yeast genetic interactions have been successfully translated in to mammalian cells (Yu, Lopez et al. 2008, Conde-Pueyo, Munteanu et al. 2009, McLellan, O'Neil et al. 2009, McManus, Barrett et al. 2009), so it suggests that even if it does come with limitations, there is some level of conservation between the two organisms.

1.6.3. Identification of human synthetic lethal interactions

BRCA1/2 and PARP have a robust and reproducible synthetic lethal phenotype

Hartwell and Friend's proposal that exemplified the possibility of a synthetic lethal interaction between a genetic mutation and chemical inhibition facilitated a plethora of research in the mammalian model (Hartwell, Szankasi et al. 1997). The first model and to date the most striking example of this hypothesis coming to fruition lies in the synthetic lethal interaction found between BRCA1/2-deficient tumours and Poly(ADP-Ribose) polymerase (PARP) inhibition (Bryant, Schultz et al. 2005, Farmer, McCabe et al. 2005, Helleday 2011).

The tumour suppressor genes BRCA1 and BRCA2 are involved in the repair double strand breaks (DSB's) by Homologous Recombination (HR) (Tutt and Ashworth 2002), mutation or loss of these genes in mammalian cells can lead to an increased incidence of breast, ovarian, prostate and other cancers (Canaani 2014). PARP is an enzyme known to be involved in the repair single strand breaks (SSBs) (Strom, Johansson et al. 2011). If something goes awry in the repair of these SSBs, either naturally or by PARP inhibition, then at the point of DNA replication, the persistence of these unrepaired SSBs at replication forks will cause the fork to collapse and allow the SSBs to be converted to DSBs. The DSBs will subsequently be repaired by HR (Underhill, Toulmonde et al. 2011). It is thought that mechanistically, BRCA1/2-deficient tumours are synthetic lethal with PARP inhibition as a consequence of both the single strand break repair pathway and the HR pathway being compromised (Bryant, Schultz et al. 2005, Farmer, McCabe et al. 2005). After treatment with PARP inhibitors in BRCA1/2-deficient tumours, it is postulated that the DSBs that arise aren't able to be

repaired by HR and instead are repaired, for example via NHEJ, a process by which several chromatid aberrations are gained, ultimately resulting in cell death (Underhill, Toulmonde et al. 2011). Pre-clinically, as a 'proof of principle' different examples of BRCA-deficient cell lines and even mouse xenografts have been demonstrated to be sensitive to PARP inhibition (Bryant, Schultz et al. 2005, Farmer, McCabe et al. 2005). Consequently, the synthetic lethal relationship between BRCA1/2 and PARP was the first to be determined in mammalian cells and exploited clinically for cancer therapy as both a PARP1-inhibitor single agent or in combination with classical chemotherapies.

Other examples of synthetic lethality

Like BRCA1/2, other genes involved in HR or the DNA damage response (DDR) have been identified as sensitive to treatment with PARP inhibitors. For example; RAD51, ATM, ATR, ATRX, NBN, CHK1, CHK2, SHFM1, RPA1, mir-182, SWI5-SFR1, USP1/UAF1, CDK1, PTEN1, TMPRSS2-ERG fusion, PDS5B, as well as several Fanconi anemia proteins (Xia, Sheng et al. 2006, Lord and Ashworth 2012, Papeo, Casale et al. 2013, Canaani 2014).

The term 'BRCAness' has been adopted to describe some genes that have phenotypic traits mimicking tumours with BRCA1 and BRCA2 mutations and can be defined as a defect in double strand break repair by HR. This state of BRCAness can be induced by various tumour-specific genetic or epigenetic signatures, for example blocking sites of ubiquitination at DNA damage contributes to the proapoptotic phenotype induced by proteasome inhibitors. Proteasome inhibitors can decrease nuclear foci formation of DNA damage response molecules like RAD51, due to defective ubiquitination. These changes together can inforce this state of BRCAness (Jacquemont and Taniguchi 2007).

Oncogenic drivers, such as KRAS and MYC can also be targeted by synthetic-lethality approaches, where previously they were not thought to be 'druggable'. In a recent study, oncogenic mutations in KRAS were shown to exhibit synthetic lethality after topoisomerase inhibition (Steckel, Molina-Arcas et al. 2012) and Myc-driven cancers are found to have a synthetic lethal interaction with

mammalian target of rapamycin (mTOR)-dependent phosphorylation of eukaryotic translation initiation factor 4E binding protein-1 (4EBP1) (Pourdehnad, Truitt et al. 2013). These unique identifications are providing novel therapeutic approaches to make these commonly deregulated oncogenes druggable in the clinic.

Interestingly, synthetic lethal gene targets for VHL-mutant cancers have been identified recently in a shRNA synthetic lethal screen. As mentioned previously, VHL is the most frequently mutated gene in ccRCC, with BAF180 (PBRM1) being the second. A screen of 100 shRNA vectors, targeting 88 kinases, was performed to identify synthetic lethal 'hits' that inhibit viability of VHL-/- renal carcinoma cells. This screen identified multiple hits including CDK6, MET and MAP2K1 (MEK1) and found that small molecule inhibition of Cdk4/6 had preferential activity against VHL-/- renal carcinoma cells (Bommi-Reddy, Almeciga et al. 2008). This suggests that shRNA screening for synthetic lethality has the potential to identify novel therapeutic targets.

1.6.4. Limitations and translational challenges

Excluding the translation of the BRCA/PARP interaction from hypothesis to clinical therapy, there have been very few other interactions that have successfully progressed from discovery to the clinic. For several years we have had extensive knowledge of synthetic lethal interactions in mammalian cells, and though progress has been relatively slow, there are still endless interactions to be exploited and great potential for valuable therapeutic elucidation of these relationships.

One of the contributing factors to this slow progression is the lack of potent inhibitors that are specific to a single target and that are cell permeable (Fece de la Cruz, Gapp et al. 2015). Most chemical inhibitors have a broad spectrum of potential cellular targets (Lehar, Stockwell et al. 2008), so regardless of an impartial, systematic approach to identifying targets, actually targeting them with available inhibitors in a gene-specific manner is a challenge. There is a very

real concern that genetic synthetic lethal interactions may never have pharmacological representation (Nijman and Friend 2013).

Another factor that hinders the translation of synthetic lethal interactions is our restricted understanding of how they are influenced by the tumour microenvironment, along with genetic and epigenetic variation (Nijman and Friend 2013). Most cancers do not harbour just one mutation, there are generally multiple driver and passenger mutations that contribute to tumour progression (Pon and Marra 2015) and therefore it is important to take in to account the context of the molecular heterogeneity that is exhibited in individual cancers when treating therapeutically. A good example of where looking at the overall context of the tumour has paid off in the clinic is in colon cancer cells that harbour mutations in the BRAF gene. These cancers do not respond to BRAF inhibitors and are not targetable by chemical inhibition. However, it was found that these cancers deterred the effects of BRAF inhibition by a feedback mechanism that promotes signalling by the epidermal growth factors and therefore could be successfully treated with a combination of BRAF and epidermal growth factor inhibitors (Corcoran, Ebi et al. 2012, Prahallad, Sun et al. 2012, Nijman and Friend 2013).

It will be advantageous to develop a broader understanding of how synthetic lethal interactions are influenced by multiple factors, rather than to just rule out interactions because they do not immediately validate with a single drug. In turn, this gained knowledge of tumour context should progress target validation as well as allow for the development of better biomarkers and will pave the way for precision therapy.

1.7. PolyADP-Ribose Polymerase (PARP)

When a target protein is modified with monomeric, short chains, or long branching chains of ADP-ribose (ADPR), it is a post-translational modification known as ADP-ribosylation, which can be carried out by various ADP-ribosyltransferases and polymerases (ADP-RTs and PARPs.

Poly(ADP-ribose) polymerases (PARPs) are enzymes that can transfer these poly(ADP-ribose) (PAR) groups to themselves as well as to target proteins and function within the DNA damage network (Dantzer and Santoro 2013). When DNA damage occurs, poly(ADP)ribosylation is rapidly catalysed by poly(ADP-ribose) polymerases (PARPs) at DNA lesions and it is this which subsequently facilitates DNA damage repair (Li and Yu 2015). The modifications formed by PARPs are known to be involved in a number of functions in the DNA damage response, such as detection and signalling of DNA damage, chromatin relaxation, recruitment of DNA repair factors, repair of the lesion and restoration of chromatin structure (Figure 1.14) (Curtin and Sharma 2015).

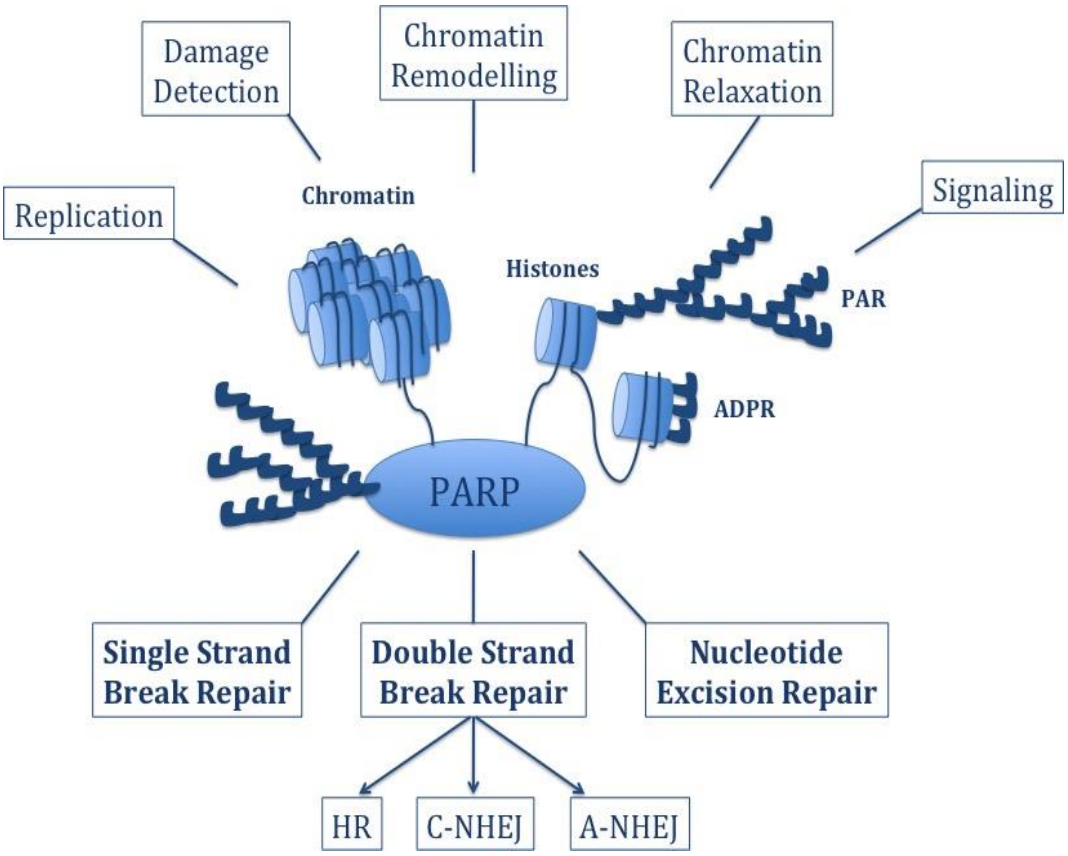

Figure 1.14. PARP affects many cellular processes. The DNA repair process is affected by the post-translational modification of PARPs and other chromatin components by mono (ADP-ribose) (ADPR) or poly (ADP-ribose) (PAR)

1.7.1. The PARP superfamily

Members of the PARP family can be found across a wide range of species and domains and have a conserved function as essential molecules from lower to higher eukaryotes. ADP-ribosyltransferases (ARTs) possess the ability to transfer ADP ribose groups from nicotine adenine dinucleotide (NAD^+) on to a single or multiple charged amino acids found on target proteins (Curtin and Sharma 2015). Specifically poly(ADP-ribosyl)ation of nuclear proteins can establish a molecular link between DNA damage and chromatin modification after DNA damage. Advancements in genome sequencing and improved genetic approaches illuminated the possibility that there was more than one enzyme involved in the conversion of NAD^+ to ADP-ribose polymers. To date there are at least eighteen proteins that contain PARP domains (Ame, Spenlehauer et al. 2004), however only 6 of these are known to have predicted or confirmed PARP activity, in which they are able to form short (oligomers) or long chains (polymers) of poly ADP-ribose (PAR) extending from the surface of the target protein (Curtin and Sharma 2015). Differences found in core motifs of the catalytic domains of these proteins account for the differences in catalytic activity (Kleine, Poreba et al. 2008).

Polymerase activity is initiated when a PARP protein binds to a free end of DNA, this allows PARP to auto-ribosylate itself and/or trans-ribosylate target proteins, which includes histones and DNA repair factors that are in close proximity to the break (Curtin and Sharma 2015). Of the six PARP proteins that are thought to have PARP activity, only three are able to bind DNA, PARP1, PARP2 and PARP3 (Curtin and Sharma 2015). The DNA binding capability of these three proteins comes from their N-terminal DNA binding domains and WGR domains that reside close to their catalytic domains (Langelier, Planck et al. 2012).

The catalytic core domain of PARPs 1, 2 and 3, which is comprised of a triad of histidine, tyrosine and glutamate residues is conserved (Johansson 1999, Kleine, Poreba et al. 2008, Langelier, Planck et al. 2012). This conservation is particularly strong in the pocket within the catalytic core that coordinates the NAD^+ substrate and it is this that is targeted by many PARP inhibitors, which act by providing a block for NAD^+ binding (Clark, Ferris et al. 1971, Johansson 1999).

Although there is strong conservation between PARPs 1, 2 and 3, there is also notable variations found in the sequences of the N-terminal binding domains, which subsequently allows each PARP to react differently to stimulation from different substrates (Johansson 1999).

As well as variations in the N-terminal domains, the length of poly ADP-ribose polymers produced by the different PARPs, while being chemically very similar, can vary greatly. For example, PARP3 typically uses mono ADP-ribose to modifiy proteins, but it is also known to generate short chains (Johansson 1999, Ame, Spenlehauer et al. 2004, Rulten, Fisher et al. 2011). However, it is still not known how polymer length, or the consequences that follow, are regulated *in vivo* and why (Hakme, Wong et al. 2008).

To date, there is a vast amount of evidence that various cellular and physiological processes are influenced by the biological properties of different PARPs (De Vos, Schreiber et al. 2012). Localisation of PARP family members to a multitude of cellular components, which include the nucleus, cytoplasm, mitochondria and vault particles, have been identified, however the function of all of the known PARPs is still to be determined (Ame, Spenlehauer et al. 2004, Hassa and Hottiger 2008). Members of the PARP family that localise primarily to the nucleus are PARPs 1, 2 and 3, as well as tankyrase 1 and 2 (aka. PARP-5a and -5b) (Schreiber, Dantzer et al. 2006, Hassa and Hottiger 2008). Other family members such as v-PARP (PARP-4), PARP-6, PARP-8, PARP-9, PARP-10 and the Bal proteins Bal1-3 (PARP-13, -14, -15) can too be found in the nucleus, however they are not restricted here (Krishnakumar and Kraus 2010).

The incredibly varied interaction between PARP family members with multiple processes gives rise to a plethora of biological outcomes, that include but aren't limited to, differentiation, development, stress responses, inflammation and cancer and therefore makes them an attractive family of proteins to research (Krishnakumar and Kraus 2010).

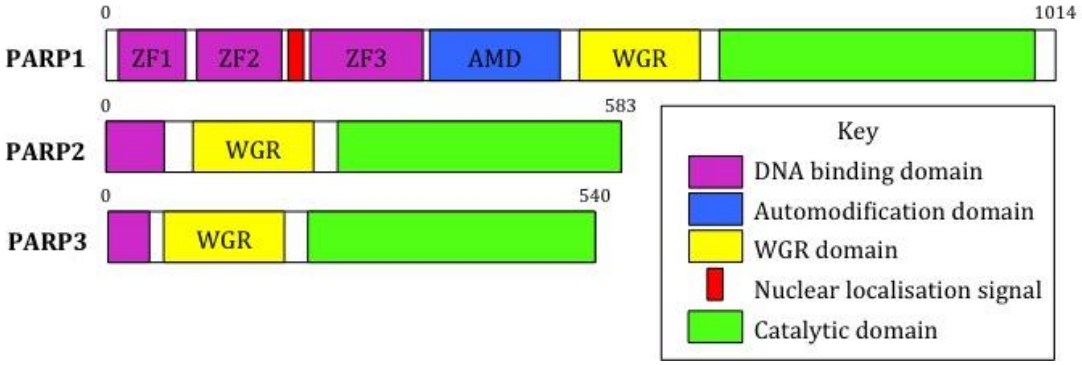

Figure 1.15. Functional domains of the key PARPs. Adapted from Rulten *et al* chapter within (Curtin and Sharma 2015).

1.7.2. PARP1

The 113-kDa human protein, PARP1, is a nuclear enzyme involved in the detection of DNA strand breaks and is the founding member of the PARP superfamily.

The most abundant and active of the three DNA-binding PARPs, PARP1 and its activation have been associated with acting downstream of multiple processes, including chromatin remodelling, transcription and telomere maintenance. PARP1 is thought to have an important role in DNA damage signalling and accelerating single strand break repair (SSBR) (Sanderson and Lindahl 2002, Fisher, Hochegger et al. 2007). It is a stable component of chromatin and accounts for 80-90% of the detectable PAR signal following DNA damage (Mullins, Giri et al. 1977, Giri, West et al. 1978, Lindahl, Satoh et al. 1995). The N-terminal domain of PARP1 is responsible for its initial recruitment to sites of DNA damage, binding to this damage, whether it be a single strand or double strand break, its mediated by the two zinc fingers in this N-terminal domain. These zinc fingers also allow for the dimerization of PARP1 (Ali, Timinszky et al. 2012).

Other repair factors are allowed to bind to sites of DNA damage after the dissociation of PARP1 from the break, this dissociation is an important step in the repair process that is mediated by auto-ribosylation of PARP1 with negatively charged PAR (Ferro and Olivera 1982, Zahradka and Ebisuzaki 1982). DNA binding and auto-modification of PARP1 attracts DNA repair proteins involved in SSBR, such as XRCC1, to the sites of damage, but is not thought to be essential for SSBR (de Murcia, Niedergang et al. 1997, Wang, Stingl et al. 1997, Shall and de Murcia 2000, El-Khamisy, Masutani et al. 2003). Recruitment of XRCC1 then acts as a scaffold for the further recruitment of other repair factors such as the end processing factors PNKP and Aprataxin and the chromain remodelers APLF and ALC1. Ligation of the repaired break is carried out by DNA ligase IIIα, which forms a heterodimer with XRCC1.

PARP1 also binds to double strand breaks (DSBs) and has been implicated in several pathways that mediate DSB repair. The homologous recombination (HR) pathway, as described in section 1.1.3.2 uses the intact sister chromatid as a

template for repair. Loss or inhibition of PARP1 is able to induce a hyper-recombination phenotype, presenting as spontaneously increased levels of sister chromatid exchange (SCE). Conversely, overexpression of PARP1 can suppress DNA damage-induced SCEs, suggesting the presence or absence of PARP1 is able to influence HR (de Murcia, Niedergang et al. 1997, Meyer, Muller et al. 2000). HR accessory factors, including breast cancer type 1 susceptibility protein (BRCA1), which forms a heterodimer with BRCA1-associated RING-domain protein 1 (BARD1), can be recruited to sites of damage by PARP1 to accelerate repair (Li and Yu 2013, Curtin and Sharma 2015). PARP1 can also recruit the RNA-binding motif protein X-linked (RBMX) to sites of damage, positively regulating HR by the stabilisation of breast cancer type 2 susceptibility protein (BRCA2) (Adamson, Smogorzewska et al. 2012).

1.7.3. PARP2

PARP2 was first identified after the embryonic fibroblasts derived from PARP1 deficient mice showed signs of residual DNA-dependent PARP activity (Shieh, Ame et al. 1998, Ame, Rolli et al. 1999). PARP2 is thought to have a key role in genome surveillance and protection and has been implicated in numerous cellular functions, which include genome and chromosome stability, heterochromatin integrity, cell death, differentiation and inflammation (Yelamos, Schreiber et al. 2008). Mammalian PARP2 is a 66.2kDa protein, with a catalytic domain that is 69% similar to that of PARP1 (Ame, Rolli et al. 1999, Oliver, Ame et al. 2004). Like PARP1, PARP2's catalytic activity is stimulated by the presence of DNA strand breaks. Their targets, which include histones, DNA repair proteins and transcription factors, as well as themselves via auto-ribosylation, suggest they have a strong involvement in chromatin structure and DNA metabolism (Schreiber, Dantzer et al. 2006).

PARP2 produces PAR that is of similar length and composition to PARP1, but it much less catalytically active, working at a rate of around 10-25% compared to PARP1 activity (Ame, Rolli et al. 1999). Similarly to PARP1, PARP2 is able to bind

DNA, with a functional DNA binding domain located at its N-terminus, together with a nuclear localisation signal (Shieh, Ame et al. 1998, Ame, Rolli et al. 1999, Leger, Bar et al. 2014).

The DNA binding domain of PARP2 has similar homology to SAP domains that can be found in numerous nuclear proteins, such as AP-endonuclease and Ku70, which are known to be involved in chromosomal organisation and DNA repair (Aravind and Koonin 2000).

PARP2 is able to form a homodimer with itself as well as a heterodimer with PARP1 and each protein can poly(ADP-ribosyl)ate the other (Schreiber, Ame et al. 2002). In PARP1 deficient systems, it is thought that PARP2 activity could compensate for this PARP1 loss, this is due to the proteins having similar targets as well as similar activity and profiles of stimulation (Curtin and Sharma 2015). As mentioned above, PARP1 and PARP2 have similar target proteins. Proteins involved in the base excision repair pathway, XRCC1 (x-ray cross complementing factor 1), DNA polymerase β and DNA ligase III, which are known partners of PARP1, have also been seen to interact with PARP2 (Schreiber, Ame et al. 2002). Like with PARP1, XRCC1 negatively regulates PARP2 activity as well as being a polymer acceptor for both PARP1 and PARP2 (Schreiber, Ame et al. 2002). To elucidate PARP2's role in the DNA damage response, Schreiber et al treated PARP2-deficient cells with the alkylating agent N-nitroso-N-methylurea (MNU) and subsequently saw a delay in the repair of breaks that was comparable to the delay seen in PARP1 deficient cells, suggesting that PARP2 has an active role in base excision repair (Schreiber, Ame et al. 2002).

It is worth mentioning that *PARP2*$^{-/-}$ mice, like *PARP1*$^{-/-}$ mice, are viable, however mice that are deficient in both genes are not, suggesting that there are overlapping essential development functions of PARP1 and PARP2 (Menissier de Murcia, Ricoul et al. 2003). Loss of PARP2 is also found to be embryonic lethal in mice in combination with ATM, where single deletion of each gene results in viable mice (Huber, Bai et al. 2004).

As mentioned, PARP2 appears to have many overlapping functions and target proteins with PARP1 and it has been stipulated that it may act in a compensatory

manner following PARP1 deletion. However, PARP1 and PARP2 deficient mice are known to also exhibit different developmental and immunological defects, which could indicate a role for PARP2 in its own specific pathways, independent of PARP1 (Yelamos, Schreiber et al. 2008, Robert, Dantzer et al. 2009).

1.7.4. PARP3

PARP3 has a mass of 60.1kDa and was first discovered by searching an expressed sequence tag library with the sequence of human PARP1, with an aim to identify novel proteins with related sequences (Johansson 1999). Structurally, PARP3 is similar to PARP2 (Figure 1.15) and has a conserved catalytic domain, as identified by crystal structure, that is similar to PARP1 and PARP2 (Ruf, Mennissier de Murcia et al. 1996, Oliver, Ame et al. 2004, Lehtio, Jemth et al. 2009). PARP3 also has a DNA binding domain at the N-terminus that is divergent to PARP1 and 2 and a WGR domain that is enriched with tryptophan, glycine and arginine (Dai, Rulten et al. 2015). In mammalian cells, two isoforms of PARP3 exist, that vary at the N-terminal domain by just seven amino acids and it is unknown if the two isoforms carry out different functions, only the short isoform is present in mice (Augustin, Spenlehauer et al. 2003).

PARP3 has diverse roles in multiple cellular processes, such as mitotic progression, maintenance of telomere stability and importantly in the damage response to repair DNA.

PARP3 is implicated in the base excision repair pathway, as well as NHEJ, through its interaction with several proteins (Rouleau, McDonald et al. 2007). The ADP-ribosyltransferase activity of PARP3 is thought to be able to be stimulated by DNA DSBs and has been shown to function together with APLF to promote NHEJ (Rulten, Fisher et al. 2011).

PARP3 also has roles in the stabilisation of the mitotic spindle and in telomere integrity by regulating the mitotic components NuMA and tankyrase 1 (Boehler, Gauthier et al. 2011). After DNA damage occurs, PARP3 is also thought to affect

the choice between repair by HR and NHEJ pathways by limiting DNA end resection (Beck, Boehler et al. 2014).

2 Materials and Methods

2.1. Materials

2.1.1. Mammalian expression plasmids

GIPZ lentiviral shRNA vectors

BAF180 and non-silencing control (NSC) GIPZ lentiviral shRNA vectors were purchased from Thermo Scientific and grown from glycerol stocks on LB (low salt) Ampicillin plates before isolating plasmid DNA using an EndoFree (Endotoxin-free) Maxi-prep kit (Qiagen). The purchased vectors contain TurboGFP fluorescent marker, which was switched out for either GFP or RFP(mCherry) with a nuclear localisation signal (NLS), using primers provided by Hung Quang Dang (as listed in Table 2.2). The GFP/NLS and mCherry/NLS PCR fusion products (as described in Figure 2.1) were cloned in to pGEM-T-Easy Vector acting as a holding vector to allow for amplification. Restriction enzymes XBaI/NotI and SpeI/NotI were used to insert the GFP/NLS and mCherry/NLS respectively in to the GIPZ shBAF180 and shControl vectors. The plasmids subsequently created were named shBAF180+GFP/NLS, shBAF180+mCherry/NLS, shNSC+GFP/NLS and shNSC+mCherry/NLS.

CRISPR Cas9 wild type/gRNA plasmids

Cas9 wild type/gRNA plasmids with five different guide RNA's were obtained from Horizon discovery as part of a free CRISPR guide program, coordinated by Chris Thorne, guide sequences as shown in Table 2.1. Due to low transfection efficiency of the Cas9/gRNA plasmids, co-transfection with a second plasmid with a selection marker was necessary. The pcDNA4-GFP-IRES-Puro plasmid was kindly provided by Prof. Keith Caldecott (University of Sussex).

Table 2.1. CRISPR Guide RNA's used in this study

Gene	Gene ID	Given Name	Sequence
PBRM1	153269	CRISPR Construct 1	ATAGAAGAAGTTGGATTCCA
PBRM1	153270	CRISPR Construct 2	CCCGCTGACACTGCTGGAAG
PBRM1	153271	CRISPR Construct 3	GGCCTGGTGTTGACACAGAA
PBRM1	153272	CRISPR Construct 4	AGGATCTACAGTTGGAAGAT
PBRM1	153272	CRISPR Construct 4	GGCAATCTACACATTAGCAA

2.1.2. Primers

Primers used in this study for cloning of GIPZ lentiviral shRNA vectors and for SURVEYOR mutation assay are shown in Table 2.2.

Table 2.2. Primers used in this study

Primer Name	Sequence
o417_pGIPZ-CMV-XbaI-F	ACGTGCTGCAGGTCCGAGGTTCTAGACGTATTACC
o418_pGIPZ-CMV-AcGFP-SpeI-R	GGTGGCAGAACTAGTTCCTCTAGTAGAGTCGGT
o419_pGIPZ-CMV-AcGFP-SpeI-F	ACCGACTCTACTAGAGGAACTAGTTCTGCCACCATGGT GAGCAAGGGCG
o420_pGIPZ-AcGFP-NotI-R	GGGGCGGAATTTGCGGCCGCTTATCTAGATCCGGTGGA TCC
o421_pGIPZ-mCherry-R1	CTTCTTTTTTGGATCAGCTCGAGATCTGAGTCCGGACT TGTACAGCTCGTCCATGCC
o422_pGIPZ-mCherry-R2	GGGCGGAATTTGCGGCCGCTTATACCTTTCTCTTCTTT TTTGGATCTACCTTTCTCTTCTTTTTTGGATCTACCTT TCTCTTCTTTTTTGGATCAGCTCG
F-CRISPR-1-4	CAAGGAAGTCCAGGGCTTA
R-CRISPR-1-4	TTGTTTCCACATGGCTATATCC
F-CRISPR-5	ACCAGGAGCATAAATCTGATG
R-CRISPR-5	AGTCTCCCATGTAGCTGGGA
F-CRISPR5(2)	GAGTATGTAGGGCCCACACAAG
R-CRISPR5(2)	GTATCATTTAAGCCCATTCCTGC

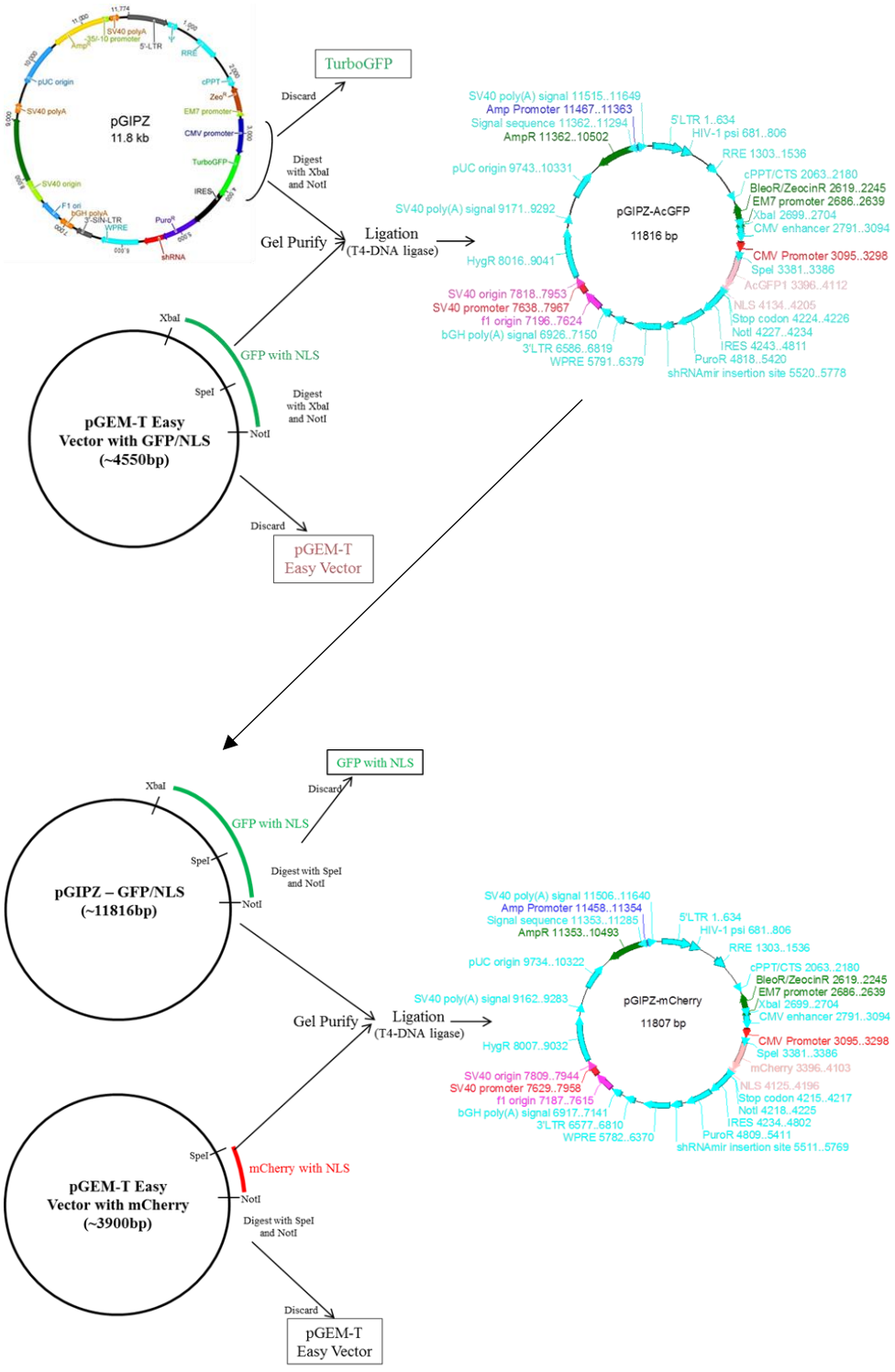

Figure 2.1. Cloning strategy for the establishment of shRNA pGIPZ vectors expressing either GFP/NLS or mCherry/NLS

2.1.3. Antibodies

In this study two commercially available human BAF180 antibodies, BAF180/PB1 (A301-591A) and BAF180 (ABE70) were purchased from Bethyl Laboratories (via Cambridge Bioscience, Cambridge, UK) and Merck Millipore (Hertfordshire, UK) respectively. Antibodies against ASF1A/B (sc-53171), BAP1 (sc-28383), CTF18 (sc-374632), GCN5 (sc-130654), HDAC1 (sc-7872), HDAC4 (sc-46672), RNF4 (sc-21351), TIP60 (sc-5727), CENPF (sc-22791) and RAD51 (sc-8349) were purchased from Santa Cruz (California, USA). 53BP1 BP13 (A300-272A antibodies were obtained from Bethyl Laboratories (via Cambridge Bioscience, Cambridge, UK), EZH2 D2C9 (5246), cleaved Caspase 3 Asp175 (9661) and H2AZ (2718) antibodies were purchased from Cell Signalling (Massachusetts, USA) and PARP1 (MCA15226) and PARP3 (ab96601) were purchased from Bio-Rad (California, USA) and AbCam (Cambridge, UK) respectively. The loading controls Alpha-actin (A5060) and Alpha-tubulin DM1A (ab7291) were obtained from Sigma-Aldrich (Dorset, UK) and AbCam (Cambridge, UK) respectively. Mouse (PO260), Goat (PO449) and Rabbit (PO448) HRP conjugated immunoglobulins for use as secondary antibodies were purchased from Dako (Denmark).

Antibody dilutions used for Western blotting, flow cytometry and immunofluorescence are further described in Table 2.3.

2.1.4. Cells

All cell lines used in this study were grown in 37^{o}C incubators with 5% CO_2 and all media was supplemented with 1% Penicillin/Streptomycin and 1% L-Glutamine purchased from Gibco (Thermo Fisher), unless otherwise stated. The human osteosarcoma cell line, U2OS, were cultured in Dulbecco's Modified Eagle Medium (DMEM) purchased from Gibco (Thermo Fisher) supplemented with 15% Foetal Bovine Serum (FBS). The lung cancer cell line, A549 and the two renal cell carcinoma cell lines, A-498 and A-704 were cultured in Minimum

Essential Media (MEM) purchased from Gibco (Thermo Fisher) supplemented with 10% FBS.The breast cancer cell line T47D and the two renal cell carcinoma cell lines, 786-0 and 769-P were cultured in Roswell Park Memorial Institute (RPMI) 1640 medium purchased from Gibco (Thermo Fisher), supplemented with 10% FBS. The renal cell carcinoma cell line Caki-1 was grown in McCoy's 5a medium from Gibco (Thermo Fisher) and was supplemented with 10% FBS. All cell lines grow as a monolayer and were allowed to grow to around 70-90% confluency before being re-plated to Corning T-75 tissue culture flasks every 3-5 days. No cell line was continually passaged for more than 6 weeks at a time to avoid sub-culturing, a decrease in cellular productivity and cellular differentiation, to name a few deleterious passage effects.

2.1.5. Radiation

Cells treated with irradiation were exposed to the radioisotope Caesium-137 (^{137}Cs 64 TBq – 1989). This radiation source emits radiation in the form of gamma rays and to a lesser extent, high-energy beta particles. As this source decays over time, the reading as of January 2016 was 6.2Gy/min.

Table 2.3. Antibodies used in this study

Antibody	Clonality (Isotope)	Company (Product Number)	Molecular Weight / Dilution
Primary Antibodies			
Anti-Actin	Rabbit Polyclonal (IgG)	Sigma-Aldrich (A5060)	42kDa (1:5000)
Anti-ASF1A/B (4A1/3)	Mouse Monoclonal (IgG2a)	Santa Cruz (sc-53171)	23kDa (1:200)
Anti-BAF180/PB1	Rabbit Polyclonal (Whole IgG)	Bethyl (A301-591A)	193kDa (1:500)
Anti-BAF180	Rabbit Polyclonal (Whole IgG)	Millipore (ABE70)	193kDa (1:500)
Anti-BAP1 (C-4)	Mouse Monoclonal (IgG1)	Santa Cruz (sc-28383)	80kDa (1:500)
Anti-Cleaved Caspase-3 (Asp175)	Rabbit Polyclonal	Cell Signaling (9661)	17/19kDa (1:500)
Anti-CENPF	Rabbit Polyclonal (IgG)	Santa Cruz (sc-22791)	330kDa (1:1000)
Anti-CTF18 (F-1)	Mouse Monoclonal (IgG2a)	Santa Cruz (sc-374632)	107kDa (1:200)
Anti-EZH2 (D2C9)	Rabbit Polyclonal (IgG)	Cell Signalling (5246)	98kDa (1:1000)
Anti-GCN5 (2384C5-2a)	Mouse Monoclonal (IgG2b)	Santa Cruz (sc-130654)	94kDa (1:200)
Anti-HDAC1 (H-51)	Rabbit Polyclonal (IgG)	Santa Cruz (sc-7872)	55kDa (1:200)
Anti-HDAC4 (A-4)	Mouse Monoclonal (IgG2b)	Santa Cruz (sc-46672)	140kDa (1:90)
Anti-Histone H2A.Z	Rabbit Polyclonal	Cell Signalling (2718)	14 kDa (1:1000)
Anti-PARP1	Mouse Monoclonal (IgG1)	Biorad (MCA1522G)	113kDa Full Length – 89kDa Cleaved PARP (1:2000)
Anti-PARP3	Rabbit Polyclonal (IgG)	AbCam (ab96601)	60kDa (1:500)
Anti-RAD51 (H-92)	Rabbit Polyclonal (IgG)	Santa Cruz (sc-8349)	37kDa (1:200)
Anti-RNF4 (C-15)	Goat Polyclonal (IgG)	Santa Cruz (sc-21351)	21kDa (1:200)
Anti-TIP60 (K17)	Goat Polyclonal (IgG)	Santa Cruz (sc-5727)	58kDa (1:200)
Anti-α-Tubulin (DM1A)	Mouse Monoclonal (IgG1)	AbCam (ab7291)	50kDa (1:10000)
Anti-53BP1 (BP13)	Rabbit Polyclonal (Whole IgG)	Bethyl (A300-272A)	220kDa (1:800)
Secondary Antibodies			
Rabbit-anti-mouse HRP immunoglobulin	Polyclonal (IgG)	Dako (PO260)	1:5000
Goat-anti-rabbit HRP immunoglobulin	Polyclonal (IgG)	Dako (PO448)	1:5000
Rabbit-anti-goat HRP immunoglobulin	Polyclonal (IgG)	Dako (PO449)	1:5000

2.2. Methods

2.2.1. siRNA knockdowns

siRNA knockdowns were carried out using either HiPerfect transfection reagent (Qiagen) or Lipofectamine RNAiMAX reagent (Invitrogen). Cell lines were typically seeded at a density of 1-3x10^5 cells per 6cm dish in 3ml appropriate media and siRNA knockdowns were carried out as per the specific manufacturer's instructions, using either single siRNA sequences or SMARTpool's of four siRNA's (Dharmacon ON-TARGETplus) on the day of seeding as well as 24 hours later. Treated cells were left for 72 hours from first transfection before being detached using 0.05% Tryspin-EDTA (Gibco) and were either harvested for whole cell extracts or taken on to further experiments.

2.2.2. Whole cell extracts

Cells were grown in either 6cm or 10cm dishes until confluent or until a specific time-point and de-attached using 0.05% Trypsin-EDTA (Gibco), which was deactivated by FBS containing media about 1 minute after Trypsin addition. Cells were pelleted by centrifugation at 1500 rpm at 4^{o}C for 5 minutes. Pellets were washed twice with ice cold phosphate-buffered saline (PBS) and were either stored at -20^{o}C or processed immediately. Whole cell extracts were prepared from the pellets using an edited version of Tanaka's method (Tanaka et al., 1992). Method edited by Cornelia Meisenberg. The pellet was re-suspended in 1ml ice cold PBS and centrifuged at 3600 rpm at 4^{o}C for 10 minutes and the supernatant was carefully removed. Pellets were re-suspended in around 4 packed cell volumes (PCV's) of IP lysis buffer containing 20mM Tris-HCL ph7.5, 10mM EDTA ph 8.0, 100mM NaCl, 1% Triton X-100 and freshly added protease inhibitors (950µl IP lysis buffer with 50µl protease inhibitors). The cells were mixed thoroughly by rocking at 4^{o}C for 30 minutes and subsequently sheered by two rounds of sonication set to 30 seconds on/30 seconds off pulses, using the

Diagenode Bioruptor sonicating water bath. Cell lysate was centrifuged at 13000 rpm at 4°C for 10 minutes. Supernatant was carefully collected and stored at -20°C or -80°C for long term storage until needed.

2.2.3. Protein concentration - Bradford assay

The Bradford assay was used to measure the protein concentrations of whole cell extracts for western blotting, using Bio-Rad protein assay reagent (Bio-Rad). 2µl of whole cell extract sample were diluted in 18µl ddH_20 and further diluted in 980µl of the dye reagent at 1 x concentration. A blank sample was used to standardize sample readings and absorbance measurements at an optical density of 595 nm were read using a UV spectrophotometer. A reference BSA protein standard at 0.2mg/ml sample was also measured for calculation of protein concentration.

2.2.4. Western blotting – SDS-PAGE

Proteins were resolved on 8, 10, 12 or 15% separating gels depending on the size of the protein of interest by sodium dodecyl sulfate (SDS) polyacrylamide gel electrophoresis (PAGE). Separating gel solutions were made as described in Table 2.4 below and poured between 1.5mm Mini-PROTEAN spacer plates (Bio-Rad) leaving a 1-1.5 inch gap for the stacking gel. A layer of isopropanol was swiftly added to the top of the separating gel allowing it to set with a straight edge. The isopropanol was completely removed before the stacking gel solution (see Table 2.4) was added to the gel cast along with a protein gel comb and was allowed to set.

Table 2.4. Separation and stacking gel components for SDS-PAGE

Gel Type	8%	10%	12%	15%	Stacking (2ml)
ddH20	2.9ml	2.5ml	2.1ml	1.5ml	1.0ml
Separation buffer	1.5ml	1.5ml	1.5ml	1.5ml	--
Stacking buffer	--	--	--	--	0.5ml
APS	75µl	75µl	75µl	75µl	25µl
TEMED	7.5µl	7.5µl	7.5µl	7.5µl	2.5µl
Acrylamide (30% - 37:5:1)	1.6ml	2.0ml	2.4ml	3.0ml	0.5ml

Protein concentration was determined by Bradford assay (as described in 2.2.3) to allow for accurate loading. 20-40µg of whole cell extract was diluted in 4x NuPAGE LDS Sample Buffer (Novex, Thermo Fisher) with 5% 2-Mercaptoethanol (BME) freshly added, before being denatured at 95^{o}C for 5-10 minutes. The previously made gels were transferred to Mini-PROTEAN Tetra Vertical Electrophoresis Cell tanks (Bio-Rad), which were then filled with 1x SDS-PAGE running buffer. Samples were loaded in the gel alongside a molecular weight ladder, Precision Plus Protein Dual Color Standards (Bio-Rad) and run at 150 V for approximately 1 hour or until the dye front reached the bottom of the gel. Resolved proteins were then immobilised on nitrocellulose membrane (GE Healthcare) at 250 mA with constant Amps for 90 minutes in SDS-PAGE transfer buffer. Membranes were then blocked in 5% Milk-TBST (Tris-Buffered Saline and Tween 20) or 3% BSA-TBST for 1 hour at room temperature. Membranes were either left whole or cut with a sterile scalpel to further incubate with specific antibodies. Appropriate primary antibodies were diluted in 5% Milk-TBST or 3% BSA-TBST and added to the membrane, before being transferred to 4^{o}C overnight with shaking. The membrane was washed three times for 5 minutes with PBS and then incubated for at least 1 hour with a similarly diluted secondary antibody. Membranes were washed again with PBS three times and then proteins were visualised on film using enhanced chemiluminescence (ECL).

2.2.5. Agarose gel electrophoresis

1% agarose gels were generally used throughout the study to analyse DNA samples, however in experiments such as the SURVEYOR mutation detection assay (as described in 2.2.15), where DNA fragments smaller than 500 bp are separated, 2% gels were used. Agarose powder (Sigma) was added to 1 x TAE buffer and heated using a microwave until completely dissolved. The mixture was allowed to cool for about 5 minutes before ethidium bromide was added to a final concentration of around 0.2-0.5µg/ml (usually around 1µl/40ml). The agarose mixture was poured in to a gel tray with gel combs and allowed to set. Gels were placed in to gel tanks filled with 1 x TAE buffer and DNA samples diluted in 6x loading buffer (NEB) were loaded alongside either 1 kb or 100 bp DNA ladders (NEB), depending on the expected size of DNA fragments, for size comparison. Electrophoresis was carried out, running the gels at around 90-120V, depending on gel size, for 30 minutes before DNA bands were analysed using UV transillumination.

2.2.6. Gel Purification

DNA bands were observed from agarose gels after separation by electrophoresis, using UV transillumination. Correct bands were excised from the gel using a sterile scalpel and DNA was subsequently purified using QIAquick Gel Extraction Kit (Qiagen), following the manufacturer's instructions.

2.2.7. Restriction Digests

Double and single restriction digests were typically set up using restriction enzymes and CutSmart Buffer purchased from NEB. 1-3µg DNA, usually around 2-5µl, was typically digested in a 50µl reaction, composed of 5µl 10x CutSmart buffer, 1µl of each restriction enzyme and made up to the total volume with

sterile water. Digestions were typically left for at least 1 hour, sometimes overnight, at 37°C. Digestions were analysed by agarose gel electrophoresis (see section 2.2.5) and correct fragments were gel purified (see section 2.2.6) before being ligated in to a secondary plasmid.

2.2.8. Ligation

20µl ligation reactions were carried out using T4 DNA ligase (NEB), 10x T4 DNA Ligase Buffer (NEB), sterile water and a given ratio of purified DNA insert to vector. The amount of insert needed for a specific ratio was calculated by first observing the standard 1:1 ratio:

[Length Insert (kb) / Length Vector (kb)] x ng of Vector = ng insert needed for 1:1

Typically a 4:1 Insert : Vector ratio was used. Ligation reactions were incubated for at least 15 minutes at room temperature, but in most cases were typically left overnight before being transformed in to XL1-Blue Competent *E. Coli* cells (as described in section 2.2.9).

2.2.9. XL1-Blue E. Coli transformation

Freshly prepared ligation reactions (As described in 2.2.8) or plasmid DNA (around 100-200ng) were added to 50µl XL1-Blue competent cells that had previously been thawed on ice for 15 minutes. The DNA/*E. Coli* mixture was gently pipetted and incubated on ice for 40 minutes. The cells were heat shocked in a 42°C water bath for 40 seconds and then placed back on ice. 500µl LB broth, without antibiotic, was added and cells were allowed to recover at 37°C for 1 hour. Cells were pelleted using a bench top centrifuge at 1500rpm for 1 minute and all but 100µl of the supernatant was subsequently discarded. The cell pellet was re-suspended in the remaining supernatant and spread on LB plates containing the appropriate antibiotics and further incubated at 37°C overnight.

2.2.10. Blue-white screening of bacterial colonies

100µl of 100mM IPTG (Isopropyl β-D-1-thiogalactopyranoside) and 20µl of 50mg/ml XGal (5-bromo-4-chloro-3-indolyl-β-D-galactopyranoside) were spread over solid LB plates with appropriate antibiotics and allowed to dry prior to use in transformation reactions (as described in 2.2.9). Blue white screening was used to analyse the correct intake of recombinant *E. Coli* containing plasmids by the production of blue or white colonies formed by either functional β-galactosidase (encoded by the lacZ gene) or disrupted/inactivated β-galactosidase production respectively.

2.2.11. PCR Amplification of DNA

PCR amplifications were carried out using the high-fidelity DNA polymerase, Phusion (NEB) and a typical 50µl reaction was set up on ice as follows:

Component	**50µl Reaction**
MilliQ H_20	To 50 µl
5X Phusion HF Buffer	10 µl
5mM dNTPs	2 µl
10 µM Forward Primer	1 µl
10 µM Reverse Primer	1 µl
Template DNA	Variable
Phusion DNA Polymerase	0.5 µl

PCR reaction mixtures were immediately transferred to a bench top themocycler for amplification.

A typical PCR cycling programme was as follows:

Step	Temperature	Time
Initial Denaturation	98°C	2 min
30 Cycles – **Denature**	98°C	10 secs
Annealing	60°C	30 secs
Extension	72°C	3 min
Final Extension	72°C	10 min
Finish Hold	4°C	Infinite

PCR products were either stored at 4oC or 1-5µl was immediately analysed by agarose gel electrophoresis (as described in section 2.2.5).

2.2.12. Stable shRNA cell line transfection

Using both the unaltered and the altered pGIPZ shRNA plasmids (as described in 2.1.1), cells were seeded at a density of $2x10^5$ per well in a 24 well plate and transfected with the plasmid DNA 24 hours later as per the manufacturer's instructions (Thermo Scientific). After optimisation of the protocol, 4µg rather than the recommended 1µg of DNA was used, as well as 6µl rather than the suggested range of 1-2.8µl of TurboFect was diluted in 100µl OptiMEM. Transgene expression was analysed in the 24-48-hour period following transfection and cells that appeared to express either the GFP or mCherry fluorescent proteins were put under continuous puromycin (Fisher Scientific) antibiotic selection. Antibiotic dose response curves were carried out for each cell line to determine the minimum dose of antibiotic to kill any non-transfected cells, details of which are noted in the table below:

Cell Line	Puromycin Dose
U2OS	1.5 µg/ml
A549	0.75 µg/ml
786-0	0.9 µg/ml
T47D	1 µg/ml

2.2.13. CRISPR cell line transfection

Creation of BAF180 CRISPR knockout cell lines, using guide RNA's (section 2.1.1.) was carried out with direction from Chris Thorne (Horizon Discovery), however optimisation of their protocol, as well as the introduction of a secondary plasmid (section 2.1.1.) was required to achieve significant transfection levels. Cells were seeded at a density of $5x10^4$ cells per well in a 24 well plate and were transfected 24 hours later. A transfection reagent comprised of 100µl OptiMEM, 2µl TurboFect, 0.5µg of each given CRISPR construct and 0.25µg of the empty vector pcDNA4-GFP-IRES-Puro was incubated for 30 minutes and then added drop wise to the cells. Transient GFP expression from the empty vector plasmid was analysed 24 hours later and successfully transfected cells were put under puromycin antibiotic selection for 3-5 days. Successfully transfected cells were grown for gDNA extraction (section 2.2.14) and the success of each CRISPR guide was determined using the SURVEYOR mutation detection assay (see section 2.2.15). A single CRISPR guide was then chosen as 'most efficient' and cells that had been previously transfected with that guide were single cell diluted to establish a clonogenic cell line. Single clones were grown to confluency in 96 well plates and then split to three new 96 well plates, one for continuous passage, one for genomic DNA extraction and one for freezing. Genomic DNA was harvested from these plates (section 2.2.14) and successful clones were determined again by the SURVEYOR mutation detection assay (section 2.2.15). Any clones that appeared to have the mutation introduced by the CRISPR guide was then expanded and BAF180 expression was checked by Western blotting (section 2.2.4) as well as by sequencing (GATC-biotech).

2.2.14. Genomic DNA extraction

Genomic DNA extraction from cultured cells – Large scale format

U2OS and 786-0 cells were grown in 10cm tissue culture dishes and harvested when confluent, giving a typical yield of around $4x10^6$ cells. Harvested cells were

pelleted by centrifugation at 1500 rpm for 5 minutes and then re-suspended in 500µl Tail lysis buffer for genomic DNA extraction, composed of 50mM Tris-HCL, pH 8.8, 100mM EDTA, 100mM NaCl and 1% SDS. To this, 500µl Phenol/Chloroform/Isoamyl (25:24:1) alcohol was added and cells were agitated until an emulsion formed. The samples were centrifuged in a bench top microfuge at maximum speed for 5 minutes, here you can observe the lysis solution forming three distinct layers. The top layer, or aqueous phase, was carefully removed to a new Eppendorf and 200µl saturated NaCl (5-6M) was added and then the mixture was shaken vigorously for 5 minutes before being centrifuged for 10 minutes at maximum speed. The supernatant was carefully poured in to a new Eppendorf and 700µl Isopropanol was added and mixed by inversion. At this stage you can see the DNA appear as a cloud within the solution. The solution was then spun again at maximum speed for 10 minutes, revealing a very clear, spread out pellet of DNA. The pellet was washed with 70% ethanol for 1 minute and further centrifuged for 5 minutes at maximum speed, forming a smaller, more compact pellet. An appropriate amount of TE buffer was added to the pellet and was then left at room temperature overnight to aid DNA re-suspension.

Genomic DNA extraction from cultured cells - 96 well plate format

Genomic DNA was harvested from 96 well plates as set out by Sigma-Aldrich in a technical bulletin that describes the harvesting of genomic DNA after delivery of zinc finger nucleases (http://www.sigmaaldrich.com/content/dam/sigma-aldrich/docs/Sigma/Bulletin/1/ckozfndbul.pdf).

2.2.15. SURVEYOR mutation detection assay

The detection of mutated/deleted DNA sequences, introduced by the transfection of CRISPR guides to cells, was carried out using the SURVEYOR mutation detection kit (Transgenomic). Genomic DNA was harvested from CRISPR gRNA transfected ‘test’ cells as well as from untreated ‘control’ cells (as described in

2.2.14) and the specific region of interest, i.e. where the CRISPR guide should 'cut' the DNA, was amplified by PCR (section 2.2.11) using primers listed in Table 2.2. The PCR products were analysed on 2% agarose gels. Alongside 'test' and 'control' DNA samples, the SURVEYOR mutation detection kit provides two reference plasmid DNAs, Control C and Control G, which were also PCR amplified, as per the manufacturer's instructions. The PCR amplified DNA samples were then hybridized to form hetero- and homoduplexes. A typical set up of this reaction was as follows:

PCR Amplified Component	Amount
SURVEYOR Control C	30 µl
SURVEYOR Control C + Control G	15 µl + 15 µl
Untreated 'Control' Cells	40 µl
CRISPR gRNA treated Cells	40 µl
Control Cells + CRISPR gRNA Cells	20 µl + 20 µl

The hybridization reaction tubes were secured with Eppendorf cap locks, to stop the lids from popping open, and were heated in a heat block at 95^{o}C for 5 minutes. The entire block was then allowed to cool to 30^{o}C before digesting the samples with the SURVEYOR nuclease exactly as described in the manufacturer's instructions. A typical set up of this digestion reaction was as follows:

For SURVEYOR Control C and Control C + Control G Reactions	
Component	**Amount**
Hybridized Sample	12 µl
0.15M MgCl2	1.2 µl
SURVEYOR Enhancer S	1 µl
SURVEYOR Nuclease S	1 µl
Stop Solution (added after incubation)	1.5 µl

For 'Control' and 'Test' hetero- and homoduplexes	
Component	**Amount**
Hybridized Sample	30 µl
0.15M MgCl2	3 µl
SURVEYOR Enhancer S	1 µl
SURVEYOR Nuclease S	1 µl
Stop Solution (added after incubation)	3.5 µl

The digestions were mixed gently by vortex and subsequently incubated at 42°C for 60 minutes. Immediately after the incubation period, the SURVEYOR Stop Solution was added to each reaction and products were either stored at -20°C or analysed by agarose gel electrophoresis immediately (section 2.2.5). Homoduplexes appear on 2% agarose gels as a single DNA band, whereas heteroduplexes are cleaved by the SURVEYOR nuclease enzyme and will appear as fragmented DNA.

2.2.16. CellTiter-Glo viability assay

Viability after siRNA gene knockdown

For viability assays performed after siRNA treatment, cells were treated as described in 2.2.1, harvesting those 72 hours after primary transfection. Cells were counted and re-seeded at a density of $3x10^3$ per well in triplicate per condition in to a flat bottom white 96 well microplate (Nunc – Thermo Scientific). Viable or metabolically active cells, determined by quantification of active ATP, were measured 24 hours later. CellTiter-Glo reagent (Promega) was added in a 1:1 ratio with media to the cells and left at room temperature for 15 minutes, luminescence was observed using the GloMAX-Multi Microplate reader (Promega).

Viability after drug treatment

Cells were seeded at a density of $8x10^3$ per well directly in to a flat bottom white 96 well microplate (Nunc – Thermo Scientific) and left to adhere. 24 hours after seeding, fresh medium was added to the cells, supplemented with drug. Drug doses were performed in triplicate wells and DMSO was used as a vehicle control in all cases. Cells were left in the supplemented medium for a further 96 hours before being treated with the CellTiter-Glo reagent as described above.

2.2.17. High-throughput siRNA screening

shBAF180+GFP/NLS and shControl+mCherry/NLS U2OS cells were seeded at a 1:1 density of 8000 cells per well in 96-well plates. Cells were reverse transfected with a RNAi library of 446 genes with Lipofectamine RNAi MAX at a final siRNA concentration of 20nM. Cells were grown for 72 hours, permeabilised, fixed in 4% PFA and stained with DAPI. Screened cells were imaged at 10x magnification in 16 frames per well, imaging more than 10,000 cells per well.

2.2.18. Clonogenic survival assay

Clonogenic survival after siRNA gene knockdown

siRNA knockdowns were carried out as described in 2.2.1 and at the 72 hour time point after primary transfection, cells were either harvested for Western blot (section 2.2.4) or were seeded to 6cm dishes at a density of 300 cells per dish, in triplicate per condition. Cells were allowed to grow for 12-14 days, or until visible colonies were observed. Media was discarded from the plates and cells were stained with methylene blue for 1 hour. The methylene blue stain was washed away gently with water and plates were allowed to dry before scoring colonies using a Stuart Scientific SC6 colony counter (Sigma-Aldrich). Any colony that appeared to contain 50 cells or more was counted and the surviving fraction was worked out as a percentage of the siRNA treated cells compared to siControl cells.

Clonogenic survival after drug treatment (+/- Irradiation)

Cells were plated to 10cm dishes at a density of 300 cells per plate in 9ml of appropriate medium and were left to adhere for at least 4 hours, or overnight if seeding took place late in the evening and treatment was carried out early the next morning to ensure cells haven't gone through a cellular division before treatment. The cells were then treated with varying doses of drug in triplicate,

made up in 1ml of appropriate medium and this was added to the medium already in culture, making a total plate media volume of 10ml. The plates were incubated for 12-14 days or until visible colonies were observed. The plates were stained and counted as described above. For plates treated with irradiation as well as drug, the lowest concentration of drug where you are able to observe a difference was determined and varying doses of gamma irradiation was inflicted on the plates containing the 300 adhered cells, after addition of the drug.

2.2.19. Immunofluorescence

Cells were grown in 96 well plates and siRNA treated in the same manner as described in the high-throughput siRNA screen (section 2.2.17). When cells were 70-90% confluent, media was removed and cells were washed with PBS before fixing in 4% paraformaldehyde for 10 minutes. Cells were washed twice with PBS and were either immediately subjected to antibody staining or were kept at 4^{o}C for up to 72 hours. PBS was removed and cellular membranes were permeabilized with PBS + 0.2% Triton X-100 for 3 minutes before being incubated in primary antibody (at appropriate dilution) in PBS + 2% w/v BSA for 1 hour. Cells were washed three times with PBS before incubating with secondary antibody (at appropriate dilution) in PBS + 2% w/v BSA for 30 minutes at room temperature in the dark. Cells were washed three times with PBS, incubated with DAPI and visualised at 20x objective using the EVOS fluorescent digital inverted microscope.

2.2.20. Flow Cytometric Immunofluorescence Analysis

For flow cytometric immunofluorescence analysis, U2OS stable shControl and shBAF180 cells were seeded at a density of around 1x10^{6} in 10 cm dishes and cultured for 24 hours before the addition of the drugs Olaparib and Camptothecin at stated doses in duplicate per dose/time point. Cells were harvested at 0, 24, 48, 72 and 96 hour time points and pelleted by centrifugation at 1500 rpm for 5

minutes. To fix the cells, 1ml 70% Ethanol (EtOH) was added drop wise to the pellets whilst gently vortexing, storing the fixed cells at -20^{o}C until the final time point is harvested. Once all samples are collected, the fixed cells are then pelleted by centrifugation at 1000 rpm for 3 minutes and gently washed in PBS before a second round of centrifugation. The cells are then re-suspended in 1ml PBS + 0.1% BSA using a Gilson pipette and centrifuged again before re-suspending in 2ml PBS + 0.5% BSA + 0.25% Triton X-100 and incubated on ice for 15 minutes and subsequently centrifuged again at 1000 rpm for 3 minutes. The pellet, depending on size was then re-suspended in 50-100µl PBS + 0.5% BSA + 0.25% Triton X-100 cleaved Caspase 3 Asp175 (9661) at 1:500 dilution and incubated at room temperature for at least 1 hour. The cells were then washed with PBS + 0.5% BSA + 0.25% Triton X-100, re-pelleted by centrifugation and further incubated in 50-100µl PBS + 0.5% BSA + 0.25% Triton X-100 with anti-rabbit 488 secondary antibody at a 1:500 dilution at room temperature in the dark for 30 minutes. Cells were then washed with PBS + 0.5% BSA + 0.25% Triton X-100 and re-suspended in 200-400µl Propidium Iodide (PI) solution with 5µg/ml PI and 100µg/ml RNAase I and incubated at room temperature in the dark for 15 minutes. Samples were then transferred to 4^{o}C for overnight storage. Cells were passed through a fine-gauge needle prior to sampling on the BD Accuri C6 plus flow cytometer (BD Bioscience).

2.2.21. RAD51 foci formation assay

For RAD51 foci formation, U2OS cells were seeded at a density of 3x10^{5} in to two 6cm tissue culture dishes in 3ml of medium per dish. A transfection reagent composed of 200µl OptiMEM (Gibco), 12µl HiPerfect (Qiagen) and 6µl of either siControl or siBAF180 (ON-TARGETplus SMARTpool Dharmacon) at 20µM stock was then added drop wise to the cells. 24 hours later the transfection reagent was made as before and was added to the area of two sterile coverslips in fresh 6cm dishes. The cells were gently detached, using trypsin and were re-seeded to the new 6cm dishes containing coverslips. 48 hours later, or when cells appear almost confluent on the coverslips, Aphidicolin (Sigma-Aldrich) was added to the

medium at a dilution of 1:1000 to prevent S phase cells from progressing to G2. One coverslip from each dish was then taken to a new dish and washed twice with PBS, permeabilization of the cellular membrane was then achieved by adding PBS + 0.2% Triton to the cells for no more than 60 seconds. The cells were then fixed in 4% paraformaldehyde for 10 minutes before being washed three times with PBS and stored at 4^{o}C. The coverslips that remain in the 6cm dishes with media were irradiated with gamma radiation to the extent of 3 Gy and were returned to the 37^{o}C incubator with 5% CO_2 for 2 hours before being permeabilised and fixed as described previously. Coverslips were either antibody stained immediately or stored at 4^{o}C for up to 72 hours. If immediately sampling coverslips, PBS was removed and slips were incubated in PBS with 1:200 dilution of Anti-RAD51 (sc-8349) primary antibody for 1 hour, with 1:200 dilution of Rabbit Cy3 secondary antibody for 30 minutes, with 1:1000 dilution of Anti-CENPF (sc-22791) primary antibody for 1 hour and finally with a 1:400 dilution of Alexa-488 secondary antibody for 30 minutes. Between each antibody addition, coverslips were washed with PBS three times. Coverslips were then mounted to microscope slides using VECTASHIELD Antifade Mounting Medium with DAPI (Vector Laboratories). RAD51 foci were scored by eye in G2 positive cells only using the Zeiss 3D microscope.

3. Hypothesis driven synthetic lethal screen

3.1. Introduction

The principle of synthetic lethality, as described fully in section 1.6, defines a genetic relationship between a pair of genes, where the loss of either gene is permissive for cell survival but the combinatory loss of both genes together is resultant in cell death or a retardation of growth. Synthetic lethality can be observed in genes that act in the same biochemical pathway as well as in distinct, but compensatory pathways (Pan, Ye et al. 2006).

Originally, the phenomenon of synthetic lethality was exploited to elucidate functional relationships between genes in yeast, but more recently the principle has been harnessed in the search for targeted cancer therapy. As previously described, there have been multiple examples where yeast genetic interactions have been translated to mammalian cells (Yu, Lopez et al. 2008, Conde-Pueyo, Munteanu et al. 2009, McLellan, O'Neil et al. 2009, McManus, Barrett et al. 2009). Using this potentially translatable observation as well as the data from three independent synthetic lethal screens in yeast, we identified eight genes with synthetic lethal interactions with yeast homologues of BAF180 (Rsc1 and Rsc2) to take forward for experimentation in mammalian cells (Table 3.1). Of the many potential synthetic lethal candidate genes that could be explored, we chose these eight due to their strong sequence conservation from yeast to mammalian cells, they were all synthetic lethal or synthetic sick with Rsc1 and/or Rsc2, the deletion of all genes alone are not thought to be deleterious to 'normal' cells and they are all potentially targetable by drugs.

Of the eight genes identified as potentially synthetic lethal with BAF180, four of them, Asf1 (ASF1A, ASF1B), CTF18 and SLX5 (RNF4), were identified in a screen that sought to use global genetic analysis to identify novel synthetic fitness or lethality defect interactions in the DNA integrity network of *S. cerevisiae* (Pan, Ye et al. 2006).

Yeast Gene	Mammalian Gene	Synthetic Lethal/Synthetic Sick with rsc2	Synthetic Lethal/Synthetic Sick with rsc1	Enzyme	References
ASF1	ASF1A and ASF1B	Synthetic Lethality	N/A	No, but conserved hydrophobic groove flanked by strong electronegative surface potential/binding sites	Pan X et al 2006
CTF18	hCTF18	Synthetic Growth Defect	N/A	ATPase	Pan X et al 2006
RPD3	RPD3L1/HDAC1	Synthetic Lethality	Synthetic Lethality	HDAC	Lin YY, et al 2008
GCN5	KAT2A/GCN5/GCN5L2	Synthetic Lethality	Synthetic Lethality	HAT	Cairns BR, et al 1999
HDA1	HDAC4	Synthetic Lethality	Synthetic Growth Defect	HDAC	Lin YY, et al 2008
ESA1	KAT5/TIP60	Synthetic Lethality	Synthetic Lethality	HAT	Lin YY, et al 2008
SLX5	RNF4	Synthetic Growth Defect	Synthetic Growth Defect	E3 Ubiquitin-protein ligase	Pan X et al 2006

Table 3.1. Hypothesis driven gene candidates. Candidate genes were chosen based on their synthetic lethal relationship with BAF180's yeast homologs Rsc1 and Rsc2

Anti-silencing function 1 (Asf1) is a histone chaperone that participates in both nucleosome assembly and disassembly (Park and Luger 2008, Krebs and Tora 2009, Oh, Ruskoski et al. 2012). Asf1 is a histone H3/H4 chaperone in the context of DNA replication and together with CAF-1 and PCNA works to assemble nucleosomes on replicated DNA (Franco, Lam et al. 2005, Sanematsu, Takami et al. 2006, Groth, Corpet et al. 2007, Miller, Yang et al. 2008). Cells that have lost the Asf1 protein have impairments in DNA replication (Schulz and Tyler 2006). In mammalian cells there are two isoforms of Asf1, which are ASF1A and ASF1B. These mammalian isoforms have a highly conserved N-terminus, which acts as a binding interface for both the H3.1-H4 replicative histones and the H3.3-H4 replacement histones (De Koning, Corpet et al. 2007, Corpet, De Koning et al. 2011). Like Asf1 in yeast, the mammalian isoforms also interact with CAF-1 in the replication-coupled assembly pathway (Mello, Sillje et al. 2002). A good representation of the conservation between yeast Asf1 and the two human isoforms can be seen when human ASF1A introduced in to yeast is able to rescue the DNA damage response defect created from the depletion of endogenous Asf1 (Tamburini, Carson et al. 2005, Corpet, De Koning et al. 2011). Furthermore, introduction of human ASF1B to Asf1 depleted yeast cells can compensate for the associated growth defects and the sensitivity to replication stress (Tamburini, Carson et al. 2005, Corpet, De Koning et al. 2011).

The rather aptly named Chromosome transmission fidelity protein 18 (CTF18) is required for the faithful segregation of chromosomes (Hanna, Kroll et al. 2001). It is a component of the CTF18-RFC complex, composed of Ctf18, Ctf8, Dcc1 along with four small subunits (Rfc2-5) of replication factor C (RFC), which as a whole is necessary for sister chromatid cohesion and faithful chromosome transmission (Mayer, Gygi et al. 2001, Bylund and Burgers 2005). Loss of CTF18 is associated with a severe sister chromatid cohesion defect, failed maintenance of telomeres, and results in a preanaphase accumulation of cells that depends on the spindle assembly checkpoint. CTF18-defective cells have an increased sensitivity to microtubule depolymerizing drugs and hypersensitivity to the chemotherapeutic drugs methyl methanesulfonate (MMS) and hydroxyurea (HU) (Hanna, Kroll et al. 2001, Mayer, Gygi et al. 2001, Kubota, Hiraga et al. 2011).

RING finger protein 4 (RNF4), also known as small nuclear RING finger protein (SNURF) (Moilanen, Poukka et al. 1998) is an E3 ubiquitin-protein ligase that mediates the proteasomal degradation of several proteins including the promyelocytic leukaemia (PML) protein and the transcriptional activator PEA3. A C3HC4 (RING-HC)-type RING finger motif resides at RNF4s C-terminal domain (Moilanen, Poukka et al. 1998). RNF4 is the best characterised SUMO targeted ubiquitin ligase (STUbL) in human cells. STUbLs can contain individual or multiple SUMO interacting motifs (SIMs) that can recognise SUMO chains and target poly-SUMOylated proteins for proteasome-mediated degradation. RNF4, using SIMs, can recognise SUMO chains, for example the poly-SUMOylated PML, acting to ubiquitinate the PML as well as the poly-SUMO chains attached to it, subsequently directing PML for proteasomal degradation (Tatham, Geoffroy et al. 2008). RNF4 has also been associated with chromosome alignment and spindle assembly by the regulation of the kinetochore complex CENPH-CENPI-CENPK, targeting poly-SUMOylated CENPI for proteasomal degradation (Hickey, Wilson et al. 2012).

Using genome wide analysis, Lin et al found that the yeast homologs of our two candidate HDACs, HDAC1 and HDAC4 and one HAT gene, KAT5 (TIP60), were all synthetic lethal with the BAF180 yeast homologue Rsc2 (Lin, Qi et al. 2008). Yeast counterparts of HDAC1 and KAT5 were also synthetic lethal with Rsc1 however HDAC4 had a less severe phenotype, exhibiting a synthetic growth defect with Rsc1 upon double deletion (Lin, Qi et al. 2008).

Histone (lysine) acetyltransferase 5 (KAT5), also referred to as TIP60 and denoted as such in this thesis, is the catalytic subunit of the nucleosome acetyltransferase of H4 (NuA4)/TIP60 complex. NuA4 primarily acetylates the nucleosomal histones H4 and H2A to mediate transcriptional activation of various genes, but is also a regulator of the cellular response to DNA damage, apoptosis, cell signalling and cell cycle control (Doyon and Cote 2004, Sun, Jiang et al. 2005, Brown, Bourke et al. 2016). Mammalian NuA4, which confusingly is also referred to as TIP60, is a multi-protein complex (Jha, Gupta et al. 2013, Mahajan and Stanley 2014). Yeast NuA4 has 13 subunits with the Esa1 subunit as the catalytic core, homologous to TIP60 (Doyon and Cote 2004). TIP60 has a

direct role in histone exchange, working with SRCAP and p400 to remove H2A/H2B dimers and replace them with H2A.Z/H2B (Cai, Jin et al. 2005, Ruhl, Jin et al. 2006, Wong, Cox et al. 2007). The hypoxia inducible factor 1A (HIF1A) is known to interact with and recruit TIP60 to chromatin and TIP60 is thought to be required for HIF1A-dependent chromatin modification and RNA polymerase II activation in hypoxia (Perez-Perri, Dengler et al. 2016). An important role for TIP60 is in the regulation of the repair of DNA DSBs via acetylation and subsequent activation of ATM and other proteins involved in the DDR (Sapountzi, Logan et al. 2006, Judes, Rifai et al. 2015).

Our final candidate gene, KAT2A (GCN5), was identified as synthetic lethal with both Rsc1 and Rsc2 in a small scale screen that aimed to identify whether RSC together with the SAGA genes were required for cell viability (Cairns, Schlichter et al. 1999). GCN5 is a histone acetyltransferase (HAT) that is part of the SAGA (SPT-ADA-GCN5 acetylase) coactivator complex and was first identified in the yeast *S. cerevisiae*, working to promote transcriptional activation in specific genes within chromatin (Martinez, Palhan et al. 2001). In mammalian cells there are two homologs of GCN5, GCN5L and PCAF, which have been found in multiple different complexes that resemble the yeast SAGA complex, the PCAF complex, TFTC (TATA-binding-protein-free TAF_{II}-containing complex), STAGA (SPT3-TAF_{II}31-GCN5L acetylase) and more recently the ATAC complex, which resembles the ATAC (Ada Two-A containing) complex in Drosophila (Wang, Faiola et al. 2008) (Martinez, Palhan et al. 2001, Wang, Faiola et al. 2008, Guelman, Kozuka et al. 2009). These multi-protein complexes are involved in a wide range of biological processes by acetylating histones H3 and H4 as well as several non-histone proteins, therefore regulating chromatin and gene specific transcription (Wang, Faiola et al. 2008). Yeast GCN5 is synthetic lethal with both homologues of BAF180 Rsc1 and Rsc2 (Cairns 1999). In mammalian cells it is known as KAT2A and the relationship between it and BAF180 has not been fully explored.

In addition to our hypothesis driven candidate synthetic lethal genes that were chosen based on our knowledge of yeast gene interactions, we also used current mammalian cell literature as well as our knowledge of the genes frequently

mutated in renal cell carcinoma to identify two more potential synthetic lethal with BAF180 gene candidates: BAP1 and EZH2.

As discussed in section 1.3.3, BAP1 is known to be one of the four main drivers of tumourigenesis in ccRCC, mutated at a frequency of around 15% in all tumours. Although it has been classified as a main driver mutation in ccRCC, these mutations do not tend to correlate with PBRM1 mutation. Mutations that occur in BAP1 in ccRCC are also though to exhibit different biology as well as leading to a different prognosis and overall survival (OS), when comparing to ccRCC's with mutations in PBRM1. This, together with the mutually exclusive relationship observed between these mutation frequencies, suggested that they could be exploited therapeutically in a synthetic lethal manner.

EZH2 is the catalytic subunit of the polycomb repressive complex 2 (PRC2) and works by catalysing the methylation of lysine 27 on histone H3, which is a chromatin modification that is associated with transcriptionally repressed heterochromatin.
Recently, in our lab, it has been shown that depletion of EZH2, results in the formation of fewer H2AK119ub foci in irradiated cells, a phenotype that is mirrored in both BAF180 and BMI1 (PRC1) depleted cells. This suggests that PRC2 is required for IR-induced H2AK119ub and that PRC2 may promote PRC1 activity at sites of DNA damage (Kakarougkas, Ismail et al. 2014). It was also observed that similar to cells lacking the PBAF complex, there was a delay in the repair of a subset of DSBs at early time points following IR in EZH2 depleted cells and this is consistent with the idea that a failure to repress transcription flanking DSBs impeded efficient repair. It was postulated that PBAF remodels chromatin surrounding DSBs in order to facilitate PRC2 and therefore PCR1 activity toward their respective substrates (Kakarougkas, Ismail et al. 2014).

Wilson et al describe an imbalanced epigenetic antagonism between the SWI/SNF complex and the PRC2 complex (Wilson, Wang et al. 2010). They find that loss of a core SWI/SNF subunit, SNF5, in cancer cells results in the upregulation of EZH2 and that inactivation of EZH2 activity ultimately blocks tumour progression in mouse models (Wilson, Wang et al. 2010). An observation that could be exploited therapeutically in vivo.

Since this finding, multiple other studies have arisen to determine if this synthetic lethal interaction between SNF5 and EZH2 could be reproduced with other subunits of the SWI/SNF complex (Kim, Kim et al. 2015).
It was shown recently that cancers that lack the ARID1A, PBRM1 and SMARCA4 subunits of SWI/SNF were dependent on both the catalytic and non-catalytic activity of EZH2 (Kim, Kim et al. 2015). It was also found that treatment of ARID1A-mutated ovarian cancer cells with EZH2 methyltransferase inhibitors resulted in synthetic lethality (Bitler, Aird et al. 2015). In a combinatory approach, Fillmore et al found that treatment with EZH2 inhibitors in BRG1 and EGFR mutated non-small-cell lung cancers sensitized these tumours to treatment with TopoII inhibitors, presenting a new therapeutic strategy in a genetically complex disease (Fillmore, Xu et al. 2015). Our aim was to determine whether this synthetic lethal phenotype could be reproduced in BAF180 deficient cancers.

3.2. Aims

The aim of this work was to use a hypothesis driven approach to explore and validate synthetic lethal interactions in BAF180-depleted cells.

3.3. A subset of yeast synthetic lethal interactions are not conserved in mammalian cells

To identify which candidate genes selected by yeast high-throughput screen data (Figure 3.1a) could have conserved synthetic lethal interactions between yeast and mammalian cells we first carried out viability assays after siRNA depletion. U2OS cells were transfected with short interfering RNA targeting human BAF180 mRNA or a nonsense scrambled control mRNA as well as the candidate genes ASF1A, ASF1B, CTF18, HDAC1, HDAC4 and TIP60 and the viability measured (Figure 3.1b). Western blotting (Figure 3.1c) was used to confirm knockdown.

For both ASF1A and ASF1B there was no significant decrease in viability in cells depleted for both ASF1 and BAF180 when compared to appropriate controls (Figure 3.1b). However, although not significant statistically, knockdown of ASF1B did appear to decrease viability of BAF180 depleted cells more favourably compared to the control. Similarly, no significant synthetic lethal interaction was detected between either HDAC1 or HDAC4 and BAF180.

While the synthetic lethal interaction between TIP60 and BAF180 was not significant in these assays, there was a trend towards reduced viability in the cells depleted of both relative to either single depletion (Figure 3.1b), and further analyses uncovered a significant relationship (Hopkins, McGregor et al. 2016). The reasons for the lack of synthetic lethality in these assays are not clear, but may be due to variation in knockdown efficiency between assays.

A

Gene	Protein
ASF1A	Histone chaperone ASF1A (Anti-silencing function 1A)
ASF1B	Histone chaperone ASF1B (Anti-silencing function 1B)
CTF18	Chromosome transmission fidelity protein 18 homolog
KAT2A (GCN5)	Histone acetyltransferase KAT2A
HDAC1	Histone deacetylase 1
HDAC4	Histone deacetylase 4
RNF4	E3 ubiquitin-protein ligase RNF4
KAT5 (TIP60)	Histone acetyltransferase KAT5

B

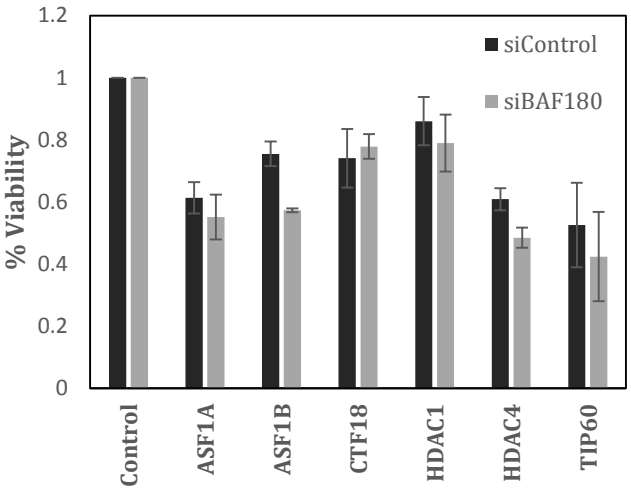

C

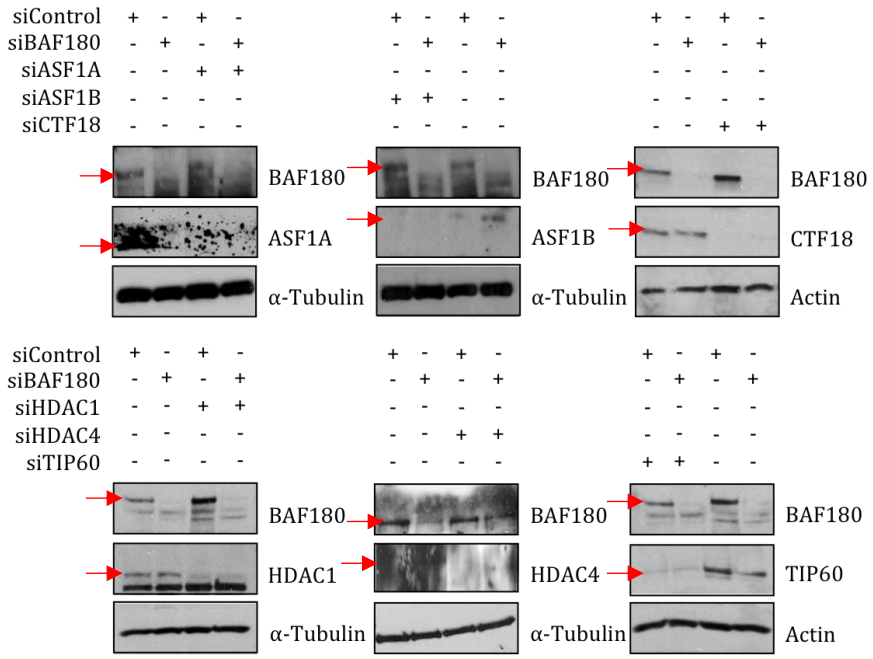

Figure 3.1. A subset of yeast synthetic lethal interactions are not conserved in mammalian cells. (A) List of gene candidates chosen for hypothesis driven synthetic lethal mini screen. (B) U20S cells were transfected with short interfering RNA targeting human BAF180 mRNA, as well as a scrambled 'control' siRNA and either ASF1A, ASF1B, CTF18, HDAC1, HDAC4 or TIP60 mRNA (C) Western blot analysis of siRNA treated U20S cells. Whole cell extracts were analysed with the indicated antibodies, using either actin or α-tubulin as a loading control.

3.4. U2OS cells have reduced viability after co-depletion of BAF180 and RNF4

Cell titre glow viability assays were performed with cells depleted of BAF180 and/or RNF4 to investigate a potential synthetic lethal relationship. There was an 18% difference in average viability is seen between cells treated with siRNF4 alone, compared to RNF4 and BAF180 siRNA treatment, with a p value of 0.086, determined by student T-test. Although the p value is not statistically significant, the trend is very reproducible. The siRNA depletion of RNF4 was not efficient, raising the possibility that further depletion would lead to more substantial effects on viability.

3.5. U2OS cells have a reduced viability after co-depletion of BAF180 and GCN5

To establish if there was a conserved synthetic lethal interaction between KAT2A and BAF180, we used siRNA transfection in U2OS cells to knock down KAT2A alone, BAF180 alone and the two together and then viability was measured. We observed a significant reduction in viability after siRNA knockdown of KAT2A together with BAF180 (Figure 3.3a). Knockdown efficiency was determined by Western blotting (Figure 3.3b). These data suggests that the histone acetyltransferase KAT2A has a synthetic lethal interaction with BAF180.

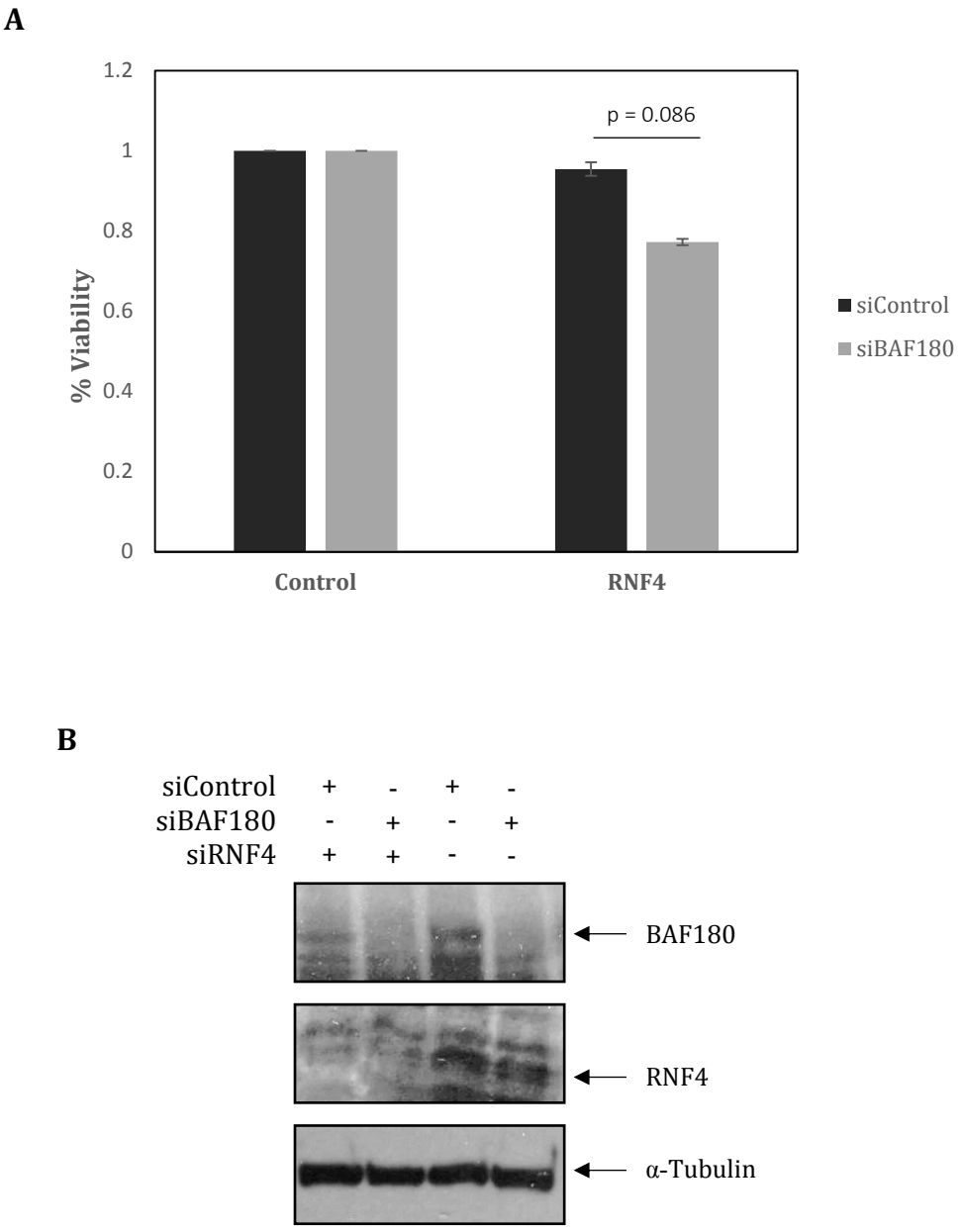

Figure 3.2. U20S cells have reduced viability after co-depletion of BAF180 and RNF4. (A) Viability was measured following siRNA treatment targeting either human BAF180 or RNF4 mRNA was introduced in to U20S cells alongside a sequence of scrambled or 'control' siRNA. (B) Western blot analysis of siRNA treated U20S cells. Whole cell extracts were prepared and analysed using antibodies raised against BAF180 or RNF4, using or α-tubulin as a loading control.

A

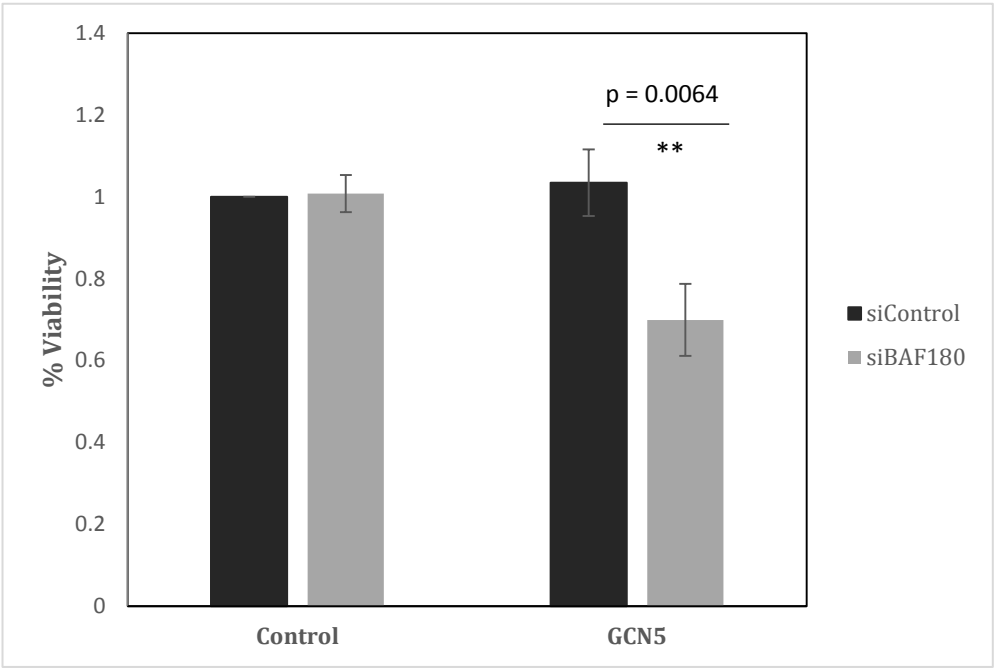

B

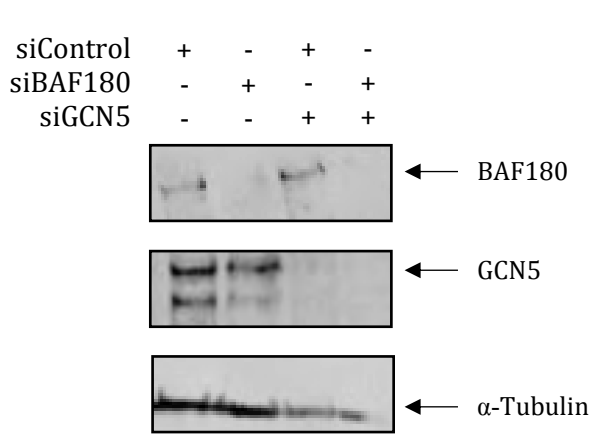

Figure 3.3 U20S cells have reduced viability after co-depletion of BAF180 and GCN5. (A) Cell viability was observed after siRNA transfection of siBAF180, siGCN5 and siControl, in U20S cells. siRNA knockdown of both GCN5 and BAF180 in U20S cells results in a reduction of cell viability compared to each of the individual knockdowns. (B) Western blot analysis of siRNA treated U20S cells using antibodies raised against BAF180 or GCN5, using α-tubulin as a loading control.

3.6. Depletion of EZH2 in BAF180 shU2OS cells results in a synthetic lethal interaction

This hypothesis was tested in stable U2OS cell lines expressing short hairpin RNA (shRNA) targeting BAF180 or a control sequence described in Chapter 4. Clonogenic survival assays were carried out after siRNA depletion of either human EZH2 mRNA or a scrambled 'control' mRNA. shBAF180 cells were significantly more sensitive to EZH2 knockdown in three independent experiments (Figure 3.4a). A representative western blot of this knockdown is shown in (Figure 4.3). To confirm efficient siRNA knockdown of EZH2, whole cell extracts were harvested 72 hours after primary transfection and were analysed by western blot (Figure 3.4b). Interestingly, there appears to be increased EZH2 levels in the shBAF180 cells compared with the shControl cells (Figure 3.4b). This is consistent with the finding by Wilson et al, where they see an overexpression of EZH2 after the loss of SNF5 (Wilson, Wang et al. 2010). These data suggest a synthetic lethal interaction between BAF180 deficiency and EZH2 loss.

To further investigate this interaction, we used the drug GSK126, which acts by inhibiting the methyltransferase activity of EZH2. The cells deficient in BAF180 were inherently more sensitive to treatment with GSK126 at all doses, in agreement with Kim et al (Kim, Kim et al. 2015). These data suggest that EZH2 inhibitors may be a new therapeutic treatment for BAF180-mutated cancers, such as ccRCC.

A

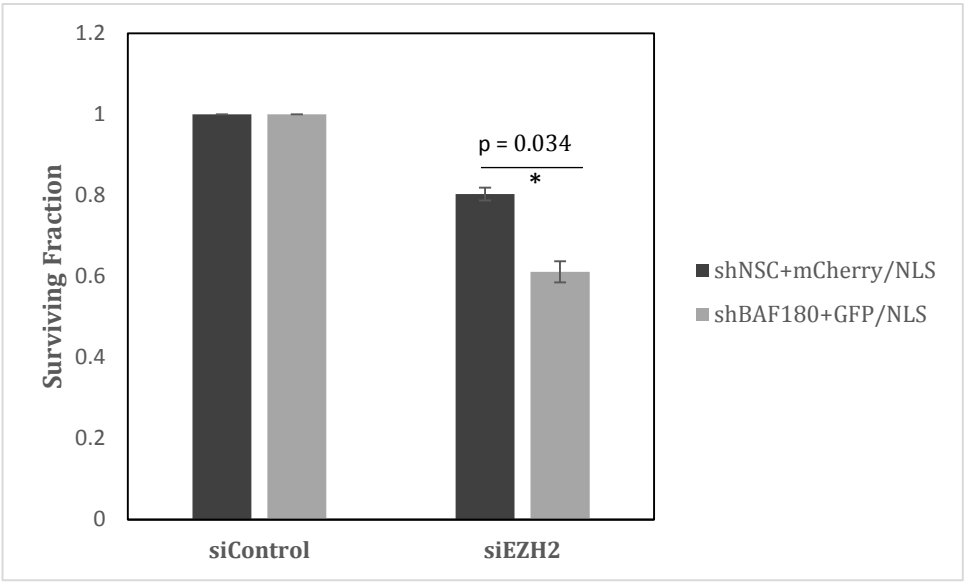

B

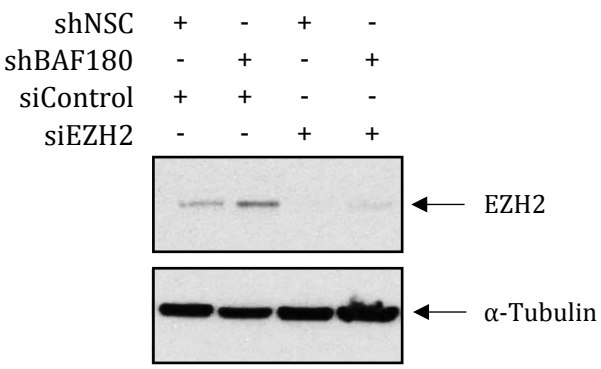

C

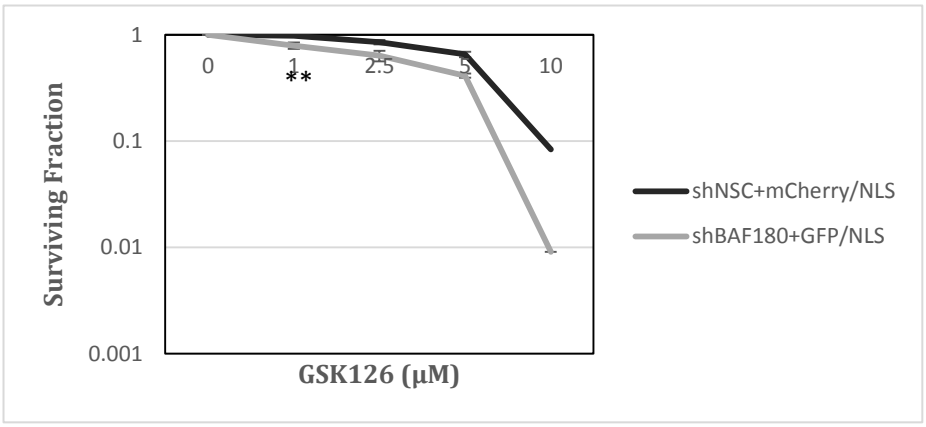

Figure 3.4 BAF180 depleted shU20S are more sensitive to EZH2 siRNA and inhibitors. (A) shBAF180 cells (see chapter 4) were more sensitive to EZH2 knockdown in clonogenic survival assays (n=3). Statistical significance is represented by * for $p<0.05$, as analysed by Student's t-test. (B) Western Blot analysis of depletion of EZH2 in shControl and shBAF180 cells. (C) shBAF180 cells were more sensitive to treatment with GSK126 than control cells in clonogenic survival assays.

3.7. BAP1 and BAF180 are synthetic lethal

3.7.1. BAF180 depleted shU2OS are more sensitive to depletion of BAP1

To test the hypothesis that BAF180 and BAP1 exhibit a synthetic lethal interaction we first tested survival after siRNA knockdown in shControl and shBAF180 cells. Colony formation assays were carried out in triplicate to assess viability changes in these stable U2OS cells after knockdown with both siControl and siBAP1 (Figure 3.5a).

First, we found that BAP1 depletion reduced the viability of both shControl and shBAF180 cells (Figure 3.5a). It is the hope that depletion of a single gene that we wish to exploit therapeutically would not have such a significant effect on our 'normal' cell population. However, we know that cancer cells can grow efficiently without the presence of BAP1 in vivo and so a severe reduction in total cell viability here may be specific to U2OS cells. Alternatively, there may be off target siRNA effects. Nevertheless, there was still a small, yet statistically significant decrease in the surviving fraction of shBAF180 cells compared to shControl (Figure 3.5a). The knockdown efficiency was assessed by Western blot (Figure 3.5b).

3.7.2. BAP1 and BAF180 are synthetic lethal in a ccRCC model

To investigate the relationship between BAF180 and BAP1 in a more clinically relevant manner, we then decided to look at cell viability after BAP1 and BAF180 siRNA depletion in a panel of renal cell cancers. The A704 and 769-P cell lines were derived from human ccRCC and have inactivating mutations in BAF180 and BAP1 respectively. In the renal cells, A704, lacking BAF180, cell viability is greatly compromised after further depletion of BAP1 (Figure 3.6a). Similarly, but not as strikingly, depletion of BAF180 in a BAP1 mutant cell line, 769-P, also

resulted in a reduction of viability compared to siControl only (Figure 3.6a). By Western blot analysis, we find that the A704 cell line harbouring the BAF180 mutation leads to a total loss of protein. Whereas the 769-P cell line that harbours the BAP1 mutation, does not abrogate protein expression but does result in a loss of function (Pena-Llopis, Vega-Rubin-de-Celis et al. 2012). Together, these data suggest that BAP1 is synthetic lethal with BAF180 in a number of systems, including U2OS, as well as the more clinically relevant ccRCC system.

A

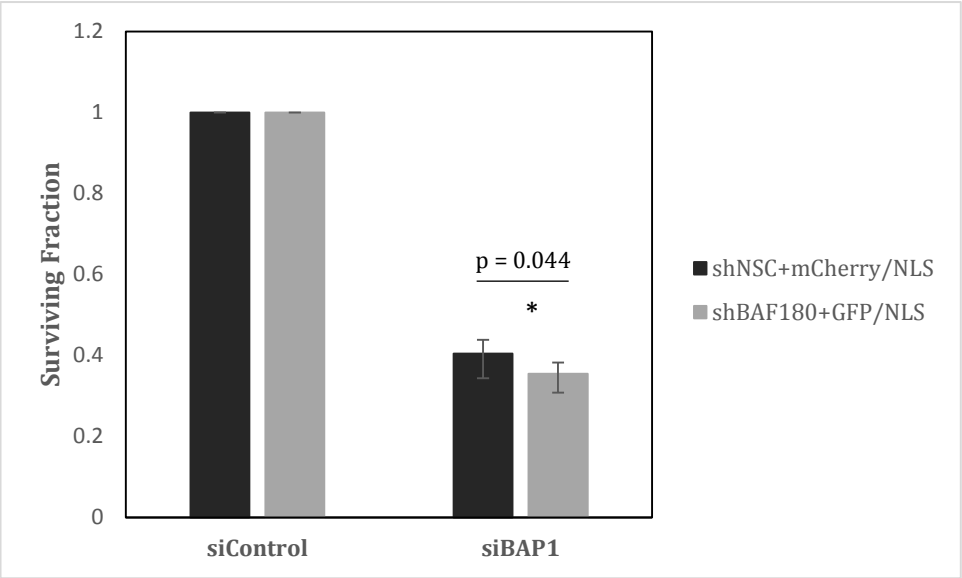

B

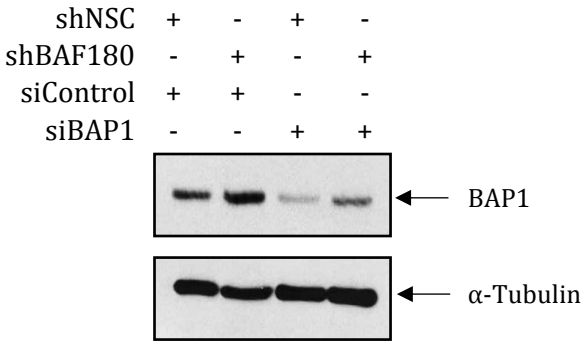

Figure 3.5 BAF180 depleted shU20S are more sensitive to depletion of BAP1. (A) shBAF180 cells (see Chapter 4) were more sensitive to siRNA knockdown of BAP1 in triplicate experiments. Statistical significance is represented by * for $p<0.05$, as analysed by Student t-test. (B) Western Blot Analysis of siRNA treated shU20S cells. Whole cell extracts were prepared and separated by 8% SDS-PAGE gels, transferred to nitrocellulose and probed with antibodies raised against BAP1. α-tubulin was used as a loading control

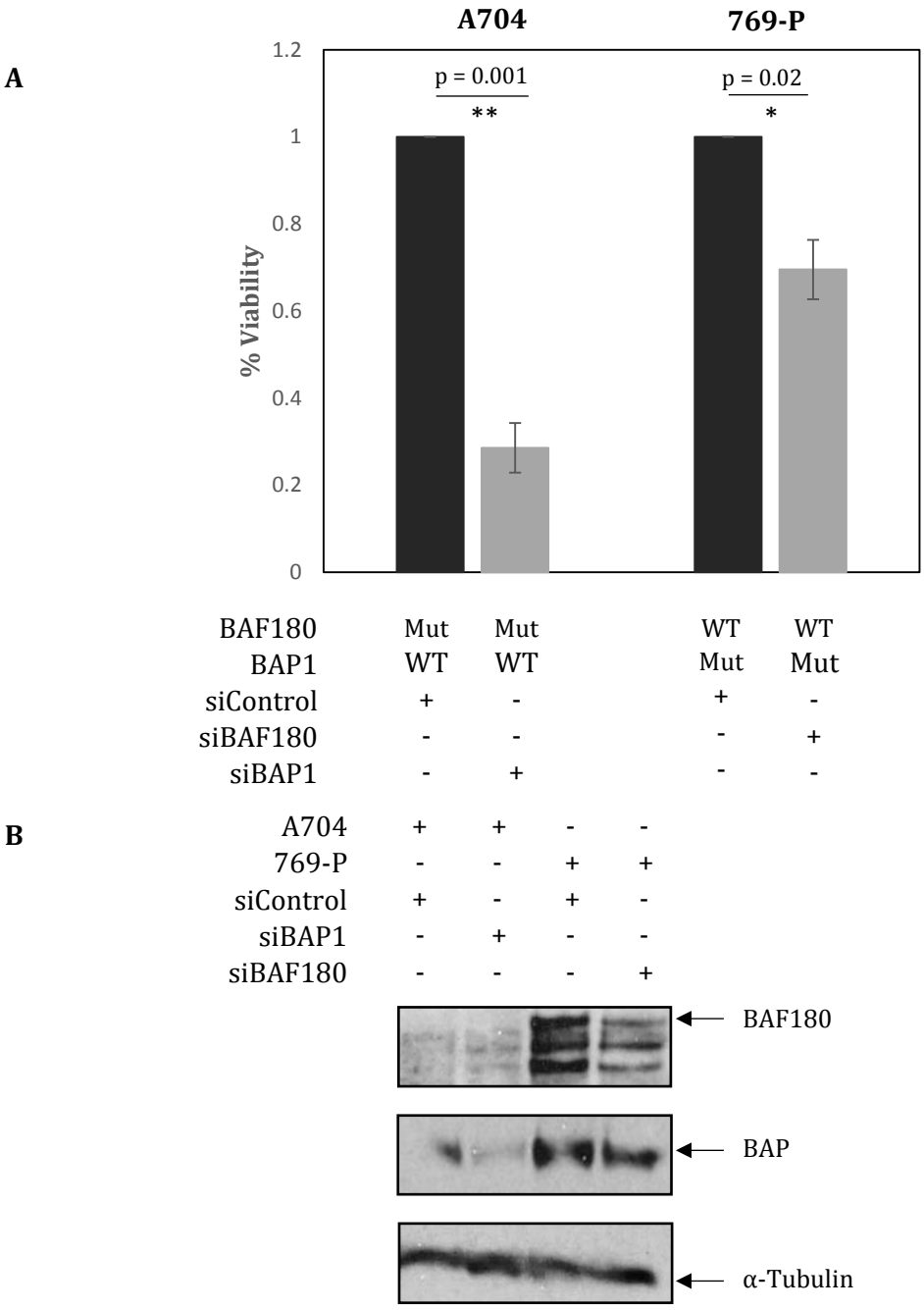

Figure 3.6 BAP1 and BAF180 are synthetic lethal in a ccRCC model (A) Promega Cell Titre Glo Viability Assay in RCC's. siRNA against human BAP1 as well as scrambled or 'control' siRNA was transfected in to the BAF180 lacking A704 renal cancer cell line and likewise, BAF180 siRNA was transfected in to the BAP1 mutated renal cell line 769-P, using Lipofectamine RNAiMAX transfection reagent. 72hrs after primary transfection the cells were re-seeded in triplicate per condition to 96 well plates. Viable cells were measured 24 hours later using cell titre glo reagent. Both the A704 and 769-P cell lines showed a sensitivity to siRNA knockdown of BAP1 and BAF180 respectively, suggesting a synthetic lethal interaction between the two genes. (B) Western blot analysis of siRNA treated renal cells.

3.8. Discussion

In this chapter we demonstrated that multiple genes exhibit a synthetic lethal phenotype when knocked down in mammalian cells in combination with BAF180 (PBRM1). Consistent with data from yeast high-throughput synthetic fitness screening (Cairns, Schlichter et al. 1999, Pan, Ye et al. 2006, Lin, Qi et al. 2008), we found that RNF4 and GCN5 (KAT2A) have a conserved synthetic lethal interaction with mammalian BAF180. While not statistically significant in the assays carried out in this study, we have illuminated a possible synthetic lethal interaction between BAF180 and ASF1B, HDAC4 and TIP60 that have potential to be validated with further testing.

In corroboration with multiple studies that identify EZH2 as an essential gene in cancers that have lost subunits of the SWI/SNF complex (Wilson, Wang et al. 2010, Bitler, Aird et al. 2015, Fillmore, Xu et al. 2015, Kim, Kim et al. 2015), we were able to confirm a synthetic lethal relationship between BAF180 and EZH2 that can be applied to clinical therapy using drugs that target EZH2s methyltransferase activity, such as GSK126.

We also identified BAP1 as a synthetic lethal interactor of BAF180, which could be exploited clinically with the use of BAP1 inhibitors.

A summary of all synthetic lethal interactions studies in this chapter are shown in Table 3.2.

Gene Name	BAF180 SL Rationale	Assay Used	SL interaction with BAF180
ASF1A	Synthetic Lethal with Rsc2	Viability Assay	No
ASF1B	Synthetic Lethal with Rsc2	Viability Assay	No
CTF18	Synthetic Growth Defect with Rsc2	Viability Assay	No
HDAC1	Synthetic Lethal with Rsc1 and Rsc2	Viability Assay	No
HDAC4	Synthetic Lethal with Rsc2, Synthetic Growth Fefect with Rsc1	Viability Assay	No
TIP60 (KAT5)	Synthetic Lethal with Rsc1 and Rsc2	Viability Assay	Yes
RNF4	Synthetic Growth Defect with Rsc1 and Rsc2	Viability Assay	Yes
GCN5 (KAT2A)	Synthetic Lethal with Rsc1 and Rsc2	Viability Assay	Yes
EZH2	Required for survival in SWI/SNF mutated cancers	Clonogenic Survival Assay	Yes
BAP1	Also a driver of ccRCC, mutually exclusive with BAF180	Clonogenic Survival Assay	Yes

Table 3.2. Overview of interactions tested in hypothesis driven screen. *Note: While ASF1B and HDAC4 are noted as not synthetic lethal with BAF180 in this table, this conclusion is limited to this specific viability assay. For these genes the data looked promising, though not statistically significant.

3.8.1. Histone acetyltransferases and synthetic lethality with BAF180

Two histone acetyltransferases (HAT) genes have been identified as being synthetic lethal with mammalian BAF180 from this data, TIP60 (KAT5) and GCN5 (KAT2A).

As mentioned, TIP60 is the catalytic subunit of the NuA4/TIP60 complex and has well established roles in the regulation of the DNA DSB response (Ikura, Ogryzko et al. 2000, Sun, Jiang et al. 2005). TIP60 has also been linked to regulating faithful mitotic chromosome segregation via the acetylation of Aurora B, with TIP60 working to stabilize Aurora B's activity during the transition from metaphase to anaphase (Mo, Zhuang et al. 2016). Work in our lab has shown that BAF180 also regulates mitotic stability, but unlike TIP60, BAF180 promotes the correct establishment of centromere cohesion, subsequently preventing genome instability and aneuploidy (Brownlee, Chambers et al. 2014). One possibility is that a combined defect in both mechanisms could be the contributing cause of the synthetic lethal effect we see (Figure 3.1) (Hopkins, McGregor et al. 2016).

The second and more convincing evidence of synthetic lethality between BAF180 and HAT genes was seen with GCN5 (Figure 3.3). GCN5 was found to be synthetic lethal with BAF180's yeast homologs Rsc1 and Rsc2 (Cairns, Schlichter et al. 1999).

Bromodomains are found in many proteins and are important for the regulation of transcription and chromatin structure and can be found in proteins with HAT activity, like GCN5 as well as in members of the SWI/SNF family, including BAF180 (Jeanmougin, Wurtz et al. 1997, Winston and Allis 1999). Bromodomains bind to the amino-terminal tails of histones H3 and H4 (Ornaghi, Ballario et al. 1999) and function as acetyl-lysine binding motifs (Dhalluin, Carlson et al. 1999). In GCN5 the bromodomains are not thought to play an important role (Candau, Zhou et al. 1997), however genetic cooperativity has been found between the bromodomains of Rsc4, another homologue of BAF180, and GCN5. Lys14 of histone H3 is the preferred site of acetylation by GCN5 and is also a critical residue for Rsc4 bromodomain function. It could be speculated that loss of this

interaction between both bromodomain containing complexes, including loss of acetylation at Lys14 of histone H3, could be the underlying reason for the synthetic lethality found in this study.

3.8.2. Possible mechanisms for synthetic lethality between BAF180 and RNF4

As previously mentioned, RNF4 is an E3 ubiquitin-protein ligase that is one of the most characterised SUMO targeted ubiquitin ligase (STUbL) in mammalian cells. Ubiquitylation and SUMOylation can simply be described as the covalent attachment of ubiquitin and/or SUMO polypeptides to target proteins, thus providing a mechanism to regulate cellular functions, which is important for the maintenance of genome stability (Jackson and Durocher 2013). These post-translational modifications are important for the coordination of multiple pathways, including the DNA damage recognition pathway, the cell signalling pathway and DNA repair (Jackson and Durocher 2013). Work in our lab has shown BA180 to have an important role in the repriming of replication downstream from replication forks that have been blocked at sites of DNA damage (Niimi, Chambers et al. 2012). Depletion of BAF180 after DNA-damage with UV-irradiation, resulted in a reduction of PCNA ubiquitination as well as unmodified chromatin-associated PCNA and the STUbL E3 ligase that ubiquitinates PCNA, Rad18. Interestingly, we found that the BAH domains of BAF180 are specifically required for the ubiquitination of PCNA (Niimi, Hopkins et al. 2015). The cooperation between BAF180 and ubiquitylating ligases could explain the mechanism behind the synthetic lethality observed after double depletion of BAF180 and RNF4. In vitro, the ubiquitylation targets of STUbLs are relatively unspecific (Sun, Leverson et al. 2007), so it is possible that RNF4 acts to compensate for the decrease in Rad18 after BAF180 depletion and when this compensatory pathway is removed, could result in replication fork collapse and subsequently the cell death we observe in Figure 3.2.

Alternatively, I found that depletion of BAF180 results in a defect in HR (Chapter 6). Inactivation of RNF4 in both mammalian and chicken cells results in the defective repair of DNA DSBs by both HR and NHEJ (Galanty, Belotserkovskaya et al. 2012, Luo, Zhang et al. 2012, Yin, Seifert et al. 2012). Therefore, it is plausible to assume that loss of two pathways that are responsible for the repair of damaged DNA via HR and NHEJ could be sufficient to trigger apoptosis in these cells.

Although RNF4 is potentially targetable by drugs, there are currently no known inhibitors, making the transition from bench to clinic more difficult than with other genes we have found to be synthetic lethal with BAF180 in this study.

3.8.3. Synthetic lethality by targeting EZH2 methyltransferase activity in BAF180-mutated cancers

EZH2 is an epigenetic regulator that silences the expression of its target genes (Bitler, Aird et al. 2016). EZH2 is upregulated in a variety of cancers including breast, prostate and lymphomas and can often be associated with advance staging of tumour progression and poor prognosis, suggesting it has an important role in oncogenic transformation (Varambally, Dhanasekaran et al. 2002, Bracken, Pasini et al. 2003, Simon and Lange 2008, Wilson, Wang et al. 2010). It is already known that there is a genetic dependence on EZH2 in cancers that lack the SNF5 subunit of SWI/SNF and that the complexes they belong to are antagonistic with each other (Wilson, Wang et al. 2010). EZH2 catalyses the methylation of lysine 27 on histone H3, which is associated with transcriptionally repressed heterochromatin. Whereas the catalytic activity exhibited by SWI/SNF complexes is associated with euchromatin, an open, relaxed state of chromatin that is transcriptionally active. It is thought that the chromatin remodelling activities mediated by SWI/SNF complexes can be counteracted by polycomb proteins, such as EZH2.

In this study, congruent to the findings between EZH2 and SNF5 (Wilson, Wang et al. 2010), we observe an increase in EZH2 protein expression after BAF180 loss, suggesting there may be a functional relationship between BAF180 and EZH2 in

oncogenic transformation. And in agreement with Kim et al(Kim, Kim et al. 2015), we found that treatment with GSK126 in BAF180 (PBRM1) mutant cell lines results in impaired colony formation. These data suggest that like SNF5, BAF180 deficiency also leads to upregulated EZH2 expression and that survival of our BAF180-deficient cancer cells is directly dependent on this upregulated EZH2. This is a phenotype that can be exploited therapeutically using inhibitors against EZH2 in cancers that are deficient in BAF180.

It has been shown that the ARID1A subunit of SWI/SNF and EZH2 have antagonistic roles and regulate many genes that overlap (Bitler, Aird et al. 2016). In ARID1A mutated ovarian clear cell carcinoma (OCCC), PIK3IP1 was found to contribute to the observed synthetic lethality seen after these ARID1A –deficient cancers were treated with EZH2 inhibitors. PIK3IP1 is a target gene that was reactivated after EZH2 inhibition in ARID1A mutated OCCC, subsequently responsible for triggering apoptosis, leading to cell specific killing of the ARID1A-mutated cancer cells but not wild type cells. They suggest using EZH2 inhibitors in combination with an inhibitor of the PI3K/AKT pathway to achieve a greater clinical benefit in OCCC. This is something to consider with the synthetic lethality observed in our case with BAF180 and EZH2. Further investigation in to target genes that are potentially upregulated after EZH2 inhibition in BAF180-deficient cancers could generate a new approach to therapeutic treatment of ccRCC. The discovery of another target that could be inhibited in combination with EZH2 inhibitors would result in a much greater clinical benefit for cancers that lack BAF180, like ccRCC.

3.8.4. Therapeutic exploitation of the mutually exclusive BAF180 and BAP1 mutations for treatment of ccRCC

Meta-analysis (Pena-Llopis, Christie et al. 2013) and independent validation (Hakimi, Ostrovnaya et al. 2013) have determined that mutations in BAP1 and BAF180 (PBRM1) tend to be mutually exclusive in ccRCC (Pena-Llopis, Vega-Rubin-de-Celis et al. 2012, Kapur, Christie et al. 2014).

As previously mentioned, mutation exclusivity often suggests that two genes function in the same pathway, which could itself result in synthetic lethality. However, in the case of BAP1 and BAF180, it is more likely that the two genes function in two different pathways. As mentioned before BAF180 and BAP1 mutations give rise to markedly different clinical outcomes, they have non-overlapping gene expression signatures and BAP1 mutations are associated with high Fuhrman grade (a widely used grading system for renal cell carcinoma, on a scale of I-IV, where grade I is associated with best prognosis and grade IV the worst) and mTORC1 activation while PBRM1 mutations are associated with low Fuhrman grade and a lack of mTORC1 activation, supporting the argument that BAP1 and BAF180 must act in two distinct pathways (Brugarolas 2013). Work in our lab has speculated a role for BAF180 in HR and it is known that loss of BAP1 results in impaired recruitment of HR factors like BRCA1 and RAD51 (Ismail, Davidson et al. 2014). Therefore, combined loss of two pathways that contribute to HR, together with other impaired pathways and factors due to loss of either gene, is most likely to be the underlying reason why these two genes exhibit a synthetic lethal relationship. To exploit this interaction clinically, it would be useful to test this synthetic lethality with inhibitors against BAP1.

4. Cell line generation

4.1. Introduction

The manipulation of cell lines in scientific research is important for the functional study of specific genes, to observe what effect the loss or gain of these genes has on the cells. There are multiple ways of carrying out gene manipulation in human cell lines in culture, but the two I will focus on in this chapter are the formation of stable cell lines through shRNA knockdowns and the production of gene knockout cells using CRISPR technology.

4.1.1. RNA Interference (RNAi)

RNA interference (RNAi), also known as co-suppression, post-transcriptional gene silencing (PTGS) and quelling, has proved itself a valuable tool for the study of gene function in mammalian cells in recent years. The mechanism was first discovered in the nematode *Caenorhabditis elegans* after double-stranded RNA (dsRNA) delivered by injection resulted in the sequence specific silencing of genes (Fire, Xu et al. 1998). It is believed that the natural endogenous function of RNAi works to protect the genome against invasion from dynamic genetic elements that form aberrant RNA or dsRNA in a host cell when they are activated, such as transposons and viruses (Elbashir, Lendeckel et al. 2001). The principle of RNAi works by specifically degrading the sequence of the host mRNA after double-stranded RNA (dsRNA) that is homologous to the target sequence is delivered through the cytoplasm (Fire, Xu et al. 1998). An endogenous complex called RISC (RNA-induced silencing complex) is involved in the enzymatic pathway used to degrade target gene expression. RISC, with assistance from the proteins Argonaute (Ago) and dsRNA binding proteins, allows for the loading of the guide siRNA strand to the complex, which is then able to localise the guide to the complementary sequence of mRNA. This mRNA is cleaved by the protein Ago and subsequently degraded by other endogenous

nucleases (Elbashir, Lendeckel et al. 2001, Moore, Guthrie et al. 2010). The mechanism of RNAi is served by several methods, the simplest being the transfection of chemically synthesized short interfering RNA oligonucleotides (siRNAs) in to the cytosol and the method that I will focus on here, which involves the use of short hairpin RNAs (shRNAs) (Moore, Guthrie et al. 2010). shRNAs can be introduced to cells via transfection within plasmid vectors, where the shRNAs are encoded within and transcribed from these vectors by RNA pol III or modified pol II promoters (Moore, Guthrie et al. 2010). Delivery of shRNAs to cells can also be achieved by the infection of the cell using virally produced vectors (Moore, Guthrie et al. 2010). The benefit of using shRNA rather than siRNA is that due to cytosolic delivery, siRNA gene knockdowns are transient, whereas shRNAs allow for the production of a stable gene knockdown within a cell line (Moore, Guthrie et al. 2010). shRNAs are typically formed of two complementary sequences that are between 19-22 base pairs in length, these are linked by a short loop of 4-11 nucleotides, which is reminiscent of the naturally occurring microRNA (miRNA) hairpin. After transcription, the endogenous enzyme Dicer detects the shRNA sequence in the cytosol. Dicer enables the processing of dsRNA and pre-microRNAs to synthesize functional intermediates such as siRNA duplexes and miRNAs, that can subsequently bind to the target mRNA and are incorporated in to the RISC complex for sequence-specific gene degradation (Vermeulen, Behlen et al. 2005, Moore, Guthrie et al. 2010).

The shRNA plasmids used in this study were expressed as unique human microRNA-30 (miR-30) primary transcripts and were designed to add a Drosha processing site to the hairpin construct, which is thought to increase gene-silencing efficiency (Boden, Pusch et al. 2004). Drosha is a nuclease that mediates initial miRNA processing in the nucleus from pri-miRNA to pre-miRNA, which is further processed by Dicer in to mature miRNAs (Lee, Ahn et al. 2003). Using a cell line with stable depletion of a protein has several experimental advantages over transient depletion. For example, it would not be possible to create a long-term cell line using siRNA gene knockdowns when taking in to consideration that the oligonucleotide concentration is diluted over time during normal cells division and constant transfection with siRNA can become extremely

expensive over time. We therefore created multiple shRNA-expressing cell lines. I will discuss exactly how these cell lines were generated in detail in section 4.3.

4.1.2. CRISPR/Cas9 targeted genome editing

Clustered, regularly interspaced, short, palindromic repeats (CRISPR) technology is rapidly becoming the gold standard method used to introduce precise and targeted changes in the genome of living cells. Endogenous CRISPR, together with CRISPR-associated (Cas) genes, are essential in adaptive immunity in both bacteria and archaea, providing a defence mechanism that eradicates invading genetic material (Barrangou, Fremaux et al. 2007). CRISPR is defined as genetic code that incorporates short repetitions of base sequences followed by spacer DNA segments. It is a bacterial system that normally functions in adaptive immunity. This mechanism observed in bacteria has been subsequently exploited and adapted in to a form of genome editing that is essential in mainstream research today. The CRISPR/Cas9 technology that has developed from this knowledge of bacteria uses the endonuclease activity of Cas9 along with a synthetic guide RNA, that can be tailored to your specific gene, to introduce a double strand break at that specific location within the genome. When these breaks are recognised within the cell, DNA repair pathways are stimulated to repair these breaks, either by NHEJ or HR (Ran, Hsu et al. 2013). NHEJ will most typically be used to repair double strand breaks that are introduced in this manner, this pathway choice is error prone and introduces insertions and deletions, resulting in frameshift mutations in the genes coding sequence (Figure 4.1).

HR can also be used to repair DNA DSBs induced by CRISPR/Cas9. This can be exploited by providing a donor sequence with modifications at a target site (Ran, Hsu et al. 2013).

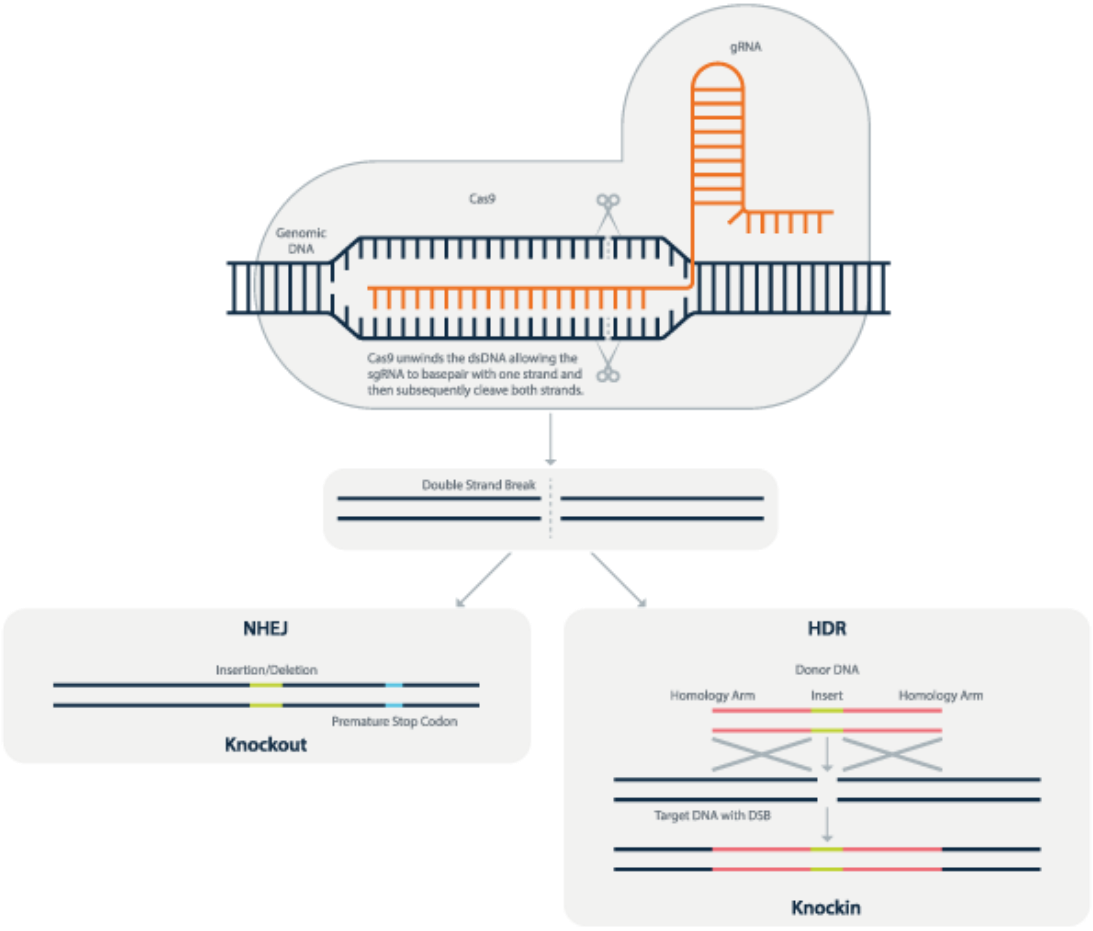

Figure 4.1. Cells will repair DNA DSBs by NHEJ or HDR after CRISPR treatment. Taken from Horizon Discovery.

4.2. Aims

The aim of the work described in this chapter was to create multiple cell lines with reduced/null BAF180 protein expression by shRNA depletion as well as CRISPR knockout for use in the experiments discussed in this thesis as well as to understand the biological impact of BAF180 in cells.

4.3. Establishing stably depleted BAF180 cell lines using GIPZ lentiviral shRNA

To establish cell lines that have stably reduced BAF180 expression, we chose to use BAF180 and non-silencing control (NSC) GIPZ lentiviral shRNA vectors. Six different BAF180 shRNA constructs were acquired from Thermo Scientific, each targeting different regions of mammalian BAF180. Four of the BAF180 shRNA constructs targeted BAF180s bromodomains, in either bromodomains 2, 3, 4 or 6 (Figure 4.2a). The remaining two constructs targeted sequences either in the second BAH domain or the C-terminal region (Figure 4.2a). Important features of the mammalian expression plasmid include TurboGFP for monitoring transgene expression, a puromycin resistance gene for selection of successfully transfected cells and, of course, the short hairpin RNA (Figure 4.2b). The TurboGFP and shRNA are part of a bicistronic transcript, driven by the human cytomegalovirus (hCMV) promoter.

After transfection of the constructs, GFP expression was monitored over a period of 10-15 days in the presence of puromycin selection (Figure 4.2.c). Puromycin resistant colonies were isolated, and Western blot analysis was carried out on whole cell extracts, revealing that all of the constructs apart from one (targeting bromodomain 4 of BAF180), resulted in good depletion of BAF180 protein levels (Figure 4.2d). Cells expressing construct 1 seemed to consistently show good levels of BAF180 reduction and so were chosen to be taken into future experiments.

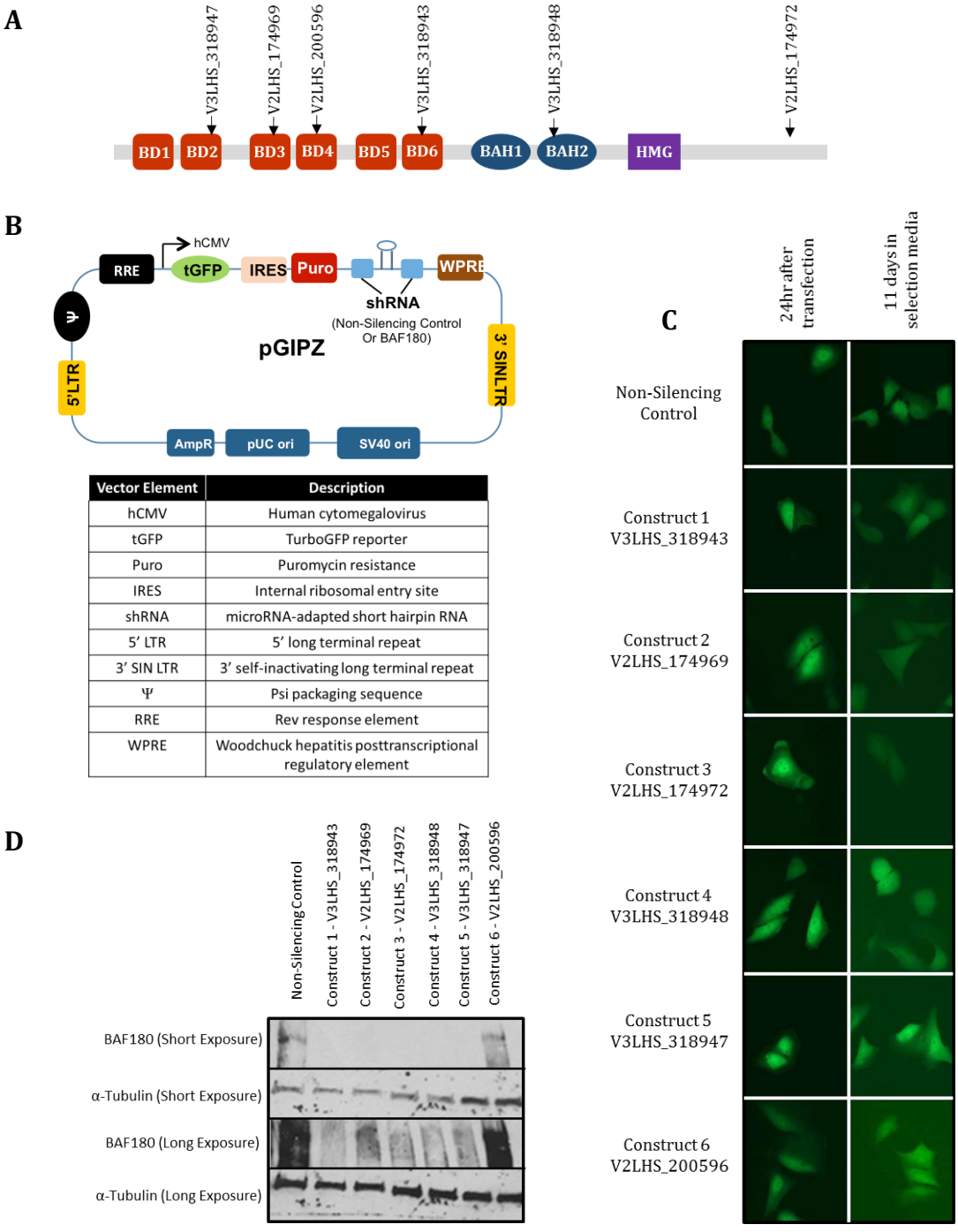

Vector Element	Description
hCMV	Human cytomegalovirus
tGFP	TurboGFP reporter
Puro	Puromycin resistance
IRES	Internal ribosomal entry site
shRNA	microRNA-adapted short hairpin RNA
5′ LTR	5′ long terminal repeat
3′ SIN LTR	3′ self-inactivating long terminal repeat
Ψ	Psi packaging sequence
RRE	Rev response element
WPRE	Woodchuck hepatitis posttranscriptional regulatory element

Figure 4.2. Establishing six BAF180 shRNA stable U20S cell lines using GIPZ lentiviral shRNA. (A) Illustration showing the domains of BAF180 and where each BAF180 shRNA sequence targets. (B) Features of the GIPZ lentiviral shRNA plasmid. Purchased from Thermo Scientific. (C) Representative images of GFP expressed 24 hours after transfection of each shRNA construct and 11 days after being under Puromycin selection. (D) Western blot showing knockdown efficiency of each shRNA construct.

For the purpose of the high-throughput siRNA screen (HTS), which I will talk about in chapter 5, it was necessary to have cell lines that were visually distinguishable when mixed together. To this end we then went about establishing sets of cell lines that expressed different fluorescent proteins. Using the shRNA constructs purchased from Thermo Scientific (shBAF180 – construct 1/V3LHS_318943 and shControl) we set about exchanging the TurboGFP for either GFP or mCherry with a nuclear localisation signal (Figure 4.3a), resulting in the following constructs, shNSC+mCherry/NLS, shNSC+GFP/NLS, shBAF180+mCherry/NLS and shBAF180+GFP/NLS.

To build a set of cell lines that were able to be used in the HTS as well as cell lines that were useful for other ongoing projects in the lab, we chose to express these modified plasmids in the osteosarcoma cell line U2OS, the lung cancer cell line A549, the breast cancer cell line T47D and the renal cell line 786-0, which is the most clinically relevant. Sixteen stable cell lines were established from these transfections and a representative image of one set of the U2OS cell lines created can be seen in Figure 4.3b. Whole cell extracts were gathered from all cell lines and BAF180 protein expression levels were analysed by western blot. A representative BAF180 blot is shown in Figure 4.3c, showing reduced levels of BAF180 in U2OS cells expressing the modified shBAF180+GFP/NLS, in comparison with the corresponding shNSC+mCherry/NLS control.

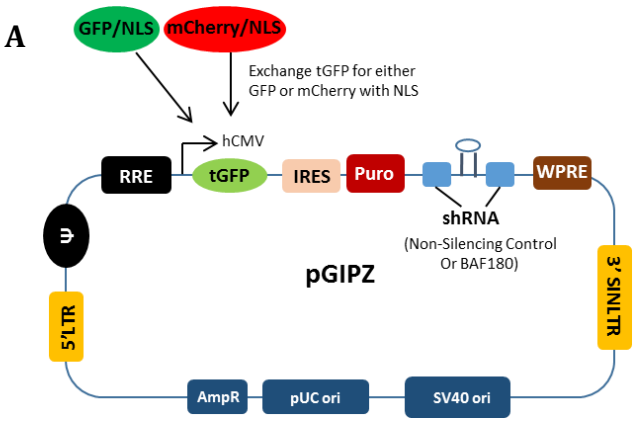

Vector Element	Description
hCMV	Human cytomegalovirus
tGFP	TurboGFP reporter
Puro	Puromycin resistance
IRES	Internal ribosomal entry site
shRNA	microRNA-adapted short hairpin RNA
5′ LTR	5′ long terminal repeat
3′ SIN LTR	3′ self-inactivating long terminal repeat
Ψ	Psi packaging sequence
RRE	Rev response element
WPRE	Woodchuck hepatitis posttranscriptional regulatory element

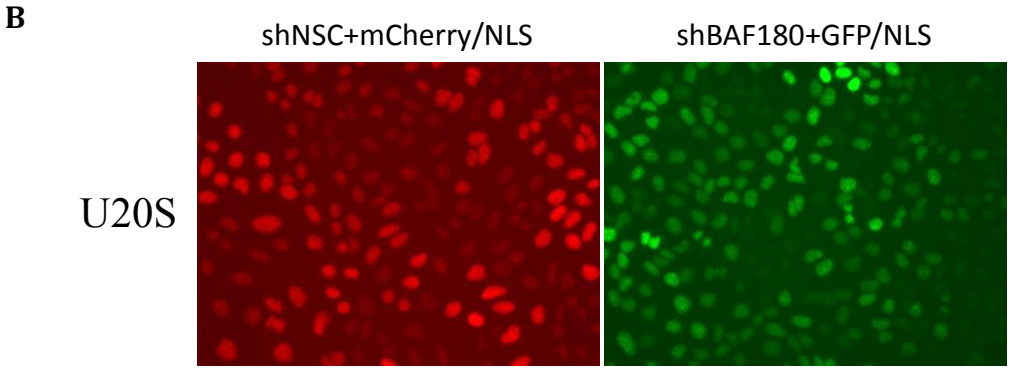

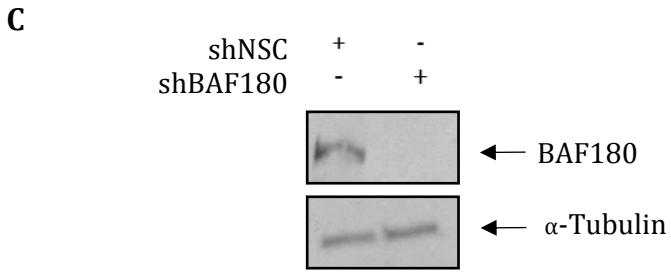

Figure 4.3. Substitution of TurboGFP for either GFP or mCherry with a nuclear localisation signal. (A) Illustration of the exchange of flurophores in shControl and shBAF180 GIPZ constructs (described in text). (B) Representative images of one of the sets of cell lines established from manipulated shRNA constructs. (C) Western blot showing BAF180 expression after transfection with either shControl or shBAF180 constructs.

4.4. Establishing BAF180 CRISPR Knockout cell lines

Genome engineering techniques are constantly evolving and CRISPR gene manipulations are becoming the gold standard. Five CRISPR guide RNAs were tested (Figure 4.4a) and these guides, like our shRNA constructs, targeted different areas of mammalian BAF180. We chose to create BAF180 CRISPR knockouts in the cell lines U2OS as well as the renal cells 786-0. A renal carcinoma cell line was chosen for clinical relevance, as we know that BAF180 is frequently mutated in ccRCC. 786-0 cells have a 3n copy number for BAF180 (PBRM1) and U2OS are well known to be aneuploid, making the full knockout of each copy of the gene would be slightly more difficult in these cell lines, than a cell line with normal ploidy. The guides from Horizon were integrated as part of an 'all in one' plasmid, that contained the Cas9 enzyme needed to introduce the break, DasherGFP to act as a transient marker of successful transfection, and the target guide sequence (Figure 4.4b - left). Transfection of the U2OS and 786-0 cells with each of our five CRISPR guides was originally not successful. Instead we harnessed the principle of co-transfection with the empty vector pcDNA4-GFP-IRES-Puro (kindly given to us by the Caldecott Lab – University of Sussex) to introduce a puromycin selection marker and a nuclear GFP signal, in contrast to the CRISPR constructs that express a cytosolic DasherGFP. Co-transfection with both plasmids allowed us to place the cells under antibiotic selection long enough to ensure the resultant population would only be cells that had successfully taken up both plasmids. A representative image of the two forms of GFP expressed by U2OS cells after transfection with both the CRISPR plasmid and the pcDNA4-GFP-IRES-Puro plasmid is seen in Figure 4.4c. Figure 4.5 provides an overview of the CRISPR process, showing a step-by-step break down of the multiple steps carried out from initial transfection with these two plasmids to confirming the final knockout clones.

A

PBRM1 CRISPR Guide RNA	Sequence
1	ATAGAAGAAGTTGGATTCCA
2	CCCGCTGACACTGCTGGAAG
3	GGCCTGGTGTTGACACAGAA
4	AGGATCTACAGTTGGAAGAT
5	GGCAATCTACACATTAGCAA

B

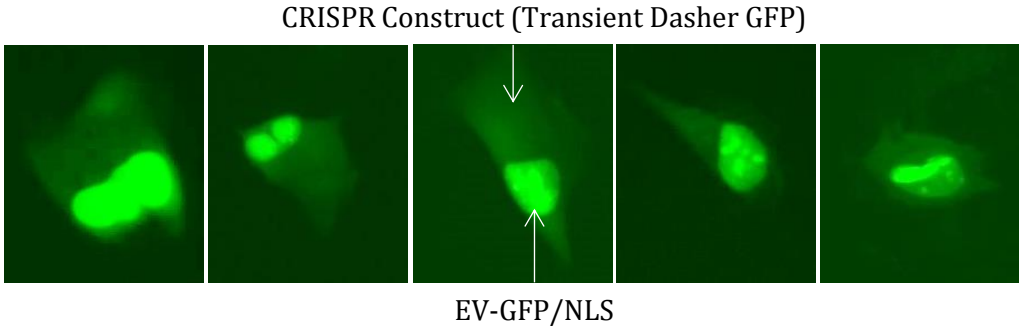

Figure 4.4. Establishment of a BAF180 CRISPR Knockout cell line. (A) Table showing target sequences of five BAF180 CRISPR guide RNAs. (donated from Horizon Discovery as part of their free CRISPR guide initiative. (B) Representative image of both types of GFP expression created by co-transfection of plasmids in U20S cells.

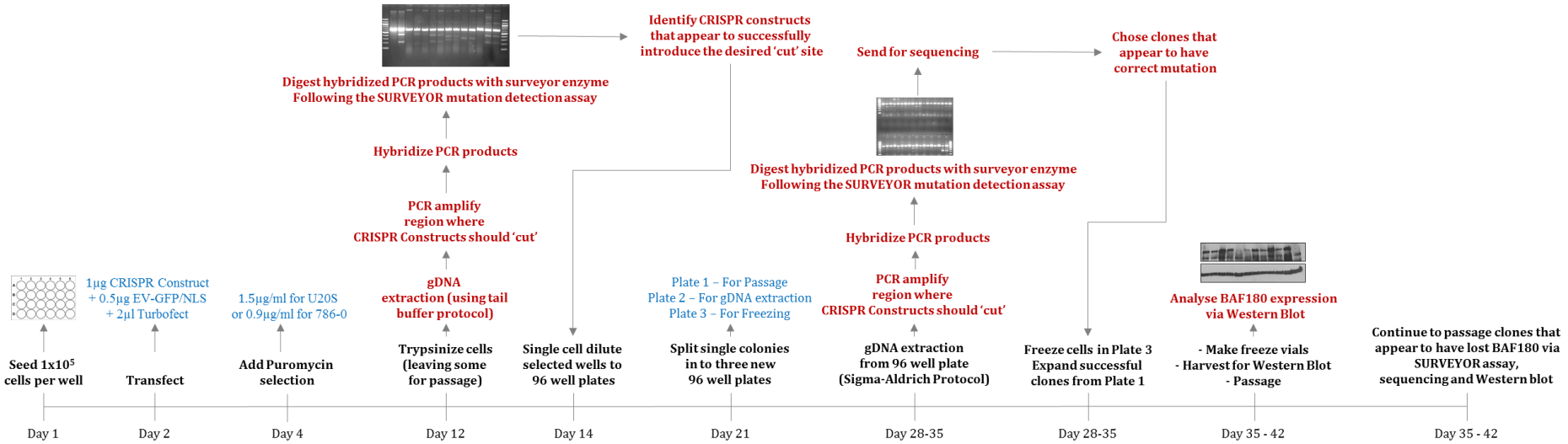

Figure 4.5. Scheme of establishing a BAF180 CRISPR Knockout cell line. A detailed flow diagram to show the lengthy and in-depth steps carried out to create a BAF180 CRISPR knockout cell line, from initial transfection of the cells to validation of successful clones.

After ensuring that we were getting successful transfection in our cells we then wanted to identify which CRISPR guide was working the most efficiently in a pooled population. U2OS and 786-0 cells were transfected with each CRISPR gRNA along with the pcDNA4 plasmid and were allowed to expand enough to harvest genomic DNA and continue to culture the samples. Genomic DNA was prepared and analysed by PCR using primers in Table 2.2 from test samples and in non-transfected control cells. CRISPR guides 1-4 were all in a region small enough to be serviced by one set of primers and CRISPR guide 5 targeted a region further away, requiring its own set of primers. Test and control PCR products were hybridized together and subsequently digested using the SURVEYOR mutation detection assay and visualised by gel electrophoresis. Homoduplexes appear on gels as a single DNA band, whereas heteroduplexes are cleaved by the SURVEYOR nuclease enzyme and will appear as fragmented DNA. Therefore, products that are digested by the nuclease in to multiple fragments suggest there is a mixed population of DNA, suggesting that genetic alterations have been introduced in the test samples. Pooled populations of U2OS cells transfected with all CRISPR constructs resulted in digested products when analysed by gel electrophoresis (Figure 4.6a). Control gDNA that was amplified with the PCR primers for constructs 1-4 and construct 5 treated with the SURVEYOR nuclease, as expected showed a homogeneous population, represented by a single band when analysed by electrophoresis (Figure 4.6a/b). If the pooled population of transfected cells had all been efficiently targeted by the CRISPR gRNA then you would expect to see a homogeneous population and a single band when analysed alone and a heteroduplex when mixed with the control gDNA. We observed a heteroduplex in all U2OS test samples when digested by themselves as well as when digested with the control, suggesting not all cells in our pooled population were successfully transfected and would require single cell clonal expansion to determine which cells had been successfully targeted (Figure 4.6a). The CRISPR guide efficiency appeared to be significantly lower in pooled populations of 786-0 cells, with only one guide, construct 2, appearing as a heteroduplex (Figure 4.6b).

A

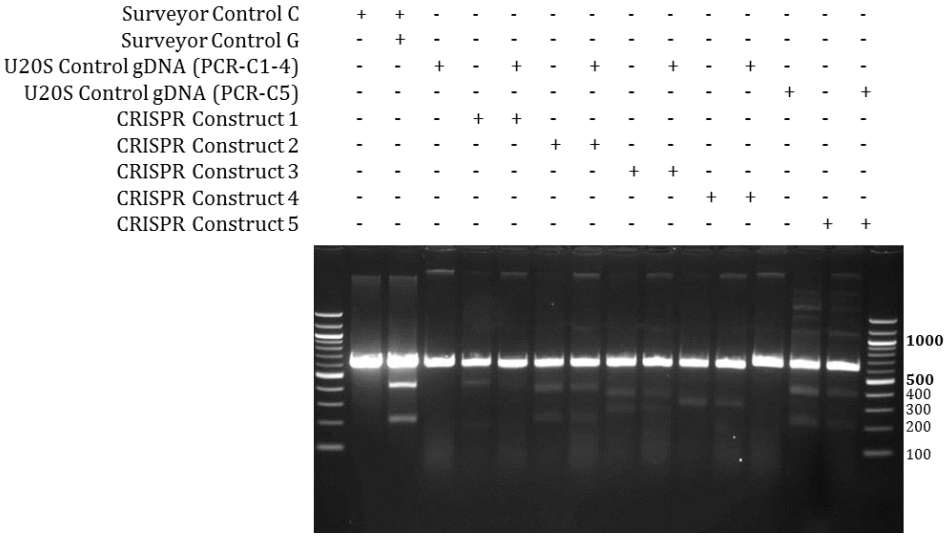

B

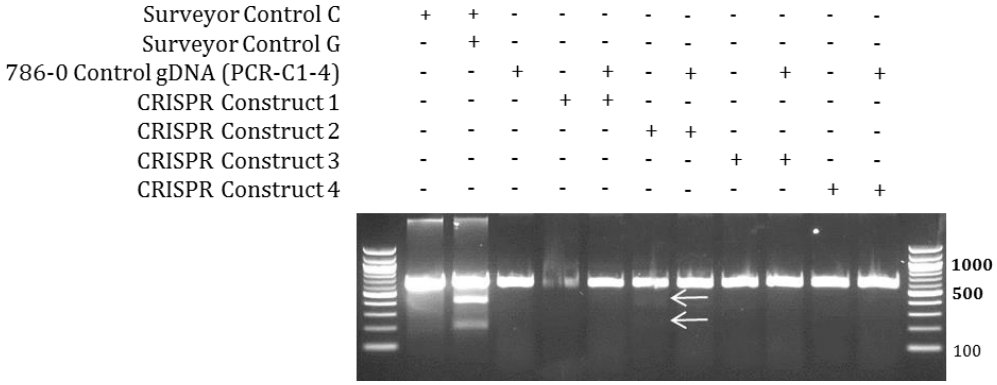

Figure 4.6. Identification of most efficient BAF180 CRISPR construct. Cells were initially transfected with each CRISPR guide to assess which guide would be most likely to establish a BAF180 KO cell line. Genomic DNA was harvested from treated and untreated cells and were hybridized together before treatment with the surveyor nucleases. Cleavage by surveyor nucleases indicates a heterogeneous population in the hybridization mixture. (A) Surveyor nuclease assay carried out using PCR amplified gDNA from U20S cells transfected with CRISPR guide RNAs. (B) Surveyor nuclease assay carried out using PCR amplified gDNA from 786-0 cells transfected with CRISPR guide RNAs.

To establish full knockout cell lines, we next had to isolate clonal populations from single cells. For this we chose to dilute the U2OS cells that had been transfected with both constructs 2 and 3 and the 786-0 cells that had been transfected with construct 2. Genomic DNA was harvested from the 96 well plates as described in 2.2.14, PCR amplified and digested with SURVEYOR nuclease as before. Multiple clones were analysed per cell line and representative analyses are shown in Figure 4.7a, Figure 4.8a and Figure 4.9a.

Twelve U2OS-based clones generated from CRISPR guide 2 were chosen for further analysis. Many appeared to have a reduced level of BAF180 protein expression, but two in particular, clones 26 and 39 had little or no BAF180 expression (Figure 4.7b). Stocks from all clones were frozen and have been stored in liquid nitrogen for future use.

Four 786-0 based clones were further investigated and all appeared to have lost BAF180 expression (Figure 4.8b). However, upon sequencing these clones, wild type BAF180 sequences were detected, raising the possibility that we did not have a full knockout cell line. Again all clones were frozen and stored in liquid nitrogen for future use.

Of the U2OS cells transfected with CRISPR guide 3, we chose five clones for further analysis, of which three appeared to have lost all or most BAF180 protein expression (Figure 4.9b). Sequencing analysis confirmed a deletion in the DNA sequence targeted by CRISPR construct 3 in clone 15 (Appendix Figure 1) and this clone chosen for use in further experiments. Although sequencing and western blot analysis (Figure 4.9b) was consistent with BAF180 knockout in our U2OS CRISPR-C3-Clone 15 cells, we noticed that there were still proteins detected by the BAF180 antibody, albeit at lower molecular weight and lower abundance than the normal BAF180 protein signal. To work out if these remaining bands were related to BAF180, we treated U2OS and our BAF180 knockout cells with either control siRNA or BAF180 siRNA. Using two different BAF180 antibodies, we found that the extra bands did in fact decrease in intensity after BAF180 siRNA treatment, suggesting that some form of BAF180 remains within these knockouts (Figure 4.10). These data may suggest that there is a truncated version of the

protein present in these cells as it runs at a molecular weight below the observable full length BAF180 band.

Importantly, however the cell line exhibits phenotypes that are in accord with BAF180 knockdown, such as an increased nucleus size and increased micronuclei (C. Meisenberg – unpublished data), suggesting that these putative truncated forms of BAF180 may not be functional, at least for these activities.

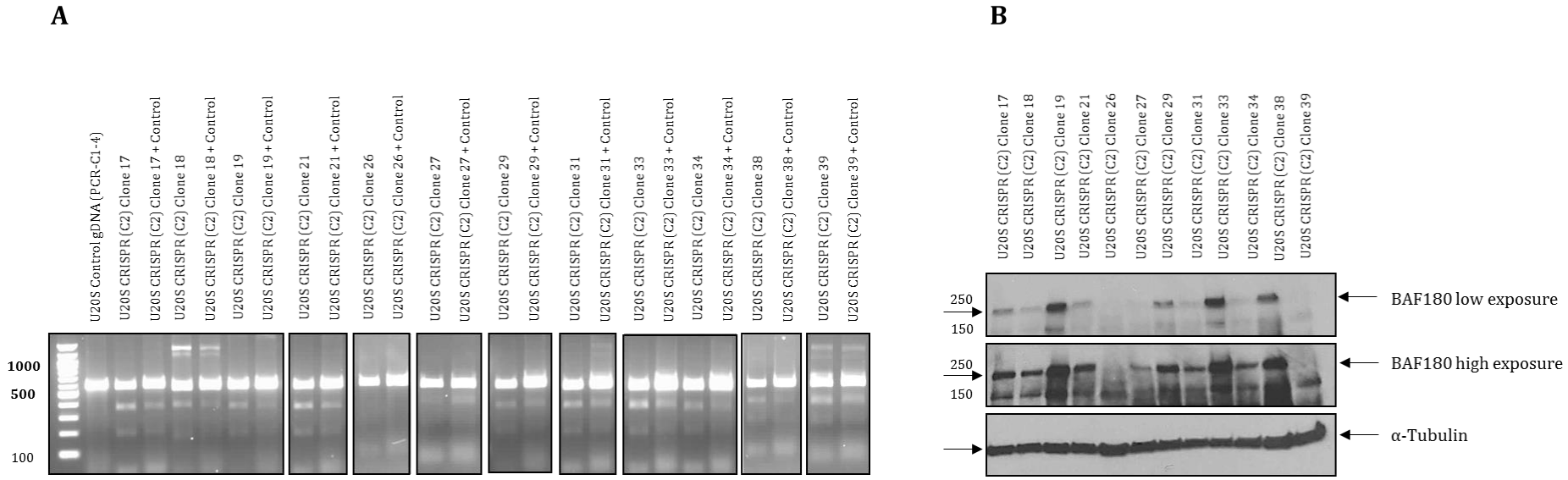

Figure 4.7. Identification of successful BAF180 Knockout clones in U20S using CRISPR guide 2. Cells transfected with the BAF180 CRISPR guide 2 were diluted to leave a single cell and allowed to form individual clones. Genomic DNA was extracted from various clones and was PCR amplified using specific primers that lie either side of the DNA sequence targeted by the CRISPR guide RNA (A) SURVEYOR nuclease assay. Agarose gel electrophoresis showing digestion products of multiple U20S clones that appear to have a heterogeneous population after cleavage by surveyor nuclease enzymes. (B) Western blot showing BAF180 protein expression corresponding to the U20S BAF180 CRISPR clones analysed in (A).

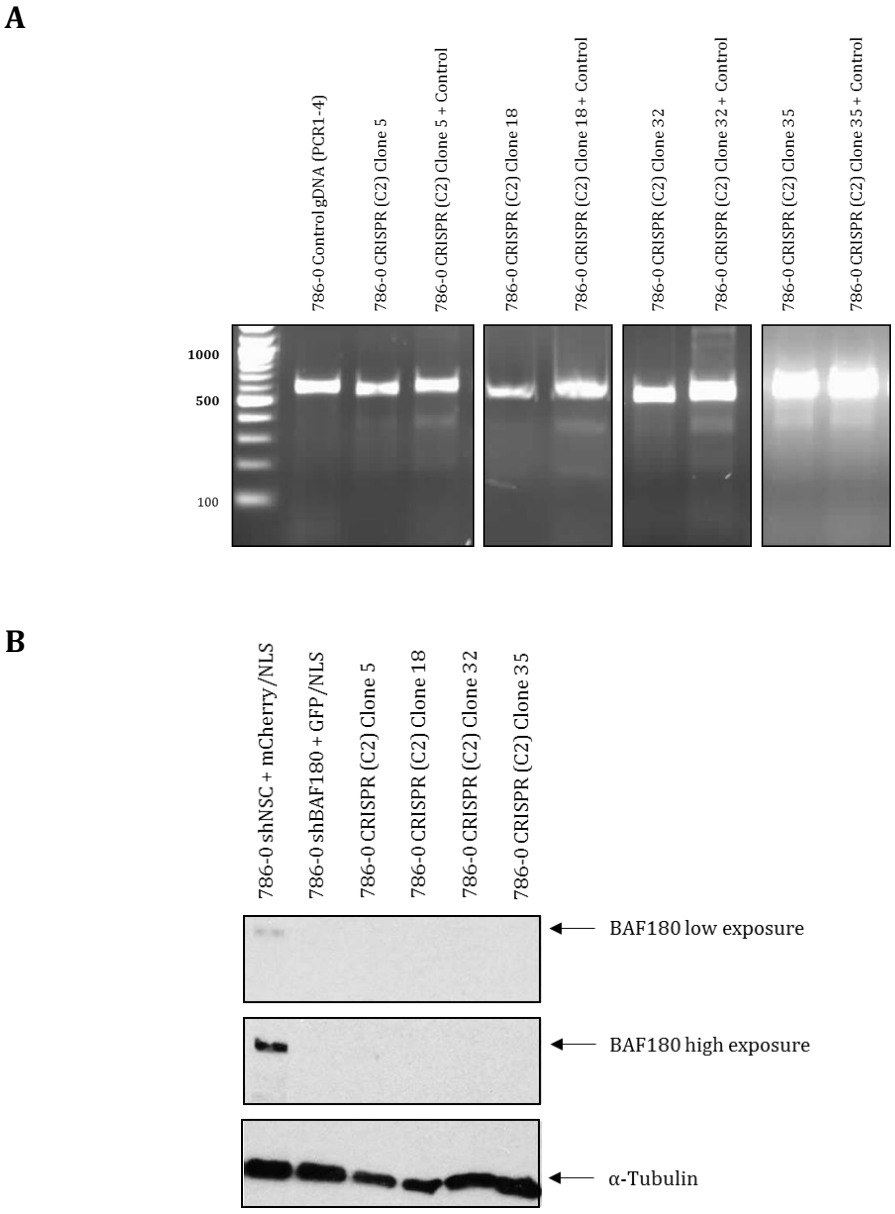

Figure 4.8. Identification of successful BAF180 Knockout clones in 786-0 using CRISPR guide 2. Cells transfected with the BAF180 CRISPR guide 2 were diluted to leave a single cell and allowed to form individual clones. Genomic DNA was extracted from various clones and was PCR amplified using specific primers that lie either side of the DNA sequence targeted by the CRISPR guide RNA (A) Surveyor nuclease assay. Agarose gel electrophoresis showing digestion products of multiple 786-0 clones that appear to have a heterogeneous population after cleavage by surveyor nuclease enzymes. (B) Western blot showing BAF180 protein expression corresponding to the 786-0 BAF180 CRISPR clones analysed in (A), using our shControl and shBAF180 786-0 cell lines as reference.

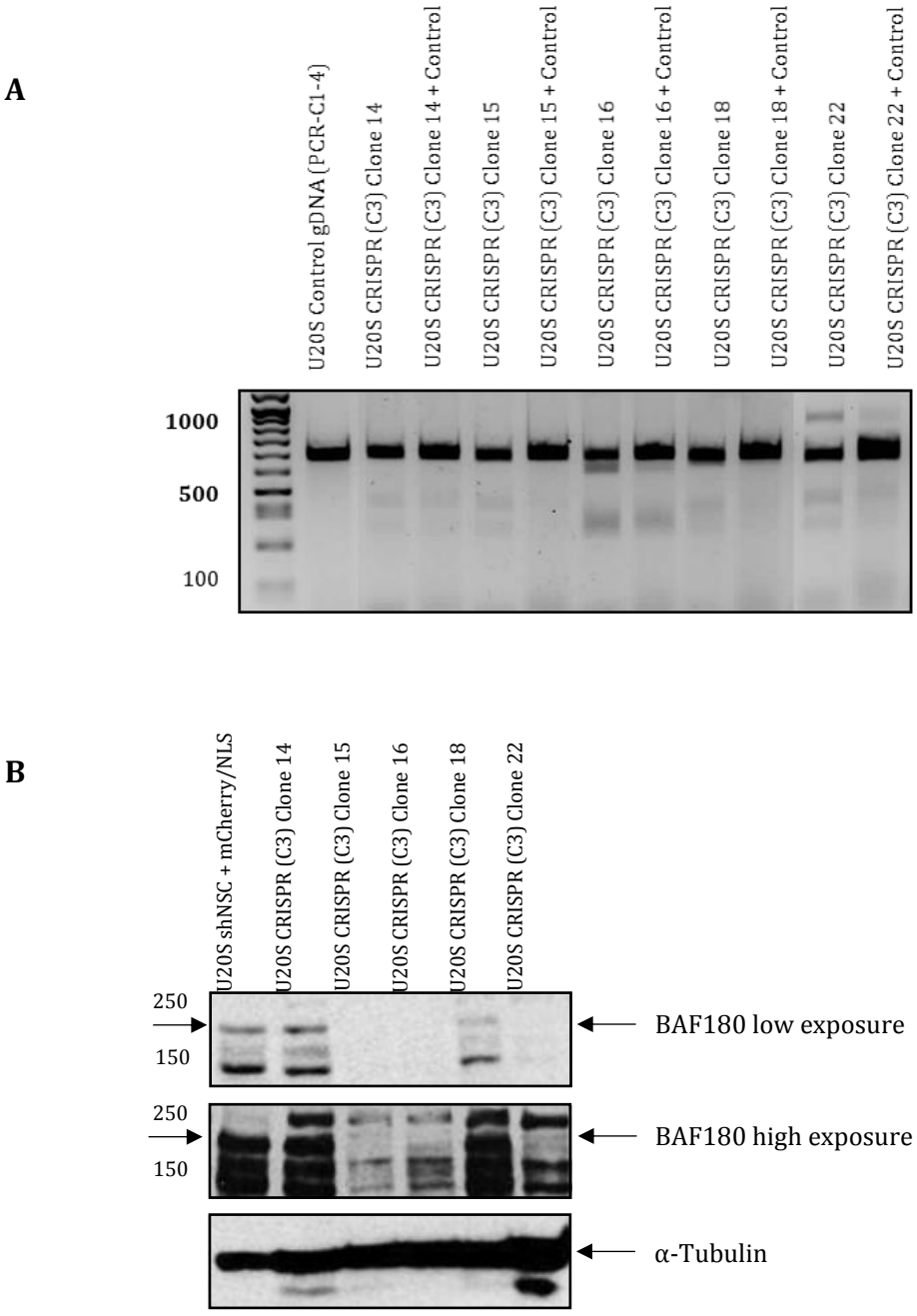

Figure 4.9. Identification of successful BAF180 Knockout clones in U20S using CRISPR guide 3. Cells transfected with the BAF180 CRISPR guide 3 were single cell diluted and allowed to form individual clones. Genomic DNA was extracted from various clones and was PCR amplified using specific primers that lie either side of the DNA sequence targeted by the CRISPR guide RNA (A) Surveyor nuclease assay. Agarose gel electrophoresis showing digestion products of multiple U20S clones that appear to have a heterogeneous population after cleavage by surveyor nuclease enzymes. (B) Western blot showing BAF180 protein expression corresponding to the U20S BAF180 CRISPR clones analysed in (A). Clone 15 was chosen as the most likely to have a full BAF180 knockout.

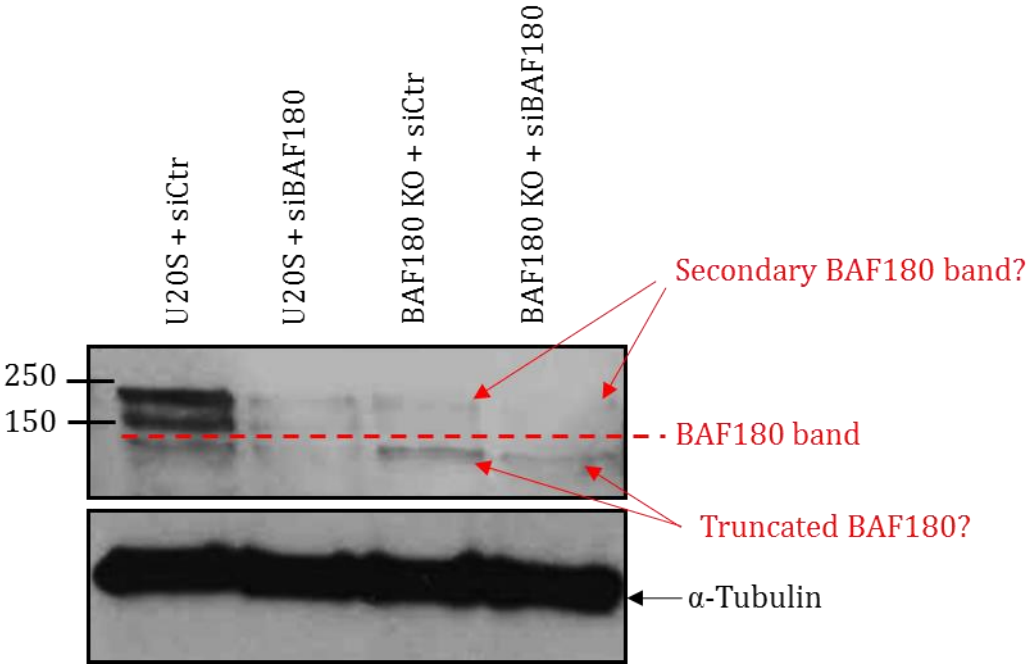

Figure 4.10. A truncated version of BAF180 may still exist in our U20S BAF180 CRISPR Knockout cells. Western blot showing BAF180 expression after BAF180 siRNA treatment in U20S and BAF180 CRISPR KO cells.

4.5. Discussion

Here we established multiple BAF180 depleted cell lines. Four U2OS cell lines were created expressing shControl+mCherry/NLS, shControl+GFP/NLS, shBAF180+mCherry/NLS and shBAF180+GFP/NLS. Four 786-0 cell lines were created expressing shControl+mCherry/NLS, shControl+GFP/NLS, shBAF180+mCherry/NLS and shBAF180+GFP/NLS. Four T47D cell lines were created expressing shControl+mCherry/NLS, shControl+GFP/NLS, shBAF180+mCherry/NLS and shBAF180+GFP/NLS. Four A549 cell lines were created expressing shControl+mCherry/NLS, shControl+GFP/NLS, shBAF180+mCherry/NLS and shBAF180+GFP/NLS. Six U2OS cell lines were established to express the various shBAF180+TurboGFP constructs and one with the corresponding shControl+TurboGFP.

U2OS shControl and shBAF180 cells with the original TurboGFP-expressing plasmids were used by Brownlee et al in experiments identifying that BAF180 promotes cohesion and prevents genome instability and aneuploidy (Brownlee, Chambers et al. 2014). shBAF180 and shControl plasmids were also used by Niimi et al to create MRC5V1 cell lines, identifying that the BAH domain of BAF180 is required for PCNA ubiquitination (Niimi, Hopkins et al. 2015). U2OS cells expressing shControl+mCherry/NLS and shBAF180+GFP/NLS were used by myself in collaboration with V. Savic in the identification of TIP60-dependent radiation sensitivity in the absence of BAF180 (Hopkins, McGregor et al. 2016). We have also shown the creation of multiple CRISPR BAF180 knockout cell lines in U2OS and 786-0, with one line being used by other lab members for characterisation experiments.

4.5.1. The advantages and limitations of genetic engineering using shRNA

Short hairpin RNA (shRNA) is a widely used approach for the creation of stable gene knockdowns and can be achieved using viral or non-viral DNA vectors.

Both siRNA and shRNA exploit the same cellular mechanism (RISC), but choosing between the use of siRNA or shRNA to achieve your target gene knockdown depends on multiple factors, such as cell type, time demands and the need for transient versus stable integration (Moore, Guthrie et al. 2010). An increasing concern with siRNA is the probability of experiencing off-target effects due to the high concentration of cytoplasmic siRNA. Also as the cells divide, the siRNA concentration becomes more dilute and therefore creation of a long-term cell line with your target gene knockdown is unfeasible. The generation of long-term stable cell lines using shRNA, on the other hand, completely eliminates the need for multiple rounds of transfection and therefore increases the reproducibility of results (Moore, Guthrie et al. 2010).

The generation of stable knockdown cell lines using shRNA silencing of a specific target gene can be greatly beneficial, however there are limitations and this approach can be time-consuming. The benefit here though is that you can carry out long-term experiments, such as clonogenic survival assays, without having to perform multiple siRNA transfections. The benefit of establishing stable cell lines is also that you can carry out experiments on a much larger scale than if you had to use siRNA.

A limitation that we have observed with our stable shRNA cells is that BAF180 knockdown correlates with GFP intensity, rather than being standard throughout the cell population (Hopkins, McGregor et al. 2016). In collaboration with the Savic lab (University of Sussex), we observed that cells that expressed high levels of GFP appeared to have the greatest level of BAF180 knockdown (Hopkins, McGregor et al. 2016). This is not a problem when you are able to 'bin' your data based on the specific cells you want to see using microscopy (discussed in Chapter 5). But becomes a slight problem, when you are carrying out an experiment where you cannot exclude the cells that have low GFP expression and therefore higher BAF180 expression, for experiments such as clonogenic survival assays that rely on data from a relatively small number of cells.
We also observed that BAF180 protein expression levels tend to drift over time, even under constant puromycin selection (Figure 4.11) (Hopkins, McGregor et al. 2016). The puromycin selection marker, the fluorescent protein and the shRNA

are all under the control of the same mammalian CMV promoter, with the shRNA being the furthest from the promoter. It is possible that the efficiency of this promoter to drive the constitutive expression of all three elements over time may drift.

We may have seen longer silencing of BAF80 by the shRNA used in this study if we had implemented a lentiviral system for infection of the cells during stable cell production. Lentiviral systems have higher transfection efficiencies than non-viral systems, this is due to the host genome being able to stably integrate the lentiviruses, thus establishing long-term stable expression of the integrated DNA sequence. However, this process is much more involved than simple transfection and also carries drawbacks, such as nuclear accumulation cellular toxicity (Davidson and McCray 2011).

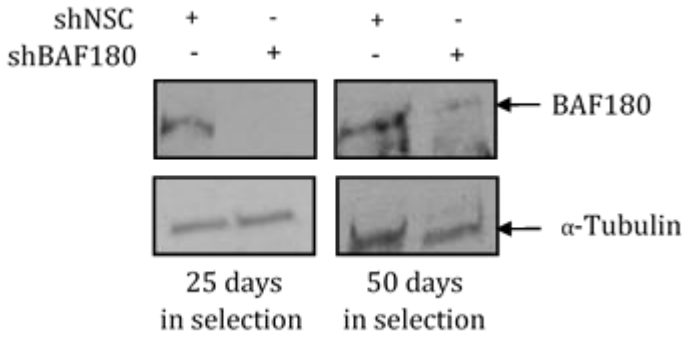

Figure 4.11. Endogenous BAF180 expression re-appears in shBAF180 U20S after continuous culture. Western blot showing BAF180 expression in shControl and shBAF180 U20S cells, 25 and 50 days after being in puromycin selection media.

4.5.2. The pros and cons of CRISPR/Cas9 gene editing

As previously mentioned, the CRISPR/ Cas systems are an RNA-based bacterial defence mechanism designed to recognise and eliminate foreign DNA from invading bacteriophage and plasmids, using the Cas endonuclease to introduce a cleavage site that is directed to a target sequence by a specific guide RNA (gRNA). The development of this advancing technology has revolutionised molecular genetics, allowing for the introduction of permanent changes to specific genes. Although the system is a relatively new technology it is rapidly becoming the gold standard choice for gene editing. This is due to the fact that CRISPR can make changes to the genetic code of a cell, resulting in a gene knockout, rather than a gene knockdown, like those achieved by siRNA and shRNA. Design of target guide RNAs is relatively simple because the target specificity relies on ribonucleotide complex formation and not protein/DNA recognition, therefore guides can be designed quickly and cheaply for any given gene sequence in the genome. However, there are limitations to the CRSIPR/Cas 9 system. The first being that establishing a CRISPR gene knock out is labour intensive and requires clonal isolation, whereas shRNA transfection and antibiotic selection is relatively quick in comparison. Screening for successful CRISPR clones can be time consuming. The CRISPR/Cas 9 system can also produce unwanted off-target effects by introducing a mutation at a non-specific locus that has similar, but not identical, sequence homology to the target sites. These off-target sites are hard to identify as you would have to sequence and scan the entire host genome to identify whether there are in fact mutations at sites with sequence similarity to the guide RNA. Sequencing the whole genome of cell lines is becoming less expensive than in previous years, but it is still extremely costly.

Although there are advantages and disadvantages to the CRISPR/Cas 9 system as well as it still being a developing technology, it remains a powerful tool for manipulating the genomes of cell lines, mice and even somatic and embryonic stem cells from mice and humans. It can be exploited as such to create sophisticated and precise models for the study of gene and cellular function and can provide deeper insights into the underlying mechanisms of human disease

(Chiang, le Sage et al. 2016). Establishment of our BAF180 CRISPR knock out cell lines provides a system where we can observe BAF180 loss in a more genetically relevant way, as opposed to relying on gene knockdowns.

5. Mammalian high-throughput synthetic lethal RNAi screen

5.1. Introduction

RNAi interference (RNAi) is an effective tool for genome-scale high-throughput analysis of gene function. The use of high-throughput screens can be exploited in many ways, for example to isolate multiple members of a functional pathway as well as implicate new genes in a given biological function, process, complex or behaviour.

When the normal function of a gene is required for a given function, RNAi knockdown may lead to a phenotype detectable in an assay that tests that function either directly or indirectly. In our case we are using shRNA knockdown cell lines treated with a library of 446 siRNAs, purchased from Dharmacon, to identify novel genes whose normal function is essential in BAF180-deficient cell lines.

Typically, before high-throughput screening can take place, it is generally necessary to incorporate bioinformatics analysis at a genome scale to identify a subset of candidate genes followed by experimental testing. As described in Chapter 3, we described a subset of hypothesis driven candidate genes that test our hypothesis as well as our chosen cell lines. From this data, we are able to progress to more inclusive high-throughput testing to identify synthetic lethal genes with BAF180-deficient cells. Data resulting from high-throughput screening must be further analysed to identify positive result 'hits'.

5.2. Aims

The aim of this work was to use a novel method of high-throughput RNAi screening to identify genes that are synthetic lethal when depleted in combination with BAF180.

5.3. siRNA screen

To identify novel genes whose expression is essential in BAF180-deficient cells, we designed a high-throughput RNA interference (RNAi) synthetic lethality screen. For this screen we selected the osteosarcoma cell line, U2OS. U2OS cells are known to be readily transfectable and amenable to high-content imaging. Two U2OS cell lines were established, as described in detail in section 4.3, by transfection with pGIPZ plasmids expressing shControl+mCherry/NLS or shBAF180+GFP/NLS Figure 5.1a. The expression of two unique fluorescent tags allows for the co-culturing of cell lines, enabling us to treat both control and BAF180-deficient cells with exactly the same conditions and measure cell response via fluorescent readout. Optimisation of screen conditions resulted in the choice to mix our red-control and green-BAF180 cell lines in a 1:1 ratio (Figure 5.1a), seeding a total of 8000 cells per well. Cells were transfected with a human siRNA library encompassing 446 human protein-coding genes, with one gene per well of a 96-well plate and each gene being targeted by a pool of 4 siRNAs (Figure 5.1a). More than 10,000 cells per well were imaged using the Olympus ScanR microscope (Figure 5.1a). Previous work with our shControl and shBAF180 U2OS cell lines identified a relationship between the level of fluorescence and shRNA construct expression (Hopkins, McGregor et al. 2016). As described in Chapter 4, our shRNA is part of a bicistronic construct, that expresses its fluorescent marker and the specific shRNA under the same CMV promoter and therefore allows us to exploit the overall GFP level as a readout for the average shRNA expression. Figure 5.1b shows representative BAF180 immunofluorescence images, identifying low expressing GFP cells that correlate with a higher BAF180 antibody signal. To eliminate cells that may still be expressing BAF180, we chose to specifically analyse shBAF180 cells with high levels of GFP. Olympus ScanR analysis software was used to analyse the images taken by the ScanR microscope. Each cell in the screen was given an arbitrary value corresponding to ‘mean fluorescence’. We created gates to count cells in each and shBAF180 with the highest mean fluorescence were normalised to

control wells that were treated with control siRNA only. Using this, a ratio was established between our high-GFP expressing BAF180-deficient cells and total mCherry expressing shControl cells. We did not restrict our analysis of the mCherry control cells by fluorescence, as level of shRNA expression in these cells was not required to be high. Each screen was repeated in triplicate and average z-scores were calculated. Using the ratio established between high expressing GFP shBAF180 cells and total mCherry cells, each well was given a value. Each of these ratios were averaged for each plate and the standard deviation for the whole plate was calculated. To determine z-scores we used the calculation:

(GFP:mCherry ratio in specific well – Plate average)/Plate STDEV = gene Z-score

These z-scores were averaged between the three screens and plotted as a waterfall graph (Figure 5.1d). Genes with negative z-scores indicate there may be a synthetic lethal interaction specifically with our BAF180-depleted cells and those with positive z-scores stimulate BAF180-depleted cell growth more than the control. Top gene 'hits' were considered in the z-score range -2.039 to -1.07 (Figure 5.2).

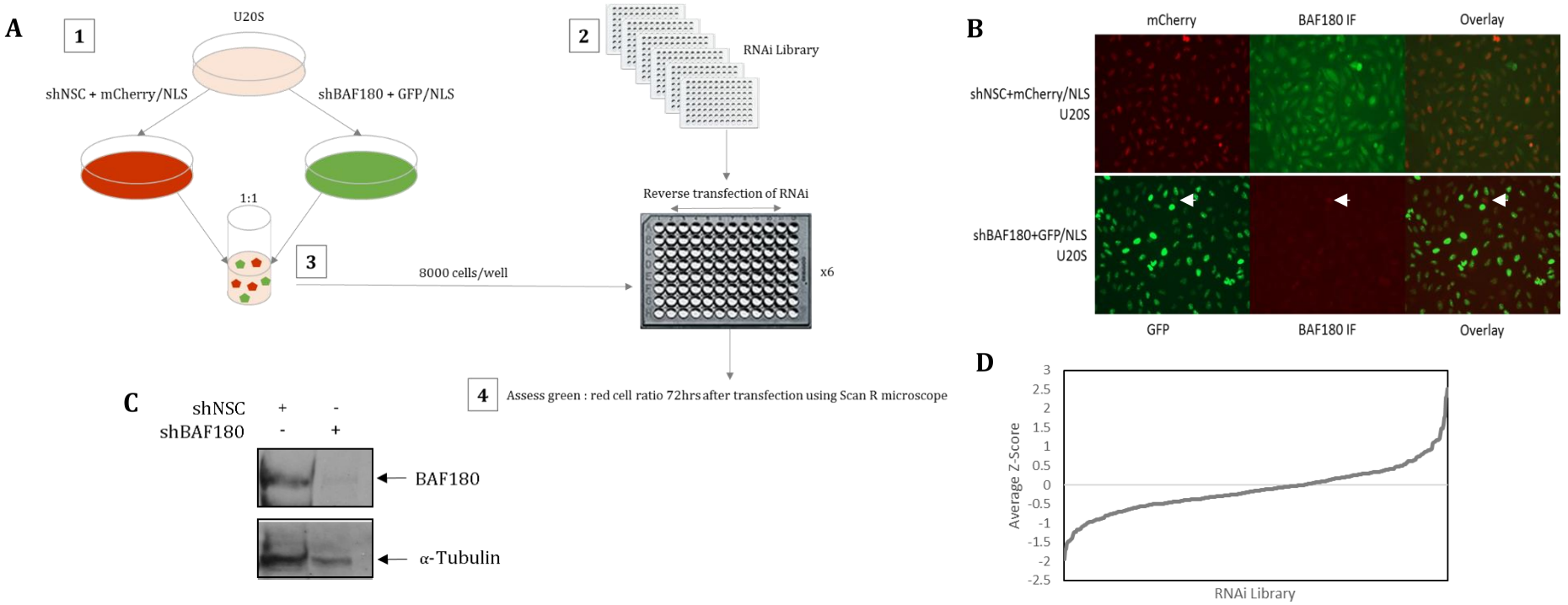

Figure 5.1. High-throughput synthetic lethal RNAi screen. (A) Schematic representation of co-culturing system used for HTS. 1. Cell lines were derived from U20S expressing control or BAF180 targeting shRNA and expressing mCherry or GFP fluorophores respectively. 2. RNAi library – Lipofectamine RNAi MAX duplex was added to 96 well plates. 3. Cell lines were mixed in a 1:1 ratio and added to RNAi – Lipofectamine duplex for reverse transfection. 4. Imaging and analysis based on mCherry:GFP ratio after siRNA treatment was carried out using ScanR microscopy. (B) Immunofluorescence analysis in shControl and shBAF180 U20S cell lines showing relative levels of BAF180 expression. The white arrow shows a representative shBAF180 cell with low GFP expression, correlating to higher BAF180 expression. (C) Western blot analysis showing relative BAF180 expression in shControl and shBAF180 cells used in the first repeat of the HTS. (D) Waterfall plot of average Z-scores ranking each siRNA from our RNAi library for synthetic lethal potential with BAF180.

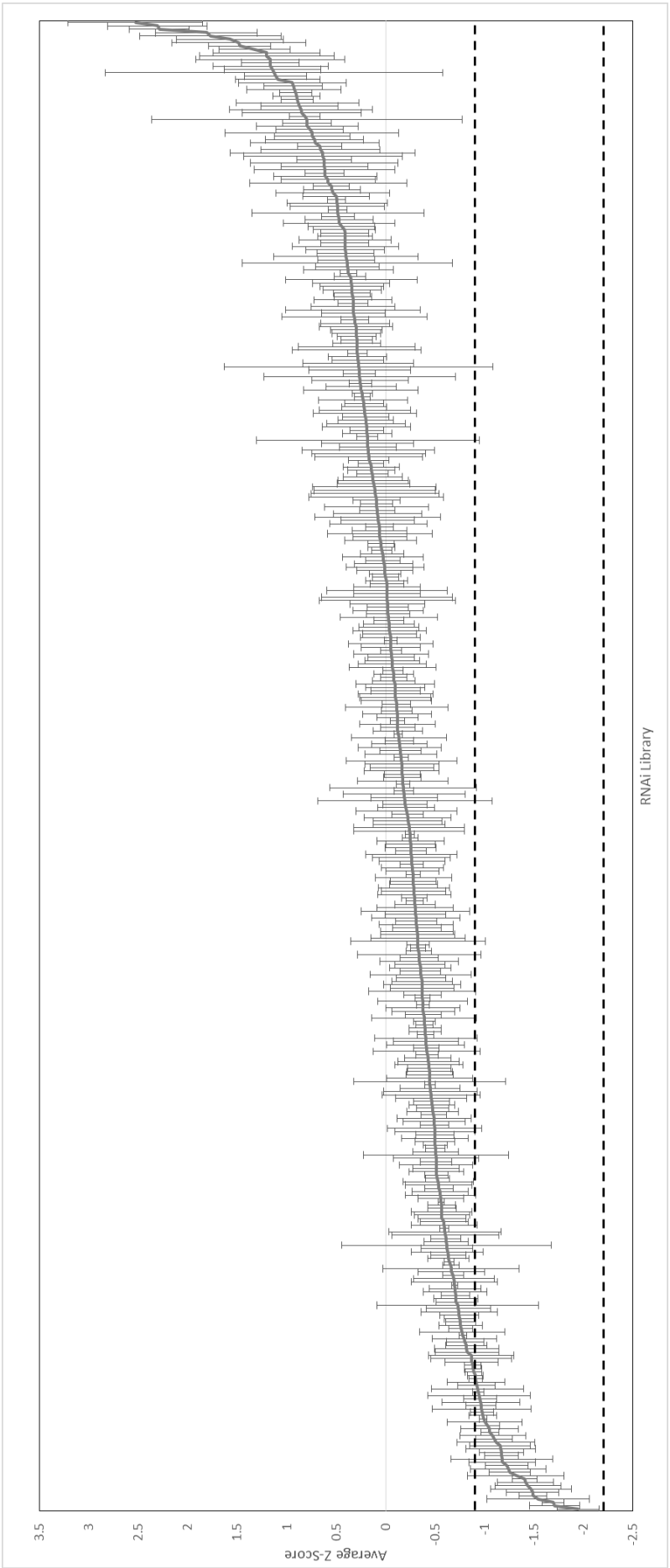

Figure 5.2. High-throughput RNAi screen results. Waterfall plot of average Z-scores for each siRNA in the library. Each siRNA is ranked for its potential to exhibit a synthetic lethal response in our BAF180 negative cells. Broken lines represent the threshold for siRNA 'hits' (between the Z-Scores of -2.039 to -1.07) that were defined as synthetic lethal with shBAF180 cells. Error bars represent standard deviation between triplicate repeats of the screen.

Screen Controls

Before a synthetic lethal screen could be carried out a number of optimisation experiments had to be performed to ensure all aspects were working sufficiently. As mentioned above, cell seeding density and ratio were established in optimisation experiments (data not shown). Transfection efficiency was optimised using immunofluorescence analysis with an antibody against 53BP1. Using this, we identified conditions for optimal transfection, Figure 5.3a shows representative.

In addition to optimisation of all conditions before running our HTS, we also added internal controls to each plate treated to confirm conditions were regulated across the screen. Due to the large number of siRNAs in our library, each screen was spread across six plates and in triplicate resulting in eighteen plates to analyse, thus these internal controls were extremely important. Each plate had multiple control wells to ensure conditions were standard throughout the screens. Wells treated with control siRNA only, as well as those treated with just transfection reagent were included to show that the seeding density was uniform from well to well and that both cell lines were viable in culture with this treatment (Figure 5.3b). siRNA against TIP60 was included as a control as in previous work we saw a reliable difference in viability between the shControl and shBAF180 U2OS cells, with shBAF180 being more sensitive to knockdown of TIP60 (Hopkins, McGregor et al. 2016). As an additional control that gave visual confirmation of successful transfection, we included control wells where the shControl and shBAF180 cells were treated with siRNA against GFP (Figure 5.3b-c). We visually assessed successful knockdown of GFP in each plate in the screen, shown by representative images in Figure 5.3c, giving us confidence in the knockdown efficiency exhibited by each screen plate.

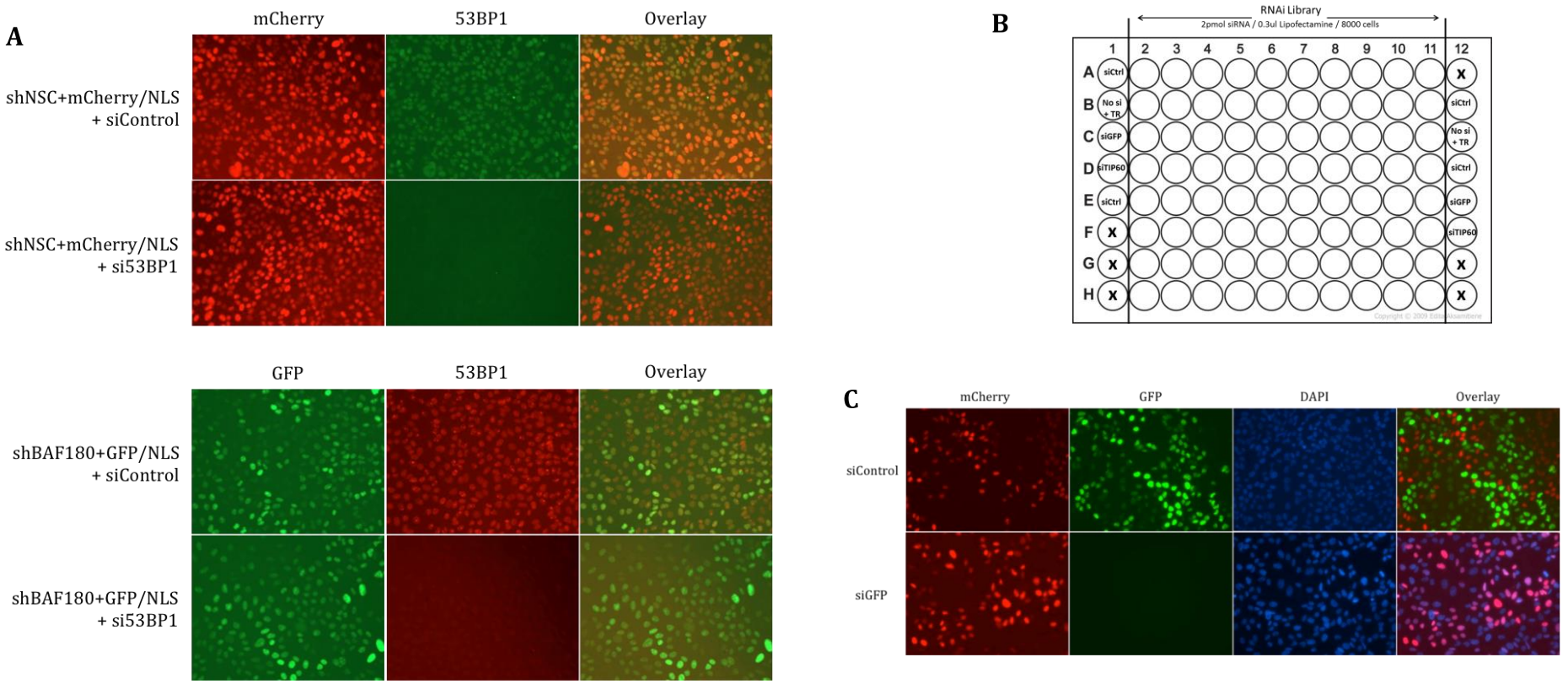

Figure 5.3. Internal screen controls. (A) Immunofluorescence images of shControl and shBAF180 U20S cells treated with control and 53BP1 siRNA under screen conditions. The antibody for 53BP1 is known to give a reliable immunofluorescence signal. Cells were treated with this siRNA under screen conditions in 96 well plates to test representative screen knockdown efficiency. (B) HTS plate lay out, including internal controls. (C) Representative images of internal test wells from HTS screen plates. Every plate in our HTS contained wells that were treated with control or GFP siRNA under the same conditions as applied to the RNAi library. Loss of GFP expression after siRNA treatment gave a visual confirmation of successful knockdown potential for each plate.

5.4. Hit selection and validation

The objective of the screen was to determine a defined hit (or hits) whose silencing in combination with BAF180 depletion resulted in synthetic lethality. From the 446 siRNAs tested in the screen, we chose 33 genes from the top 10%, as ranked by Z-score, as potential synthetic lethal interactors (Figure 5.4). The library of siRNAs included a commercially available library of genes involved in the DNA damage response (DDR), combined with a 'custom' library that was chosen by Genome Centre researchers. Many genes involved in the DDR came out as synthetic lethal hits with our BAF180-depleted cells, including the excision repair proteins ERCC6 (top hit), ERCC1 and ERCC3 to name a few. Interestingly, genes involved in cell cycle regulation, like cyclin D1 (CCND1), cyclin C (CCNC) and cyclin B1 (CCNB1) were also found to be synthetic lethal with BAF180. TIP60 (KAT5) was included as a gene in the library as well as being one of our internal screen controls. Interestingly, the siRNA targeting TIP60 from the screen library resulted in synthetic lethality with BAF180 and ranked 28th in the top hits, corroborating the interaction that we had seen previously. Another gene that was included in our hypothesis driven mini-screen (see Chapter 3), KAT2A (GCN5), was also identified as a top hit in our HTS, again the interaction being validated by different SMARTpool siRNAs. The other genes tested in our hypothesis driven mini-screen were not included in our HTS siRNA library, but the appearance of the two that were included, in our top hit list, not only validates these interactions, but also gives us confidence in the other results of the screen.

To choose genes identified in our HTS for further analysis, we first determined (in collaboration with Frances Pearl – University of Sussex) which were potentially targetable by drugs and which already had commercially available inhibitors. Of the 33 hits, five had inhibitors (at the time of study), which were DNTT, CCND1, PARP3, TP53 and CCNB1 and so were taken as a subset of hits to further validate using small inhibitors. Of the candidate gene hits that did not have an inhibitor, we chose six genes to further validate using siRNA knockdown based experiments and these were, ERCC6, PLRG1, due to their high ranking in

the HTS, as well as H2AZ, NCAPG, SMARCC1 and GCN5, due to their known interactions with chromatin.

Gene Name	Full Name	Protein Name	Z-Score	StDEV	Function	Complex
ERCC6	Excision Repair Cross-Complementation Group 6	ERCC-6	-2.04	0.33	DNA Repair - TCNER	Recruits CSA Complex (DCX(ERCC8) Complex)
DNTT	DNA Nucleotidylexotransferase	TDT	-1.94	0.37	DNA nucleotidylexotransferase activity	Ternary complex with DNTTIP2 and core histone - released from complex by PCNA
CCND1	Cyclin D1	BCL-1	-1.76	0.23	G1/S transition of mitotic cell cycle	Cyclin D1-CDK4 (DC) Complex
PARP3	poly(ADP-ribose) polymerase family member 3	ADPRTL3	-1.74	0.75	DNA repair - BER/NHEJ/HR	-
PLRG1	Pleiotropic Regulator 1	PLRG1	-1.73	0.24	mRNA splicing, via spliceosome / G1/S transition of mitotic cell cycle	PRP19-CDC5L Complex
TNP1	Transition Protein 1	STP-1	-1.71	0.68	Chromatin Remodeling - Histone removal and deposition	-
POLR2I	Polymerase (RNA) II subunit I	RPB9	-1.71	0.44	Transcription	DNA-directed RNA polymerase II Complex
H2AFZ	H2A Histone Family Member Z	H2A.Z	-1.69	0.19	Chromatin Remodeling - Histone variant	Forms heterodimer with H2B
CCNC	Cyclin C	Cyclin-C	-1.68	0.21	Transcription	Mediator Complex (when w/CDK8 - partners w/CDK3 to promote re-entry)
TP53	Tumour Protein p53	p53	-1.60	0.28	Tumour suppressor gene	TP53-HIPK2-AXIN1 complex
NCAPG	Non-SMC Condensin I Complex Subunit G	CAP-G	-1.55	0.05	DNA condensation	Condensin
ERCC1	Excision Repair Cross-Complementation Group 1	ERCC-1	-1.51	0.12	DNA repair - NER	XPF
PPP4R3B	Protein Phosphatase 4 Regulatory Subunit 3B	SMEK2	-1.49	0.24	Protein de-phosphorylation	Regulatory subunit of serine/threonine-protein phosphatase 4 (PP4)
FANCG	Fanconi Anemia Complementation Group G	XRCC9	-1.47	0.42	DNA repair	FA Core Complex
TERF2IP	TERF2 Interacting Protein	hRAP1	-1.44	0.27	Telomere maintenance	Shelterin
POLR2B	Polymerase (RNA) II subunit B	RPB2	-1.41	0.04	Transcription / DNA Repair - TCNER	DNA-directed RNA polymerase II Complex
SMARCC1	SWI/SNF related-matrix associated-actin dependent-regulator of chromatin-subfamily c-1	BAF155	-1.41	0.49	ATP-dependent chromatin remodeling	BAF/PBAF
GTF2H2	General Transcription Factor IIH Subunit 2	BTF2	-1.41	0.61	DNA Repair - TCNER	TFIIH
POLR2D	Polymerase (RNA) II Subunit D	RBP4	-1.41	0.21	Transcription / DNA Repair - TCNER	DNA-directed RNA polymerase II Complex
ANKRD52	Ankyrin Repeat Domain 52	PP6-ARS-C	-1.40	0.36	Recognition of phosphoprotein substrates	Putative regulatory subunit of protein phosphatase 6 (PP6)
POLR2H	Polymerase (RNA) II Subunit H	hRPB8	-1.39	0.17	Transcription / DNA Repair - TCNER	DNA-directed RNA polymerase II Complex
UBA1	Ubiquitin Like Modifier Activating Enzyme 1	A1S9	-1.39	0.08	Protein ubiquitination	-
WDR48	WD Repeat Domain 48	USP1-associated factor 1	-1.35	0.12	Protein de-ubiquitination	Conditional USP1,12,46
CIB1	Calcium And Integrin Binding 1	KIP or CIBP	-1.34	0.23	Calcium-dependent protein kinase inhibitor	-
FANCD2	Fanconi Anemia Complementation Group D2	FACD2	-1.34	0.05	DNA repair	FANCD2-I Complex
TFPT	TCF3 Fusion Partner	INO80F	-1.29	0.30	ATP-dependent chromatin remodeling	INO80
ERCC3	Excision Repair Cross-Complementation Group 3	XPB	-1.28	0.26	DNA repair - NER	TFIIH
KAT5	Lysine Acetyltransferase 5	HTATIP/TIP60	-1.26	0.26	Histone acetyltransferase	TIP60
CCNB1	Cyclin B1	CCNB1	-1.22	0.34	G1/S transition of mitotic cell cycle	MPF (Maturation Promoting Factor)
APTX	Aprataxin	FHA-HIT	-1.21	0.14	DNA repair - SSBR/DSBR/BER	-
BCAS2	Breast Carcinoma Amplified Sequence 2	SPF27	-1.13	0.15	mRNA splicing, via spliceosome	PRP19-CDC5L Complex
KAT2A	Lysine Acetyltransferase 2A	GCN5	-1.10	0.10	Transcription / Chromatin remodeling	SAGA + ATAC Complexes
FEN1	Flap Structure-Specific Endonuclease 1	MF1	-1.07	0.15	DNA repair	FEN1-PCNA Complex

Figure 5.4. Top gene 'hit' selection based on siRNA Z-Score ranking

Of the six genes we chose to validate using different siRNAs the most notable and convincingly reproducible synthetic lethal interaction was H2AZ. Clonogenic survival assays were carried out after siRNA knockdown of H2AZ in shControl and shBAF180 U2OS cells. shBAF180 cells were significantly more sensitive to siH2AZ knockdown (Figure 5.5a). Gene knockdown of H2AZ was confirmed by western blot analysis (Figure 5.5b). Because there was still significant protein detected after siRNA depletion, it is possible that a full reduction of H2AZ protein expression could result in a more severe synthetic lethal phenotype.

GCN5, which was independently validated in section 3.5, was identified as a hit in high-throughput screening analysis. Although this interaction had already been studied in our hypothesis driven mini-screen using cell viability as a readout (Figure 3.3), we wanted to further validate this interaction in a different way. shBAF180 U2OS cells treated with siRNA against GCN5 had a lower colony forming potential compared to the control (Figure 5.5c), providing additional evidence of a synthetic lethal interaction seen between these two genes.

In clonogenic survival assays, the siRNAs targeting ERCC6, PLRG1, NCAPG and SMARCC1 did not selectively target either the shControl or shBAF180 U2OS cell lines (Figure 5.5d), suggesting these genes are not synthetic lethal with BAF180. Many RNAi screens produce false positive results, these can be contributed to by experimental noise that is inherent in large-scale studies, bias that can be inherent in the screen assay, off-target effects and even incomplete or incorrect gene models. While these genes may be false positives, further investigation is required to determine this with confidence.

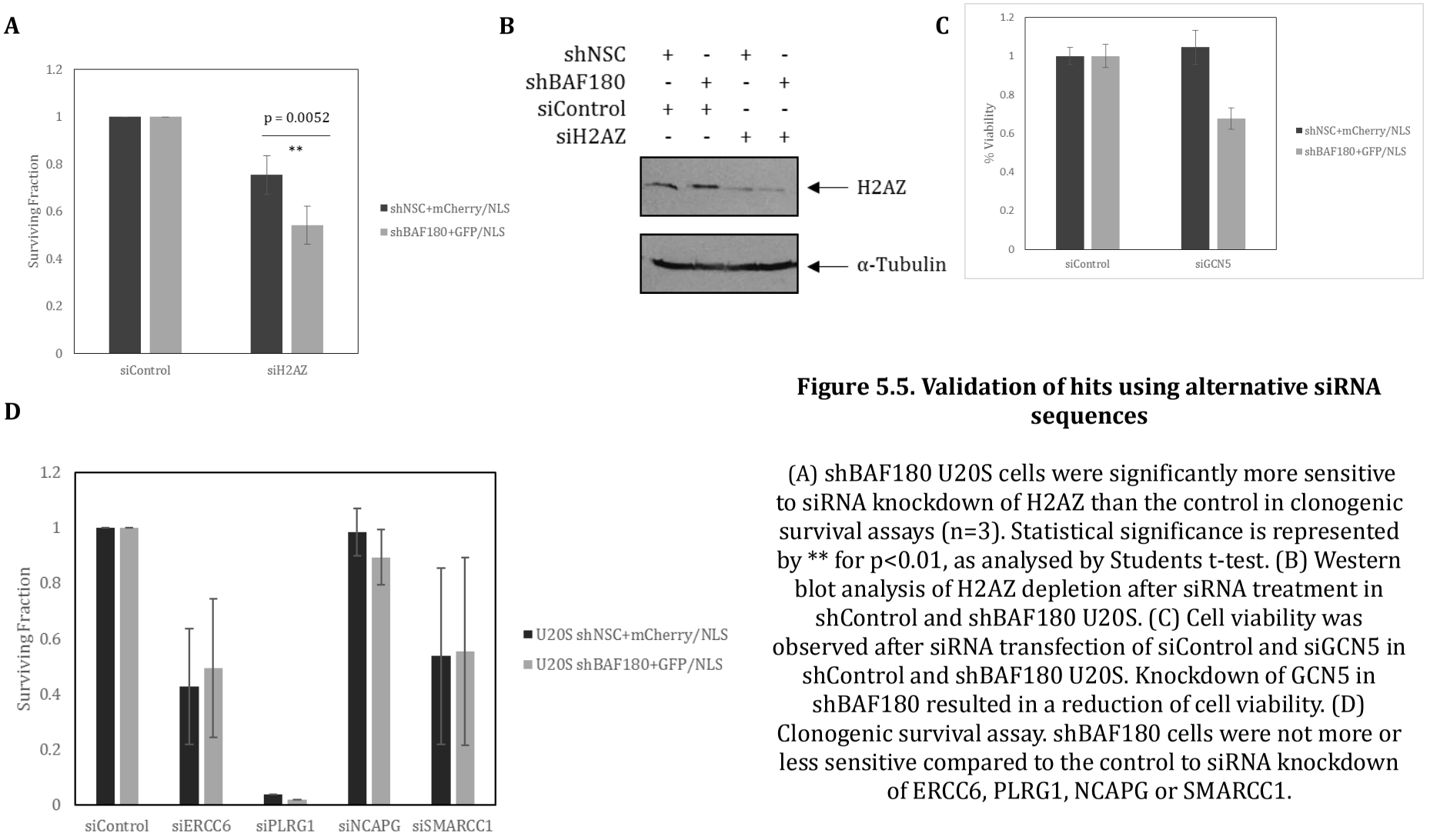

Figure 5.5. Validation of hits using alternative siRNA sequences

(A) shBAF180 U20S cells were significantly more sensitive to siRNA knockdown of H2AZ than the control in clonogenic survival assays (n=3). Statistical significance is represented by ** for $p<0.01$, as analysed by Students t-test. (B) Western blot analysis of H2AZ depletion after siRNA treatment in shControl and shBAF180 U20S. (C) Cell viability was observed after siRNA transfection of siControl and siGCN5 in shControl and shBAF180 U20S. Knockdown of GCN5 in shBAF180 resulted in a reduction of cell viability. (D) Clonogenic survival assay. shBAF180 cells were not more or less sensitive compared to the control to siRNA knockdown of ERCC6, PLRG1, NCAPG or SMARCC1.

In addition to testing synthetic lethal interactions with different siRNAs, we also wanted to investigate the conditional viability reduction in our shBAF180 U2OS cells seen in the HTS using small molecule inhibitors. As mentioned above we chose five targets with inhibitors, DNTT, CCND1, PARP3, TP53 and CCNB1 (Figure 5.6a). As a first, we used viability assays to determine if each drug had potential to selectively kill our shBAF180 U2OS before taking on to further assays.

A small difference in viability between shBAF180 and the control was seen after treatment with Genistin, a small molecule inhibitor targeting DNTT (Figure 5.6b). However, the drug seemed to aid cell growth at low concentrations with both cell lines doing better at these low concentrations compared to the 0μM control. The difference in viability between these cell lines was only seen at these low doses when both cell lines had more improved viability. Higher doses of Genistin resulted in loss of viability in an equal manner for both cell lines. Interestingly, two drugs targeting the PARP proteins, ME0328, a PARP3 specific inhibitor and Olaparib a pan inhibitor of PARP genes, selectively reduced viability in the shBAF180 U2OS cell line compared to the control (Figure 5.6c-d). We chose two small inhibitors to validate the synthetic lethal interaction between TP53 and BAF180, Cyclic Pifithrin-α-hydrobromide and Pifithrin-μ, both of which resulted in no observable difference in cell viability or colony forming potential after treatment in shControl and shBAF180 U2OS cells (Figure 5.7b-c and 5.8b-c). The drug Palbociclib (aka PD0332991) showed a slight difference in cell viability at the 7.5μM dose between the shBAF180 and shControl cells (Figure 5.9b), however no difference was apparent when investigated further in clonogenic survival assays (Figure 5.9c). It should be noted however, that the cells were more sensitive to the inhibitor in clonogenic survival assays. Thus, there is scope here to develop this assay and cannot be entirely ruled out of any further testing.

A

Drug	Gene Target
Genistin	**DNTT**
Heptelidic Acid	DNTT
ME0328	**PARP3**
Olaparib	**PARPs**
Cyclic Pifithrin-α-hydrobromide	TP53
Pifithrin-μ	TP53
Palbociclib (PD0332991)	CCND1
RO-3306	CCNB1

B

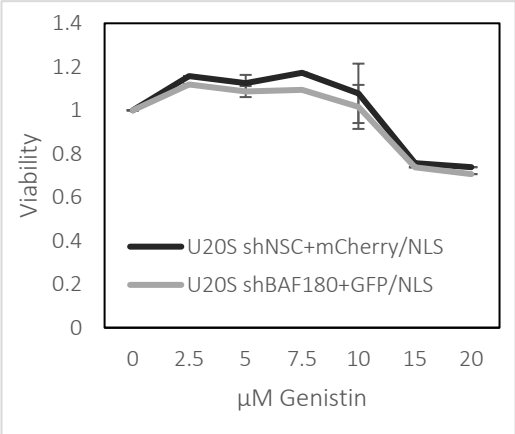

C

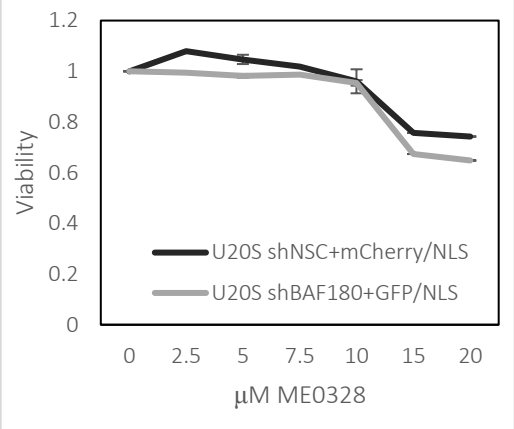

D

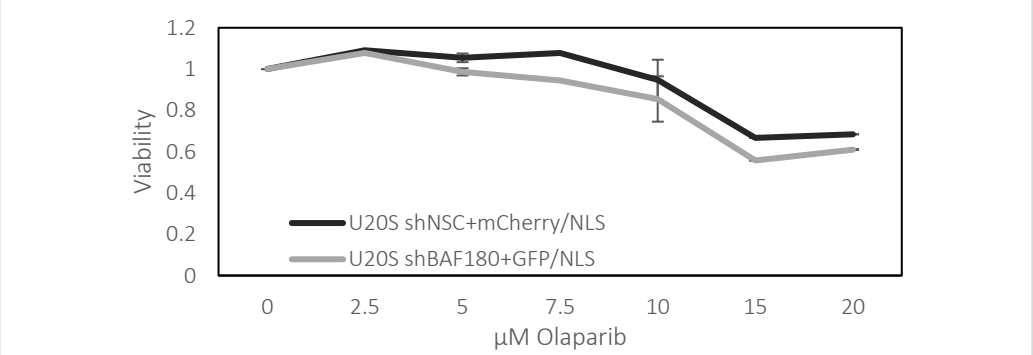

Figure 5.6. Small molecule inhibitor validation of HTS hits. (A) Inhibitors against HTS gene hits. (B) Cell viability in shControl and shBAF180 U20S after treatment with Genistin. (C-D) Cell viability in shControl and shBAF180 U20S after treatment with the PARP inhibitors ME0328 and Olaparib respectively. shBAF180 cells were slightly more sensitive to PARP inhibition that the control.

A

Drug	Gene Target
Genistin	DNTT
Heptelidic Acid	DNTT
ME0328	PARP3
Olaparib	PARPs
Cyclic Pifithrin-α-hydrobromide	**TP53**
Pifithrin-μ	TP53
Palbociclib (PD0332991)	CCND1
RO-3306	CCNB1

B

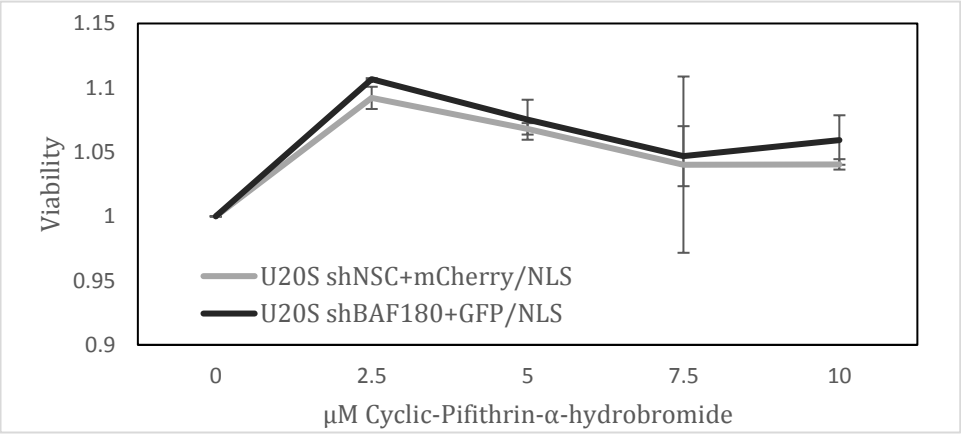

C

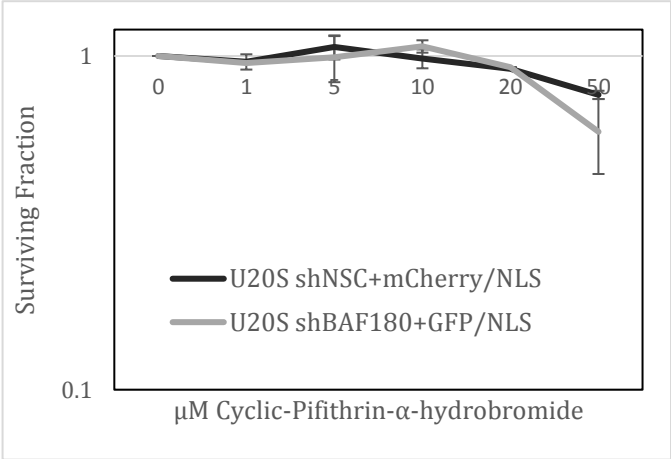

Figure 5.7. Small molecule inhibition of TP53 does not confirm HTS synthetic lethal interaction with BAF180. (A) Inhibitors against HTS gene hits. (B) Cell viability curve of shControl and shBAF180 U20S after exposure to Cyclic Pifithrin-α-hydrobromide. (C) shBAF180 U20S were no more sensitive to treatment with Cyclic Pifithrin-α-hydrobromide than the control in clonogenic survival.

A

Drug	Gene Target
Genistin	DNTT
Heptelidic Acid	DNTT
ME0328	PARP3
Olaparib	PARPs
Cyclic Pifithrin-α-hydrobromide	TP53
Pifithrin-μ	**TP53**
Palbociclib (PD0332991)	CCND1
RO-3306	CCNB1

B

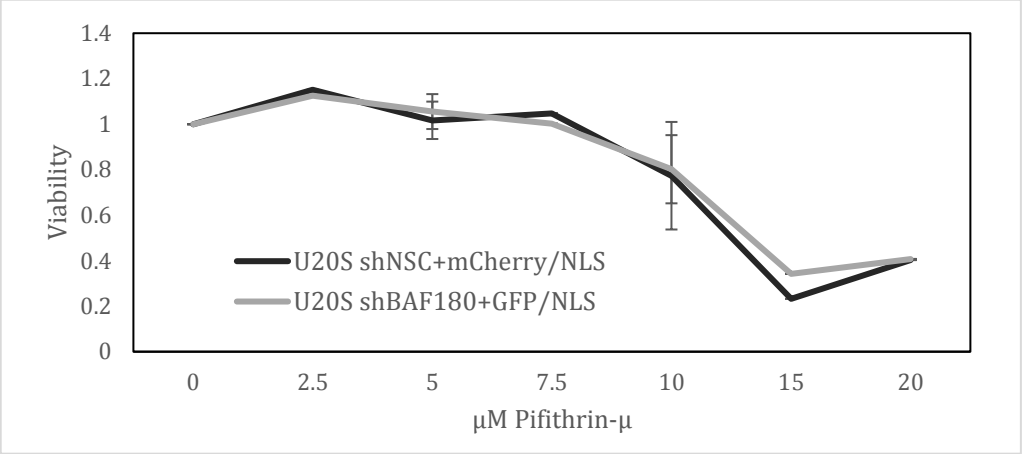

C

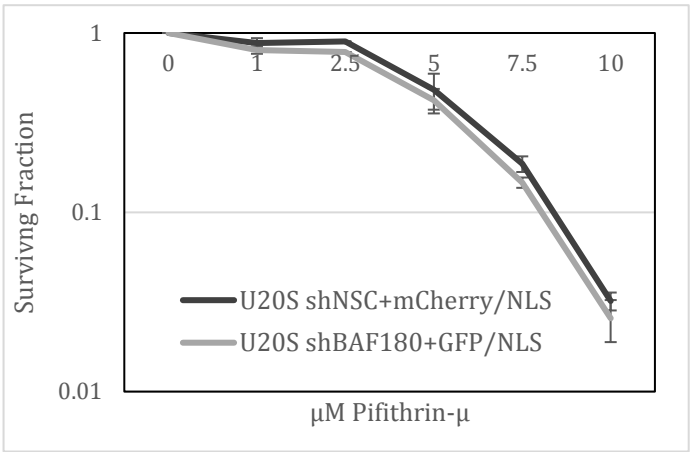

Figure 5.8. Small molecule inhibition of TP53 does not confirm HTS synthetic lethal interaction with BAF180. (A) Inhibitors against HTS gene hits. (B) Cell viability curve of shControl and shBAF180 U20S after exposure to Pifithrin-μ (C) shBAF180 U20S were no more sensitive to treatment with Pifithrin-μ than the control in clonogenic survival.

A

Drug	Gene Target
Genistin	DNTT
Heptelidic Acid	DNTT
ME0328	PARP3
Olaparib	PARPs
Cyclic Pifithrin-α-hydrobromide	TP53
Pifithrin-μ	TP53
Palbociclib (PD0332991)	**CCND1**
RO-3306	CCNB1

B

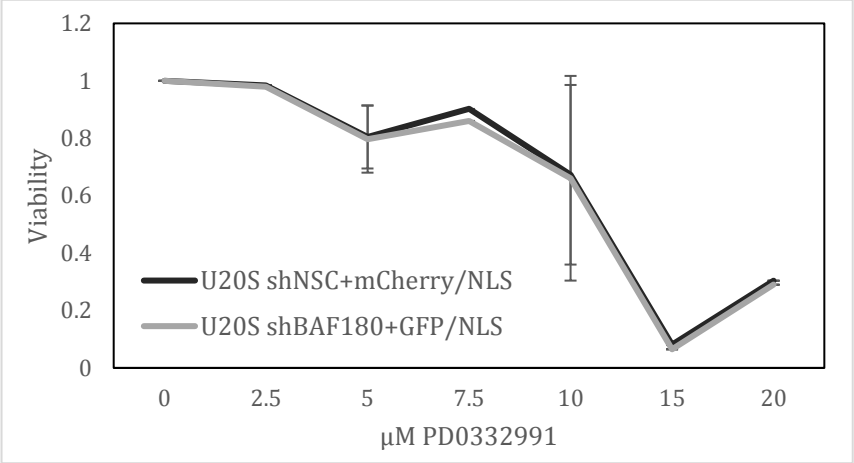

C

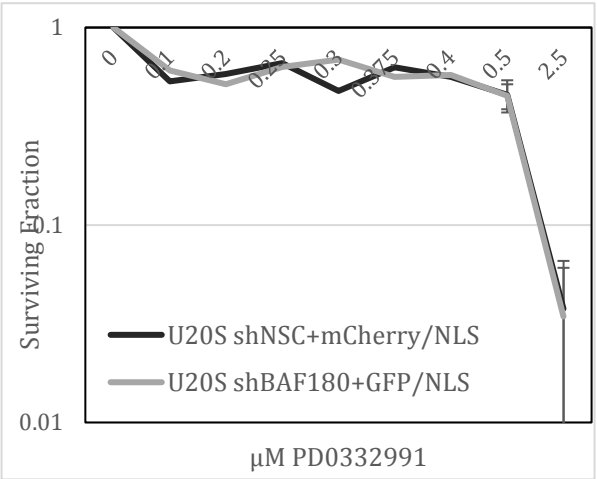

Figure 5.9. Small molecule inhibition of Cyclin D1 (CDK4/6) does not confirm HTS synthetic lethal interaction with BAF180. (A) Inhibitors against HTS gene hits. (B) Cell viability curve of shControl and shBAF180 U20S after exposure to Palbociclib(C) shBAF180 U20S were no more sensitive to treatment with Palbociclib than the control in clonogenic survival.

Heptelidic Acid, which also targets DNTT was analysed to further develop the potential synthetic relationship with BAF180. An unusual cell viability curve was seen after treatment with Heptelidic acid, possibly due to the drug precipitating in the media. Nevertheless, we did see a small difference in viability between the shBAF180 cells and the control at 2.5μM in duplicate experiments (Figure 5.10b). We therefore further tested this drug in clonogenic survival assays. We observed a consistent difference in colony forming potential between the two cell lines, with the shBAF180 cells being more sensitive to treatment with Heptelidic Acid (Figure 5.10c). While there was a consistent trend, the differences were not significant (Figure 5.10c).

The drug RO-3306, targeting CCNB1, modestly targeted BAF180-depleted cells more than the control cell line in both cell viability assays and clonogenic survival assays (Figure 5.11b-c). This difference was enhanced by the addition of IR to low dose treatment of RO-3306 in clonogenic survival assays (Figure 5.11d). As chemotherapeutic drugs are often given in combination with radiation therapy, it is important to see whether there is an increase in selective effects on viability after irradiation.

A

Drug	Gene Target
Genistin	DNTT
Heptelidic Acid	**DNTT**
ME0328	PARP3
Olaparib	PARPs
Cyclic Pifithrin-α-hydrobromide	TP53
Pifithrin-μ	TP53
Palbociclib (PD0332991)	CCND1
RO-3306	CCNB1

B

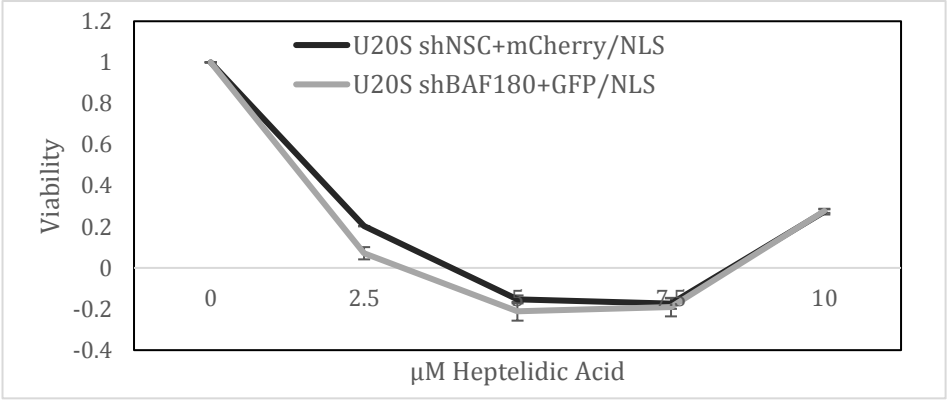

C

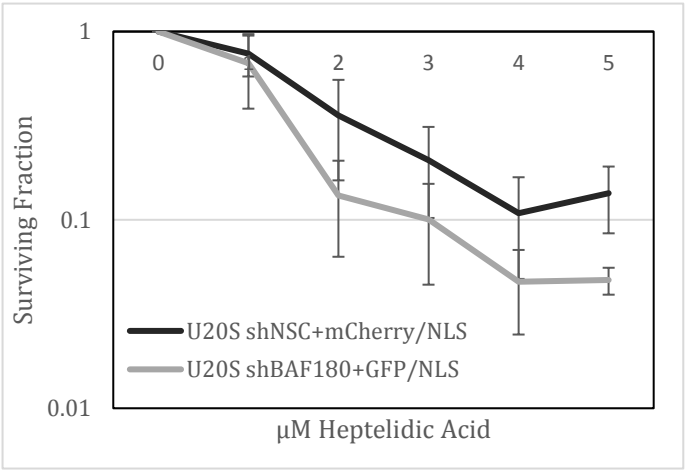

Figure 5.10. Small molecule inhibition of DNTT consistently shows a trend of synthetic lethality in shBAF180 U2OS. (A) Inhibitors against HTS gene hits. (B) Cell viability curve of shControl and shBAF180 U20S after exposure to Heptelidic Acid (n=2). shBAF180 appear marginally more sensitive to the control after treatment 2.5μM. (C) shBAF180 U20S were more sensitive to treatment with Heptelidic Acid than the control in clonogenic survival, but was not statistically significant by student t-test (n=3).

A

Drug	Gene Target
Genistin	DNTT
Heptelidic Acid	DNTT
ME0328	PARP3
Olaparib	PARPs
Cyclic Pifithrin-α-hydrobromide	TP53
Pifithrin-μ	TP53
Palbociclib (PD0332991)	CCND1
RO-3306	CCNB1

B

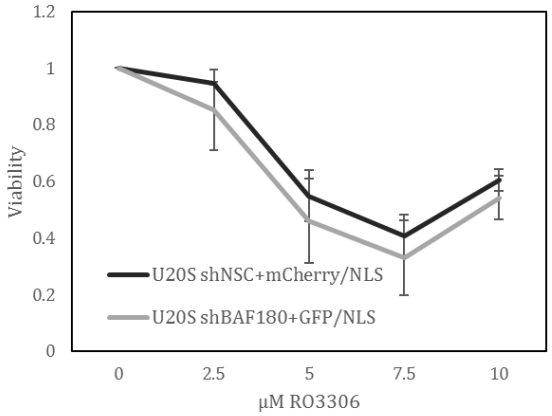

C

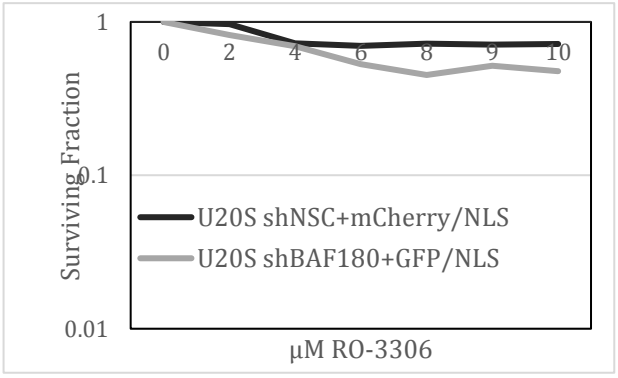

D

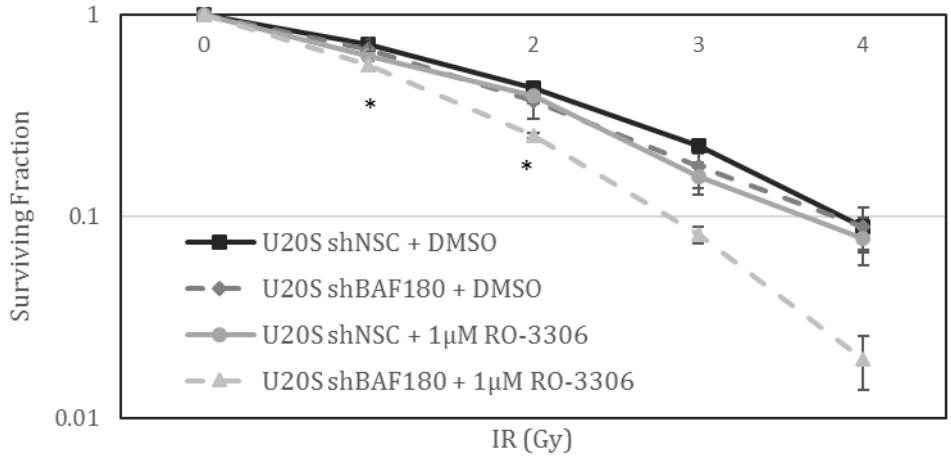

Figure 5.11. Small molecule inhibition of Cyclin B1 (CDK1) validates HTS synthetic lethal interaction with BAF180. (A) Inhibitors against HTS gene hits. (B) Cell viability curve of shControl and shBAF180 U20S after exposure to RO-3306 (n=2). shBAF180 appear marginally more sensitive to the control after treatment. (C) shBAF180 U20S were more sensitive to treatment with RO-3306 than the control in clonogenic survival, but was not statistically significant (n=3). (D) shBAF180 U20S are more sensitive to low dose treatment with RO-3306 than the control after irradiation. (n=3) Statistical significance is represented by * for $P<0.05$, as analysed by student t-test.

5.5. Discussion

The objective of our high-throughput screen was to determine a hit, or multiple hits, whose depletion in combination with BAF180 resulted in synthetic lethality. Moreover, we wanted to improve on current RNAi screening methods by developing a novel system with improved sensitivity and reproducibility. We created shBAF180 and shControl isogenic cell lines that we were able to identify when co-cultured, enabling us to observe specific cell differences within the same well microenvironment, reducing the amount of experimental variation and increase screen sensitivity and therefore giving us a better chance at potential hit validation. From a library consisting of 446 genes, we identified 33 genes as synthetic lethal gene candidates with shBAF180 U2OS cells. The RNAi library used in the screen was designed to deliberately target genes involved in the DNA damage response (DDR). We know that the DDR is essential for maintaining the genomic integrity of the cell and its disruption is one of the hallmarks of cancer. We also know that synthetic lethality can either occur due to the loss of two genes in one essential pathway, the loss of two genes in independent survival pathways or the loss of two genes in independent pathways where an essential product is normally formed.

Recent work in our lab has shown that phosphorylation of BAF180 by ATM is required for early DNA repair activity in that lack of transcriptional repression of genes flanking DNA DSBs impedes repair (Kakarougkas, Ismail et al. 2014). It is possible that loss of two genes involved in the DDR, whether they be on the same or parallel pathways, could result in synthetic lethality. It is known that defects in the DNA damage response and repair pathways lead to genomic instability in tumour cells and this instability can cause sensitivity to DNA damaging drugs more than normal cells. For example, treatment with PARP inhibitors in BRCA-negative cancers cause synthetic lethality by the combination of impairment of both single- and double-stranded DNA break repair respectively. As previously mentioned, BRCA1 and BRCA2 are important for the repair of DNA DSBs by homologous recombination (HR) and mutations here are commonly associated with breast and ovarian cancer (Hall, Friedman et al. 1992, Casey, Plummer et al.

1993, Wooster, Neuhausen et al. 1994, Parikh and Advani 1996). PARP recruits DNA repair proteins to sites of single-strand DNA breaks and if this is inhibited, stalled replication forks arise, which are typically repaired by HR (Petermann, Keil et al. 2005). In BRCA-negative cancers, treated with PARP inhibitors, PARP1 is trapped on DNA, blocking replication fork progression, which usually requires homologous recombination repair (HRR). Due to the HRR defect observed in BRCA-negative cancers, treatment with PARP inhibitors results in cell specific synthetic lethality.

We could speculate that BAF180-depleted cells are more sensitive to knockdown of other DDR genes because of impairments in two repair processes, like BRCA and PARP. However, the underlying mechanism for synthetic lethality between BAF180 and each gene identified in the HTS, must be reasoned individually.

PARP3, a gene that is implicated in the DDR, was identified as a candidate gene hit with BAF180 in the HTS and was validated by the PARP inhibitors ME3028 and Olaparib in this chapter, however the mechanism of this synthetic lethality and the further development of this interaction will be discussed in detail in Chapter 6.

5.5.1. H2A.Z is synthetic lethal when knocked down in combination with BAF180.

We identified H2AZ as a candidate gene hit in our synthetic lethal HTS with BAF180, and this interaction was validated using siRNAs non-overlapping with those used in the HTS. H2A.Z is a well-characterised variant of the canonical H2A histone and acetylation of H2A.Z is important for the regulation of gene expression. Acetylation of H2A.Z is typically associated with highly transcribed genes and a more open chromatin structure, whereas unacetylated H2A.Z is found in silent genes (Josling, Selvarajah et al. 2012) and is therefore linked to both the activation and repression of transcription. H2A.Z is also present at centromeres and is thought to have an important role in the organization of

pericentric heterochromatin centromere structure and function (Greaves, Rangasamy et al. 2007). BAF180 has well-characterised roles in transcriptional regulation, however recent work in our lab has also implicated BAF180 in sister chromatid cohesion, specifically at centromeres in mammalian cells (Brownlee, Chambers et al. 2014). The rationale behind why H2AZ and BAF180 might be synthetic lethal could therefore be explained by one of two mechanisms. Firstly, that the loss of two genes that are important for transcriptional regulation could be enough to cause synthetic lethality or secondly, that to the loss of two genes that have important functional roles at centromeres may be the cause of the observed synthetic lethality.

5.5.2. Possible mechanisms for BAF180 and SMARCC1 synthetic lethality

Although we were not able to validate the interaction found in our high-throughput screen between BAF180 and SMARCC1 with the use of non-overlapping siRNAs, it does not necessarily suggest that this 'hit' was a false positive. It is interesting to think about SMARCC1 as a candidate synthetic lethal interactor with BAF180. As discussed previously, in clear cell renal cell carcinoma VHL, PBRM1 (BAF180), BAP1 and SETD2 are frequently mutated, they also all reside on the short arm of chromosome 3p. SMARCC1 is a subunit of both SWI/SNF chromatin remodelling complexes, BAF and PBAF. Like BAF180, the gene encoding SMARCC1 is found on chromosome 3p21.31 between BAF180 and VHL. It has been determined, that given its location, ~90% of ccRCC would be expected to lose at least one SMARCC1 allele, with the second being susceptible to loss. It was also determined that statistically, by chance alone, SMARCC1 would be expected to be mutated at around 70% of the frequency of BAF180, however, its mutation rate in ccRCC are actually extremely low (Brugarolas 2013). It has been suggested that SMARCC1 may be broadly essential for survival and that mutations here may be detrimental for ccRCC. We identified SMARCC1 as the 17th out of 446 genes that are likely to be synthetic lethal with BAF180 in high-throughput siRNA screening. It is possible that if SMARCC1 is indeed required for

ccRCC cell survival, then loss of this gene could result in the synthetic lethality seen here with BAF180-depleted cells. The exploitation of SWI/SNF subunit inhibition for cancer therapy is intriguing and could provide a novel approach to the treatment of cancers that currently have poor treatment options, like ccRCC.

5.5.3. Possible mechanisms for BAF180 and Cyclin B1 synthetic lethality

As mentioned in section 1.5, in bladder cancer, PBRM1 is thought to regulate the expression of cyclin B1. Overexpression of PBRM1 is thought to reduce mRNA levels of cyclin B1 and loss of PBRM1 is thought to increase mRNA levels of cyclin B1 (Huang, Peng et al. 2015). The cell cycle is controlled by cyclins and cyclin-dependent kinases (Sherr 1996). Cyclin B1 is a key molecule for G2/M phase transition of the cell cycle and is needed for initiation of mitosis. Cyclin B1 overexpression has been linked to disease recurrence in cancers such as colorectal, prostate, breast and lung cancer to name just a few (Mashal, Lester et al. 1996, Kawamoto, Koizumi et al. 1997, Wang, Yoshimi et al. 1997, Malumbres and Barbacid 2005, Kim, Ackerson et al. 2006).

Defects in cell cycle control are essential to carcinogenesis. It has been suggested that PBRM1 reduction can induce cell cycle arrest and subsequently promotes cell proliferation (Huang, Peng et al. 2015). We have identified a synthetic lethal relationship between PBRM1 (BAF180) and cyclin B1 (CCNB1). Previous studies have shown the increase in cyclin B1 upon BAF180 depletion. It is possible that this upregulation of cyclin B1 is necessary for cancer cell survival and that the combined loss of this gene together with BAF180 may result in the inability to maintain chromatin in a transcriptionally permissive state and may be the underlying cause for the synthetic lethality seen in this study. To study this interaction further, it would be interesting to analyse our set of BAF180-depleted cell lines by western blot to see if cyclin B1 is upregulated after BAF180 loss via shRNA, CRISPR knockout or in our naturally occurring BAF180-negative cancer cell lines, A704.

In conclusion, we have presented a novel synthetic lethal high-throughput RNAi screening method that is capable of assaying synthetic lethal interactions in a cell specific manner. Multiple candidate genes were identified as synthetic lethal hits with BAF180-depleted shU2OS cells, some of which we were able to validate at a further level, however further work is required before translating this data in to something clinically relevant. PARP3 was in the top 1% of genes tested for synthetic lethality with shBAF180 cells in our screen. Due to the presence of PARP inhibitors already being used in a synthetic lethal manner in clinical studies for BRCA-deficient cancers, the translational aspect of validating this gene swiftly became extremely interesting to us. This synthetic lethal interaction and further validation of this gene will be discussed in the next chapter.

6. PARP inhibition is synthetically lethal with BAF180 loss

6.1. Introduction

Poly (ADP-ribose) Polymerase (PARP), as described in section 1.7, has a well characterised role in the repair of DNA damage. Small molecule inhibitors of PARP were originally developed to sensitize patients to chemotherapy during cancer treatment. However, more recently, PARP inhibitors have been demonstrated as a potential therapy for targeting cancers with a deficiency in the homologous recombination (HR) pathway.

PARP inhibition in BRCA mutated cancers is one of the first clinically implemented examples of harnessing the principle of synthetic lethality for cancer therapy (Lord and Ashworth 2008). BRCA1 and BRCA2 are essential for the repair of DNA double strand breaks (DSBs) and collapsed replication forks using the HR pathway. Loss of wild type BRCA1 or BRCA2, results in the complete absence of HR and the increase in the cells usage of non-conservative mechanisms to repair DSBs/replication forks (Lord and Ashworth 2008). It has been well established that the HR defect in BRCA-deficient cells is the primary cause of PARP inhibitor sensitivity (Lord and Ashworth 2008). It has been shown that deficiencies in other HR proteins can also lead to sensitivity to PARP inhibitors (McCabe, Turner et al. 2006).

Previous work in our lab has identified the SWI/SNF complex PBAF as important for mediating sister chromatid cohesion. Specifically, this activity is dependent on the BAF180 subunit of PBAF (Brownlee, Chambers et al. 2014). As described in section 1.1.3.2, the process of HR utilizes an intact sister chromatid as a repair template for the repair of damaged DNA in the S/G2 phase of the mammalian cell cycle (Kong, Ball et al. 2014). It is known that efficient homologous recombination is promoted by the recruitment of sister chromatid cohesion to DNA DSBs (Kong, Ball et al. 2014, Gelot, Guirouilh-Barbat et al. 2016). We found that cells with deficient BAF180 demonstrate phenotypes that are consistent

with a defect in cohesin-mediated DNA repair (Brownlee, Chambers et al. 2014). Therefore, it is possible that the PBAF complex may also promote HR. We identified multiple PARP genes, as being synthetic lethal with BAF180 in the RNAi screen presented in Chapter 5. In this chapter we sought to address whether a defect in HR in BAF180-deficient cells was the underlying cause for this synthetic lethal phenotype.

6.2. Aims

The aims of the work described in this chapter were firstly to validate the synthetic lethal interaction found between BAF180 and the PARP genes identified by our high-throughput screen (Chapter 5), using siRNA and drug based in vitro experiments. Secondly, to confirm that the biological interactions observed could be reproduced in multiple cell lines, using multiple PARP inhibitors. And finally, to explore a potential HR defect in BAF180 deficient cells, to uncover a mechanism of why BAF180 and PARP genes have a synthetic lethal relationship.

6.3. BAF180 and PARP genes are synthetic lethal

High-throughput screening techniques, as described in Chapter 5, identified a potential synthetic lethal interaction between BAF180 and PARP3. To validate this interaction, it was necessary to reproduce the synthetic lethal observation, using a different pool of siRNAs, to confirm that the 'hit' wasn't simply due to off target effects. In addition, when not performing high-throughput analyses, a more rigorous analysis of cell viability can be used. Therefore, using siRNA sequences targeting different regions of the gene, clonogenic survival assays were performed. This revealed a large decrease in survival after treatment with siPARP3 in shBAF180 cells (Figure 6.1a), consolidating our findings from our high-throughput screen. The fact that the interaction could be reproduced in a different assay, with a different siRNA

sequence, suggests that this interaction is robust, but would still need to be explored further.

Notably, we also identified PARP1, PARP2 and PARP4 in the screen (Figure 6.1b). Although these PARP genes did not make it to the top 'hit' list as described in Chapter 5, the BAF180 depleted shU2OS cells were still classed as more sensitive to these gene knockdowns when compared to the control. To test whether these other PARPs are genuinely synthetic lethal with loss of BAF180, we tested colony survival potential as we did for PARP3 (Figure 6.1.a), with different siRNAs to those included in the screen for PARPs 1 and 2. A striking decrease in colony formation potential was seen after depletion of PARP1 in our shBAF180 cells, whereas depletion of PARP2 resulted in no difference in survival between shBAF180 and shControl cell lines (Figure 6.1c).

Interestingly, co-depletion of PARP1, PARP2 and PARP3, reduced survival of the shBAF180 to a percentage that was lower than PARP2 siRNA alone, but marginally higher than both PARP1 and PARP3 siRNA depletions alone (Figure 6.1c). This could suggest either that the removal of PARP2 alongside PARP1 and PARP3, could slightly rescue the synthetic lethal phenotype, or that the siRNA depletions were not as effective in combination.

Western blot analysis of whole cell extracts was used to determine knockdown efficiency in these siPARP treated cells (Figure 6.1d). PARP1, which runs at 116-kDa, was significantly reduced, as expected in the cells treated with siPARP1 as well as the cells treated with siPARP1, 2 and 3. PARP3, which runs at 60-kDa, was reduced in cells treated with siPARP3 as well as cells treated with siPARP1,2 and 3.

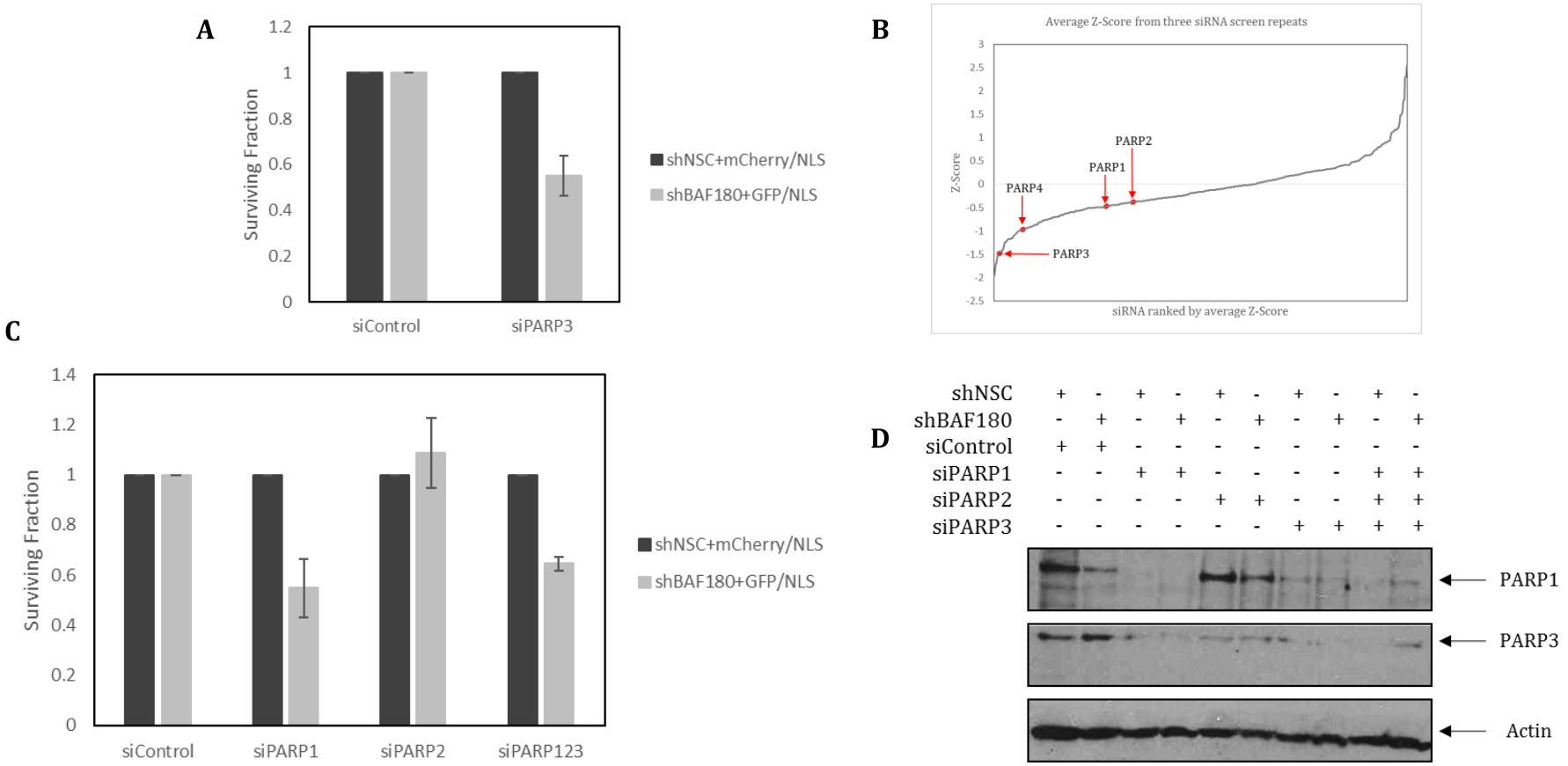

Figure 6.1 BAF180 and PARP genes are synthetic lethal

(A) shBAF180 U20S cells were sensitive to siRNA knockdown from PARP3 in clonogenic survival assays (n=3). (B) Waterfall plot of z-scores from synthetic lethal RNAi screen – PARP1,2,3 and 4 were all synthetic lethal with shBAF180 cells. (C) shBAF180 U20S were sensitive to siRNA knockdown from PARP1 and the combination of PARP1,2 and 3, but not PARP2 alone in clonogenic survival assays (n=3). (D) Western blot analysis of PARP1 and PARP3 depletion in shControl and shBAF180 U20S cells.

6.4. Multiple cell lines with depleted BAF180 are sensitive to treatment with the PARP inhibitor drug Olaparib

In parallel with the confirmation that the same synthetic lethality can be seen with various siRNA sequences against our PARP targets (Figure 6.1a-d), we wanted to replicate the conditional viability reduction in a more therapeutically relevant way, with small molecule inhibitors that are commercially available. The rationale behind validation using small molecule inhibitors as well as siRNA was multifaceted. Firstly, we can speculate that gene targeting by RNAi may not completely downregulate the targets, perhaps due to incomplete depletion of the gene. As no genes in the screen showed 100% shBAF180 specific synthetic lethality we postulated that residual gene product activity may have prevented a strong conditional response. Secondly, often loss of a protein by siRNA depletion does not always produce the same biological effects as drug inhibition. Finally, small molecule inhibitors of PARP are currently in clinical trials and are already treating cancers by exploiting the principle of synthetic lethality.

Olaparib, otherwise known as Lynparza, is known to be a potent inhibitor of PARP1 and PARP2 with some activity also against tankyrase-1 and is currently tested for the treatment of BRCA deficient cancers.

Colony survival assays were carried out using shBAF180 and shControl U2OS cells after treatment with Olaparib. BAF180 depleted cells were significantly more sensitive to treatment with Olaparib compared to the control (Figure 6.2a). This sensitivity was conserved when moving in to a different cell line (Figure 6.2b), the more clinically relevant renal cell line, 786-0. As previously described (Chapter 4), 786-0 cells were made to stably express shRNA against both BAF180 with a GFP/NLS, as well as separately a control shRNA with mCherry/NLS. The renal cells lacking BAF180 were significantly more sensitive to treatment with Olaparib, compared to the control.

A

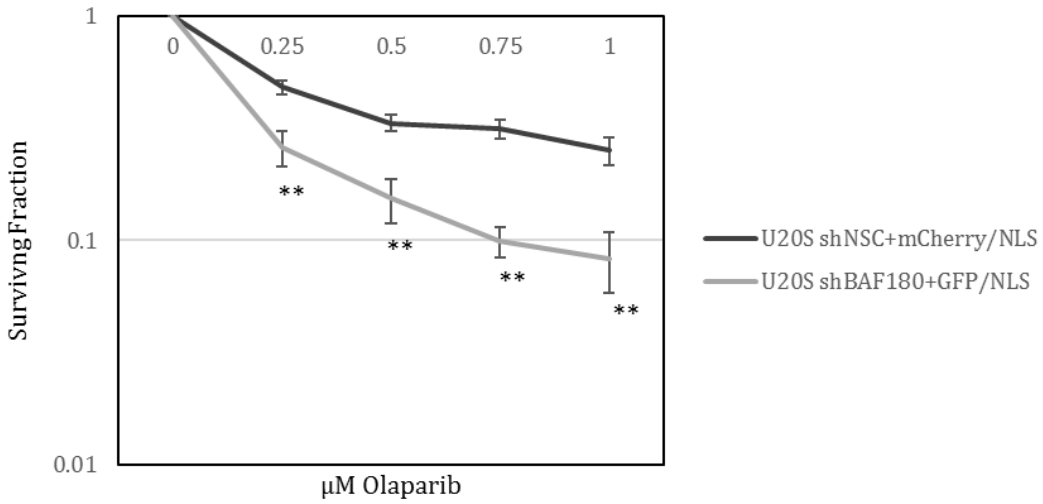

B

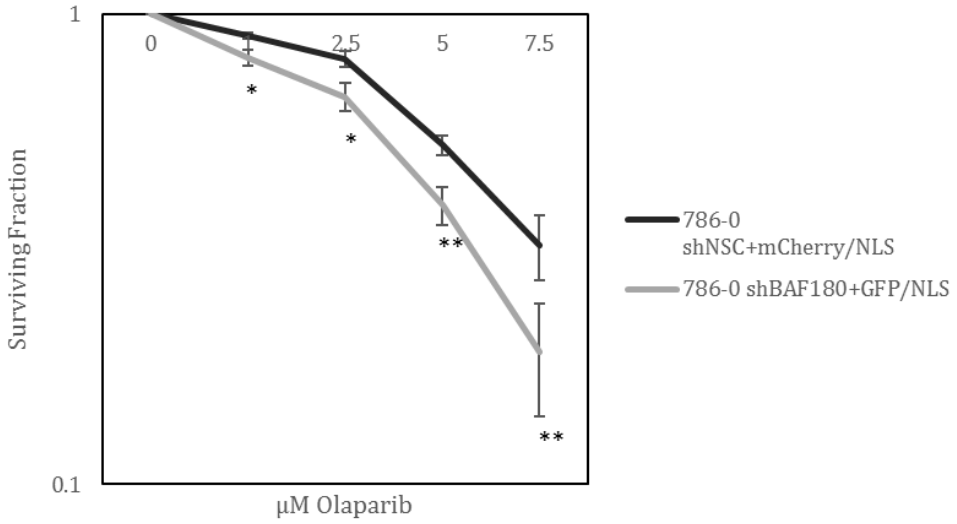

Figure 6.2. Two cell lines with depleted BAF180 are sensitive to treatment with the PARP inhibitor drug Olaparib. (A) shBAF180 U20S cells were more sensitive to treatment with Olaparib compared to the control in clonogenic survival assay. (n=3). (B) shBAF180 786-0 cells were more sensitive to treatment with Olaparib compared to the control in clonogenic survival assay. (n=3).
Statistical significance is represented by * for $p<0.05$ and ** for $p<0.01$, as analysed by Student t-test.

6.5. Sensitivity to Olaparib is not due to off target shRNA effects

When synthesising our cell lines, as described in Chapter 4, we generated stable shBAF180 cell lines with several different shRNA sequences. This provided us with an opportunity to determine whether the synthetic lethal relationship with PARP activity is a consequence of off target effects from the shRNA sequence used. We therefore performed colony survival assays with the panel of stable shBAF180 cells. Figure 6.3a shows the varying degree of sensitivity of each BAF180 shRNA construct in comparison to a U2OS only control. The construct that we chose to take forward for further modification, V3LHS_318943, which target sequence is located in the sixth of BAF180's bromodomains (Figure 6.3c), came out as one of the most sensitive to Olaparib treatment and was statistically significant at 0.5μM ($p<0.05$* - not shown in figure) (Figure 6.3a). This result was as expected, due to its modified counterpart shBAF180+GFP/NLS (U20S) being found to be sensitive to Olaparib treatment previously (Figure 6.2).

Constructs V2LHS_174969 and V2LHS_200596, which target sequences located in the third and fourth bromodomain respectively (Figure 6.3c), both show the strongest sensitivity of the constructs to PARP inhibitor treatment with statistically significant p values at each concentration ($p<0.05$* - not shown in figure). While constructs V2LHS_174972, located in the C-terminal domain and V3LHS_318948, located in the second BAH domain (Figure 6.3c), appear to be the least sensitive of the five (Figure 6.3a).

Western blot analysis (Figure 6.3b) demonstrates suppression of BAF180 protein expression in each of the shRNA constructs stable cell lines, when compared to relative BAF180 expression in control U2OS cells. Importantly, depletion of BAF180 by any of the given constructs, which target very different regions of the protein, all ultimately confer a sensitivity to the PARP inhibitor Olaparib. Together, these data suggest that the synthetic lethality between BAF180 loss and PARP inhibition is not a consequence of off target or indirect effects.

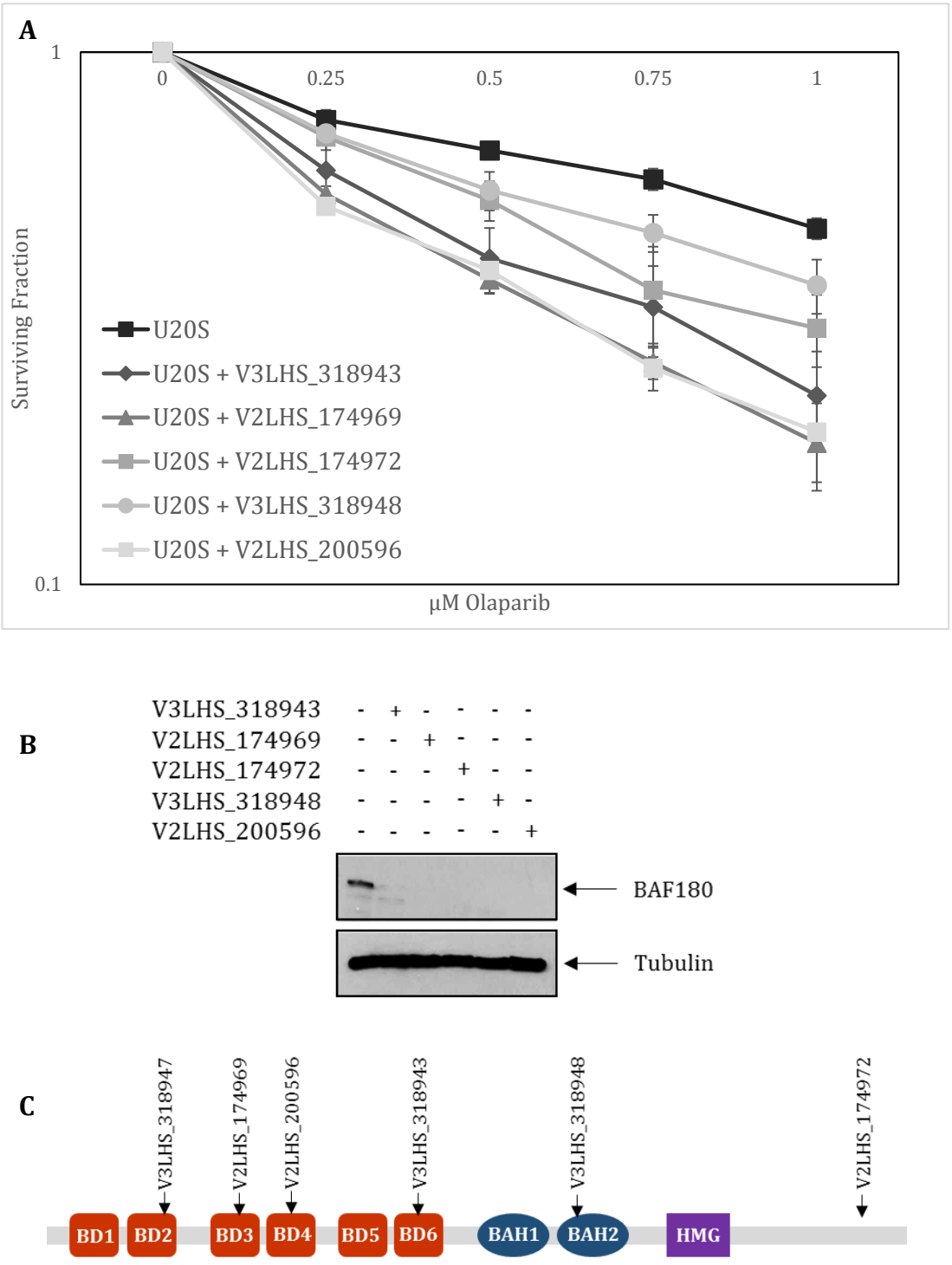

Figure 6.3 Sensitivity to Olaparib is not due to off target shRNA effects. (A) Five different shBAF180 construct expressing U20S cell lines were more sensitive to treatment with Olaparib compared to the control in clonogenic survival assays (n=3). (B) Western blot analysis of BAF180 protein expression in shBAF180 construct expressing U20S cell lines. (C) Illustration of the domains of BAF180 and where each shBAF180 construct targets.

6.6. Multiple cancer cell lines with depleted BAF180 are sensitive to the PARP inhibitor Rucaparib

To further investigate the relationship between BAF180 loss and the inhibition of PARP activity, we repeated the assays using different PARP inhibitor drugs. There are currently multiple commercially available PARP inhibitors that are in various stages of clinical trials.

Rucaparib has binding affinity with nine PARP proteins (PARP1, 2, 3, 4, 10. 15. 16. TNKS1 and TNKS2), but is thought to be a potent inhibitor specifically of PARP1, compared to Olaparib which is a potent PARP1/2 inhibitor. We chose to test Rucaparib in addition to Olaparib as we hypothesised that we may see a more dramatic synthetic lethal effect with a drug with binding affinity for both PARP1 and PARP3.

Colony survival assays were carried out in both the U2OS as well as the 786-0 stable shControl and shBAF180 cell lines, under constant exposure from the PARP inhibitor Rucaparib. Statistically significant differences in survival were observed in shBAF180 U2OS treated with Rucaparib at a subset of doses tested. Although survival differences were not significant at all doses, a reduction in colony formation ability was consistently apparent. There was a tendency for the shBAF180 renal cells to be slightly more sensitive to Rucaparib compared to shControl at the doses studied. While this was less dramatic than the differences observed in the U2OS-based cell lines, we could speculate that this may be due to the parent 786-0 cells potentially having a higher base-line level resistance to Rucaparib.

A

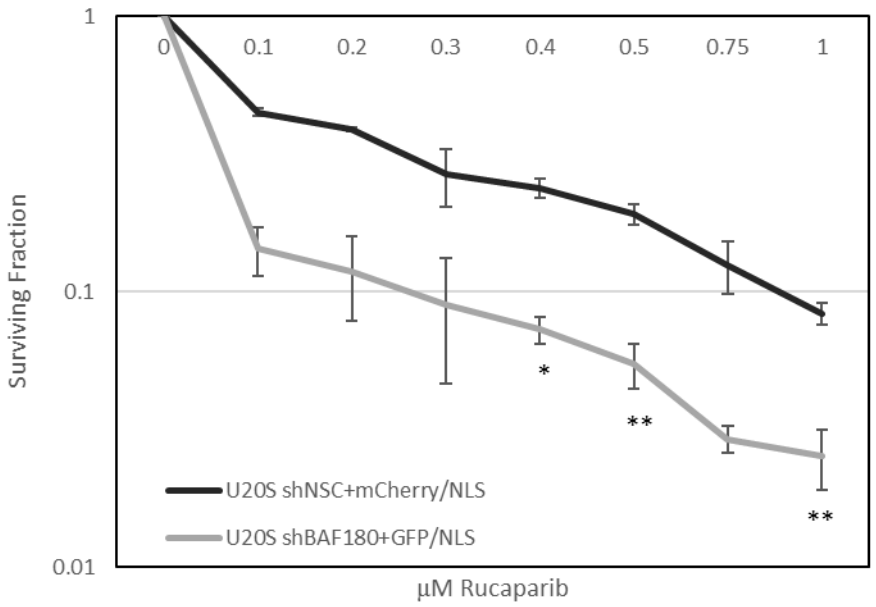

B

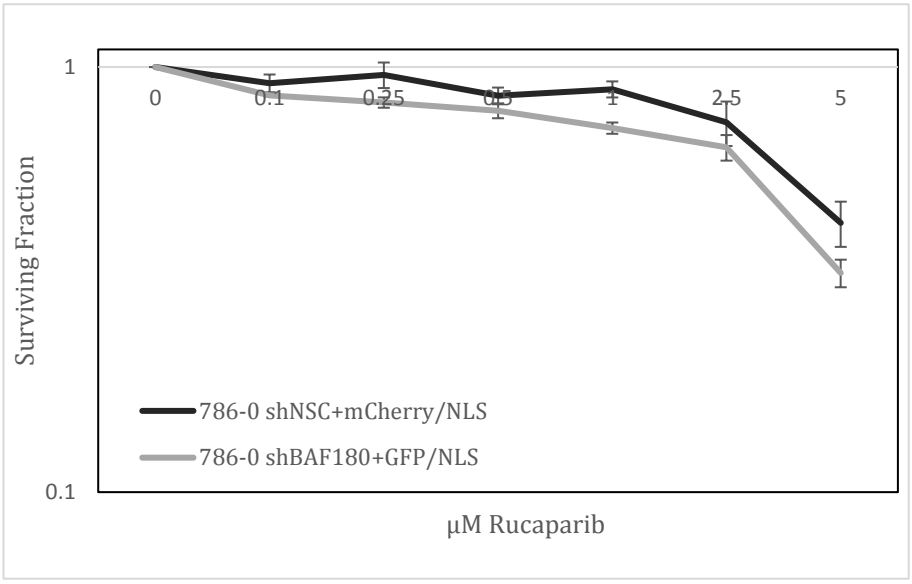

Figure 6.4 Multiple cancer cell lines with depleted BAF180 are sensitive to the PARP inhibitor Rucaparib. (A) shBAF180 U20S cells were more sensitive to treatment with Rucaparib compared to the control in clonogenic survival assay. (n=3). (B) shBAF180 786-0 cells were more sensitive to treatment with Rucaparib compared to the control in clonogenic survival assay. (n=3).
Statistical significance is represented by * for $p<0.05$ and ** for $p<0.01$, as analysed by Student t-test.

6.7. Sensitivity to Olaparib in BAF180 shU2OS is exacerbated by treatment with Ionising Radiation

We chose to combine PARP inhibition with ionising radiation (IR), to see if there was potential for amplifying problems repairing breaks in our cells with already impaired pathways.

To test how BAF180 depleted cells treated with olaparib, responded to the addition of IR, we chose a dose of olaparib that gave a small difference between cell lines and examine if we could exacerbate the difference with gamma irradiation.

shU2OS cells were irradiated in the presence of olaparib (Figure 6.5). Survival assays revealed a significant decrease in survival after the addition of Olaparib in the shBAF180 cells compared to the control at 2, 3 and 4Gy (Figure 6.5). The sensitivity to ionizing radiation after BAF180 knockdown and treatment with Olaparib, suggests that BAF180-depleted cells may have a defect in the HR pathway.

6.8. siBAF180 depleted U2OS cells exhibit a mild defect in HR

Cells that are sensitive to treatment to PARP inhibitors have a defect in HR (McCabe, Turner et al. 2006). Here we wanted to identify if the loss of BAF180 corresponded with a defect in HR. RAD51 foci formation is a readout of homologous recombination (Tarsounas, Davies et al. 2003).

Cells with a defect in HR will not be able to repair irradiation induced damage as readily and therefore will have fewer RAD51 foci. CENPF staining was used to visualise cells in the G2 stage of the cell cycle and antibodies against human RAD51 were used to visualise RAD51 foci formation, DNA content was stained using DAPI.

Here we see BAF180 depleted cells forming statistically significantly less foci per cell compared to the control, which is indicative of a partial HR defect (Figure 6.6a). Representative images illustrate the presence of RAD51 foci (Figure 6.6b).

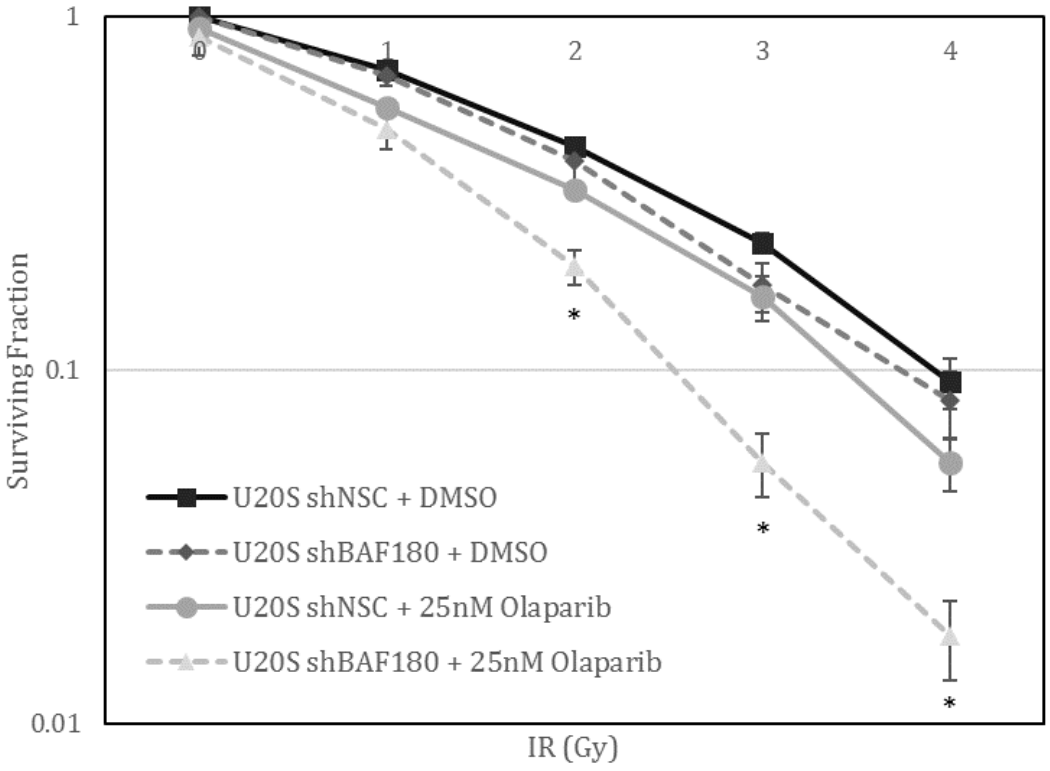

Figure 6.5 Sensitivity to Olaparib in BAF180 shU20S cells is exacerbated by treatment with IR. shBAF180 U20S cells were more sensitive to treatment with Olaparib compared to the control in clonogenic survival assay. This sensitivity was increased upon addition of IR. (n=3). Statistical significance is represented by * for $p<0.05$, as analysed by Student t-test.

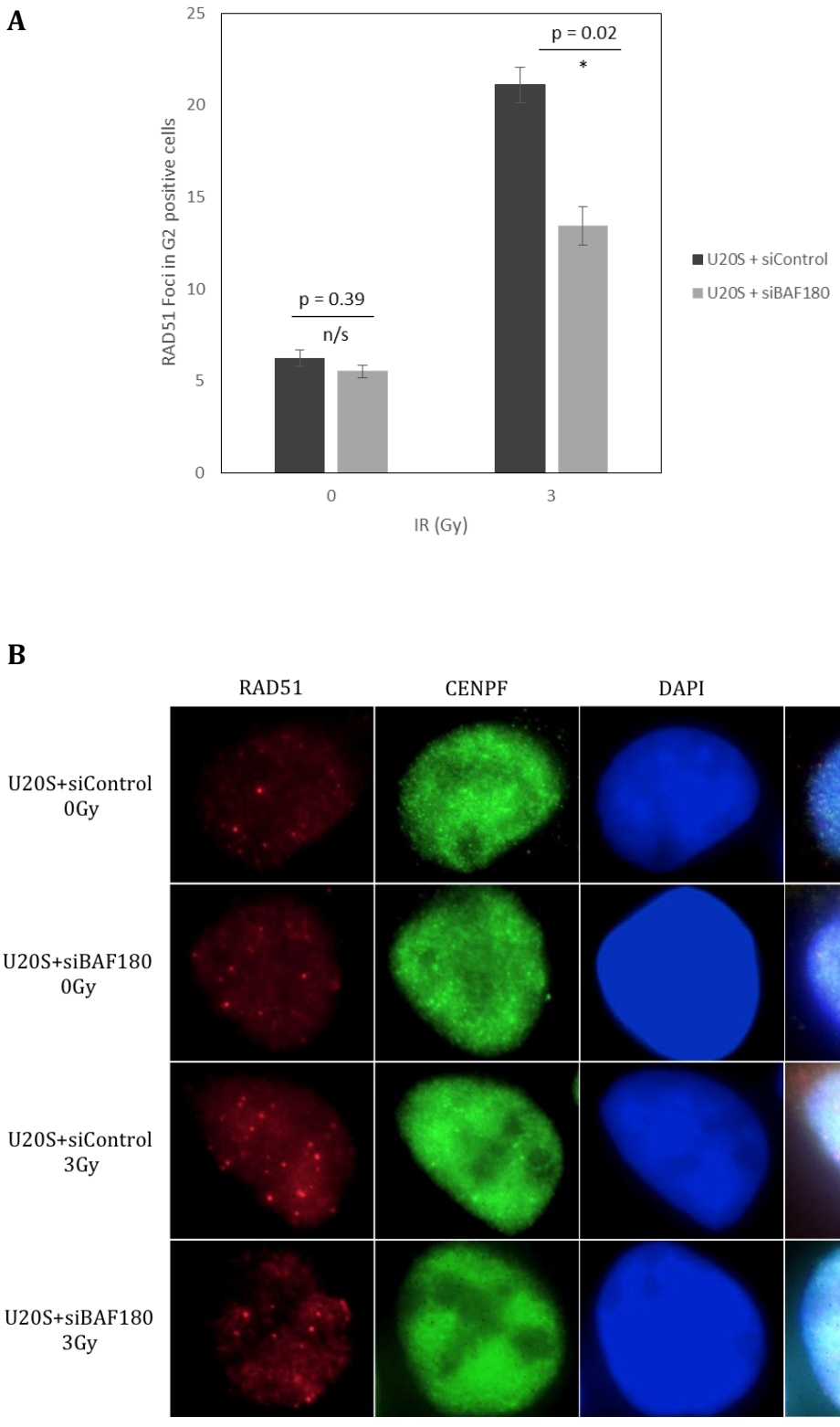

Figure 6.6 BAF180 depleted U20S cells exhibit a mild defect in HR. IR induced RAD51 focus formation in U20S cells treated with siControl or siBAF180. (A) Mean number of foci scored after 0Gy and 2 hours after 3Gy irradiation. Statistical significance is represented by * for $p<0.05$, as analysed by Student t-test. (B) Representative images of RAD51 focus formation.

6.9. Exposure of camptothecin in BAF180 shU2OS cells results in a sub G1 pile up and an increase of apoptotic cells

Camptothecin (CPT) is a Topoisomerase I inhibitor, that forms a tight complex with TOP1-DNA adducts. The stabilisation of TOP1-DNA adducts by CPT activates an ATR-dependent pathway to promote the repair of DNA damage by homologous recombination after encountering replication stress (O'Connell, Adamson et al. 2010). Consequently, cells with defects in the HR pathway display sensitivity to treatment with CPT.

6.9.1. BAF180 depleted shU2OS cells treated with camptothecin accumulate in sub G1

To further investigate the defect in HR in BAF180 deficient cells, we used the drug camptothecin and analysed the data by flow cytometry. U2OS stable shControl and shBAF180 cells were treated with camptothecin and analysed by FACS to monitor apoptotic responses and cell cycle progression.

FACS profiles showed an increase in the sub G1 population, in shBAF180 cells after treatment with camptothecin (Figure 6.7a, Figure 6.7b). Addition of camptothecin had an effect on cell viability in both cell lines, however, strikingly there was a more rapid accumulation in the sub G1 population in the shBAF180 cells compared to the control. In both the shControl and shBAF180 cells exposure to camptothecin was severely toxic after 96 hours and therefore, sub G1 population levels plateaued here (Figure 6.7a, Figure 6.7b).

6.9.2. BAF180 depleted shU2OS cells treated with camptothecin are positive for the apoptotic indicator, Caspase 3

In order to determine whether the sub-G1 population was due to apoptosis in response to CPT treatment, we monitored this response directly using antibodies raised against Caspase 3. Caspase 3 is part of the Caspase family of endoproteases, that play a key role in cell regulatory networks that control inflammation and cell death. Multiple caspases are sequentially activated during cellular apoptosis, or programmed cell death. The presence of caspase 3 in cells can be used as a readout of activation of the apoptotic pathway. Both FACS analysis (Figure 6.8a), as well as Western blot (Figure 6.8c) demonstrated that apoptosis has been stimulated in both cell lines after the treatment with camptothecin. The caspase positive fraction of cells was quantitated by gating in the FACs assays, and this suggested that the proportion of cells undergoing apoptosis was significantly higher for the shBAF180 cells (Figure 6.8a, Figure 6.8b). Another readout of apoptosis is PARP cleavage (Yang, Zhao et al. 2004). Western blot analysis showed the formation of cleaved PARP after treatment with camptothecin at early time points (Figure 6.8c), suggesting that the drug did indeed stimulate apoptosis in both cell lines.

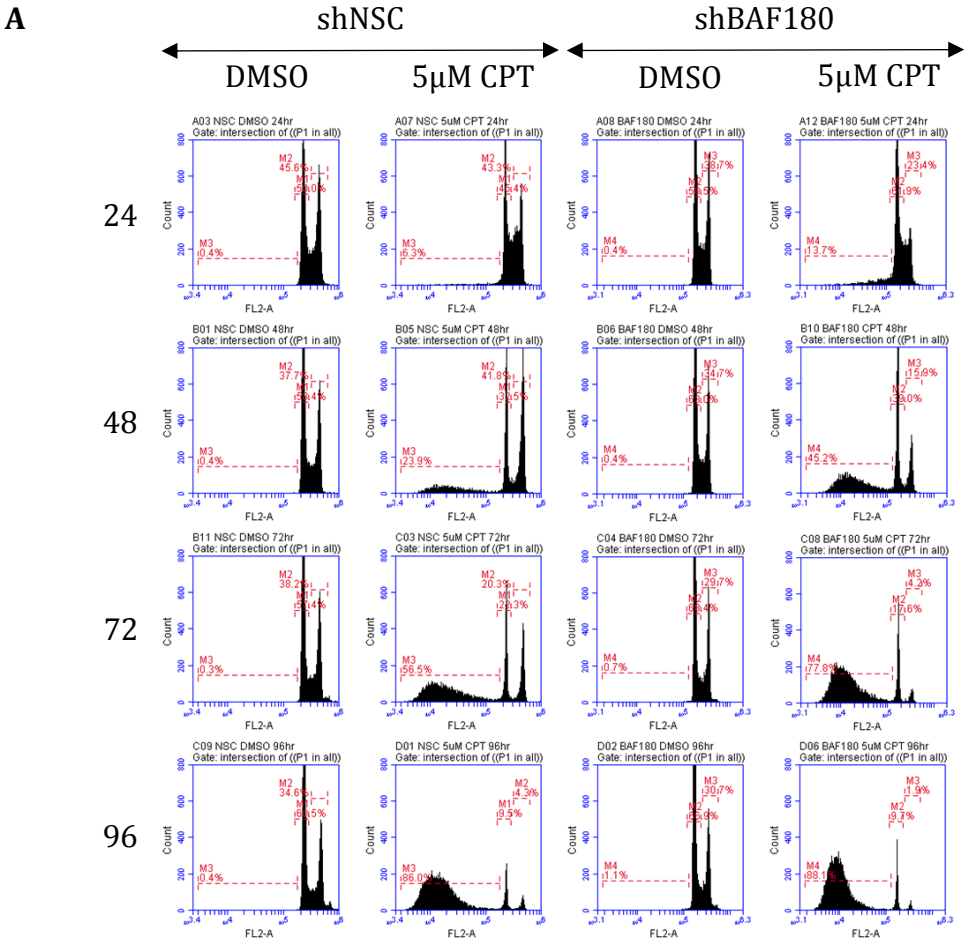

Figure 6.7. BAF180 depleted shU20S cells treated with camptothecin accumulate in sub G1. FACS analysis of shControl and shBAF180 U20S treated with camptothecin or the vehicle control DMSO at 0, 24, 48, 72 and 96 hour time points. (A) Representative cell cycle profiles after treatment with camptothecin (n=2) (B) Histogram representation of sub G1 population after camptothecin treatment.

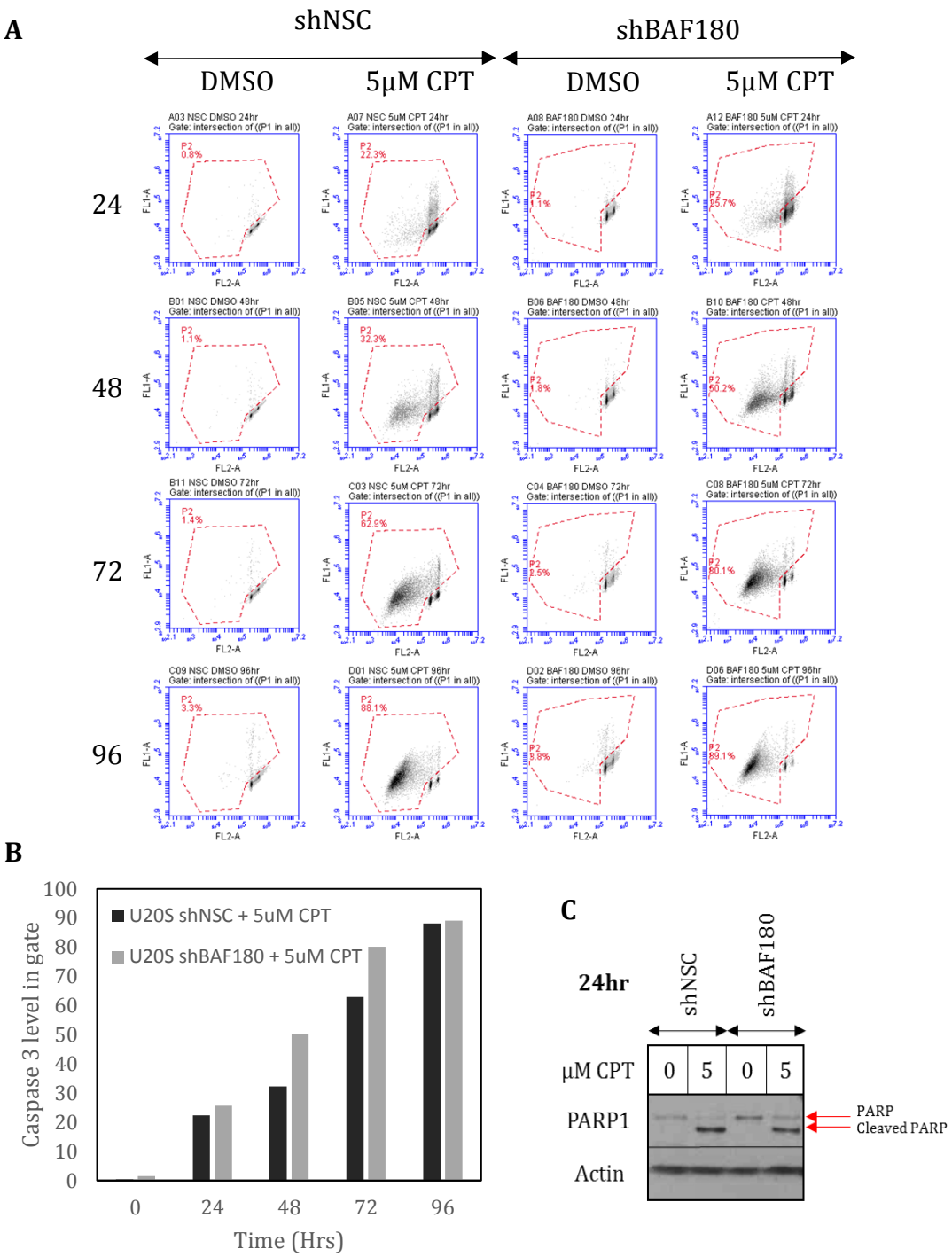

Figure 6.8. BAF180 depleted shU20S cells treated with camptothecin have more caspase 3 positive cells compared to the control. FACS analysis of shControl and shBAF180 U20S treated with camptothecin or the vehicle control DMSO at 0, 24, 48, 72 and 96 hour time points. (A) Representative caspase 3 levels after treatment with camptothecin (n=2) (B) Histogram representation of caspase 3 in gated population after camptothecin treatment. (C) Western blot of apoptosis. Analysis of PARP and cleaved PARP expression after treatment with camptothecin in shControl and shBAF180 U20S cells.

6.10. Exposure of Olaparib in BAF180 shU2OS cells results in a sub G1 accumulation and an increase of apoptotic cells

We wished to understand how our shU2OS cells were dying after treatment with the PARP inhibitor Olaparib. Our hypothesis was that the cells were being made to enter the apoptotic pathway, rather than cell death by necrosis.

6.10.1. BAF180 depleted shU2OS cells treated with Olaparib accumulate in sub G1

In order to test whether the shBAF180 cells were dying by apoptosis after PARP inhibitor treatment, U2OS stable shControl and shBAF180 cells were analysed after olaparib treatment by FACS. Addition of Olaparib to the stable U2OS cell lines shControl and shBAF180 resulted in a slight increase in the sub G1 population of both cell lines at high doses and late time points (Figure 6.9). At high doses over long periods of exposure to any drug would stimulate some level of cell death or apoptosis because the cells can no longer tolerate the treatment, but it is interesting to see that this level of apoptosis is increased significantly in the cells lacking BAF180.

6.10.2. BAF180 depleted shU2OS cells treated with Olaparib are positive for the apoptotic indicator, Caspase 3

Consistent with the data shown in Figure 6.9, a shift in the total cells apoptotic population can be seen in both cell lines at the 10 and 20uM dose of Olaparib at late time points when looking at Caspase 3 expression (Figure 6.10). Caspase 3 levels show us a clearer indication that the shBAF180 cells are more prone to enter apoptosis after Olaparib treatment, than looking at the sub G1 population alone. shBAF180 cells have an increase in Caspase-3 positive cells at all time points after treatment with 10 and 20μM Olaparib compared to the control.

These data demonstrate that loss of BAF180 results in a modest, but clear, defect in the HR pathway, which provides a potential mechanistic explanation for the sensitivity to treatment with PARP inhibitors.

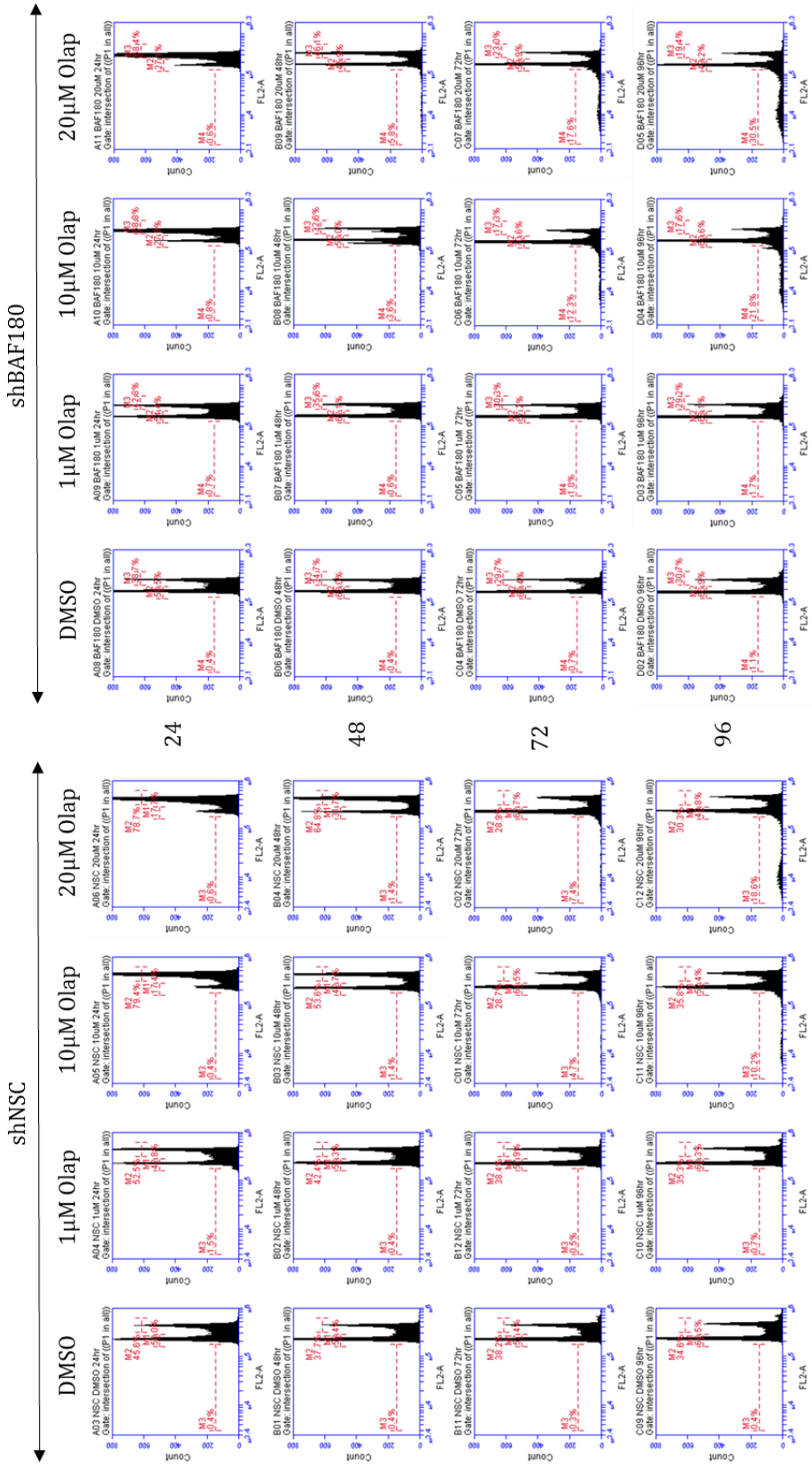

Figure 6.9. BAF180 depleted shU20S cells treated with Olaparib accumulate in sub G1.
FACS analysis of shControl and shBAF180 U20S treated with Olaparib or the vehicle control DMSO at 0, 24, 48, 72 and 96 hour time points. Representative cell cycle profiles after treatment with Olaparib (n=2).

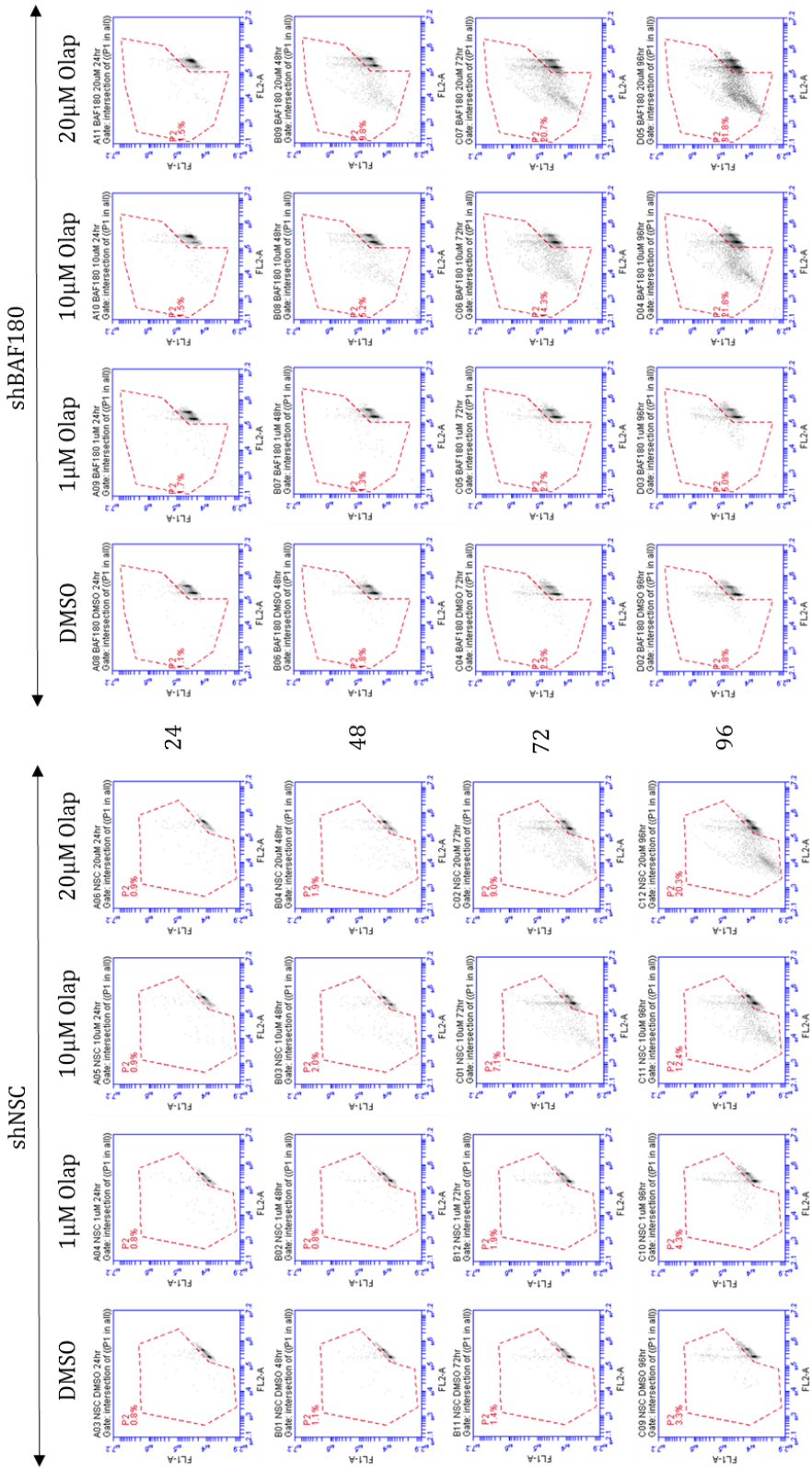

Figure 6.10. BAF180 depleted shU20S cells treated with Olaparib have more caspase 3 positive cells compared to the control. FACS analysis of shControl and shBAF180 U20S treated with Olaparib or the vehicle control DMSO at 0, 24, 48, 72 and 96 hour time points. Representative caspase 3 levels after treatment with Olaparib (n=2)

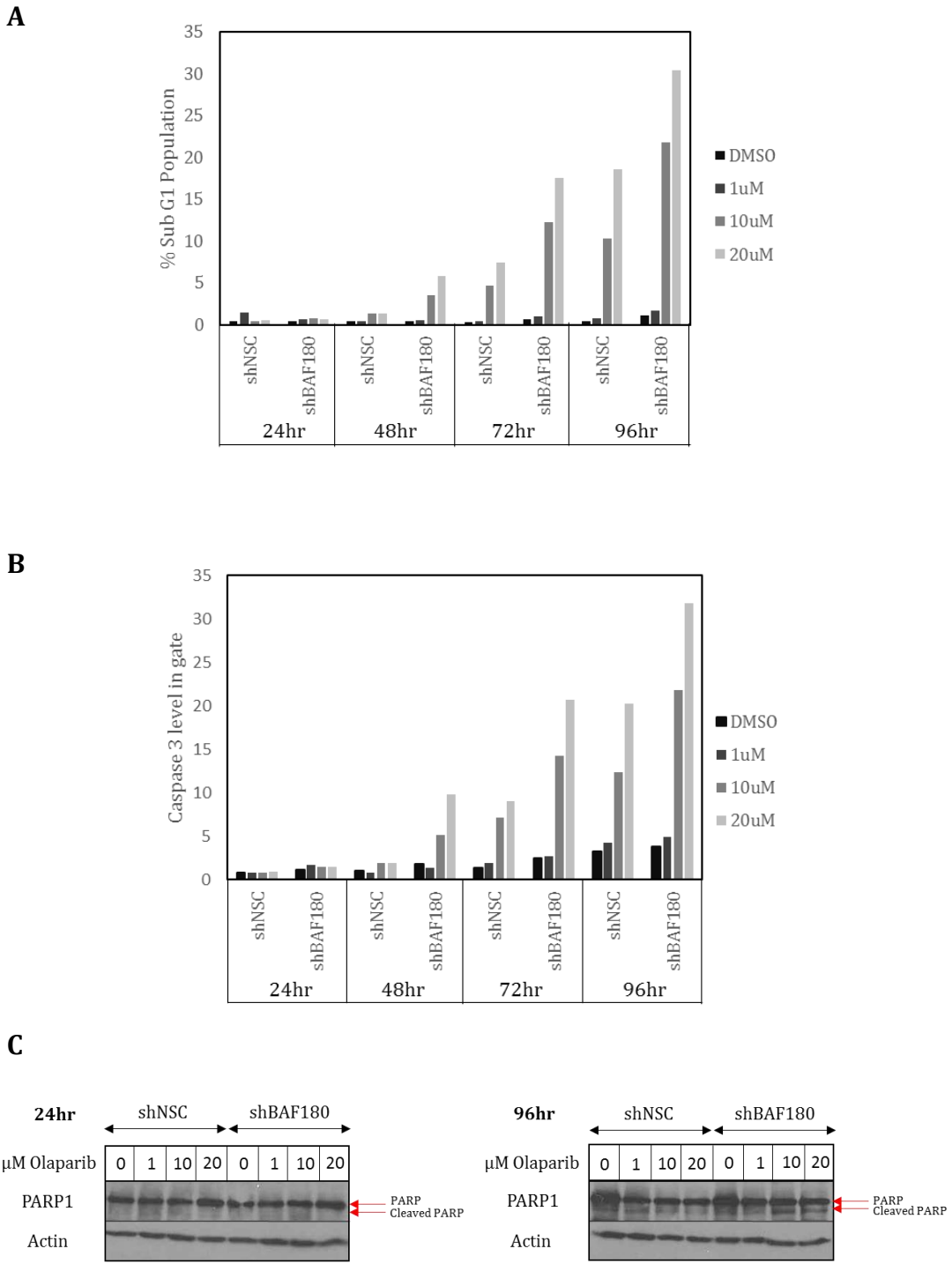

Figure 6.11. shBAF180 U20S appear to die through apoptosis after treatment with Olaparib.

FACS analysis of shControl and shBAF180 U20S treated with Olaparib or the vehicle control DMSO at 0, 24, 48, 72 and 96 hour time points. (A) Histogram representation of sub G1 population after camptothecin treatment (B) Histogram representation of caspase 3 in gated population after Olaparib treatment. (C) Western blot of apoptosis. Analysis of PARP and cleaved PARP expression after treatment with Olaparib in shControl and shBAF180 U20S cells.

6.11. Discussion

In this section we validated the siPARP:shBAF180 interaction observed in our high-throughput synthetic lethal siRNA screen, described in Chapter 5. We found that the interaction seen between PARP1 and PARP3 with shBAF180 U2OS cells was not due to off-target effects, confirming the interaction with different siRNAs and small molecule inhibitors of PARP in two different BAF180-deficient cell lines. We confirmed that multiple shBAF180 constructs expressing in U2OS cells confer sensitivity to the PARP inhibitor Olaparib, demonstrating that the synthetic lethality observed was not shRNA construct specific. We saw that sensitivity to Olaparib in shBAF180 U2OS cells was exacerbated upon addition of IR, suggesting that there may be a HR defect in BAF180-deficient cell lines. We confirmed that there is a modest defect in the HR pathway in BAF180-deficient cells by observing RAD51 foci formation and camptothecin sensitivity. And finally we demonstrated that BAF180-deficient U2OS cells treated with Olaparib show increased levels of cells in apoptosis.

6.11.1. Is there a more important role for PARP3 than the other PARP genes in regards to BAF180 synthetic lethality?

Our high-throughput screen, as discussed in Chapter 5, identified PARP3 as having the 4th highest synthetic lethal interaction with shBAF180 U2OS out of 446 siRNAs. The other PARP genes followed the same trend and were also identified as having a modest synthetic lethality with BAF180. But it is interesting to think about why this might be.

Technical errors, for example errors in pipetting on a large scale, may be responsible for why PARP3 came higher in our screen than the other PARP genes. Due to the high-throughput nature of a screen, there is more potential for variability here on such a large scale, compared with manual/individual validation. Because we further validated PARP1's synthetic lethal interaction with BAF180 at levels comparable to PARP3 (Figure 6.1a and 6.1c), it is likely that

technical errors in the HTS resulted in the more favourable killing of shBAF180 U2OS by loss of PARP3, however it is interesting to speculate why PARP3, in a PARP1-independent way, is synthetic lethal with BAF180.

PARP1 was the first gene discovered in the PARP family, is well characterised and has clear roles in the DNA damage response. However, increasing evidence demonstrates that PARP3 is too an important player in the cellular response to DNA double strand breaks (Beck, Boehler et al. 2014). It has been shown that PARP3 interacts with and PARylates Ku70/Ku80 and specifically it works together with Ku80 to limit DNA end resection and helps to make the choice between HR and NHEJ pathways (Beck, Boehler et al. 2014). PARP3 has also been found to interact with the chromatin-associated Polycomb Group (PcG) components EZH2, Suz12 and YY1 (Rouleau, McDonald et al. 2007). It has been suggested that PARP3 cooperates with EZH2 to regulate the expression and/or binding of BRCA1 at sites of DNA damage (Beck, Boehler et al. 2014). Recent work in our lab, as previously described, has linked the EZH2 containing PRC2 complex with the BAF180 containing PBAF complex. The data suggested that PBAF remodels chromatin surrounding DSBs in order to facilitate PRC2 activity and found that loss of EZH2 mirrored phenotypes exhibited by BAF180-deficent cells, for example the reduced formation of H2AK119ub foci after irradiation and the delay in the repair of a subset of DSBs at early time points following IR, suggesting that the failure to repress transcription around DSBs affects efficient repair. (Kakarougkas, Ismail et al. 2014). We could speculate that loss of two pathways responsible for interaction with EZH2 at DNA damage sites, together with the other pathways and factors affected by loss of either PARP3 or BAF180, could be the underlying reason for the synthetic lethality demonstrated here.

The most likely underlying reason for BAF180/PARP synthetic lethality is due to BAF180 contributing to the HR pathway (discussed in more detail below). However, there are other possible explanations for this observed phenotype. For example, as mentioned previously, the gene encoding BAF180, PBRM1, is located on chromosome 3p21 (Brugarolas 2013). Like BAF180, PARP3 is also found on chromosome 3p21 (Johansson 1999). In Chapter 5, we introduced the possibility

that SMARCC1 was found as a top hit from our high-throughput synthetic lethal screen with BAF180 because it also resides on chromosome 3p21. Given its location on a short chromosome arm that has multiple ccRCC genes mutated, it would be expected to be mutated by chance alone at 70% of the frequency of BAF180 (Brugarolas 2013). However, mutation of SMARCC1 in ccRCC are very rare, suggesting that the gene may be required for ccRCC survival (Brugarolas 2013). Out of 1777 kidney cancer samples tested for PARP3 mutation, just 0.11% (2 samples) harboured a mutation (Forbes, Beare et al. 2015). It is possible to speculate that after loss of VHL and BAF180 tumour suppressors, PARP3 gene expression may be essential for cell growth and may account for the synthetic lethality we observe in this study. Of course, this theory does not account for the synthetic lethality seen between BAF180 and other PARP family members such as PARP1, 2 and 4 as they are found on chromosome 1, 14 and 13 respectively.

6.11.2. BAF180-deficient cells have a defect in homologous recombination

Deficiency in the homologous recombination pathway causes cellular sensitivity to PARP inhibitors, therefore PARP inhibitor sensitivity may indicate a defect in HR directed repair. We identified a sensitivity to both Olaparib and Rucaparib in two of our BAF180-deficient cell lines (U2OS and 786-0), suggesting that there may be an underlying defect in HR in our BAF180-depleted cells causing the PARP inhibitor sensitivity.

Recent work in our lab has identified PBAF, and specifically the BAF180 subunit, as being important for mediating correct sister chromatid cohesion (Brownlee, Chambers et al. 2014). Cohesin is thought to be involved in sister chromatid HR but not NHEJ in human cells (Potts, Porteus et al. 2006). Cohesin is recruited to sites of DNA damage and facilitates sister chromatid HR by mediating local cohesion between a damaged chromatid and its intact sister template (Kim, Krasieva et al. 2002).

It is known that cohesin complex related genes, with defects in the HR pathway, are sensitive to PARP inhibition. For example, PDS5B (APRIN) is a cohesion-associated protein, that interacts with BRCA2. BRCA2 is known to interact with a number of proteins that control HR including PALB2 (Xia, Sheng et al. 2006), FANCG (Hussain, Witt et al. 2003), FANCD2 (Hussain, Wilson et al. 2004), BRCA1 (Chen, Silver et al. 1998) and DSS1 (Marston, Richards et al. 1999). Like BRCA2-deficient cells, mutations in BRCA2-binding proteins can also result in compromised HR efficiency and sensitisation to DNA damage. It was determined that PDS5B expression is required for the normal response to DNA-damaging agents, the nuclear localisation of RAD51 and BRCA2 and efficient homologous recombination (Brough, Bajrami et al. 2012). Silencing of PDS5B results in a sensitisation to the PARP inhibitor Olaparib (Brough, Bajrami et al. 2012). A number of other cohesion-associated genes, for example, RAD21, ESCO1, ESCO2 and SMC3, when silenced, have also been found to be sensitive to PARP inhibition (Bajrami, Frankum et al. 2014). This highlights the importance for factors involved in correct sister chromatid cohesion in the DNA damage response.

The yeast homologues of BAF180, Rsc1 and Rsc2 are already known to have defects in HR-dependent DNA repair (Chai, Huang et al. 2005, Oum, Seong et al. 2011). The defective sister chromatid HR at double strand break sites, in Rsc2 mutant cells specifically, is thought to be due to impaired accumulation of DSB-induced cohesin at the break (Oum, Seong et al. 2011). It is possible that mammalian BAF180, like its yeast homologues, cooperates with cohesion factors to facilitate cohesin-dependent HR. Therefore, silencing of BAF180 gives rise to defective HR and sensitivity to PARP inhibitors as seen in this study.

6.11.3. Future work

Consistent with data from the Lord lab (C. Lord – The Institute of Cancer Research – personal communication), we find that BAF180-depleted cells are sensitive to treatment with PARP inhibitors. They observe sensitivity to Olaparib, Rucaparib

and Talazoparib in siPBRM1 depleted mouse embryonic stem cells in clonogenic survival assays (C. Lord – unpublished data).

To test whether the human renal cell line, 786-0, expressing shBAF180 has a conserved synthetic lethal interaction with PARP inhibitors in a different model to those tested here, we chose to perform mouse xenografts in collaboration with Prof. Sue Eccles (The Institute of Cancer Research). Immunodeficient mice were injected with shControl and shBAF180 cells and tumours were allowed to form for twelve days before treatment was given. No significant difference in tumour volume was seen between shControl and shBAF180 after treatment with 15mg/kg Olaparib for five consecutive weeks (data not shown). In BRCA1-/- mouse xenografts, the Lord lab have previously observed a non-significant difference in tumour cell growth between the BRCA1-depleted and control cells treated with PARP inhibitor. However, upon Hematoxylin and Eosin (HE) staining of tumours, they find a higher level of necrosis in the BRCA1-depleted cells after PARP inhibitor treatment (C. Lord – unpublished data).

Ongoing work is currently being performed to determine whether, consistent with the Lord lab data, upon HE staining we will also see a higher level of necrosis in the shBAF180 cells. Failing this, we can also pursue repeating the xenograft study with a higher dose of PARP inhibitor, as retrospectively we learned that 15mg/kg is a relatively low dose treatment and standard PARP inhibitor xenograft studies use ~50mg/kg doses.

Observing the response of a human tumour to therapy is important for the progression of new drug treatments for cancer. Performing mouse xenografts with transplanted human cells is a good preliminary model for the examination of response to therapy. Our aim is to confirm that shBAF180 depleted cells are more sensitive to PARP inhibitor treatment in this model, either in decreased tumour volume or increased levels of necrosis, with an overall view to utilizing PARP inhibitors for the treatment of BAF180-null ccRCC.

References

Abat, D., O. Demirhan, N. Inandiklioglu, E. Tunc, S. Erdogan, D. Tastemir, I. N. Uslu and Z. Tansug (2014). "Genetic alterations of chromosomes, p53 and p16 genes in low- and high-grade bladder cancer." Oncol Lett **8**(1): 25-32.

Adamson, B., A. Smogorzewska, F. D. Sigoillot, R. W. King and S. J. Elledge (2012). "A genome-wide homologous recombination screen identifies the RNA-binding protein RBMX as a component of the DNA-damage response." Nat Cell Biol **14**(3): 318-328.

Agrawal, N., M. J. Frederick, C. R. Pickering, C. Bettegowda, K. Chang, R. J. Li, C. Fakhry, T. X. Xie, J. Zhang, J. Wang, N. Zhang, A. K. El-Naggar, S. A. Jasser, J. N. Weinstein, L. Trevino, J. A. Drummond, D. M. Muzny, Y. Wu, L. D. Wood, R. H. Hruban, W. H. Westra, W. M. Koch, J. A. Califano, R. A. Gibbs, D. Sidransky, B. Vogelstein, V. E. Velculescu, N. Papadopoulos, D. A. Wheeler, K. W. Kinzler and J. N. Myers (2011). "Exome sequencing of head and neck squamous cell carcinoma reveals inactivating mutations in NOTCH1." Science **333**(6046): 1154-1157.

Ahmad, K. and S. Henikoff (2002). "The histone variant H3.3 marks active chromatin by replication-independent nucleosome assembly." Mol Cell **9**(6): 1191-1200.

Ahnesorg, P., P. Smith and S. P. Jackson (2006). "XLF interacts with the XRCC4-DNA ligase IV complex to promote DNA nonhomologous end-joining." Cell **124**(2): 301-313.

Al Sarakbi, W., W. Sasi, W. G. Jiang, T. Roberts, R. F. Newbold and K. Mokbel (2009). "The mRNA expression of SETD2 in human breast cancer: correlation with clinico-pathological parameters." BMC Cancer **9**: 290.

Ali, A. A., G. Timinszky, R. Arribas-Bosacoma, M. Kozlowski, P. O. Hassa, M. Hassler, A. G. Ladurner, L. H. Pearl and A. W. Oliver (2012). "The zinc-finger domains of PARP1 cooperate to recognize DNA strand breaks." Nat Struct Mol Biol **19**(7): 685-692.

Ame, J. C., V. Rolli, V. Schreiber, C. Niedergang, F. Apiou, P. Decker, S. Muller, T. Hoger, J. Menissier-de Murcia and G. de Murcia (1999). "PARP-2, A novel mammalian DNA damage-dependent poly(ADP-ribose) polymerase." J Biol Chem **274**(25): 17860-17868.

Ame, J. C., C. Spenlehauer and G. de Murcia (2004). "The PARP superfamily." Bioessays **26**(8): 882-893.

Andres, S. N., A. Vergnes, D. Ristic, C. Wyman, M. Modesti and M. Junop (2012). "A human XRCC4-XLF complex bridges DNA." Nucleic Acids Res **40**(4): 1868-1878.

Angus-Hill, M. L., A. Schlichter, D. Roberts, H. Erdjument-Bromage, P. Tempst and B. R. Cairns (2001). "A Rsc3/Rsc30 zinc cluster dimer reveals novel roles for the chromatin remodeler RSC in gene expression and cell cycle control." Mol Cell **7**(4): 741-751.

Aravind, L. and E. V. Koonin (2000). "SAP - a putative DNA-binding motif involved in chromosomal organization." Trends Biochem Sci **25**(3): 112-114.

Aravind, L. and D. Landsman (1998). "AT-hook motifs identified in a wide variety of DNA-binding proteins." Nucleic Acids Res **26**(19): 4413-4421.

Asturias, F. J., W. H. Chung, R. D. Kornberg and Y. Lorch (2002). "Structural analysis of the RSC chromatin-remodeling complex." Proc Natl Acad Sci U S A **99**(21): 13477-13480.

Augustin, A., C. Spenlehauer, H. Dumond, J. Menissier-De Murcia, M. Piel, A. C. Schmit, F. Apiou, J. L. Vonesch, M. Kock, M. Bornens and G. De Murcia (2003). "PARP-3 localizes preferentially to the daughter centriole and interferes with the G1/S cell cycle progression." J Cell Sci **116**(Pt 8): 1551-1562.

Aymard, F., B. Bugler, C. K. Schmidt, E. Guillou, P. Caron, S. Briois, J. S. Iacovoni, V. Daburon, K. M. Miller, S. P. Jackson and G. Legube (2014). "Transcriptionally active chromatin recruits homologous recombination at DNA double-strand breaks." Nat Struct Mol Biol **21**(4): 366-374.

Baetz, K. K., N. J. Krogan, A. Emili, J. Greenblatt and P. Hieter (2004). "The ctf13-30/CTF13 genomic haploinsufficiency modifier screen identifies the yeast chromatin remodeling complex RSC, which is required for the establishment of sister chromatid cohesion." Mol Cell Biol **24**(3): 1232-1244.

Bannister, A. J. and T. Kouzarides (2005). "Reversing histone methylation." Nature **436**(7054): 1103-1106.

Beck, C., C. Boehler, J. Guirouilh Barbat, M. E. Bonnet, G. Illuzzi, P. Ronde, L. R. Gauthier, N. Magroun, A. Rajendran, B. S. Lopez, R. Scully, F. D. Boussin, V. Schreiber and F. Dantzer (2014). "PARP3 affects the relative contribution of

homologous recombination and nonhomologous end-joining pathways." Nucleic Acids Res **42**(9): 5616-5632.

Belmont, A. S. and K. Bruce (1994). "Visualization of G1 chromosomes: a folded, twisted, supercoiled chromonema model of interphase chromatid structure." J Cell Biol **127**(2): 287-302.

Benayoun, B. A., E. A. Pollina, D. Ucar, S. Mahmoudi, K. Karra, E. D. Wong, K. Devarajan, A. C. Daugherty, A. B. Kundaje, E. Mancini, B. C. Hitz, R. Gupta, T. A. Rando, J. C. Baker, M. P. Snyder, J. M. Cherry and A. Brunet (2014). "H3K4me3 breadth is linked to cell identity and transcriptional consistency." Cell **158**(3): 673-688.

Bender, A. and J. R. Pringle (1991). "Use of a Screen for Synthetic Lethal and Multicopy Suppressee Mutants to Identify 2 New Genes Involved in Morphogenesis in Saccharomyces-Cerevisiae." Molecular and Cellular Biology **11**(3): 1295-1305.

Bergink, S., F. A. Salomons, D. Hoogstraten, T. A. Groothuis, H. de Waard, J. Wu, L. Yuan, E. Citterio, A. B. Houtsmuller, J. Neefjes, J. H. Hoeijmakers, W. Vermeulen and N. P. Dantuma (2006). "DNA damage triggers nucleotide excision repair-dependent monoubiquitylation of histone H2A." Genes Dev **20**(10): 1343-1352.

Bernstein, B. E., E. L. Humphrey, R. L. Erlich, R. Schneider, P. Bouman, J. S. Liu, T. Kouzarides and S. L. Schreiber (2002). "Methylation of histone H3 Lys 4 in coding regions of active genes." Proc Natl Acad Sci U S A **99**(13): 8695-8700.

Bhaskara, S. (2015). "Histone deacetylases 1 and 2 regulate DNA replication and DNA repair: potential targets for genome stability-mechanism-based therapeutics for a subset of cancers." Cell Cycle **14**(12): 1779-1785.

Birnbaum, D. J., D. Birnbaum and F. Bertucci (2011). "Endometriosis-associated ovarian carcinomas." N Engl J Med **364**(5): 483-484; author reply 484-485.

Boehler, C., L. R. Gauthier, O. Mortusewicz, D. S. Biard, J. M. Saliou, A. Bresson, S. Sanglier-Cianferani, S. Smith, V. Schreiber, F. Boussin and F. Dantzer (2011). "Poly(ADP-ribose) polymerase 3 (PARP3), a newcomer in cellular response to DNA damage and mitotic progression." Proc Natl Acad Sci U S A **108**(7): 2783-2788.

Bommi-Reddy, A., I. Almeciga, J. Sawyer, C. Geisen, W. Li, E. Harlow, W. G. Kaelin, Jr. and D. A. Grueneberg (2008). "Kinase requirements in human cells: III.

Altered kinase requirements in VHL-/- cancer cells detected in a pilot synthetic lethal screen." Proc Natl Acad Sci U S A **105**(43): 16484-16489.

Bonisch, C. and S. B. Hake (2012). "Histone H2A variants in nucleosomes and chromatin: more or less stable?" Nucleic Acids Res **40**(21): 10719-10741.

Boone, C., H. Bussey and B. J. Andrews (2007). "Exploring genetic interactions and networks with yeast." Nat Rev Genet **8**(6): 437-449.

Bott, M., M. Brevet, B. S. Taylor, S. Shimizu, T. Ito, L. Wang, J. Creaney, R. A. Lake, M. F. Zakowski, B. Reva, C. Sander, R. Delsite, S. Powell, Q. Zhou, R. Shen, A. Olshen, V. Rusch and M. Ladanyi (2011). "The nuclear deubiquitinase BAP1 is commonly inactivated by somatic mutations and 3p21.1 losses in malignant pleural mesothelioma." Nat Genet **43**(7): 668-672.

Botuyan, M. V., J. Lee, I. M. Ward, J. E. Kim, J. R. Thompson, J. Chen and G. Mer (2006). "Structural basis for the methylation state-specific recognition of histone H4-K20 by 53BP1 and Crb2 in DNA repair." Cell **127**(7): 1361-1373.

Bourachot, B., M. Yaniv and C. Muchardt (1999). "The activity of mammalian brm/SNF2alpha is dependent on a high-mobility-group protein I/Y-like DNA binding domain." Mol Cell Biol **19**(6): 3931-3939.

Boyer, L. A., C. Logie, E. Bonte, P. B. Becker, P. A. Wade, A. P. Wolffe, C. Wu, A. N. Imbalzano and C. L. Peterson (2000). "Functional delineation of three groups of the ATP-dependent family of chromatin remodeling enzymes." J Biol Chem **275**(25): 18864-18870.

Breeden, L. and K. Nasmyth (1987). "Cell cycle control of the yeast HO gene: cis- and trans-acting regulators." Cell **48**(3): 389-397.

Brouwer, I., G. Sitters, A. Candelli, S. J. Heerema, I. Heller, A. J. de Melo, H. Zhang, D. Normanno, M. Modesti, E. J. Peterman and G. J. Wuite (2016). "Sliding sleeves of XRCC4-XLF bridge DNA and connect fragments of broken DNA." Nature **535**(7613): 566-569.

Brownlee, P. M., A. L. Chambers, R. Cloney, A. Bianchi and J. A. Downs (2014). "BAF180 promotes cohesion and prevents genome instability and aneuploidy." Cell Rep **6**(6): 973-981.

Brownlee, P. M., A. L. Chambers, A. W. Oliver and J. A. Downs (2012). "Cancer and the bromodomains of BAF180." Biochem Soc Trans **40**(2): 364-369.

Brownlee, P. M., C. Meisenberg and J. A. Downs (2015). "The SWI/SNF chromatin remodelling complex: Its role in maintaining genome stability and preventing tumourigenesis." DNA Repair (Amst) **32**: 127-133.

Brugarolas, J. (2013). "PBRM1 and BAP1 as novel targets for renal cell carcinoma." Cancer J **19**(4): 324-332.

Bryant, H. E., N. Schultz, H. D. Thomas, K. M. Parker, D. Flower, E. Lopez, S. Kyle, M. Meuth, N. J. Curtin and T. Helleday (2005). "Specific killing of BRCA2-deficient tumours with inhibitors of poly(ADP-ribose) polymerase." Nature **434**(7035): 913-917.

Burrows, A. E., A. Smogorzewska and S. J. Elledge (2010). "Polybromo-associated BRG1-associated factor components BRD7 and BAF180 are critical regulators of p53 required for induction of replicative senescence." Proc Natl Acad Sci U S A **107**(32): 14280-14285.

Cairns, B. R., Y. Lorch, Y. Li, M. Zhang, L. Lacomis, H. Erdjument-Bromage, P. Tempst, J. Du, B. Laurent and R. D. Kornberg (1996). "RSC, an essential, abundant chromatin-remodeling complex." Cell **87**(7): 1249-1260.

Cairns, B. R., A. Schlichter, H. Erdjument-Bromage, P. Tempst, R. D. Kornberg and F. Winston (1999). "Two functionally distinct forms of the RSC nucleosome-remodeling complex, containing essential AT hook, BAH, and bromodomains." Mol Cell **4**(5): 715-723.

Canaani, D. (2014). "Application of the concept synthetic lethality toward anticancer therapy: a promise fulfilled?" Cancer Lett **352**(1): 59-65.

Canudas, S. and S. Smith (2009). "Differential regulation of telomere and centromere cohesion by the Scc3 homologues SA1 and SA2, respectively, in human cells." J Cell Biol **187**(2): 165-173.

Cao, R., Y. Tsukada and Y. Zhang (2005). "Role of Bmi-1 and Ring1A in H2A ubiquitylation and Hox gene silencing." Mol Cell **20**(6): 845-854.

Carretero, M., M. Ruiz-Torres, M. Rodriguez-Corsino, I. Barthelemy and A. Losada (2013). "Pds5B is required for cohesion establishment and Aurora B accumulation at centromeres." EMBO J **32**(22): 2938-2949.

Carvalho, S., A. C. Vitor, S. C. Sridhara, F. B. Martins, A. C. Raposo, J. M. Desterro, J. Ferreira and S. F. de Almeida (2014). "SETD2 is required for DNA double-strand break repair and activation of the p53-mediated checkpoint." Elife **3**: e02482.

Cary, R. B., S. R. Peterson, J. Wang, D. G. Bear, E. M. Bradbury and D. J. Chen (1997). "DNA looping by Ku and the DNA-dependent protein kinase." Proc Natl Acad Sci U S A **94**(9): 4267-4272.

Chaban, Y., C. Ezeokonkwo, W. H. Chung, F. Zhang, R. D. Kornberg, B. Maier-Davis, Y. Lorch and F. J. Asturias (2008). "Structure of a RSC-nucleosome complex and insights into chromatin remodeling." Nat Struct Mol Biol **15**(12): 1272-1277.

Chai, B., J. Huang, B. R. Cairns and B. C. Laurent (2005). "Distinct roles for the RSC and Swi/Snf ATP-dependent chromatin remodelers in DNA double-strand break repair." Genes Dev **19**(14): 1656-1661.

Chambers, A. L. and J. A. Downs (2012). "The RSC and INO80 chromatin-remodeling complexes in DNA double-strand break repair." Prog Mol Biol Transl Sci **110**: 229-261.

Chambers, A. L., L. H. Pearl, A. W. Oliver and J. A. Downs (2013). "The BAH domain of Rsc2 is a histone H3 binding domain." Nucleic Acids Res **41**(19): 9168-9182.

Chan, D. A. and A. J. Giaccia (2011). "Harnessing synthetic lethal interactions in anticancer drug discovery." Nat Rev Drug Discov **10**(5): 351-364.

Chandrasekaran, R. and M. Thompson (2007). "Polybromo-1-bromodomains bind histone H3 at specific acetyl-lysine positions." Biochem Biophys Res Commun **355**(3): 661-666.

Charlop-Powers, Z., L. Zeng, Q. Zhang and M. M. Zhou (2010). "Structural insights into selective histone H3 recognition by the human Polybromo bromodomain 2." Cell Res **20**(5): 529-538.

Chi, T. H., M. Wan, K. Zhao, I. Taniuchi, L. Chen, D. R. Littman and G. R. Crabtree (2002). "Reciprocal regulation of CD4/CD8 expression by SWI/SNF-like BAF complexes." Nature **418**(6894): 195-199.

Chiruvella, K. K., Z. Liang and T. E. Wilson (2013). "Repair of double-strand breaks by end joining." Cold Spring Harb Perspect Biol **5**(5): a012757.

Clapier, C. R. and B. R. Cairns (2009). "The biology of chromatin remodeling complexes." Annu Rev Biochem **78**: 273-304.

Clark, J. B., G. M. Ferris and S. Pinder (1971). "Inhibition of nuclear NAD nucleosidase and poly ADP-ribose polymerase activity from rat liver by

nicotinamide and 5'-methyl nicotinamide." Biochim Biophys Acta **238**(1): 82-85.

Conde-Pueyo, N., A. Munteanu, R. V. Sole and C. Rodriguez-Caso (2009). "Human synthetic lethal inference as potential anti-cancer target gene detection." BMC Syst Biol **3**: 116.

Corcoran, R. B., H. Ebi, A. B. Turke, E. M. Coffee, M. Nishino, A. P. Cogdill, R. D. Brown, P. Della Pelle, D. Dias-Santagata, K. E. Hung, K. T. Flaherty, A. Piris, J. A. Wargo, J. Settleman, M. Mino-Kenudson and J. A. Engelman (2012). "EGFR-mediated re-activation of MAPK signaling contributes to insensitivity of BRAF mutant colorectal cancers to RAF inhibition with vemurafenib." Cancer Discov **2**(3): 227-235.

Costanzo, M., A. Baryshnikova, J. Bellay, Y. Kim, E. D. Spear, C. S. Sevier, H. Ding, J. L. Koh, K. Toufighi, S. Mostafavi, J. Prinz, R. P. St Onge, B. VanderSluis, T. Makhnevych, F. J. Vizeacoumar, S. Alizadeh, S. Bahr, R. L. Brost, Y. Chen, M. Cokol, R. Deshpande, Z. Li, Z. Y. Lin, W. Liang, M. Marback, J. Paw, B. J. San Luis, E. Shuteriqi, A. H. Tong, N. van Dyk, I. M. Wallace, J. A. Whitney, M. T. Weirauch, G. Zhong, H. Zhu, W. A. Houry, M. Brudno, S. Ragibizadeh, B. Papp, C. Pal, F. P. Roth, G. Giaever, C. Nislow, O. G. Troyanskaya, H. Bussey, G. D. Bader, A. C. Gingras, Q. D. Morris, P. M. Kim, C. A. Kaiser, C. L. Myers, B. J. Andrews and C. Boone (2010). "The genetic landscape of a cell." Science **327**(5964): 425-431.

Critchlow, S. E., R. P. Bowater and S. P. Jackson (1997). "Mammalian DNA double-strand break repair protein XRCC4 interacts with DNA ligase IV." Curr Biol **7**(8): 588-598.

Curtin, N. J. and R. A. Sharma (2015). "PARP Inhibitors for Cancer Therapy Preface." Parp Inhibitors for Cancer Therapy **83**: V-Viii.

Dai, X., S. L. Rulten, C. You, K. W. Caldecott and Y. Wang (2015). "Identification and Functional Characterizations of N-Terminal alpha-N-Methylation and Phosphorylation of Serine 461 in Human Poly(ADP-ribose) Polymerase 3." J Proteome Res **14**(6): 2575-2582.

Dalgliesh, G. L., K. Furge, C. Greenman, L. Chen, G. Bignell, A. Butler, H. Davies, S. Edkins, C. Hardy, C. Latimer, J. Teague, J. Andrews, S. Barthorpe, D. Beare, G. Buck, P. J. Campbell, S. Forbes, M. Jia, D. Jones, H. Knott, C. Y. Kok, K. W. Lau, C. Leroy, M. L. Lin, D. J. McBride, M. Maddison, S. Maguire, K. McLay, A. Menzies, T.

Mironenko, L. Mulderrig, L. Mudie, S. O'Meara, E. Pleasance, A. Rajasingham, R. Shepherd, R. Smith, L. Stebbings, P. Stephens, G. Tang, P. S. Tarpey, K. Turrell, K. J. Dykema, S. K. Khoo, D. Petillo, B. Wondergem, J. Anema, R. J. Kahnoski, B. T. Teh, M. R. Stratton and P. A. Futreal (2010). "Systematic sequencing of renal carcinoma reveals inactivation of histone modifying genes." Nature **463**(7279): 360-363.

Dantzer, F. and R. Santoro (2013). "The expanding role of PARPs in the establishment and maintenance of heterochromatin." FEBS J **280**(15): 3508-3518.

Davis, A. J. and D. J. Chen (2013). "DNA double strand break repair via non-homologous end-joining." Transl Cancer Res **2**(3): 130-143.

de Murcia, J. M., C. Niedergang, C. Trucco, M. Ricoul, B. Dutrillaux, M. Mark, F. J. Oliver, M. Masson, A. Dierich, M. LeMeur, C. Walztinger, P. Chambon and G. de Murcia (1997). "Requirement of poly(ADP-ribose) polymerase in recovery from DNA damage in mice and in cells." Proc Natl Acad Sci U S A **94**(14): 7303-7307.

De Vos, M., V. Schreiber and F. Dantzer (2012). "The diverse roles and clinical relevance of PARPs in DNA damage repair: current state of the art." Biochem Pharmacol **84**(2): 137-146.

Dechassa, M. L., A. Sabri, S. Pondugula, S. R. Kassabov, N. Chatterjee, M. P. Kladde and B. Bartholomew (2010). "SWI/SNF has intrinsic nucleosome disassembly activity that is dependent on adjacent nucleosomes." Mol Cell **38**(4): 590-602.

Denslow, S. A. and P. A. Wade (2007). "The human Mi-2/NuRD complex and gene regulation." Oncogene **26**(37): 5433-5438.

Dhalluin, C., J. E. Carlson, L. Zeng, C. He, A. K. Aggarwal and M. M. Zhou (1999). "Structure and ligand of a histone acetyltransferase bromodomain." Nature **399**(6735): 491-496.

Diderich, K., M. Alanazi and J. H. Hoeijmakers (2011). "Premature aging and cancer in nucleotide excision repair-disorders." DNA Repair (Amst) **10**(7): 772-780.

Dobzhansky, T. (1946). "Genetics of Natural Populations. Xiii. Recombination and Variability in Populations of Drosophila Pseudoobscura." Genetics **31**(3): 269-290.

Drotschmann, K., W. Yang, F. E. Brownewell, E. T. Kool and T. A. Kunkel (2001). "Asymmetric recognition of DNA local distortion. Structure-based functional studies of eukaryotic Msh2-Msh6." J Biol Chem **276**(49): 46225-46229.

El-Khamisy, S. F., M. Masutani, H. Suzuki and K. W. Caldecott (2003). "A requirement for PARP-1 for the assembly or stability of XRCC1 nuclear foci at sites of oxidative DNA damage." Nucleic Acids Res **31**(19): 5526-5533.

Farmer, H., N. McCabe, C. J. Lord, A. N. Tutt, D. A. Johnson, T. B. Richardson, M. Santarosa, K. J. Dillon, I. Hickson, C. Knights, N. M. Martin, S. P. Jackson, G. C. Smith and A. Ashworth (2005). "Targeting the DNA repair defect in BRCA mutant cells as a therapeutic strategy." Nature **434**(7035): 917-921.

Fece de la Cruz, F., B. V. Gapp and S. M. Nijman (2015). "Synthetic lethal vulnerabilities of cancer." Annu Rev Pharmacol Toxicol **55**: 513-531.

Fei, J., N. Kaczmarek, A. Luch, A. Glas, T. Carell and H. Naegeli (2011). "Regulation of nucleotide excision repair by UV-DDB: prioritization of damage recognition to internucleosomal DNA." PLoS Biol **9**(10): e1001183.

Ferro, A. M. and B. M. Olivera (1982). "Poly(ADP-ribosylation) in vitro. Reaction parameters and enzyme mechanism." J Biol Chem **257**(13): 7808-7813.

Fisher, A. E., H. Hochegger, S. Takeda and K. W. Caldecott (2007). "Poly(ADP-ribose) polymerase 1 accelerates single-strand break repair in concert with poly(ADP-ribose) glycohydrolase." Mol Cell Biol **27**(15): 5597-5605.

Fitch, M. E., S. Nakajima, A. Yasui and J. M. Ford (2003). "In vivo recruitment of XPC to UV-induced cyclobutane pyrimidine dimers by the DDB2 gene product." J Biol Chem **278**(47): 46906-46910.

Francis, N. J., A. J. Saurin, Z. Shao and R. E. Kingston (2001). "Reconstitution of a functional core polycomb repressive complex." Mol Cell **8**(3): 545-556.

Franklin, R. E. and R. G. Gosling (1953). "Molecular configuration in sodium thymonucleate." Nature **171**(4356): 740-741.

Fryland, T., J. H. Christensen, J. Pallesen, M. Mattheisen, J. Palmfeldt, M. Bak, J. Grove, D. Demontis, J. Blechingberg, H. S. Ooi, M. Nyegaard, M. E. Hauberg, N. Tommerup, N. Gregersen, O. Mors, T. J. Corydon, A. L. Nielsen and A. D. Borglum (2016). "Identification of the BRD1 interaction network and its impact on mental disorder risk." Genome Med **8**(1): 53.

Fujita, N., D. L. Jaye, M. Kajita, C. Geigerman, C. S. Moreno and P. A. Wade (2003). "MTA3, a Mi-2/NuRD complex subunit, regulates an invasive growth pathway in breast cancer." Cell **113**(2): 207-219.

Gerlinger, M., S. Horswell, J. Larkin, A. J. Rowan, M. P. Salm, I. Varela, R. Fisher, N. McGranahan, N. Matthews, C. R. Santos, P. Martinez, B. Phillimore, S. Begum, A. Rabinowitz, B. Spencer-Dene, S. Gulati, P. A. Bates, G. Stamp, L. Pickering, M. Gore, D. L. Nicol, S. Hazell, P. A. Futreal, A. Stewart and C. Swanton (2014). "Genomic architecture and evolution of clear cell renal cell carcinomas defined by multiregion sequencing." Nat Genet **46**(3): 225-233.

Gerlinger, M., A. J. Rowan, S. Horswell, J. Larkin, D. Endesfelder, E. Gronroos, P. Martinez, N. Matthews, A. Stewart, P. Tarpey, I. Varela, B. Phillimore, S. Begum, N. Q. McDonald, A. Butler, D. Jones, K. Raine, C. Latimer, C. R. Santos, M. Nohadani, A. C. Eklund, B. Spencer-Dene, G. Clark, L. Pickering, G. Stamp, M. Gore, Z. Szallasi, J. Downward, P. A. Futreal and C. Swanton (2012). "Intratumor heterogeneity and branched evolution revealed by multiregion sequencing." N Engl J Med **366**(10): 883-892.

Gillet, L. C. and O. D. Scharer (2006). "Molecular mechanisms of mammalian global genome nucleotide excision repair." Chem Rev **106**(2): 253-276.

Giri, C. P., M. H. West, M. L. Ramirez and M. Smulson (1978). "Nuclear protein modification and chromatin substructure. 2. Internucleosomal localization of poly(adenosine diphosphate-ribose) polymerase." Biochemistry **17**(17): 3501-3504.

Gnarra, J. R., K. Tory, Y. Weng, L. Schmidt, M. H. Wei, H. Li, F. Latif, S. Liu, F. Chen, F. M. Duh and et al. (1994). "Mutations of the VHL tumour suppressor gene in renal carcinoma." Nat Genet **7**(1): 85-90.

Goodarzi, A. A. and P. A. Jeggo (2013). "The repair and signaling responses to DNA double-strand breaks." Adv Genet **82**: 1-45.

Goodarzi, A. A., Y. Yu, E. Riballo, P. Douglas, S. A. Walker, R. Ye, C. Harer, C. Marchetti, N. Morrice, P. A. Jeggo and S. P. Lees-Miller (2006). "DNA-PK autophosphorylation facilitates Artemis endonuclease activity." EMBO J **25**(16): 3880-3889.

Goodwin, G. H. and R. H. Nicolas (2001). "The BAH domain, polybromo and the RSC chromatin remodelling complex." Gene **268**(1-2): 1-7.

Gordon, F., K. Luger and J. C. Hansen (2005). "The core histone N-terminal tail domains function independently and additively during salt-dependent oligomerization of nucleosomal arrays." J Biol Chem **280**(40): 33701-33706.

Gossage, L., M. Murtaza, A. F. Slatter, C. P. Lichtenstein, A. Warren, B. Haynes, F. Marass, I. Roberts, S. J. Shanahan, A. Claas, A. Dunham, A. P. May, N. Rosenfeld, T. Forshew and T. Eisen (2014). "Clinical and pathological impact of VHL, PBRM1, BAP1, SETD2, KDM6A, and JARID1c in clear cell renal cell carcinoma." Genes Chromosomes Cancer **53**(1): 38-51.

Gottlieb, T. M. and S. P. Jackson (1993). "The DNA-dependent protein kinase: requirement for DNA ends and association with Ku antigen." Cell **72**(1): 131-142.

Grawunder, U., M. Wilm, X. Wu, P. Kulesza, T. E. Wilson, M. Mann and M. R. Lieber (1997). "Activity of DNA ligase IV stimulated by complex formation with XRCC4 protein in mammalian cells." Nature **388**(6641): 492-495.

Green, G. R., P. Collas, A. Burrell and D. L. Poccia (1995). "Histone phosphorylation during sea urchin development." Semin Cell Biol **6**(4): 219-227.

Groisman, R., J. Polanowska, I. Kuraoka, J. Sawada, M. Saijo, R. Drapkin, A. F. Kisselev, K. Tanaka and Y. Nakatani (2003). "The ubiquitin ligase activity in the DDB2 and CSA complexes is differentially regulated by the COP9 signalosome in response to DNA damage." Cell **113**(3): 357-367.

Grunstein, M. (1997). "Histone acetylation in chromatin structure and transcription." Nature **389**(6649): 349-352.

Guan, B., T. L. Wang and M. Shih Ie (2011). "ARID1A, a factor that promotes formation of SWI/SNF-mediated chromatin remodeling, is a tumor suppressor in gynecologic cancers." Cancer Res **71**(21): 6718-6727.

Hakimi, A. A., I. Ostrovnaya, B. Reva, N. Schultz, Y. B. Chen, M. Gonen, H. Liu, S. Takeda, M. H. Voss, S. K. Tickoo, V. E. Reuter, P. Russo, E. H. Cheng, C. Sander, R. J. Motzer, J. J. Hsieh and R. C. C. C. G. A. R. N. i. cc (2013). "Adverse outcomes in clear cell renal cell carcinoma with mutations of 3p21 epigenetic regulators BAP1 and SETD2: a report by MSKCC and the KIRC TCGA research network." Clin Cancer Res **19**(12): 3259-3267.

Hakme, A., H. K. Wong, F. Dantzer and V. Schreiber (2008). "The expanding field of poly(ADP-ribosyl)ation reactions. 'Protein Modifications: Beyond the Usual Suspects' Review Series." EMBO Rep **9**(11): 1094-1100.

Hampel, H., W. L. Frankel, E. Martin, M. Arnold, K. Khanduja, P. Kuebler, H. Nakagawa, K. Sotamaa, T. W. Prior, J. Westman, J. Panescu, D. Fix, J. Lockman, I. Comeras and A. de la Chapelle (2005). "Screening for the Lynch syndrome (hereditary nonpolyposis colorectal cancer)." N Engl J Med **352**(18): 1851-1860.

Hanahan, D. and R. A. Weinberg (2000). "The hallmarks of cancer." Cell **100**(1): 57-70.

Hanahan, D. and R. A. Weinberg (2011). "Hallmarks of cancer: the next generation." Cell **144**(5): 646-674.

Hanawalt, P. C. and G. Spivak (2008). "Transcription-coupled DNA repair: two decades of progress and surprises." Nat Rev Mol Cell Biol **9**(12): 958-970.

Happel, N. and D. Doenecke (2009). "Histone H1 and its isoforms: contribution to chromatin structure and function." Gene **431**(1-2): 1-12.

Harbour, J. W., M. D. Onken, E. D. Roberson, S. Duan, L. Cao, L. A. Worley, M. L. Council, K. A. Matatall, C. Helms and A. M. Bowcock (2010). "Frequent mutation of BAP1 in metastasizing uveal melanomas." Science **330**(6009): 1410-1413.

Hartlerode, A. J. and R. Scully (2009). "Mechanisms of double-strand break repair in somatic mammalian cells." Biochem J **423**(2): 157-168.

Hartman, J. L. t., B. Garvik and L. Hartwell (2001). "Principles for the buffering of genetic variation." Science **291**(5506): 1001-1004.

Hartwell, L. H., P. Szankasi, C. J. Roberts, A. W. Murray and S. H. Friend (1997). "Integrating genetic approaches into the discovery of anticancer drugs." Science **278**(5340): 1064-1068.

Hassa, P. O. and M. O. Hottiger (2008). "The diverse biological roles of mammalian PARPS, a small but powerful family of poly-ADP-ribose polymerases." Front Biosci **13**: 3046-3082.

Helleday, T. (2011). "The underlying mechanism for the PARP and BRCA synthetic lethality: clearing up the misunderstandings." Mol Oncol **5**(4): 387-393.

Hillenmeyer, M. E., E. Fung, J. Wildenhain, S. E. Pierce, S. Hoon, W. Lee, M. Proctor, R. P. St Onge, M. Tyers, D. Koller, R. B. Altman, R. W. Davis, C. Nislow and G. Giaever (2008). "The chemical genomic portrait of yeast: uncovering a phenotype for all genes." Science **320**(5874): 362-365.

Ho, L., R. Jothi, J. L. Ronan, K. Cui, K. Zhao and G. R. Crabtree (2009). "An embryonic stem cell chromatin remodeling complex, esBAF, is an essential component of the core pluripotency transcriptional network." Proc Natl Acad Sci U S A **106**(13): 5187-5191.

Holmes, A. M. and J. E. Haber (1999). "Double-strand break repair in yeast requires both leading and lagging strand DNA polymerases." Cell **96**(3): 415-424.

Hsu, J. M., J. Huang, P. B. Meluh and B. C. Laurent (2003). "The yeast RSC chromatin-remodeling complex is required for kinetochore function in chromosome segregation." Mol Cell Biol **23**(9): 3202-3215.

Huang, L., Y. Peng, G. Zhong, W. Xie, W. Dong, B. Wang, X. Chen, P. Gu, W. He, S. Wu, T. Lin and J. Huang (2015). "PBRM1 suppresses bladder cancer by cyclin B1 induced cell cycle arrest." Oncotarget **6**(18): 16366-16378.

Huber, A., P. Bai, J. M. de Murcia and G. de Murcia (2004). "PARP-1, PARP-2 and ATM in the DNA damage response: functional synergy in mouse development." DNA Repair (Amst) **3**(8-9): 1103-1108.

Iizuka, M. and M. M. Smith (2003). "Functional consequences of histone modifications." Curr Opin Genet Dev **13**(2): 154-160.

Isakoff, M. S., C. G. Sansam, P. Tamayo, A. Subramanian, J. A. Evans, C. M. Fillmore, X. Wang, J. A. Biegel, S. L. Pomeroy, J. P. Mesirov and C. W. Roberts (2005). "Inactivation of the Snf5 tumor suppressor stimulates cell cycle progression and cooperates with p53 loss in oncogenic transformation." Proc Natl Acad Sci U S A **102**(49): 17745-17750.

Iyama, T. and D. M. Wilson, 3rd (2013). "DNA repair mechanisms in dividing and non-dividing cells." DNA Repair (Amst) **12**(8): 620-636.

Jackson, J. D. and M. A. Gorovsky (2000). "Histone H2A.Z has a conserved function that is distinct from that of the major H2A sequence variants." Nucleic Acids Res **28**(19): 3811-3816.

Jacquemont, C. and T. Taniguchi (2007). "Proteasome function is required for DNA damage response and fanconi anemia pathway activation." Cancer Res **67**(15): 7395-7405.

Jeggo, P. A. and J. A. Downs (2014). "Roles of chromatin remodellers in DNA double strand break repair." Exp Cell Res **329**(1): 69-77.

Jensen, D. E., M. Proctor, S. T. Marquis, H. P. Gardner, S. I. Ha, L. A. Chodosh, A. M. Ishov, N. Tommerup, H. Vissing, Y. Sekido, J. Minna, A. Borodovsky, D. C. Schultz, K. D. Wilkinson, G. G. Maul, N. Barlev, S. L. Berger, G. C. Prendergast and F. J. Rauscher, 3rd (1998). "BAP1: a novel ubiquitin hydrolase which binds to the BRCA1 RING finger and enhances BRCA1-mediated cell growth suppression." Oncogene **16**(9): 1097-1112.

Jeong, K. W., K. Kim, A. J. Situ, T. S. Ulmer, W. An and M. R. Stallcup (2011). "Recognition of enhancer element-specific histone methylation by TIP60 in transcriptional activation." Nat Struct Mol Biol **18**(12): 1358-1365.

Jiricny, J. (2013). "Postreplicative mismatch repair." Cold Spring Harb Perspect Biol **5**(4): a012633.

Johansson, M. (1999). "A human poly(ADP-ribose) polymerase gene family (ADPRTL): cDNA cloning of two novel poly(ADP-ribose) polymerase homologues." Genomics **57**(3): 442-445.

Jonasch, E., P. A. Futreal, I. J. Davis, S. T. Bailey, W. Y. Kim, J. Brugarolas, A. J. Giaccia, G. Kurban, A. Pause, J. Frydman, A. J. Zurita, B. I. Rini, P. Sharma, M. B. Atkins, C. L. Walker and W. K. Rathmell (2012). "State of the science: an update on renal cell carcinoma." Mol Cancer Res **10**(7): 859-880.

Jones, P. A. and S. B. Baylin (2007). "The epigenomics of cancer." Cell **128**(4): 683-692.

Jones, S., T. L. Wang, M. Shih Ie, T. L. Mao, K. Nakayama, R. Roden, R. Glas, D. Slamon, L. A. Diaz, Jr., B. Vogelstein, K. W. Kinzler, V. E. Velculescu and N. Papadopoulos (2010). "Frequent mutations of chromatin remodeling gene ARID1A in ovarian clear cell carcinoma." Science **330**(6001): 228-231.

Jones, S., X. Zhang, D. W. Parsons, J. C. Lin, R. J. Leary, P. Angenendt, P. Mankoo, H. Carter, H. Kamiyama, A. Jimeno, S. M. Hong, B. Fu, M. T. Lin, E. S. Calhoun, M. Kamiyama, K. Walter, T. Nikolskaya, Y. Nikolsky, J. Hartigan, D. R. Smith, M. Hidalgo, S. D. Leach, A. P. Klein, E. M. Jaffee, M. Goggins, A. Maitra, C. Iacobuzio-

Donahue, J. R. Eshleman, S. E. Kern, R. H. Hruban, R. Karchin, N. Papadopoulos, G. Parmigiani, B. Vogelstein, V. E. Velculescu and K. W. Kinzler (2008). "Core signaling pathways in human pancreatic cancers revealed by global genomic analyses." Science **321**(5897): 1801-1806.

Kadiyala, V. and C. L. Smith (2014). "Minireview: The versatile roles of lysine deacetylases in steroid receptor signaling." Mol Endocrinol **28**(5): 607-621.

Kadoch, C., D. C. Hargreaves, C. Hodges, L. Elias, L. Ho, J. Ranish and G. R. Crabtree (2013). "Proteomic and bioinformatic analysis of mammalian SWI/SNF complexes identifies extensive roles in human malignancy." Nat Genet **45**(6): 592-601.

Kadyrov, F. A., L. Dzantiev, N. Constantin and P. Modrich (2006). "Endonucleolytic function of MutLalpha in human mismatch repair." Cell **126**(2): 297-308.

Kaelin, W. G. (2005). "The von Hippel-Lindau tumor suppressor protein: roles in cancer and oxygen sensing." Cold Spring Harb Symp Quant Biol **70**: 159-166.

Kaelin, W. G., Jr. (2005). "The concept of synthetic lethality in the context of anticancer therapy." Nat Rev Cancer **5**(9): 689-698.

Kaeser, M. D., A. Aslanian, M. Q. Dong, J. R. Yates, 3rd and B. M. Emerson (2008). "BRD7, a novel PBAF-specific SWI/SNF subunit, is required for target gene activation and repression in embryonic stem cells." J Biol Chem **283**(47): 32254-32263.

Kakarougkas, A., A. Ismail, A. L. Chambers, E. Riballo, A. D. Herbert, J. Kunzel, M. Lobrich, P. A. Jeggo and J. A. Downs (2014). "Requirement for PBAF in transcriptional repression and repair at DNA breaks in actively transcribed regions of chromatin." Mol Cell **55**(5): 723-732.

Kamakaka, R. T. and S. Biggins (2005). "Histone variants: deviants?" Genes Dev **19**(3): 295-310.

Kapetanaki, M. G., J. Guerrero-Santoro, D. C. Bisi, C. L. Hsieh, V. Rapic-Otrin and A. S. Levine (2006). "The DDB1-CUL4ADDB2 ubiquitin ligase is deficient in xeroderma pigmentosum group E and targets histone H2A at UV-damaged DNA sites." Proc Natl Acad Sci U S A **103**(8): 2588-2593.

Kapur, P., S. Pena-Llopis, A. Christie, L. Zhrebker, A. Pavia-Jimenez, W. K. Rathmell, X. J. Xie and J. Brugarolas (2013). "Effects on survival of BAP1 and

PBRM1 mutations in sporadic clear-cell renal-cell carcinoma: a retrospective analysis with independent validation." Lancet Oncol **14**(2): 159-167.
Kasten, M. M., C. R. Clapier and B. R. Cairns (2011). "SnapShot: Chromatin remodeling: SWI/SNF." Cell **144**(2): 310 e311.
Kawai, H., H. Li, S. Avraham, S. Jiang and H. K. Avraham (2003). "Overexpression of histone deacetylase HDAC1 modulates breast cancer progression by negative regulation of estrogen receptor alpha." Int J Cancer **107**(3): 353-358.
Kennison, J. A. and J. W. Tamkun (1988). "Dosage-dependent modifiers of polycomb and antennapedia mutations in Drosophila." Proc Natl Acad Sci U S A **85**(21): 8136-8140.
Kia, S. K., M. M. Gorski, S. Giannakopoulos and C. P. Verrijzer (2008). "SWI/SNF mediates polycomb eviction and epigenetic reprogramming of the INK4b-ARF-INK4a locus." Mol Cell Biol **28**(10): 3457-3464.
Kim, Y. J. and D. M. Wilson, 3rd (2012). "Overview of base excision repair biochemistry." Curr Mol Pharmacol **5**(1): 3-13.
Kinzler, K. W. and B. Vogelstein (1997). "Cancer-susceptibility genes. Gatekeepers and caretakers." Nature **386**(6627): 761, 763.
Kleine, H., E. Poreba, K. Lesniewicz, P. O. Hassa, M. O. Hottiger, D. W. Litchfield, B. H. Shilton and B. Luscher (2008). "Substrate-assisted catalysis by PARP10 limits its activity to mono-ADP-ribosylation." Mol Cell **32**(1): 57-69.
Krejci, L., V. Altmannova, M. Spirek and X. Zhao (2012). "Homologous recombination and its regulation." Nucleic Acids Res **40**(13): 5795-5818.
Krishnakumar, R. and W. L. Kraus (2010). "The PARP side of the nucleus: molecular actions, physiological outcomes, and clinical targets." Mol Cell **39**(1): 8-24.
Krokan, H. E. and M. Bjoras (2013). "Base excision repair." Cold Spring Harb Perspect Biol **5**(4): a012583.
Lane, D. P. (1992). "Cancer. p53, guardian of the genome." Nature **358**(6381): 15-16.
Lange, M., B. Kaynak, U. B. Forster, M. Tonjes, J. J. Fischer, C. Grimm, J. Schlesinger, S. Just, I. Dunkel, T. Krueger, S. Mebus, H. Lehrach, R. Lurz, J. Gobom, W. Rottbauer, S. Abdelilah-Seyfried and S. Sperling (2008). "Regulation of muscle development by DPF3, a novel histone acetylation and methylation

reader of the BAF chromatin remodeling complex." Genes Dev **22**(17): 2370-2384.

Langelier, M. F., J. L. Planck, S. Roy and J. M. Pascal (2012). "Structural basis for DNA damage-dependent poly(ADP-ribosyl)ation by human PARP-1." Science **336**(6082): 728-732.

Langelier, M. F., A. A. Riccio and J. M. Pascal (2014). "PARP-2 and PARP-3 are selectively activated by 5' phosphorylated DNA breaks through an allosteric regulatory mechanism shared with PARP-1." Nucleic Acids Res **42**(12): 7762-7775.

Latif, F., K. Tory, J. Gnarra, M. Yao, F. M. Duh, M. L. Orcutt, T. Stackhouse, I. Kuzmin, W. Modi, L. Geil and et al. (1993). "Identification of the von Hippel-Lindau disease tumor suppressor gene." Science **260**(5112): 1317-1320.

Lee, H. S., J. H. Park, S. J. Kim, S. J. Kwon and J. Kwon (2010). "A cooperative activation loop among SWI/SNF, gamma-H2AX and H3 acetylation for DNA double-strand break repair." EMBO J **29**(8): 1434-1445.

Lee, J. H. and T. T. Paull (2004). "Direct activation of the ATM protein kinase by the Mre11/Rad50/Nbs1 complex." Science **304**(5667): 93-96.

Lee, J. H. and T. T. Paull (2005). "ATM activation by DNA double-strand breaks through the Mre11-Rad50-Nbs1 complex." Science **308**(5721): 551-554.

Leger, K., D. Bar, N. Savic, R. Santoro and M. O. Hottiger (2014). "ARTD2 activity is stimulated by RNA." Nucleic Acids Res **42**(8): 5072-5082.

Lehar, J., B. R. Stockwell, G. Giaever and C. Nislow (2008). "Combination chemical genetics." Nat Chem Biol **4**(11): 674-681.

Lehmann, A. R., A. Niimi, T. Ogi, S. Brown, S. Sabbioneda, J. F. Wing, P. L. Kannouche and C. M. Green (2007). "Translesion synthesis: Y-family polymerases and the polymerase switch." DNA Repair (Amst) **6**(7): 891-899.

Lehtio, L., A. S. Jemth, R. Collins, O. Loseva, A. Johansson, N. Markova, M. Hammarstrom, A. Flores, L. Holmberg-Schiavone, J. Weigelt, T. Helleday, H. Schuler and T. Karlberg (2009). "Structural basis for inhibitor specificity in human poly(ADP-ribose) polymerase-3." J Med Chem **52**(9): 3108-3111.

Leschziner, A. E., A. Saha, J. Wittmeyer, Y. Zhang, C. Bustamante, B. R. Cairns and E. Nogales (2007). "Conformational flexibility in the chromatin remodeler RSC

observed by electron microscopy and the orthogonal tilt reconstruction method." Proc Natl Acad Sci U S A **104**(12): 4913-4918.
Li, M. and X. Yu (2013). "Function of BRCA1 in the DNA damage response is mediated by ADP-ribosylation." Cancer Cell **23**(5): 693-704.
Li, M. and X. Yu (2015). "The role of poly(ADP-ribosyl)ation in DNA damage response and cancer chemotherapy." Oncogene **34**(26): 3349-3356.
Li, M., H. Zhao, X. Zhang, L. D. Wood, R. A. Anders, M. A. Choti, T. M. Pawlik, H. D. Daniel, R. Kannangai, G. J. Offerhaus, V. E. Velculescu, L. Wang, S. Zhou, B. Vogelstein, R. H. Hruban, N. Papadopoulos, J. Cai, M. S. Torbenson and K. W. Kinzler (2011). "Inactivating mutations of the chromatin remodeling gene ARID2 in hepatocellular carcinoma." Nat Genet **43**(9): 828-829.
Lia, G., E. Praly, H. Ferreira, C. Stockdale, Y. C. Tse-Dinh, D. Dunlap, V. Croquette, D. Bensimon and T. Owen-Hughes (2006). "Direct observation of DNA distortion by the RSC complex." Mol Cell **21**(3): 417-425.
Liao, L., J. R. Testa and H. Yang (2015). "The roles of chromatin-remodelers and epigenetic modifiers in kidney cancer." Cancer Genet **208**(5): 206-214.
Lin, Y. Y., Y. Qi, J. Y. Lu, X. Pan, D. S. Yuan, Y. Zhao, J. S. Bader and J. D. Boeke (2008). "A comprehensive synthetic genetic interaction network governing yeast histone acetylation and deacetylation." Genes Dev **22**(15): 2062-2074.
Lindahl, T., M. S. Satoh, G. G. Poirier and A. Klungland (1995). "Post-translational modification of poly(ADP-ribose) polymerase induced by DNA strand breaks." Trends Biochem Sci **20**(10): 405-411.
Liu, T. and J. Huang (2016). "DNA End Resection: Facts and Mechanisms." Genomics Proteomics Bioinformatics **14**(3): 126-130.
Lohr, J. G., P. Stojanov, M. S. Lawrence, D. Auclair, B. Chapuy, C. Sougnez, P. Cruz-Gordillo, B. Knoechel, Y. W. Asmann, S. L. Slager, A. J. Novak, A. Dogan, S. M. Ansell, B. K. Link, L. Zou, J. Gould, G. Saksena, N. Stransky, C. Rangel-Escareno, J. C. Fernandez-Lopez, A. Hidalgo-Miranda, J. Melendez-Zajgla, E. Hernandez-Lemus, A. Schwarz-Cruz y Celis, I. Imaz-Rosshandler, A. I. Ojesina, J. Jung, C. S. Pedamallu, E. S. Lander, T. M. Habermann, J. R. Cerhan, M. A. Shipp, G. Getz and T. R. Golub (2012). "Discovery and prioritization of somatic mutations in diffuse large B-cell lymphoma (DLBCL) by whole-exome sequencing." Proc Natl Acad Sci U S A **109**(10): 3879-3884.

Lorch, Y., B. R. Cairns, M. Zhang and R. D. Kornberg (1998). "Activated RSC-nucleosome complex and persistently altered form of the nucleosome." Cell **94**(1): 29-34.

Lorch, Y., B. Maier-Davis and R. D. Kornberg (2010). "Mechanism of chromatin remodeling." Proc Natl Acad Sci U S A **107**(8): 3458-3462.

Lord, C. J. and A. Ashworth (2012). "The DNA damage response and cancer therapy." Nature **481**(7381): 287-294.

Lu, C., H. D. Han, L. S. Mangala, R. Ali-Fehmi, C. S. Newton, L. Ozbun, G. N. Armaiz-Pena, W. Hu, R. L. Stone, A. Munkarah, M. K. Ravoori, M. M. Shahzad, J. W. Lee, E. Mora, R. R. Langley, A. R. Carroll, K. Matsuo, W. A. Spannuth, R. Schmandt, N. B. Jennings, B. W. Goodman, R. B. Jaffe, A. M. Nick, H. S. Kim, E. O. Guven, Y. H. Chen, L. Y. Li, M. C. Hsu, R. L. Coleman, G. A. Calin, E. B. Denkbas, J. Y. Lim, J. S. Lee, V. Kundra, M. J. Birrer, M. C. Hung, G. Lopez-Berestein and A. K. Sood (2010). "Regulation of tumor angiogenesis by EZH2." Cancer Cell **18**(2): 185-197.

Lucchesi, J. C. (1968). "Synthetic Lethality and Semi-Lethality among Functionally Related Mutants of Drosophila Melanogaster." Genetics **59**(1): 37-&.

Luger, K., A. W. Mader, R. K. Richmond, D. F. Sargent and T. J. Richmond (1997). "Crystal structure of the nucleosome core particle at 2.8 A resolution." Nature **389**(6648): 251-260.

Lynch, H. T., P. M. Lynch, S. J. Lanspa, C. L. Snyder, J. F. Lynch and C. R. Boland (2009). "Review of the Lynch syndrome: history, molecular genetics, screening, differential diagnosis, and medicolegal ramifications." Clin Genet **76**(1): 1-18.

Ma, Y., U. Pannicke, K. Schwarz and M. R. Lieber (2002). "Hairpin opening and overhang processing by an Artemis/DNA-dependent protein kinase complex in nonhomologous end joining and V(D)J recombination." Cell **108**(6): 781-794.

Macher-Goeppinger, S., M. Keith, K. E. Tagscherer, S. Singer, J. Winkler, T. G. Hofmann, S. Pahernik, S. Duensing, M. Hohenfellner, J. Kopitz, P. Schirmacher and W. Roth (2015). "PBRM1 (BAF180) protein is functionally regulated by p53-induced protein degradation in renal cell carcinomas." J Pathol **237**(4): 460-471.

Mahaney, B. L., M. Hammel, K. Meek, J. A. Tainer and S. P. Lees-Miller (2013). "XRCC4 and XLF form long helical protein filaments suitable for DNA end

protection and alignment to facilitate DNA double strand break repair." Biochem Cell Biol **91**(1): 31-41.

Malik, H. S. and S. Henikoff (2003). "Phylogenomics of the nucleosome." Nat Struct Biol **10**(11): 882-891.

Malu, S., V. Malshetty, D. Francis and P. Cortes (2012). "Role of non-homologous end joining in V(D)J recombination." Immunol Res **54**(1-3): 233-246.

Mandriota, S. J., K. J. Turner, D. R. Davies, P. G. Murray, N. V. Morgan, H. M. Sowter, C. C. Wykoff, E. R. Maher, A. L. Harris, P. J. Ratcliffe and P. H. Maxwell (2002). "HIF activation identifies early lesions in VHL kidneys: evidence for site-specific tumor suppressor function in the nephron." Cancer Cell **1**(5): 459-468.

Masliah-Planchon, J., I. Bieche, J. M. Guinebretiere, F. Bourdeaut and O. Delattre (2015). "SWI/SNF chromatin remodeling and human malignancies." Annu Rev Pathol **10**: 145-171.

Matsuoka, S., B. A. Ballif, A. Smogorzewska, E. R. McDonald, 3rd, K. E. Hurov, J. Luo, C. E. Bakalarski, Z. Zhao, N. Solimini, Y. Lerenthal, Y. Shiloh, S. P. Gygi and S. J. Elledge (2007). "ATM and ATR substrate analysis reveals extensive protein networks responsive to DNA damage." Science **316**(5828): 1160-1166.

McKenna, E. S. and C. W. Roberts (2009). "Epigenetics and cancer without genomic instability." Cell Cycle **8**(1): 23-26.

McLellan, J., N. O'Neil, S. Tarailo, J. Stoepel, J. Bryan, A. Rose and P. Hieter (2009). "Synthetic lethal genetic interactions that decrease somatic cell proliferation in Caenorhabditis elegans identify the alternative RFC CTF18 as a candidate cancer drug target." Mol Biol Cell **20**(24): 5306-5313.

McManus, K. J., I. J. Barrett, Y. Nouhi and P. Hieter (2009). "Specific synthetic lethal killing of RAD54B-deficient human colorectal cancer cells by FEN1 silencing." Proc Natl Acad Sci U S A **106**(9): 3276-3281.

Measday, V., K. Baetz, J. Guzzo, K. Yuen, T. Kwok, B. Sheikh, H. Ding, R. Ueta, T. Hoac, B. Cheng, I. Pot, A. Tong, Y. Yamaguchi-Iwai, C. Boone, P. Hieter and B. Andrews (2005). "Systematic yeast synthetic lethal and synthetic dosage lethal screens identify genes required for chromosome segregation." Proc Natl Acad Sci U S A **102**(39): 13956-13961.

Medina, P. P., J. Carretero, M. F. Fraga, M. Esteller, D. Sidransky and M. Sanchez-Cespedes (2004). "Genetic and epigenetic screening for gene alterations of the

chromatin-remodeling factor, SMARCA4/BRG1, in lung tumors." Genes Chromosomes Cancer **41**(2): 170-177.

Medina, P. P., O. A. Romero, T. Kohno, L. M. Montuenga, R. Pio, J. Yokota and M. Sanchez-Cespedes (2008). "Frequent BRG1/SMARCA4-inactivating mutations in human lung cancer cell lines." Hum Mutat **29**(5): 617-622.

Menissier de Murcia, J., M. Ricoul, L. Tartier, C. Niedergang, A. Huber, F. Dantzer, V. Schreiber, J. C. Ame, A. Dierich, M. LeMeur, L. Sabatier, P. Chambon and G. de Murcia (2003). "Functional interaction between PARP-1 and PARP-2 in chromosome stability and embryonic development in mouse." EMBO J **22**(9): 2255-2263.

Menoni, H., D. Gasparutto, A. Hamiche, J. Cadet, S. Dimitrov, P. Bouvet and D. Angelov (2007). "ATP-dependent chromatin remodeling is required for base excision repair in conventional but not in variant H2A.Bbd nucleosomes." Mol Cell Biol **27**(17): 5949-5956.

Meyer, R., M. Muller, S. Beneke, J. H. Kupper and A. Burkle (2000). "Negative regulation of alkylation-induced sister-chromatid exchange by poly(ADP-ribose) polymerase-1 activity." Int J Cancer **88**(3): 351-355.

Millan-Arino, L., A. B. Islam, A. Izquierdo-Bouldstridge, R. Mayor, J. M. Terme, N. Luque, M. Sancho, N. Lopez-Bigas and A. Jordan (2014). "Mapping of six somatic linker histone H1 variants in human breast cancer cells uncovers specific features of H1.2." Nucleic Acids Res **42**(7): 4474-4493.

Mo, D., C. Li, J. Liang, Q. Shi, N. Su, S. Luo, T. Zeng and X. Li (2015). "Low PBRM1 identifies tumor progression and poor prognosis in breast cancer." Int J Clin Exp Pathol **8**(8): 9307-9313.

Mohrmann, L. and C. P. Verrijzer (2005). "Composition and functional specificity of SWI2/SNF2 class chromatin remodeling complexes." Biochim Biophys Acta **1681**(2-3): 59-73.

Morin, R. D., M. Mendez-Lago, A. J. Mungall, R. Goya, K. L. Mungall, R. D. Corbett, N. A. Johnson, T. M. Severson, R. Chiu, M. Field, S. Jackman, M. Krzywinski, D. W. Scott, D. L. Trinh, J. Tamura-Wells, S. Li, M. R. Firme, S. Rogic, M. Griffith, S. Chan, O. Yakovenko, I. M. Meyer, E. Y. Zhao, D. Smailus, M. Moksa, S. Chittaranjan, L. Rimsza, A. Brooks-Wilson, J. J. Spinelli, S. Ben-Neriah, B. Meissner, B. Woolcock, M. Boyle, H. McDonald, A. Tam, Y. Zhao, A. Delaney, T. Zeng, K. Tse, Y. Butterfield,

I. Birol, R. Holt, J. Schein, D. E. Horsman, R. Moore, S. J. Jones, J. M. Connors, M. Hirst, R. D. Gascoyne and M. A. Marra (2011). "Frequent mutation of histone-modifying genes in non-Hodgkin lymphoma." Nature **476**(7360): 298-303.

Muller, P., S. Park, E. Shor, D. J. Huebert, C. L. Warren, A. Z. Ansari, M. Weinreich, M. L. Eaton, D. M. MacAlpine and C. A. Fox (2010). "The conserved bromo-adjacent homology domain of yeast Orc1 functions in the selection of DNA replication origins within chromatin." Genes Dev **24**(13): 1418-1433.

Mullins, D. W., Jr., C. P. Giri and M. Smulson (1977). "Poly(adenosine diphosphate-ribose) polymerase: the distribution of a chromosome-associated enzyme within the chromatin substructure." Biochemistry **16**(3): 506-513.

Musselman, C. A., M. E. Lalonde, J. Cote and T. G. Kutateladze (2012). "Perceiving the epigenetic landscape through histone readers." Nat Struct Mol Biol **19**(12): 1218-1227.

Natsume, T., C. A. Muller, Y. Katou, R. Retkute, M. Gierlinski, H. Araki, J. J. Blow, K. Shirahige, C. A. Nieduszynski and T. U. Tanaka (2013). "Kinetochores coordinate pericentromeric cohesion and early DNA replication by Cdc7-Dbf4 kinase recruitment." Mol Cell **50**(5): 661-674.

Neigeborn, L. and M. Carlson (1984). "Genes affecting the regulation of SUC2 gene expression by glucose repression in Saccharomyces cerevisiae." Genetics **108**(4): 845-858.

Ng, H. H., F. Robert, R. A. Young and K. Struhl (2002). "Genome-wide location and regulated recruitment of the RSC nucleosome-remodeling complex." Genes Dev **16**(7): 806-819.

Nickerson, M. L., M. B. Warren, J. R. Toro, V. Matrosova, G. Glenn, M. L. Turner, P. Duray, M. Merino, P. Choyke, C. P. Pavlovich, N. Sharma, M. Walther, D. Munroe, R. Hill, E. Maher, C. Greenberg, M. I. Lerman, W. M. Linehan, B. Zbar and L. S. Schmidt (2002). "Mutations in a novel gene lead to kidney tumors, lung wall defects, and benign tumors of the hair follicle in patients with the Birt-Hogg-Dube syndrome." Cancer Cell **2**(2): 157-164.

Nicolas, R. H. and G. H. Goodwin (1996). "Molecular cloning of polybromo, a nuclear protein containing multiple domains including five bromodomains, a truncated HMG-box, and two repeats of a novel domain." Gene **175**(1-2): 233-240.

Niimi, A., A. L. Chambers, J. A. Downs and A. R. Lehmann (2012). "A role for chromatin remodellers in replication of damaged DNA." Nucleic Acids Res **40**(15): 7393-7403.

Niimi, A., S. R. Hopkins, J. A. Downs and C. Masutani (2015). "The BAH domain of BAF180 is required for PCNA ubiquitination." Mutat Res **779**: 16-23.

Nijman, S. M. (2011). "Synthetic lethality: general principles, utility and detection using genetic screens in human cells." FEBS Lett **585**(1): 1-6.

Nijman, S. M. and S. H. Friend (2013). "Cancer. Potential of the synthetic lethality principle." Science **342**(6160): 809-811.

Nishi, R., S. Alekseev, C. Dinant, D. Hoogstraten, A. B. Houtsmuller, J. H. Hoeijmakers, W. Vermeulen, F. Hanaoka and K. Sugasawa (2009). "UV-DDB-dependent regulation of nucleotide excision repair kinetics in living cells." DNA Repair (Amst) **8**(6): 767-776.

Niu, X., T. Zhang, L. Liao, L. Zhou, D. J. Lindner, M. Zhou, B. Rini, Q. Yan and H. Yang (2012). "The von Hippel-Lindau tumor suppressor protein regulates gene expression and tumor growth through histone demethylase JARID1C." Oncogene **31**(6): 776-786.

Noguchi, K., A. Vassilev, S. Ghosh, J. L. Yates and M. L. DePamphilis (2006). "The BAH domain facilitates the ability of human Orc1 protein to activate replication origins in vivo." EMBO J **25**(22): 5372-5382.

Norris, A., M. A. Bianchet and J. D. Boeke (2008). "Compensatory interactions between Sir3p and the nucleosomal LRS surface imply their direct interaction." PLoS Genet **4**(12): e1000301.

Norris, A. and J. D. Boeke (2010). "Silent information regulator 3: the Goldilocks of the silencing complex." Genes Dev **24**(2): 115-122.

Ogiwara, H., A. Ui, A. Otsuka, H. Satoh, I. Yokomi, S. Nakajima, A. Yasui, J. Yokota and T. Kohno (2011). "Histone acetylation by CBP and p300 at double-strand break sites facilitates SWI/SNF chromatin remodeling and the recruitment of non-homologous end joining factors." Oncogene **30**(18): 2135-2146.

Old, R. W. and H. R. Woodland (1984). "Histone genes: not so simple after all." Cell **38**(3): 624-626.

Oliver, A. W., J. C. Ame, S. M. Roe, V. Good, G. de Murcia and L. H. Pearl (2004). "Crystal structure of the catalytic fragment of murine poly(ADP-ribose) polymerase-2." Nucleic Acids Res **32**(2): 456-464.

Oliver, A. W., S. A. Jones, S. M. Roe, S. Matthews, G. H. Goodwin and L. H. Pearl (2005). "Crystal structure of the proximal BAH domain of the polybromo protein." Biochem J **389**(Pt 3): 657-664.

Onishi, M., G. G. Liou, J. R. Buchberger, T. Walz and D. Moazed (2007). "Role of the conserved Sir3-BAH domain in nucleosome binding and silent chromatin assembly." Mol Cell **28**(6): 1015-1028.

Ornaghi, P., P. Ballario, A. M. Lena, A. Gonzalez and P. Filetici (1999). "The bromodomain of Gcn5p interacts in vitro with specific residues in the N terminus of histone H4." J Mol Biol **287**(1): 1-7.

Oum, J. H., C. Seong, Y. Kwon, J. H. Ji, A. Sid, S. Ramakrishnan, G. Ira, A. Malkova, P. Sung, S. E. Lee and E. Y. Shim (2011). "RSC facilitates Rad59-dependent homologous recombination between sister chromatids by promoting cohesin loading at DNA double-strand breaks." Mol Cell Biol **31**(19): 3924-3937.

Pan, H., R. Jia, L. Zhang, S. Xu, Q. Wu, X. Song, H. Zhang, S. Ge, X. L. Xu and X. Fan (2015). "BAP1 regulates cell cycle progression through E2F1 target genes and mediates transcriptional silencing via H2A monoubiquitination in uveal melanoma cells." Int J Biochem Cell Biol **60**: 176-184.

Pan, X., P. Ye, D. S. Yuan, X. Wang, J. S. Bader and J. D. Boeke (2006). "A DNA integrity network in the yeast Saccharomyces cerevisiae." Cell **124**(5): 1069-1081.

Papeo, G., E. Casale, A. Montagnoli and A. Cirla (2013). "PARP inhibitors in cancer therapy: an update." Expert Opin Ther Pat **23**(4): 503-514.

Park, J. H., E. J. Park, H. S. Lee, S. J. Kim, S. K. Hur, A. N. Imbalzano and J. Kwon (2006). "Mammalian SWI/SNF complexes facilitate DNA double-strand break repair by promoting gamma-H2AX induction." EMBO J **25**(17): 3986-3997.

Parsons, D. W., S. Jones, X. Zhang, J. C. Lin, R. J. Leary, P. Angenendt, P. Mankoo, H. Carter, I. M. Siu, G. L. Gallia, A. Olivi, R. McLendon, B. A. Rasheed, S. Keir, T. Nikolskaya, Y. Nikolsky, D. A. Busam, H. Tekleab, L. A. Diaz, Jr., J. Hartigan, D. R. Smith, R. L. Strausberg, S. K. Marie, S. M. Shinjo, H. Yan, G. J. Riggins, D. D. Bigner, R. Karchin, N. Papadopoulos, G. Parmigiani, B. Vogelstein, V. E. Velculescu and K.

W. Kinzler (2008). "An integrated genomic analysis of human glioblastoma multiforme." Science **321**(5897): 1807-1812.

Pasqualucci, L., V. Trifonov, G. Fabbri, J. Ma, D. Rossi, A. Chiarenza, V. A. Wells, A. Grunn, M. Messina, O. Elliot, J. Chan, G. Bhagat, A. Chadburn, G. Gaidano, C. G. Mullighan, R. Rabadan and R. Dalla-Favera (2011). "Analysis of the coding genome of diffuse large B-cell lymphoma." Nat Genet **43**(9): 830-837.

Pavlovich, C. P. and L. S. Schmidt (2004). "Searching for the hereditary causes of renal-cell carcinoma." Nat Rev Cancer **4**(5): 381-393.

Pena-Llopis, S., A. Christie, X. J. Xie and J. Brugarolas (2013). "Cooperation and antagonism among cancer genes: the renal cancer paradigm." Cancer Res **73**(14): 4173-4179.

Pena-Llopis, S., S. Vega-Rubin-de-Celis, A. Liao, N. Leng, A. Pavia-Jimenez, S. Wang, T. Yamasaki, L. Zhrebker, S. Sivanand, P. Spence, L. Kinch, T. Hambuch, S. Jain, Y. Lotan, V. Margulis, A. I. Sagalowsky, P. B. Summerour, W. Kabbani, S. W. Wong, N. Grishin, M. Laurent, X. J. Xie, C. D. Haudenschild, M. T. Ross, D. R. Bentley, P. Kapur and J. Brugarolas (2012). "BAP1 loss defines a new class of renal cell carcinoma." Nat Genet **44**(7): 751-759.

Peng, G., E. K. Yim, H. Dai, A. P. Jackson, I. Burgt, M. R. Pan, R. Hu, K. Li and S. Y. Lin (2009). "BRIT1/MCPH1 links chromatin remodelling to DNA damage response." Nat Cell Biol **11**(7): 865-872.

Peters, A. H., S. Kubicek, K. Mechtler, R. J. O'Sullivan, A. A. Derijck, L. Perez-Burgos, A. Kohlmaier, S. Opravil, M. Tachibana, Y. Shinkai, J. H. Martens and T. Jenuwein (2003). "Partitioning and plasticity of repressive histone methylation states in mammalian chromatin." Mol Cell **12**(6): 1577-1589.

Peterson, C. L. and G. Almouzni (2013). "Nucleosome dynamics as modular systems that integrate DNA damage and repair." Cold Spring Harb Perspect Biol **5**(9).

Pfister, S. X., S. Ahrabi, L. P. Zalmas, S. Sarkar, F. Aymard, C. Z. Bachrati, T. Helleday, G. Legube, N. B. La Thangue, A. C. Porter and T. C. Humphrey (2014). "SETD2-dependent histone H3K36 trimethylation is required for homologous recombination repair and genome stability." Cell Rep **7**(6): 2006-2018.

Phelan, M. L., S. Sif, G. J. Narlikar and R. E. Kingston (1999). "Reconstitution of a core chromatin remodeling complex from SWI/SNF subunits." Mol Cell **3**(2): 247-253.

Pines, A., M. G. Vrouwe, J. A. Marteijn, D. Typas, M. S. Luijsterburg, M. Cansoy, P. Hensbergen, A. Deelder, A. de Groot, S. Matsumoto, K. Sugasawa, N. Thoma, W. Vermeulen, H. Vrieling and L. Mullenders (2012). "PARP1 promotes nucleotide excision repair through DDB2 stabilization and recruitment of ALC1." J Cell Biol **199**(2): 235-249.

Piva, F., M. Santoni, M. R. Matrana, S. Satti, M. Giulietti, G. Occhipinti, F. Massari, L. Cheng, A. Lopez-Beltran, M. Scarpelli, G. Principato, S. Cascinu and R. Montironi (2015). "BAP1, PBRM1 and SETD2 in clear-cell renal cell carcinoma: molecular diagnostics and possible targets for personalized therapies." Expert Rev Mol Diagn **15**(9): 1201-1210.

Poccia, D. L. and G. R. Green (1992). "Packaging and unpackaging the sea urchin sperm genome." Trends Biochem Sci **17**(6): 223-227.

Pon, J. R. and M. A. Marra (2015). "Driver and passenger mutations in cancer." Annu Rev Pathol **10**: 25-50.

Pourdehnad, M., M. L. Truitt, I. N. Siddiqi, G. S. Ducker, K. M. Shokat and D. Ruggero (2013). "Myc and mTOR converge on a common node in protein synthesis control that confers synthetic lethality in Myc-driven cancers." Proc Natl Acad Sci U S A **110**(29): 11988-11993.

Prahallad, A., C. Sun, S. Huang, F. Di Nicolantonio, R. Salazar, D. Zecchin, R. L. Beijersbergen, A. Bardelli and R. Bernards (2012). "Unresponsiveness of colon cancer to BRAF(V600E) inhibition through feedback activation of EGFR." Nature **483**(7387): 100-103.

Rankin, E. B., J. E. Tomaszewski and V. H. Haase (2006). "Renal cyst development in mice with conditional inactivation of the von Hippel-Lindau tumor suppressor." Cancer Res **66**(5): 2576-2583.

Ray, A., S. N. Mir, G. Wani, Q. Zhao, A. Battu, Q. Zhu, Q. E. Wang and A. A. Wani (2009). "Human SNF5/INI1, a component of the human SWI/SNF chromatin remodeling complex, promotes nucleotide excision repair by influencing ATM recruitment and downstream H2AX phosphorylation." Mol Cell Biol **29**(23): 6206-6219.

Redon, C., D. Pilch, E. Rogakou, O. Sedelnikova, K. Newrock and W. Bonner (2002). "Histone H2A variants H2AX and H2AZ." Curr Opin Genet Dev **12**(2): 162-169.

Reeves, R. and M. S. Nissen (1990). "The A.T-DNA-binding domain of mammalian high mobility group I chromosomal proteins. A novel peptide motif for recognizing DNA structure." J Biol Chem **265**(15): 8573-8582.

Reisman, D., S. Glaros and E. A. Thompson (2009). "The SWI/SNF complex and cancer." Oncogene **28**(14): 1653-1668.

Rice, J. C., S. D. Briggs, B. Ueberheide, C. M. Barber, J. Shabanowitz, D. F. Hunt, Y. Shinkai and C. D. Allis (2003). "Histone methyltransferases direct different degrees of methylation to define distinct chromatin domains." Mol Cell **12**(6): 1591-1598.

Richmond, T. J. and C. A. Davey (2003). "The structure of DNA in the nucleosome core." Nature **423**(6936): 145-150.

Robert, I., F. Dantzer and B. Reina-San-Martin (2009). "Parp1 facilitates alternative NHEJ, whereas Parp2 suppresses IgH/c-myc translocations during immunoglobulin class switch recombination." J Exp Med **206**(5): 1047-1056.

Roberts, C. W., S. A. Galusha, M. E. McMenamin, C. D. Fletcher and S. H. Orkin (2000). "Haploinsufficiency of Snf5 (integrase interactor 1) predisposes to malignant rhabdoid tumors in mice." Proc Natl Acad Sci U S A **97**(25): 13796-13800.

Robertson, K. D., S. Ait-Si-Ali, T. Yokochi, P. A. Wade, P. L. Jones and A. P. Wolffe (2000). "DNMT1 forms a complex with Rb, E2F1 and HDAC1 and represses transcription from E2F-responsive promoters." Nat Genet **25**(3): 338-342.

Rogakou, E. P., C. Boon, C. Redon and W. M. Bonner (1999). "Megabase chromatin domains involved in DNA double-strand breaks in vivo." J Cell Biol **146**(5): 905-916.

Romero, O. A. and M. Sanchez-Cespedes (2014). "The SWI/SNF genetic blockade: effects in cell differentiation, cancer and developmental diseases." Oncogene **33**(21): 2681-2689.

Ropars, V., P. Drevet, P. Legrand, S. Baconnais, J. Amram, G. Faure, J. A. Marquez, O. Pietrement, R. Guerois, I. Callebaut, E. Le Cam, P. Revy, J. P. de Villartay and J. B. Charbonnier (2011). "Structural characterization of filaments formed by

human Xrcc4-Cernunnos/XLF complex involved in nonhomologous DNA end-joining." Proc Natl Acad Sci U S A **108**(31): 12663-12668.

Ropero, S. and M. Esteller (2007). "The role of histone deacetylases (HDACs) in human cancer." Mol Oncol **1**(1): 19-25.

Rossio, V., E. Galati, M. Ferrari, A. Pellicioli, T. Sutani, K. Shirahige, G. Lucchini and S. Piatti (2010). "The RSC chromatin-remodeling complex influences mitotic exit and adaptation to the spindle assembly checkpoint by controlling the Cdc14 phosphatase." J Cell Biol **191**(5): 981-997.

Rouleau, M., D. McDonald, P. Gagne, M. E. Ouellet, A. Droit, J. M. Hunter, S. Dutertre, C. Prigent, M. J. Hendzel and G. G. Poirier (2007). "PARP-3 associates with polycomb group bodies and with components of the DNA damage repair machinery." J Cell Biochem **100**(2): 385-401.

Ruf, A., J. Mennissier de Murcia, G. de Murcia and G. E. Schulz (1996). "Structure of the catalytic fragment of poly(AD-ribose) polymerase from chicken." Proc Natl Acad Sci U S A **93**(15): 7481-7485.

Rulten, S. L., A. E. Fisher, I. Robert, M. C. Zuma, M. Rouleau, L. Ju, G. Poirier, B. Reina-San-Martin and K. W. Caldecott (2011). "PARP-3 and APLF function together to accelerate nonhomologous end-joining." Mol Cell **41**(1): 33-45.

Saha, A., J. Wittmeyer and B. R. Cairns (2002). "Chromatin remodeling by RSC involves ATP-dependent DNA translocation." Genes Dev **16**(16): 2120-2134.

Saha, A., J. Wittmeyer and B. R. Cairns (2006). "Chromatin remodelling: the industrial revolution of DNA around histones." Nat Rev Mol Cell Biol **7**(6): 437-447.

Sanchez, R. and M. M. Zhou (2009). "The role of human bromodomains in chromatin biology and gene transcription." Curr Opin Drug Discov Devel **12**(5): 659-665.

Sanderson, R. J. and T. Lindahl (2002). "Down-regulation of DNA repair synthesis at DNA single-strand interruptions in poly(ADP-ribose) polymerase-1 deficient murine cell extracts." DNA Repair (Amst) **1**(7): 547-558.

Sankin, A., A. A. Hakimi, N. Mikkilineni, I. Ostrovnaya, M. T. Silk, Y. Liang, R. Mano, M. Chevinsky, R. J. Motzer, S. B. Solomon, E. H. Cheng, J. C. Durack, J. A. Coleman, P. Russo and J. J. Hsieh (2014). "The impact of genetic heterogeneity

on biomarker development in kidney cancer assessed by multiregional sampling." Cancer Med **3**(6): 1485-1492.

Sartori, A. A., C. Lukas, J. Coates, M. Mistrik, S. Fu, J. Bartek, R. Baer, J. Lukas and S. P. Jackson (2007). "Human CtIP promotes DNA end resection." Nature **450**(7169): 509-514.

Sato, Y., T. Yoshizato, Y. Shiraishi, S. Maekawa, Y. Okuno, T. Kamura, T. Shimamura, A. Sato-Otsubo, G. Nagae, H. Suzuki, Y. Nagata, K. Yoshida, A. Kon, Y. Suzuki, K. Chiba, H. Tanaka, A. Niida, A. Fujimoto, T. Tsunoda, T. Morikawa, D. Maeda, H. Kume, S. Sugano, M. Fukayama, H. Aburatani, M. Sanada, S. Miyano, Y. Homma and S. Ogawa (2013). "Integrated molecular analysis of clear-cell renal cell carcinoma." Nat Genet **45**(8): 860-867.

Savic, V., B. Yin, N. L. Maas, A. L. Bredemeyer, A. C. Carpenter, B. A. Helmink, K. S. Yang-Iott, B. P. Sleckman and C. H. Bassing (2009). "Formation of dynamic gamma-H2AX domains along broken DNA strands is distinctly regulated by ATM and MDC1 and dependent upon H2AX densities in chromatin." Mol Cell **34**(3): 298-310.

Scharer, O. D. (2013). "Nucleotide excision repair in eukaryotes." Cold Spring Harb Perspect Biol **5**(10): a012609.

Schmidt, L., F. M. Duh, F. Chen, T. Kishida, G. Glenn, P. Choyke, S. W. Scherer, Z. Zhuang, I. Lubensky, M. Dean, R. Allikmets, A. Chidambaram, U. R. Bergerheim, J. T. Feltis, C. Casadevall, A. Zamarron, M. Bernues, S. Richard, C. J. Lips, M. M. Walther, L. C. Tsui, L. Geil, M. L. Orcutt, T. Stackhouse, J. Lipan, L. Slife, H. Brauch, J. Decker, G. Niehans, M. D. Hughson, H. Moch, S. Storkel, M. I. Lerman, W. M. Linehan and B. Zbar (1997). "Germline and somatic mutations in the tyrosine kinase domain of the MET proto-oncogene in papillary renal carcinomas." Nat Genet **16**(1): 68-73.

Schneider, R., A. J. Bannister, F. A. Myers, A. W. Thorne, C. Crane-Robinson and T. Kouzarides (2004). "Histone H3 lysine 4 methylation patterns in higher eukaryotic genes." Nat Cell Biol **6**(1): 73-77.

Schreiber, V., J. C. Ame, P. Dolle, I. Schultz, B. Rinaldi, V. Fraulob, J. Menissier-de Murcia and G. de Murcia (2002). "Poly(ADP-ribose) polymerase-2 (PARP-2) is required for efficient base excision DNA repair in association with PARP-1 and XRCC1." J Biol Chem **277**(25): 23028-23036.

Schreiber, V., F. Dantzer, J. C. Ame and G. de Murcia (2006). "Poly(ADP-ribose): novel functions for an old molecule." Nat Rev Mol Cell Biol **7**(7): 517-528.

Shain, A. H., C. P. Giacomini, K. Matsukuma, C. A. Karikari, M. D. Bashyam, M. Hidalgo, A. Maitra and J. R. Pollack (2012). "Convergent structural alterations define SWItch/Sucrose NonFermentable (SWI/SNF) chromatin remodeler as a central tumor suppressive complex in pancreatic cancer." Proc Natl Acad Sci U S A **109**(5): E252-259.

Shain, A. H. and J. R. Pollack (2013). "The spectrum of SWI/SNF mutations, ubiquitous in human cancers." PLoS One **8**(1): e55119.

Shall, S. and G. de Murcia (2000). "Poly(ADP-ribose) polymerase-1: what have we learned from the deficient mouse model?" Mutat Res **460**(1): 1-15.

Shanbhag, N. M., I. U. Rafalska-Metcalf, C. Balane-Bolivar, S. M. Janicki and R. A. Greenberg (2010). "ATM-dependent chromatin changes silence transcription in cis to DNA double-strand breaks." Cell **141**(6): 970-981.

Shao, Z., F. Raible, R. Mollaaghababa, J. R. Guyon, C. T. Wu, W. Bender and R. E. Kingston (1999). "Stabilization of chromatin structure by PRC1, a Polycomb complex." Cell **98**(1): 37-46.

Shenoy, N. and L. Pagliaro (2016). "Sequential pathogenesis of metastatic VHL mutant clear cell renal cell carcinoma: putting it together with a translational perspective." Ann Oncol **27**(9): 1685-1695.

Shieh, W. M., J. C. Ame, M. V. Wilson, Z. Q. Wang, D. W. Koh, M. K. Jacobson and E. L. Jacobson (1998). "Poly(ADP-ribose) polymerase null mouse cells synthesize ADP-ribose polymers." J Biol Chem **273**(46): 30069-30072.

Skiniotis, G., D. Moazed and T. Walz (2007). "Acetylated histone tail peptides induce structural rearrangements in the RSC chromatin remodeling complex." J Biol Chem **282**(29): 20804-20808.

Soutourina, J., V. Bordas-Le Floch, G. Gendrel, A. Flores, C. Ducrot, H. Dumay-Odelot, P. Soularue, F. Navarro, B. R. Cairns, O. Lefebvre and M. Werner (2006). "Rsc4 connects the chromatin remodeler RSC to RNA polymerases." Mol Cell Biol **26**(13): 4920-4933.

Steckel, M., M. Molina-Arcas, B. Weigelt, M. Marani, P. H. Warne, H. Kuznetsov, G. Kelly, B. Saunders, M. Howell, J. Downward and D. C. Hancock (2012). "Determination of synthetic lethal interactions in KRAS oncogene-dependent

cancer cells reveals novel therapeutic targeting strategies." Cell Res **22**(8): 1227-1245.

Stern, M., R. Jensen and I. Herskowitz (1984). "Five SWI genes are required for expression of the HO gene in yeast." J Mol Biol **178**(4): 853-868.

Stransky, N., A. M. Egloff, A. D. Tward, A. D. Kostic, K. Cibulskis, A. Sivachenko, G. V. Kryukov, M. S. Lawrence, C. Sougnez, A. McKenna, E. Shefler, A. H. Ramos, P. Stojanov, S. L. Carter, D. Voet, M. L. Cortes, D. Auclair, M. F. Berger, G. Saksena, C. Guiducci, R. C. Onofrio, M. Parkin, M. Romkes, J. L. Weissfeld, R. R. Seethala, L. Wang, C. Rangel-Escareno, J. C. Fernandez-Lopez, A. Hidalgo-Miranda, J. Melendez-Zajgla, W. Winckler, K. Ardlie, S. B. Gabriel, M. Meyerson, E. S. Lander, G. Getz, T. R. Golub, L. A. Garraway and J. R. Grandis (2011). "The mutational landscape of head and neck squamous cell carcinoma." Science **333**(6046): 1157-1160.

Strom, C. E., F. Johansson, M. Uhlen, C. A. Szigyarto, K. Erixon and T. Helleday (2011). "Poly (ADP-ribose) polymerase (PARP) is not involved in base excision repair but PARP inhibition traps a single-strand intermediate." Nucleic Acids Res **39**(8): 3166-3175.

Stucki, M., J. A. Clapperton, D. Mohammad, M. B. Yaffe, S. J. Smerdon and S. P. Jackson (2005). "MDC1 directly binds phosphorylated histone H2AX to regulate cellular responses to DNA double-strand breaks." Cell **123**(7): 1213-1226.

Su, D., Q. Hu, Q. Li, J. R. Thompson, G. Cui, A. Fazly, B. A. Davies, M. V. Botuyan, Z. Zhang and G. Mer (2012). "Structural basis for recognition of H3K56-acetylated histone H3-H4 by the chaperone Rtt106." Nature **483**(7387): 104-107.

Sugasawa, K., Y. Okuda, M. Saijo, R. Nishi, N. Matsuda, G. Chu, T. Mori, S. Iwai, K. Tanaka, K. Tanaka and F. Hanaoka (2005). "UV-induced ubiquitylation of XPC protein mediated by UV-DDB-ubiquitin ligase complex." Cell **121**(3): 387-400.

Tang, L., E. Nogales and C. Ciferri (2010). "Structure and function of SWI/SNF chromatin remodeling complexes and mechanistic implications for transcription." Prog Biophys Mol Biol **102**(2-3): 122-128.

Tauchi, H., J. Kobayashi, K. Morishima, D. C. van Gent, T. Shiraishi, N. S. Verkaik, D. vanHeems, E. Ito, A. Nakamura, E. Sonoda, M. Takata, S. Takeda, S. Matsuura and K. Komatsu (2002). "Nbs1 is essential for DNA repair by homologous recombination in higher vertebrate cells." Nature **420**(6911): 93-98.

Thompson, M. (2009). "Polybromo-1: the chromatin targeting subunit of the PBAF complex." Biochimie **91**(3): 309-319.

Titus, L. C., T. R. Dawson, D. J. Rexer, K. J. Ryan and S. R. Wente (2010). "Members of the RSC chromatin-remodeling complex are required for maintaining proper nuclear envelope structure and pore complex localization." Mol Biol Cell **21**(6): 1072-1087.

Tomlinson, I. P., N. A. Alam, A. J. Rowan, E. Barclay, E. E. Jaeger, D. Kelsell, I. Leigh, P. Gorman, H. Lamlum, S. Rahman, R. R. Roylance, S. Olpin, S. Bevan, K. Barker, N. Hearle, R. S. Houlston, M. Kiuru, R. Lehtonen, A. Karhu, S. Vilkki, P. Laiho, C. Eklund, O. Vierimaa, K. Aittomaki, M. Hietala, P. Sistonen, A. Paetau, R. Salovaara, R. Herva, V. Launonen, L. A. Aaltonen and C. Multiple Leiomyoma (2002). "Germline mutations in FH predispose to dominantly inherited uterine fibroids, skin leiomyomata and papillary renal cell cancer." Nat Genet **30**(4): 406-410.

Tong, A. H., M. Evangelista, A. B. Parsons, H. Xu, G. D. Bader, N. Page, M. Robinson, S. Raghibizadeh, C. W. Hogue, H. Bussey, B. Andrews, M. Tyers and C. Boone (2001). "Systematic genetic analysis with ordered arrays of yeast deletion mutants." Science **294**(5550): 2364-2368.

Tsabar, M. and J. E. Haber (2013). "Chromatin modifications and chromatin remodeling during DNA repair in budding yeast." Curr Opin Genet Dev **23**(2): 166-173.

Tsai, C. J., S. A. Kim and G. Chu (2007). "Cernunnos/XLF promotes the ligation of mismatched and noncohesive DNA ends." Proc Natl Acad Sci U S A **104**(19): 7851-7856.

Tutt, A. and A. Ashworth (2002). "The relationship between the roles of BRCA genes in DNA repair and cancer predisposition." Trends Mol Med **8**(12): 571-576.

Underhill, C., M. Toulmonde and H. Bonnefoi (2011). "A review of PARP inhibitors: from bench to bedside." Ann Oncol **22**(2): 268-279.

van Haaften, G., G. L. Dalgliesh, H. Davies, L. Chen, G. Bignell, C. Greenman, S. Edkins, C. Hardy, S. O'Meara, J. Teague, A. Butler, J. Hinton, C. Latimer, J. Andrews, S. Barthorpe, D. Beare, G. Buck, P. J. Campbell, J. Cole, S. Forbes, M. Jia, D. Jones, C. Y. Kok, C. Leroy, M. L. Lin, D. J. McBride, M. Maddison, S. Maquire, K.

McLay, A. Menzies, T. Mironenko, L. Mulderrig, L. Mudie, E. Pleasance, R. Shepherd, R. Smith, L. Stebbings, P. Stephens, G. Tang, P. S. Tarpey, R. Turner, K. Turrell, J. Varian, S. West, S. Widaa, P. Wray, V. P. Collins, K. Ichimura, S. Law, J. Wong, S. T. Yuen, S. Y. Leung, G. Tonon, R. A. DePinho, Y. T. Tai, K. C. Anderson, R. J. Kahnoski, A. Massie, S. K. Khoo, B. T. Teh, M. R. Stratton and P. A. Futreal (2009). "Somatic mutations of the histone H3K27 demethylase gene UTX in human cancer." Nat Genet **41**(5): 521-523.

VanDemark, A. P., M. M. Kasten, E. Ferris, A. Heroux, C. P. Hill and B. R. Cairns (2007). "Autoregulation of the rsc4 tandem bromodomain by gcn5 acetylation." Mol Cell **27**(5): 817-828.

Varela, I., P. Tarpey, K. Raine, D. Huang, C. K. Ong, P. Stephens, H. Davies, D. Jones, M. L. Lin, J. Teague, G. Bignell, A. Butler, J. Cho, G. L. Dalgliesh, D. Galappaththige, C. Greenman, C. Hardy, M. Jia, C. Latimer, K. W. Lau, J. Marshall, S. McLaren, A. Menzies, L. Mudie, L. Stebbings, D. A. Largaespada, L. F. Wessels, S. Richard, R. J. Kahnoski, J. Anema, D. A. Tuveson, P. A. Perez-Mancera, V. Mustonen, A. Fischer, D. J. Adams, A. Rust, W. Chan-on, C. Subimerb, K. Dykema, K. Furge, P. J. Campbell, B. T. Teh, M. R. Stratton and P. A. Futreal (2011). "Exome sequencing identifies frequent mutation of the SWI/SNF complex gene PBRM1 in renal carcinoma." Nature **469**(7331): 539-542.

Ventii, K. H., N. S. Devi, K. L. Friedrich, T. A. Chernova, M. Tighiouart, E. G. Van Meir and K. D. Wilkinson (2008). "BRCA1-associated protein-1 is a tumor suppressor that requires deubiquitinating activity and nuclear localization." Cancer Res **68**(17): 6953-6962.

Versteege, I., N. Sevenet, J. Lange, M. F. Rousseau-Merck, P. Ambros, R. Handgretinger, A. Aurias and O. Delattre (1998). "Truncating mutations of hSNF5/INI1 in aggressive paediatric cancer." Nature **394**(6689): 203-206.

Vyas, S., I. Matic, L. Uchima, J. Rood, R. Zaja, R. T. Hay, I. Ahel and P. Chang (2014). "Family-wide analysis of poly(ADP-ribose) polymerase activity." Nat Commun **5**: 4426.

Wagener, N., D. Holland, J. Bulkescher, I. Crnkovic-Mertens, K. Hoppe-Seyler, H. Zentgraf, M. Pritsch, S. Buse, J. Pfitzenmaier, A. Haferkamp, M. Hohenfellner and F. Hoppe-Seyler (2008). "The enhancer of zeste homolog 2 gene contributes to

cell proliferation and apoptosis resistance in renal cell carcinoma cells." Int J Cancer **123**(7): 1545-1550.

Wagner, E. J. and P. B. Carpenter (2012). "Understanding the language of Lys36 methylation at histone H3." Nat Rev Mol Cell Biol **13**(2): 115-126.

Wakasugi, M., A. Kawashima, H. Morioka, S. Linn, A. Sancar, T. Mori, O. Nikaido and T. Matsunaga (2002). "DDB accumulates at DNA damage sites immediately after UV irradiation and directly stimulates nucleotide excision repair." J Biol Chem **277**(3): 1637-1640.

Walker, J. R., R. A. Corpina and J. Goldberg (2001). "Structure of the Ku heterodimer bound to DNA and its implications for double-strand break repair." Nature **412**(6847): 607-614.

Wang, A. H., N. R. Bertos, M. Vezmar, N. Pelletier, M. Crosato, H. H. Heng, J. Th'ng, J. Han and X. J. Yang (1999). "HDAC4, a human histone deacetylase related to yeast HDA1, is a transcriptional corepressor." Mol Cell Biol **19**(11): 7816-7827.

Wang, J., L. Liu, Y. Qu, W. Xi, Y. Xia, Q. Bai, Y. Xiong, Q. Long, J. Xu and J. Guo (2016). "Prognostic value of SETD2 expression in patients with metastatic renal cell carcinoma treated with tyrosine kinase inhibitors." J Urol.

Wang, K., J. Kan, S. T. Yuen, S. T. Shi, K. M. Chu, S. Law, T. L. Chan, Z. Kan, A. S. Chan, W. Y. Tsui, S. P. Lee, S. L. Ho, A. K. Chan, G. H. Cheng, P. C. Roberts, P. A. Rejto, N. W. Gibson, D. J. Pocalyko, M. Mao, J. Xu and S. Y. Leung (2011). "Exome sequencing identifies frequent mutation of ARID1A in molecular subtypes of gastric cancer." Nat Genet **43**(12): 1219-1223.

Wang, W., J. Cote, Y. Xue, S. Zhou, P. A. Khavari, S. R. Biggar, C. Muchardt, G. V. Kalpana, S. P. Goff, M. Yaniv, J. L. Workman and G. R. Crabtree (1996). "Purification and biochemical heterogeneity of the mammalian SWI-SNF complex." EMBO J **15**(19): 5370-5382.

Wang, X., N. G. Nagl, D. Wilsker, M. Van Scoy, S. Pacchione, P. Yaciuk, P. B. Dallas and E. Moran (2004). "Two related ARID family proteins are alternative subunits of human SWI/SNF complexes." Biochem J **383**(Pt 2): 319-325.

Wang, Z. Q., L. Stingl, C. Morrison, M. Jantsch, M. Los, K. Schulze-Osthoff and E. F. Wagner (1997). "PARP is important for genomic stability but dispensable in apoptosis." Genes Dev **11**(18): 2347-2358.

Watanabe, R., A. Ui, S. Kanno, H. Ogiwara, T. Nagase, T. Kohno and A. Yasui (2014). "SWI/SNF factors required for cellular resistance to DNA damage include ARID1A and ARID1B and show interdependent protein stability." Cancer Res **74**(9): 2465-2475.

Watson, J. D. and F. H. Crick (1953). "Molecular structure of nucleic acids; a structure for deoxyribose nucleic acid." Nature **171**(4356): 737-738.

Weier, H. U. (2001). "DNA fiber mapping techniques for the assembly of high-resolution physical maps." J Histochem Cytochem **49**(8): 939-948.

Weissman, B. and K. E. Knudsen (2009). "Hijacking the chromatin remodeling machinery: impact of SWI/SNF perturbations in cancer." Cancer Res **69**(21): 8223-8230.

Whelan, G., E. Kreidl, G. Wutz, A. Egner, J. M. Peters and G. Eichele (2012). "Cohesin acetyltransferase Esco2 is a cell viability factor and is required for cohesion in pericentric heterochromatin." EMBO J **31**(1): 71-82.

Wiegand, K. C., S. P. Shah, O. M. Al-Agha, Y. Zhao, K. Tse, T. Zeng, J. Senz, M. K. McConechy, M. S. Anglesio, S. E. Kalloger, W. Yang, A. Heravi-Moussavi, R. Giuliany, C. Chow, J. Fee, A. Zayed, L. Prentice, N. Melnyk, G. Turashvili, A. D. Delaney, J. Madore, S. Yip, A. W. McPherson, G. Ha, L. Bell, S. Fereday, A. Tam, L. Galletta, P. N. Tonin, D. Provencher, D. Miller, S. J. Jones, R. A. Moore, G. B. Morin, A. Oloumi, N. Boyd, S. A. Aparicio, M. Shih Ie, A. M. Mes-Masson, D. D. Bowtell, M. Hirst, B. Gilks, M. A. Marra and D. G. Huntsman (2010). "ARID1A mutations in endometriosis-associated ovarian carcinomas." N Engl J Med **363**(16): 1532-1543.

Wilkins, M. H., A. R. Stokes and H. R. Wilson (1953). "Molecular structure of deoxypentose nucleic acids." Nature **171**(4356): 738-740.

Wilson, B. G. and C. W. Roberts (2011). "SWI/SNF nucleosome remodellers and cancer." Nat Rev Cancer **11**(7): 481-492.

Wilson, B. G., X. Wang, X. Shen, E. S. McKenna, M. E. Lemieux, Y. J. Cho, E. C. Koellhoffer, S. L. Pomeroy, S. H. Orkin and C. W. Roberts (2010). "Epigenetic antagonism between polycomb and SWI/SNF complexes during oncogenic transformation." Cancer Cell **18**(4): 316-328.

Woodcock, C. L. and S. Dimitrov (2001). "Higher-order structure of chromatin and chromosomes." Curr Opin Genet Dev **11**(2): 130-135.

Wu, Q., T. Ochi, D. Matak-Vinkovic, C. V. Robinson, D. Y. Chirgadze and T. L. Blundell (2011). "Non-homologous end-joining partners in a helical dance: structural studies of XLF-XRCC4 interactions." Biochem Soc Trans **39**(5): 1387-1392, suppl 1382 p following 1392.

Wunsch, A. M., K. Reinhardt and J. Lough (1991). "Normal transitions in synthesis of replacement histones H2A.Z and H3.3 during differentiation of dystrophic myotube cells. A brief note." Mech Ageing Dev **59**(3): 299-305.

Xia, B., Q. Sheng, K. Nakanishi, A. Ohashi, J. Wu, N. Christ, X. Liu, M. Jasin, F. J. Couch and D. M. Livingston (2006). "Control of BRCA2 cellular and clinical functions by a nuclear partner, PALB2." Mol Cell **22**(6): 719-729.

Xia, W., S. Nagase, A. G. Montia, S. M. Kalachikov, M. Keniry, T. Su, L. Memeo, H. Hibshoosh and R. Parsons (2008). "BAF180 is a critical regulator of p21 induction and a tumor suppressor mutated in breast cancer." Cancer Res **68**(6): 1667-1674.

Xue, Y., J. C. Canman, C. S. Lee, Z. Nie, D. Yang, G. T. Moreno, M. K. Young, E. D. Salmon and W. Wang (2000). "The human SWI/SNF-B chromatin-remodeling complex is related to yeast rsc and localizes at kinetochores of mitotic chromosomes." Proc Natl Acad Sci U S A **97**(24): 13015-13020.

Yamaguchi, H. and M. C. Hung (2014). "Regulation and Role of EZH2 in Cancer." Cancer Res Treat **46**(3): 209-222.

Yan, Z., K. Cui, D. M. Murray, C. Ling, Y. Xue, A. Gerstein, R. Parsons, K. Zhao and W. Wang (2005). "PBAF chromatin-remodeling complex requires a novel specificity subunit, BAF200, to regulate expression of selective interferon-responsive genes." Genes Dev **19**(14): 1662-1667.

Yaneva, M., T. Kowalewski and M. R. Lieber (1997). "Interaction of DNA-dependent protein kinase with DNA and with Ku: biochemical and atomic-force microscopy studies." EMBO J **16**(16): 5098-5112.

Yelamos, J., V. Schreiber and F. Dantzer (2008). "Toward specific functions of poly(ADP-ribose) polymerase-2." Trends Mol Med **14**(4): 169-178.

Yi, C. and C. He (2013). "DNA repair by reversal of DNA damage." Cold Spring Harb Perspect Biol **5**(1): a012575.

Yu, H., H. Pak, I. Hammond-Martel, M. Ghram, A. Rodrigue, S. Daou, H. Barbour, L. Corbeil, J. Hebert, E. Drobetsky, J. Y. Masson, J. M. Di Noia and B. Affar el (2014).

"Tumor suppressor and deubiquitinase BAP1 promotes DNA double-strand break repair." Proc Natl Acad Sci U S A **111**(1): 285-290.

Yu, L., A. Lopez, A. Anaflous, B. El Bali, A. Hamal, E. Ericson, L. E. Heisler, A. McQuibban, G. Giaever, C. Nislow, C. Boone, G. W. Brown and M. Bellaoui (2008). "Chemical-genetic profiling of imidazo[1,2-a]pyridines and -pyrimidines reveals target pathways conserved between yeast and human cells." PLoS Genet **4**(11): e1000284.

Yue, F., W. Li, J. Zou, Q. Chen, G. Xu, H. Huang, Z. Xu, S. Zhang, P. Gallinari, F. Wang, W. L. McKeehan and L. Liu (2015). "Blocking the association of HDAC4 with MAP1S accelerates autophagy clearance of mutant Huntingtin." Aging (Albany NY) **7**(10): 839-853.

Yun, M. H. and K. Hiom (2009). "CtIP-BRCA1 modulates the choice of DNA double-strand-break repair pathway throughout the cell cycle." Nature **459**(7245): 460-463.

Zahradka, P. and K. Ebisuzaki (1982). "A shuttle mechanism for DNA-protein interactions. The regulation of poly(ADP-ribose) polymerase." Eur J Biochem **127**(3): 579-585.

Zeng, L., Q. Zhang, S. Li, A. N. Plotnikov, M. J. Walsh and M. M. Zhou (2010). "Mechanism and regulation of acetylated histone binding by the tandem PHD finger of DPF3b." Nature **466**(7303): 258-262.

Zhang, J., L. Ding, L. Holmfeldt, G. Wu, S. L. Heatley, D. Payne-Turner, J. Easton, X. Chen, J. Wang, M. Rusch, C. Lu, S. C. Chen, L. Wei, J. R. Collins-Underwood, J. Ma, K. G. Roberts, S. B. Pounds, A. Ulyanov, J. Becksfort, P. Gupta, R. Huether, R. W. Kriwacki, M. Parker, D. J. McGoldrick, D. Zhao, D. Alford, S. Espy, K. C. Bobba, G. Song, D. Pei, C. Cheng, S. Roberts, M. I. Barbato, D. Campana, E. Coustan-Smith, S. A. Shurtleff, S. C. Raimondi, M. Kleppe, J. Cools, K. A. Shimano, M. L. Hermiston, S. Doulatov, K. Eppert, E. Laurenti, F. Notta, J. E. Dick, G. Basso, S. P. Hunger, M. L. Loh, M. Devidas, B. Wood, S. Winter, K. P. Dunsmore, R. S. Fulton, L. L. Fulton, X. Hong, C. C. Harris, D. J. Dooling, K. Ochoa, K. J. Johnson, J. C. Obenauer, W. E. Evans, C. H. Pui, C. W. Naeve, T. J. Ley, E. R. Mardis, R. K. Wilson, J. R. Downing and C. G. Mullighan (2012). "The genetic basis of early T-cell precursor acute lymphoblastic leukaemia." Nature **481**(7380): 157-163.

Zhang, Y., C. L. Smith, A. Saha, S. W. Grill, S. Mihardja, S. B. Smith, B. R. Cairns, C. L. Peterson and C. Bustamante (2006). "DNA translocation and loop formation mechanism of chromatin remodeling by SWI/SNF and RSC." Mol Cell **24**(4): 559-568.

Zhang, Z. K., K. P. Davies, J. Allen, L. Zhu, R. G. Pestell, D. Zagzag and G. V. Kalpana (2002). "Cell cycle arrest and repression of cyclin D1 transcription by INI1/hSNF5." Mol Cell Biol **22**(16): 5975-5988.

Zhao, Q., Q. E. Wang, A. Ray, G. Wani, C. Han, K. Milum and A. A. Wani (2009). "Modulation of nucleotide excision repair by mammalian SWI/SNF chromatin-remodeling complex." J Biol Chem **284**(44): 30424-30432.

Zhou, Y. and T. T. Paull (2013). "DNA-dependent protein kinase regulates DNA end resection in concert with Mre11-Rad50-Nbs1 (MRN) and ataxia telangiectasia-mutated (ATM)." J Biol Chem **288**(52): 37112-37125.

Zlatanova, J. and A. Thakar (2008). "H2A.Z: view from the top." Structure **16**(2): 166-179.

APPENDIX

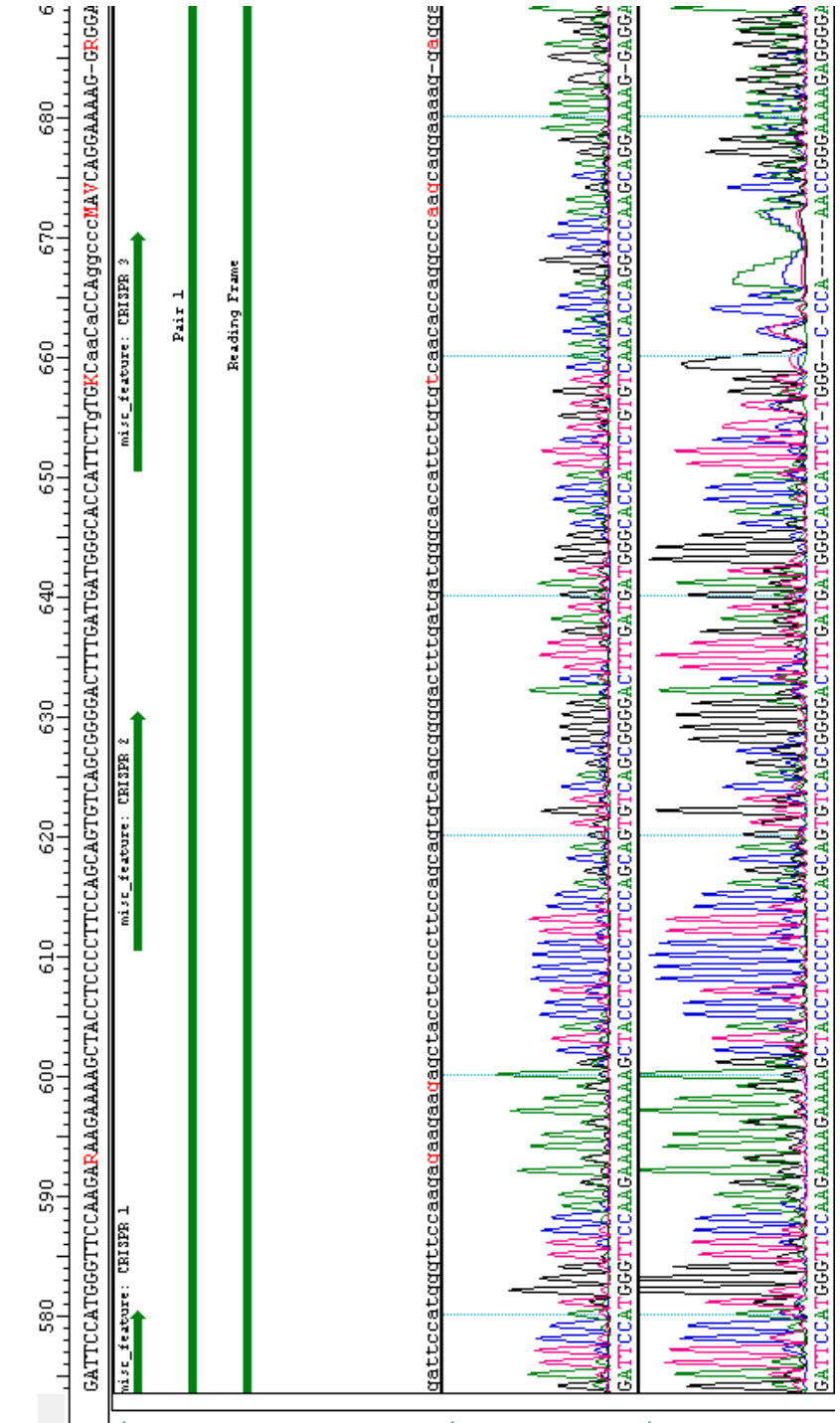

Appendix Figure 1. Sequence alignment of CRISPR knockout U2OS.

PUBLICATIONS